

Metabolic Signatures of Pneumonia in Critical Care: A Paradigm Shift in Diagnosis and Therapeutic Monitoring

David Benjamin Antcliffe

Section of Anaesthetics, Pain Medicine and Intensive Care, Imperial College
London, Charing Cross Hospital, London, UK.

2015

A thesis submitted to Imperial College London for the degree of Doctorate of
Philosophy

Supervisors:

Dr. Anthony C. Gordon

Section of Anaesthetics, Pain Medicine and Intensive Care, Imperial College
London, Charing Cross Hospital, London, UK.

Professor Masao Takata

Section of Anaesthetics, Pain Medicine and Intensive Care, Imperial College
London, Chelsea and Westminster Hospital, London, UK.

Professor George B. Hanna

Department of Surgery and Cancer, Imperial College London, St Mary's
Hospital, London, UK.

ABSTRACT

Pneumonia and ventilator associated pneumonia (VAP) are a frequent cause for admission to Intensive Care and complication of ventilation respectively. VAP occurs in 10-40% of patients requiring mechanical ventilation and is associated with increased mortality, morbidity and healthcare costs. Diagnosis can be difficult due to poor predictive value of clinical features and low specificity of radiological changes. Bronchoscopic techniques are often invasive, may not be suitable for all patients and are not without complications. New tests are required to improve the diagnosis of these conditions allowing early, appropriate antibiotic treatment.

In this study several techniques were used to explore the value of profiling of a range of biofluids obtained from ventilated patients as an aid to diagnosis of pneumonia. Patients were recruited from Intensive Care with either a diagnosis of pneumonia or brain injury. Those with brain injuries were tracked to identify patients who developed VAP. Serum, urine and exhaled breath condensate (EBC) were collected from all patients.

Metabonomics, an approach that identifies changes in metabolic profiles associated with disease, was applied using proton nuclear magnetic resonance spectroscopy to both blood and urine and with mass spectrometry (MS) to exhaled breath condensate. Following from the metabonomic work a panel of inflammatory mediators, including cytokines and eicosanoids were measured in serum using MS and flow cytometry to explore the inflammatory changes in these patients.

Overall metabolic and inflammatory profiling of serum showed potential as an adjunct to clinical diagnosis especially when combined with clinical data. Analysis of urine and EBC proved more challenging due the number of drug metabolites and low concentration of metabolites they respectively contained. In summary this study has added to the field by demonstrating the potential for profiling techniques of serum from critically ill patients to assist in the diagnosis of both pneumonia and VAP.

DECLARATION

I hereby declare that I am the sole author of this thesis and that all work within it is my own. Any individuals who carried out work in collaboration with the author are appropriately credited. I authorise the library of the University of London to lend this thesis to other institutions or individuals.

Signed:

Date: 18th June 2015

David B. Antcliffe

COPYRIGHT DECLARATION

The copyright of this thesis rests with the author and is made available under a Creative Commons Attribution Non-Commercial No Derivatives licence. Researchers are free to copy, distribute or transmit the thesis on the condition that they attribute it, that they do not use it for commercial purposes and that they do not alter, transform or build upon it. For any reuse or redistribution, researchers must make clear to others the licence terms of this work

PRESENTATIONS

Oral Presentations

D Antcliffe, B Jiménez, K Veselkov, E Holmes, G Hanna, M Takata, A C Gordon. Diagnosing pneumonia on the Intensive Care Unit with serum ^1H NMR spectroscopy. European Society of Intensive Care Medicine Congress. Intensive Care Medicine. 2014: 40(S1); S237-8. Oral Presentation.

D Antcliffe, K Veselkov, JTM Pearce, J Kinross, AC Gordon. Trajectory analysis of clinical variables to improve diagnosis of ventilator associated pneumonia in patients with brain injury. European Society of Intensive Care Medicine Congress. Intensive Care Medicine. 2013: 39(S2); S312-3. Poster Corner Presentation.

Poster Presentations

D Antcliffe, A Wolfer, K O'Dea, G Hanna, M Takata, E Holmes, A C Gordon. Profiling of Eicosanoids and Cytokines as an aid to diagnosing pneumonia on Intensive Care. American Thoracic Society Conference. Am J Respir Crit Care Med. 2015: 191; A6462.

A Wolfer, **D Antcliffe**, A Gordon, E Holmes, J Nicholson. Targeted oxylipin profiling for clinical diagnostic: a novel insight in ventilator associated pneumonia. Mass Spectrometry Applications to the Clinical Lab Conference, San Diego, March 2015.

D Antcliffe, B Jiménez , K Veselkov , E Holmes , J K Nicholson , G Hanna, M Takata, A C Gordon. NMR based metabonomic analysis of serum from patients with pneumonia on the intensive care unit. Journal of Intensive Care Society. 2014 15(1) Suppl 1; s98

D Antcliffe, P Boshier, B Jimenez, A Gordon, M Takata, E Holmes, J Nicholson, N Marczin, G Hanna. ^1H NMR analysis of exhaled breath condensate from patients developing pneumonia after major surgery. Poster Presentation at the Wellcome Trust Exploring Host-Microbiome Interactions in Health and Disease Conference, Cambridge, 2012.

ACKNOWLEDGEMENTS

I am greatly indebted to my supervisors Dr Anthony Gordon, Professor Masao Takata and Professor George Hanna for their continued guidance, encouragement and support during the course of my study.

I would also like to express my gratitude to the following people who have helped me during the course of my research.

Dr. Beatriz Jimenez – for guidance, advice and assistance during NMR studies

Mr. Arnaud Wolfer – for guidance, advice and assistance during MS profiling of eicosanoids

Prof. Elaine Holmes – for guidance and advice over all scientific aspects of this study

Dr. Kieran O’Dea – for guidance, advice and assistance with flow cytometry

Dr. Kirill Veselkov – for advice regarding multivariate data processing

Dr. Julia Denes – for guidance and assistance with MS processing of breath condensate

Dr Piers Boshier – for guidance and advice regarding breath condensate collection and processing

A great deal of thanks goes to my wife and family without whose support this thesis would not have been possible.

This study was funded via the Imperial College National Institute for Health Research Biomedical Research Centre and via an Intensive Care Foundation Young Investigator Award.

TABLE OF CONTENTS

ABSTRACT	3
DECLARATION	4
PRESENTATIONS	5
ACKNOWLEDGEMENTS	6
TABLE OF CONTENTS	7
LIST OF FIGURES	13
LIST OF TABLES	18
LIST OF ABBREVIATIONS	20
SECTION I - LITERATURE REVIEW	24
1. LITERATURE REVIEW	25
1.1 Pneumonia	25
1.1.1 Incidence	25
1.1.2 Pathogenesis	25
1.1.3 Outcomes	27
1.1.4 Diagnosis	27
1.1.4.1 Clinical Features	27
1.1.4.2 Biomarkers	28
1.1.4.3 Radiology	29
1.2 Ventilator Associated Pneumonia	29
1.2.1 Pathology	29
1.2.2 Epidemiology	30
1.2.3 Risk Factors	30
1.2.3.1 Surgery	31
1.2.3.2 Stress Ulcer Prophylaxis and Positioning	31
1.2.3.3 Intubation	32
1.2.3.4 Antibiotics	32
1.2.4 Aetiological Agents	32
1.2.5 Mortality, Morbidity and Health Care Costs	33
1.2.6 Diagnosis	33
1.2.6.1 Clinical Features	33
1.2.6.2 Radiology	34

1.2.6.3 Microbiology	34
1.2.6.4 Scoring Systems	35
1.2.6.5 Biomarkers	37
1.3 Metabonomics	38
1.3.1 ¹ H Nuclear Magnetic Resonance Spectroscopy	38
1.3.2 Mass Spectrometry	44
1.3.3 Data Analysis	45
1.3.3.1 Principal Component Analysis	46
1.3.3.2 Supervised Analysis	46
1.3.3.3 Pre-processing	49
1.4 Metabonomics of Sepsis and Pneumonia	49
1.4.1 Pneumonia	51
1.4.2 Critical Care	52
1.5 Oxylipins and Cytokines	53
1.6 Breath Analysis	56
1.6.1 Metabonomics of Exhaled Breath Condensate – ¹ H-NMR Spectroscopy	57
1.6.2 Metabonomics of Exhaled Breath Condensate – Mass Spectrometry	58
1.7 Hypothesis and Aims	59
1.7.1 Hypothesis	59
1.7.2 Aims	59
SECTION II - METHODOLOGY	61
2. PROTOCOLS AND METHODS	62
2.1 Patient Recruitment	62
2.1.1 Consent	63
2.1.2 Sample Collection	63
2.1.2.1 Serum	63
2.1.2.2 Urine	64
2.1.2.3 Exhaled Breath Condensate	65
2.1.3 Clinical Data Collection	67
2.1.4 Patient Follow Up	67
2.2 Diagnosis of Pneumonia	67
2.2.1 Brain Injury Patients Developing Ventilator Associated Pneumonia	67

2.2.2 Pneumonia	70
2.3 Specific Processing	73
2.4 Statistical Analysis	73
2.5 Patient Details	78
SECTION III – CLINICAL STUDIES	84
3. ¹H-NMR ANALYSIS OF SERUM AND URINE	85
3.1 Summary	85
3.2 Background	85
3.3 Aims	87
3.4 Protocols	88
3.4.1 Patient Recruitment and Sample Collection	88
3.4.2 Sample Processing	88
3.4.2.1 Serum	88
3.4.2.2 Urine	89
3.4.3 ¹ H-NMR 1D Experimental Data Acquisition	89
3.4.3.1 Serum	89
3.4.3.2 Urine	90
3.4.4 Pre-Processing	90
3.4.5 Statistical Analysis	91
3.4.5 Metabolite Identification	92
3.5 Results	92
3.5.1 Patients	92
3.5.2 Serum	95
3.5.2.1 10 Minutes vs 15 Minutes of Centrifugation	95
3.5.2.2 Brain Injury vs Pneumonia	97
3.5.2.3 Brain Injury vs VAP	105
3.5.2.4 Time Course	108
3.5.3 Urine	115
3.5.3.1 Brain Injury vs Pneumonia	115
3.5.3.2 Brain Injury vs VAP	118
3.5.3.3 Time Course	118
3.5.3.4 Treatment Effect	123

3.6 Discussion	126
3.7 Conclusion	134
4. SERUM INFLAMMASOME PROFILING	135
4.1 Summary	135
4.2 Background	135
4.3 Aims	137
4.4 Protocols	138
4.4.1 Patient Recruitment and Sample Collection	138
4.4.2 Eicosanoid Measurement	138
4.4.2.1 Isotopically Labelled Internal Standards	139
4.4.2.2 Standard Mixtures	139
4.4.2.3 Sample Preparation	140
4.4.2.4 Solid Phase Extraction	140
4.4.2.5 UPLC and Mass Spectrometry	141
4.4.2.6 Data Pre-processing	142
4.4.2 Cytokine Measurement	142
4.4.3.1 Assay Buffer	143
4.4.3.2 Sample Preparation	143
4.4.3.3 Standard Curves	143
4.4.3.4 Fluorescent Beads	144
4.4.3.5 Preparation of Plates	145
4.4.3.6 Flow Cytometry	146
4.4.3.7 Data Pre-processing	149
4.4.3 Statistical Analysis	149
4.5 Results	150
4.5.1 Patients	150
4.5.2 Eicosanoids	153
4.5.2.1 Evaluation of Batch Effect	154
4.5.2.2 Brain Injury vs. Pneumonia	154
4.5.2.3 Brain Injury vs VAP	160
4.5.3 Cytokines	160
4.5.3.1 Evaluation of Batch Effect	160

4.5.3.2 <i>Brain Injury vs. Pneumonia</i>	161
4.5.3.3 <i>Brain Injury vs VAP</i>	165
4.5.4 <i>Combining Eicosanoids and Cytokines</i>	167
4.5.4.1 <i>Brain Injury vs. Pneumonia</i>	167
4.5.4.2 <i>Brain Injury vs. VAP</i>	169
4.5.4.3 <i>Time Course</i>	173
4.5.4.4 <i>Correlation</i>	179
4.6 Discussion	183
4.7 Conclusions	193
5. EXHALED BREATH CONDENSATE	194
5.1 Summary	194
5.2 Background	194
5.3 Aims	198
5.4 Protocols	198
5.4.1 <i>Patient Recruitment and Sample Collection</i>	198
5.4.2 ¹ H-NMR Spectroscopy	199
5.4.2.1 ¹ H-NMR Experiments	199
5.4.2.2 <i>Freeze Drying</i>	200
5.4.2.3 <i>Effect of Collection Equipment</i>	204
5.4.2.4 <i>Summary of ¹H-NMR</i>	210
5.4.3 <i>Mass Spectrometry</i>	210
5.4.3.1 <i>Data Processing</i>	211
5.4.3.2 <i>Statistical Analysis</i>	211
5.5 Results	212
5.5.1 <i>Patients</i>	212
5.5.2 <i>Evaluation of Batch Effect</i>	212
5.5.3 <i>Collection Equipment</i>	218
5.5.4 <i>Brain Injury vs. Pneumonia</i>	218
5.5.5 <i>Brain Injury vs. VAP</i>	221
5.5.6 <i>Time Course</i>	222
5.6 Discussion	228
5.7 Conclusion	234

6. MULTIVARIATE ANALYSIS OF CLINICAL DATA	235
6.1 Summary	235
6.2 Background	235
6.3 Aims	237
6.4 Protocols	238
6.4.1 Patient Recruitment	238
6.4.2 Clinical Data	238
6.4.3 Metabolic and Inflammatory Data	239
6.4.4 Statistical Analysis	241
6.5 Results	242
6.5.1 Patients	242
6.5.2 Clinical Data Models	242
6.5.2.1 Brain Injury vs Pneumonia	242
6.5.2.2 Brain Injury vs VAP	248
6.5.3 Combining Clinical Variables with Metabonomic and Inflammazome Data	251
6.5.3.1 Brain Injury vs Pneumonia	251
6.5.3.1.1 Clinical and Metabonomic Data	251
6.5.3.1.2 Clinical and Inflammatory Data	252
6.5.3.1.3 Clinical, Metabonomic and Inflammatory Data	254
6.5.3.2 Brain Injury vs VAP	257
6.5.3.2.1 Clinical and Metabonomic Data	257
6.5.3.2.2 Clinical and Inflammatory Data	259
6.5.3.2.3 Clinical, Metabonomic and Inflammatory Data	260
6.6 Discussion	267
6.7 Conclusion	279
7. FINAL CONCLUSIONS	280
8. REFERENCES	287
9. APPENDICES	318

LIST OF FIGURES

Figure 1.1 - Schematic diagram of an NMR spectrometer	39
Figure 1.2 - Chemical shifts for common metabolite structural components	40
Figure 1.3 - Representation of J-coupling in NMR spectrometry	41
Figure 1.4 - Example ¹ H-NMR CPMG spectrum	42
Figure 1.5 - Example 2D Total Correlation Spectroscopy experiment	43
Figure 1.6 - Schematic diagram of a mass spectrometer	44
Figure 1.7 - Schematic diagram illustrating Principal Component Analysis	47
Figure 1.8 - Representation of eicosanoid metabolism	54
Figure 2.1 - Components of the RTube™ exhaled breath condensate collection device	66
Figure 2.2 - Study classification pathway for patients admitted with brain injuries	71
Figure 2.3 - Study classification for patients admitted for ventilation with a presumed diagnosis of pneumonia	72
Figure 2.4 - Breakdown of recruited patients	79
Figure 3.1 - PCA scores plot comparing ¹ H-NMR data from serum samples centrifuged for 10 and 15 minutes	96
Figure 3.2 - PCA scores plots comparing ¹ H-NMR data from serum samples from patients with pneumonia and brain injuries at the first sampling time point	98
Figure 3.3 - Comparison of ¹ H-NMR spectra from the outlying patients	99
Figure 3.4 - OPLS-DA score plot comparing serum ¹ H-NMR data from patients with pneumonia and brain injuries at the start of ventilation	100
Figure 3.5 - OPLS-DA regression coefficient plot showing the serum metabolites separating patients with pneumonia from those with brain injuries	102
Figure 3.6 - Detail of the OPLS-DA regression coefficient plot showing the serum metabolites separating patients with pneumonia from those with brain injuries	103
Figure 3.7 - OPLS-DA score plot comparing serum ¹ H-NMR data from patients with VAP and brain injuries.	106
Figure 3.8 - OPLS-DA regression coefficient plot showing the serum metabolites separating patients with VAP from those with brain injuries	107

Figure 3.9 - OPLS-DA regression coefficient plot showing the serum metabolites separating patients with brain injuries at time point 1 and 4	109
Figure 3.10 - OPLS-DA regression coefficient plot showing the serum metabolites separating patients with pneumonia at time point 1 and 4	110
Figure 3.11 - OPLS-DA regression coefficient plot showing the serum metabolites separating patients with brain injuries without pneumonia at time point 4 from those with VAP	112
Figure 3.12 - PCA scores plots comparing urine ¹ H-NMR spectra from patients with pneumonia and brain injuries at the first sampling time point	113
Figure 3.13 - OPLS-DA regression coefficient plot showing the urine metabolites separating the outliers from the PCA.	114
Figure 3.14 - OPLS-DA model comparing urine ¹ H-NMR data from patients with pneumonia and brain injuries at the start of ventilation	116
Figure 3.15 - OPLS-DA regression coefficient plot showing the urine metabolites separating those with pneumonia from those with brain injuries	117
Figure 3.16 - OPLS-DA regression coefficient plot showing the urine metabolites separating time point 1 and 4 for those patients with brain injuries	119
Figure 3.17 - OPLS-DA regression coefficient plot showing the urine metabolites separating time point 1 and 4 for those patients with pneumonia	120
Figure 3.18 - OPLS-DA regression coefficient plot showing the urine metabolites separating patients with brain injuries and no VAP at time point 4 and those with VAP	122
Figure 3.19 - OPLS-DA scores plot and regression coefficient plot showing the urine metabolites separating patients receiving tazocin compared with those not on antibiotics. STOCYSY regression coefficient plot showing correlation of potential peaks associated with tazocin.	124
Figure 4.1 - Schematic diagram of the set up plate measurement of serum cytokines with flow cytometry	145
Figure 4.2 - Example plots demonstrating how individual cytokines were identified and quantified using flow cytometry	147
Figure 4.3 - PCA, OPLS-DA scores plots and OPLS-DA loadings plot examining the effect of batch on eicosanoid measurement	155
Figure 4.4 - PCA scores and loading plots comparing serum eicosanoid measurement from patients with pneumonia and brain injuries at the start of ventilation	158
Figure 4.5 - OPLS-DA scores and loadings plots comparing serum eicosanoid measurements from patients with pneumonia and brain injuries at the start of ventilation	159

Figure 4.6 - PCA, OPLS-DA scores plots and OPLS-DA loadings plot examining the effect of batch on cytokine measurement	162
Figure 4.7 - OPLS-DA scores and loadings plots comparing serum cytokine measurements from patients with pneumonia and brain injuries at the start of ventilation	164
Figure 4.8 - OPLS-DA scores and loadings plots comparing serum cytokine measurements from patients with brain injuries and VAP	166
Figure 4.9 - OPLS-DA scores and loadings plots comparing serum cytokine and eicosanoid measurements from patients with pneumonia and brain injuries at the start of ventilation	168
Figure 4.10 - OPLS-DA scores and loadings plots comparing serum cytokine and eicosanoid measurements from patients with pneumonia and brain injuries who never developed pneumonia at the start of ventilation	170
Figure 4.11 - OPLS-DA scores and loadings plots comparing serum cytokine and eicosanoid measurements from patients with brain injuries at the start of ventilation and those with VAP	171
Figure 4.12 - OPLS-DA scores and loadings plots comparing serum cytokine and eicosanoid measurements from patients with brain injuries who never developed pneumonia at the start of ventilation to those with VAP	172
Figure 4.13 - OPLS-DA scores and loadings plots comparing serum cytokine and eicosanoid measurements from time points 1 and 4 from patients with brain injuries who did not develop pneumonia.	174
Figure 4.14 - OPLS-DA scores and loadings plots and hierarchical dendrograms comparing serum cytokine and eicosanoid measurements from the fourth time point from brain injured patients who did not develop pneumonia to the those with VAP	175
Figure 4.15 - Univariate comparison of the most important inflammatory mediators separating the final time point from brain injured patients without VAP to the time point that pneumonia developed in those with VAP	178
Figure 4.16 - Correlation heat maps demonstrating the correlation between cytokines and eicosanoids for all patients, those with pneumonia and those with brain injuries	180
Figure 5.1 - Comparison of spectra acquired from various NMR experiments on exhaled breath condensate from a healthy control subject	201
Figure 5.2 - Comparison of spectra acquired from various NMR experiments on exhaled breath condensate from a ventilated patient	203
Figure 5.3 - Comparison of the effect on NMR spectra of freeze drying exhaled breath condensate samples from a healthy volunteer	205
Figure 5.4 - Comparison of the effect on NMR spectra of freeze drying and reconstitution to different volumes exhaled breath condensate samples from a ventilated patient	207

Figure 5.5 - Comparison of NMR spectra from D ₂ O, TSP and a freeze dried exhaled breath condensate sample	208
Figure 5.6 - Comparison of NMR spectra obtained from blanks prepared in the RTube™ exhaled breath condensate collection device	209
Figure 5.7 - PCA scores plot comparing exhaled breath condensate by MS batch	214
Figure 5.8 - PCA scores plot comparing blanks run with MS by batch with example MS spectra	215
Figure 5.9 - PCA scores plot comparing exhaled breath condensate samples by batch after the subtraction of signals found within the blank samples	217
Figure 5.10 - PCA scores plot comparing exhaled breath condensate from patients admitted with pneumonia and brain injuries	219
Figure 5.11 - OPLS-DA scores plot, before and after cross validation, and equivalent s-plot comparing exhaled breath condensate samples collected from patients admitted with pneumonia and brain injuries	220
Figure 5.12 - OPLS-DA scores plot, before and after cross validation, and equivalent s-plot comparing exhaled breath condensate samples collected from patients admitted with brain injuries at time points 1 and 4	223
Figure 5.13 - OPLS-DA scores plot, before and after cross validation, and equivalent s-plot comparing exhaled breath condensate samples collected from patients admitted with brain injuries at time point 4 who did not develop pneumonia and those with VAP	226
Figure 6.1 - PCA scores and loadings plots comparing clinical data from patients admitted with pneumonia and brain injuries with and without the component of the CPIS score	243
Figure 6.2 - OPLS-DA scores plots, before and after cross validation, comparing clinical data from patients admitted with brain injuries to those with pneumonia	246
Figure 6.3 - OPLS-DA scores plots, before and after cross validation, comparing clinical data from patients admitted with brain injuries to those with VAP	249
Figure 6.4 - OPLS-DA scores plots, before and after cross validation, comparing clinical, metabolic and inflammatory data from patients admitted with brain injuries to those with pneumonia	255
Figure 6.5 - OPLS-DA scores plots, before and after cross validation, comparing clinical, metabolic and inflammatory data from patients admitted with brain injuries to those with pneumonia, using only variables with a VIP>1.0	256
Figure 6.6 - OPLS-DA scores plots, before and after cross validation, comparing clinical, integral metabolic and inflammatory data from patients admitted with brain injuries to those with VAP, using only variables with a VIP>2.0	262
Figure 6.7 - OPLS-DA scores plots, before and after cross validation, comparing clinical, full	263

spectral metabolic and inflammatory data from patients admitted with brain injuries to those with VAP, using only variables with a VIP>2.0

Figure 6.8 - OPLS-DA scores plots, before and after cross validation, comparing clinical, integral metabolic and inflammatory data from patients admitted with brain injuries after an equivalent length of stay on ICU to those with VAP, using only variables with a VIP>2.0 266

LIST OF TABLES

Table 1.1 - Common causes of community acquired pneumonia	26
Table 1.2 - Reported frequencies of VAP in different ICU populations	30
Table 1.3 - Risk Factors for VAP	31
Table 1.4 - Clinical Pulmonary Infection Score	36
Table 2.1 - Clinical data collected for all enrolled patients	68
Table 2.2 - Clinical Pulmonary Infection Score used to define ventilator associated pneumonia	69
Table 2.3 - Causes of brain injury in recruited patients	80
Table 2.4 - Causes of pneumonia in recruited patients	80
Table 2.5 - Clinical features of all included patients	82
Table 2.6 - Organisms causing pneumonia	83
Table 3.1 - Clinical features of patients included for metabonomic analysis	93
Table 4.1- Concentrations of cytokine standards	144
Table 4.2 - Clinical features of patients included for inflammatory profiling	152
Table 4.3 - Quantifiable and Unquantifiable eicosanoids	153
Table 4.4 - Univariate comparison of the most important inflammatory mediators separating the final time point from brain injured patients without VAP to the time point that pneumonia developed in those with VAP	177
Table 5.1 - Metabolites identified in exhaled breath condensate previously in the literature	196
Table 5.2 - Clinical features of patients included for exhaled breath condensate analysis	213
Table 5.3 - Most discriminant m/z ratios that differentiate brain injury from pneumonia	221
Table 5.4 - Most discriminant m/z ratios that differentiated brain injuries from VAP	222
Table 5.5 - Most discriminant m/z ratios that differentiated time point 1 from time point 4 samples from patients with brain injuries	224
Table 5.6 - Most discriminant m/z ratios that differentiated time point 1 from time point 4 samples from patients with pneumonia	225
Table 5.7 - Most discriminant m/z ratios that differentiated VAP from brain injured patients	227

with brain injuries who had spent a similar amount of time on intensive care.

Table 5.8 - Most discriminant m/z ratios that differentiated brain injured patients at time point 1 that did and did not develop VAP	228
Table 6.1 - Conversion table of litres of oxygen to FiO_2	239
Table 6.2 - Clinical variables used for multivariate analysis	240
Table 6.3 - Discriminant clinical features for the OPLS-DA model comparing patients with brain injuries to those with pneumonia using clinical data	247
Table 6.4 - Discriminant clinical features for the OPLS-DA model comparing patients with brain injuries to those with VAP using clinical data	248
Table 6.5 - Discriminant clinical features for the OPLS-DA model comparing patients with brain injuries who has sent an equivalent time on ICU to those with VAP using clinical data	250
Table 6.6 - Integrals of metabolites with the most influence on OPLS-DA model comparing brain injury with pneumonia	252
Table 6.7 - Discriminant clinical features for the OPLS-DA model comparing patients with brain injuries with pneumonia using inflammatory and clinical data	253
Table 6.8 - Discriminant clinical features for the OPLS-DA model comparing patients with brain injuries with those developing VAP using metabolic and clinical data	258
Table 6.9 - Discriminant clinical features for the OPLS-DA model comparing patients with brain injuries with those developing VAP using inflammatory and clinical data	261
Table 6.10 - Features comprising a discriminant OPLS-DA model to discriminate patients with brain injury from those with VAP using metabolic, inflammatory and clinical data	264
Table 6.11 - Features comprising a discriminant OPLS-DA model to discriminate patients with brain injury after an equivalent length of stay on ICU from those with VAP using metabolic, inflammatory and clinical data	265

LIST OF ABBREVIATIONS

10(S),17(S)-DiHDoHE - 17-Hydroxy Docosahexaenoic Acid
11(R)-HETE - 11R-Hydroxyeicosatetraenoic Acid
11,12-DHET - 11,12-Dihydroxyeicosatrienoic Acid
11,12-EET - 11,12-Epoxyeicosatrienoic Acid
11-dehydro TXB2 - 11-Dehydrothromboxane B2
12(R)-HETE - 12R-Hydroxyeicosatetraenoic Acid
12(S)-HEPE - 12S-Hydroxyeicosapentaenoic Acid
12-oxo-ETE - 12-Oxo-Eicosatetraenoic Acid
12-oxo-LTB4 - 12-Oxo-Leukotriene B4
13(S)-HODE - (13S)-Hydroxyoctadecadienoic Acid
14,15-DHET - 14,15-Dihydroxyeicosatrienoic Acid
14,15-EET - 14,15-Epoxyeicosatrienoic Acid
14-HDoHE - 14-Hydroxy docosahexaenoic Acid
15(S)-HEPE - 15S-Hydroxyeicosapentaenoic Acid
15(S)-HETE - 15S-Hydroxyeicosatetraenoic Acid
15dPGJ2 - Cyclopentenone Prostaglandin
16(R)-HETE - 16R-Hydroxyeicosatetraenoic Acid
17(S)-HDoHE - 17(S)-Hydroxy Docosahexaenoic Acid
¹H NMR - Proton Nuclear Magnetic Resonance Spectroscopy
5(S)-HETE - 5-Hydroxyeicosatetraenoic Acid
5,6-DHET - 5,6-Dihydroxyeicosatrienoic Acid
5,6-EET - 5,6-Epoxyeicosatrienoic Acid
5-oxo-ETE - 5-Oxo-eicosatetraenoic Acid
6-keto-PGF1 α - 6-Keto Prostaglandin F1 α
8(S)-HETE - 8S-Hydroxyeicosapentaenoic acid
8,9-DHET - 8,9-Dihydroxyeicosatrienoic acid
8,9-EET - 8,9-Epoxyeicosatrienoic acid
8-iso-PGF2 α - 8-Iso-Prostaglandin F2 α
9(S)-HODE - (9S)-Hydroxyoctadecadienoic Acid
AA - Arachidonic Acid
ADMA - Asymmetric Dimethyl Arginine

ALI - Acute Lung Injury
ANOVA - Analysis of Variance
APACHE II - Acute Physiology and Chronic Health Evaluation II
ARDS - Acute Respiratory Distress Syndrome
AUROC - Area Under the Receiver Operating Characteristic Curve
BAL - Bronchoalveolar Lavage
BALF - Bronchoalveolar Lavage Fluid
BI - Brain Injury
BSA - N,O-Bis(trimethylsilyl)Acetamide
CAP - Community Acquired Pneumonia
CFU - Colony Forming Units
COPD - Chronic Obstructive Pulmonary Disease
COSY - Correlation Spectroscopy
CPIS - Clinical Pulmonary Infection Score
CPMG - Carr-Purcell-Meiboom-Gill
CRP - C-Reactive Protein
CVA - Cerebrovascular Accident
D₂O - Deuterium Oxide
DGLA - Dihomo- γ -Linolenic Acid
DHA - Docosahexaenoic Acid
EBC - Exhaled Breath Condensate
EPA - Eicosapentaenoic Acid
FID - Free Induction Decay
FS - Forward Scatter
GC-MS - Gas Chromatography - Mass Spectrometry
G-CSF - Granulocyte Colony-Stimulating Factor
HDL - High Density Lipoprotein
HME - Heat and Moisture Exchanger
ICAM-1 - Intercellular Adhesion Molecule 1
ICU - Intensive Care Unit
IFN α - Interferon Alpha
IFN γ - Interferon Gamma
IL-10 - Interleukin 10

IL12p70 - Interleukin 12 p70 Subunit
IL-13 - Interleukin 13
IL-17A - Interleukin 17A
IL-1 β - Interleukin 1 β
IL-1 α - Interleukin 1 α
IL-4 - Interleukin 4
IL-6 - Interleukin 6
IL-8 - Interleukin 8
IP-10 - Interferon Gamma-Induced Protein 10
IS - Internal Standards
LA - Linoleic Acid
LAP - Latency-Associated Protein
LC-MS - Liquid Chromatography – Mass Spectrometry
LC-MS/MS - Liquid Chromatography Tandem Mass Spectrometry
LDL - Low Density Lipoprotein
LTB4 - Leukotriene B4
LTC4 - Leukotriene C4
LTD4 - Leukotriene D4
LTE4 - Leukotriene E4
MAP - Mean Arterial Pressure
MCP-1 - Monocyte Chemotactic Protein 1
MFI - Mean Fluorescence Intensity
MIP1 α - Macrophage Inflammatory Protein 1 α
MIP1 β - Macrophage Inflammatory Protein 1 β
MS - Mass Spectrometry
MV - Mechanical Ventilation
NMR - Nuclear Magnetic Resonance Spectroscopy
NOESY - Nuclear Overhauser Effect Spectroscopy
OPLS-DA - Orthogonal Partial Least Squared Discriminant Analysis
PBS - Phosphate Buffered Saline
PCA - Principle Component Analysis
PE - Phycoerythrin
PGD2 - Prostaglandin D2

PGE2 - Prostaglandin E2

PGF2 α - Prostaglandin F2 α

PLS - Partial Least Squares

PLS-DA - Partial Least Squared Discriminant Analysis

ppm - Parts Per Million

PSB - Protected Specimen Brushings

ROC - Receiver Operating Characteristic

SAH - Subarachnoid Haemorrhage

SOFA - Sequential Organ Failure Assessment Score

SPE - Solid Phase Extraction

SS - Side Scatter

STOCSY - Statistical Total Correlation Spectroscopy

sTREM-1 - Soluble Triggering Receptor Expressed on Myeloid Cells

TA - Tracheal Aspirate

Tetranor-PGDM - Tetranor Prostaglandin D Metabolite

Tetranor-PGEM - Tetranor Prostaglandin E Metabolite

Tetranor-PGFM - Tetranor Prostaglandin F Metabolite

TNF α - Tumour Necrosis Factor Alpha

TOCSY - Total Correlation Spectroscopy

TSP - 3-(Trimethyl-Silyl) Propionic Acid

TXB2 - Thromboxane B2

UPLC-MS/MS - Ultra Performance Liquid Chromatography Tandem Mass Spectrometry

VAP - Ventilator Associated Pneumonia

VIP - Variable Importance for the Projection

VLDL - Very Low Density Lipoprotein

Section I – Literature Review

1. LITERATURE REVIEW

1.1 Pneumonia

1.1.1 Incidence

Pneumonia is a common cause of admission to both hospital and the Intensive Care Unit (ICU). Pneumonia is defined as community acquired (CAP), in those patients without prior hospital contact, hospital acquired (HAP), in those hospitalised for at least 48-72h or aspiration pneumonia, following the aspiration of oro-gastric contents, for example in the context of impaired consciousness. Pneumonia is the commonest cause of death across all age groups from an infective cause and is the sixth leading cause of death in the USA and in the late 1990's had an incidence of 1.3-3.9% depending on age group and geographical location (1). In 2012 pneumonia was the sixth leading cause of death in men, causing 4.6% of deaths, and the fourth leading cause in women, causing 5.8% of deaths, in the United Kingdom and in both groups was the leading cause of death associated with infection (2). Within the emergency department pneumonia is the leading cause of admission in patients presenting with sepsis (3) and every year in the UK 0.5%-1% of adults have CAP of which 22-42% are admitted to hospital (4).

1.1.2 Pathogenesis

The common organisms causing CAP are dependent on the source of the patients in question, table 1.1. *Pneumococcus* is the most common organism causing CAP and its incidence increases with age (5). Certain organisms are more common in defined populations, for example *S. Aureus* may be more common in nursing home residents (5).

The role of aspiration of oro-gastric contents in the development of pneumonia is controversial (6, 7) and may be a common cause of pneumonia in those over 80 years of age. Large aspirates of gastric contents lead to a chemical pneumonitis which may lead to the development of acute respiratory

distress syndrome (ARDS), however, many episodes of aspiration go unnoticed. The most classical syndrome associated with aspiration is an anaerobic pleuropneumonia, which is associated with a cough producing purulent secretions and a cavitating pneumonia, however, this is rarely seen and more commonly aspiration pneumonia now refers to an acute lung infection developing after the aspiration of a large volume of oropharyngeal or upper gastrointestinal contents depositing a large bacterial load into the lungs (7). However, the diagnosis of aspiration in the community may be unclear where the events preceding the features of a respiratory tract infection are uncertain. Although aspiration pneumonia is classically associated with anaerobic organisms, over time the predominance of anaerobes seems to have diminished and aerobes and gram negative organisms seem to be more common. In those patients who aspirate whilst in hospital the organisms causing pneumonia appear similar to those causing other cases of hospital acquired infection with an abundance of *S. Aureus* (7).

Table 1.1 Most Common causes of community acquired pneumonia from the 2007 American Thoracic Society Consensus Guidelines (5). Organisms listed in decreasing order of frequency.

Patient Type	Aetiology
Outpatient	<i>Streptococcus pneumoniae</i> <i>Mycoplasma pneumoniae</i> <i>Haemophilus influenzae</i> <i>Chlamydophila pneumoniae</i> <i>Respiratory viruses</i>
Inpatient (non-ICU)	<i>Streptococcus pneumoniae</i> <i>Mycoplasma pneumoniae</i> <i>Chlamydophila pneumoniae</i> <i>Haemophilus influenzae</i> <i>Legionella species</i> <i>Aspiration</i> <i>Respiratory viruses</i>
Inpatient (ICU)	<i>Streptococcus pneumoniae</i> <i>Staphylococcus Aureus</i> <i>Legionella species</i> <i>Gram-negative bacilli</i> <i>Haemophilus influenzae</i>

1.1.3 Outcome

Admission to hospital in the UK with CAP is associated with a mean length of stay of 30 days with a median stay of 7 days (8). CAP is associated with a mortality of around 5-14% (4) which rises to 16.1-19.3% in those admitted depending on the route of admission to hospital (9). 1.2-10% of patients admitted to hospital will be managed in ICU and in this group mortality may reach 30% (4). Similarly an episode of hospital acquired pneumonia increases the length of stay by about 8 days and has a mortality of 30-70% (4).

Not only is pneumonia associated with a significant mortality, a recent study found that an admission with pneumonia was estimated to cost a median of €3,899 in the Netherlands with nursing care in ICU accounting for the second largest portion of spending (10). Cost to the UK from pneumonia in 1995/6 was estimated at £480 million with the majority of the cost being accounted for by inpatient care with each inpatient episode costing £1700-£5100 (8).

1.1.4 Diagnosis

1.1.4.1 Clinical Features

Although often perceived as a straight forward diagnosis there is no gold standard by which to make the diagnosis. The clinical features of CAP have been stated to be non-specific (11) and have limited value in making a diagnosis. There is limited evidence in the literature to quantify their usefulness. The use of clinical diagnostic criteria in a paediatric population to predict radiologically confirmed pneumonia had a sensitivity of 0.45, specificity of 0.66 and positive and negative predictive values of 0.25 and 0.82 respectively (12) with similar patterns being reproduced in other groups of children (13). In adults abnormal vital signs have a high degree of sensitivity (14) but lack specificity for pneumonia. With advancing age the presence of symptoms with pneumonia becomes less common (15) and some features, such as respiratory rate, may be sensitive but not specific (16) limiting their

usefulness in older patients. Decision aids have been evaluated in adult patients that use clinical features to determine the likelihood of radiological findings, on chest radiographs, consistent with pneumonia (17). In one study clinicians' judgement was found to have sensitivity of 0.74, a specificity of 0.84, a positive predictive value of 0.27 and a negative predictive value of 0.97 for radiological diagnosis in a primary care setting (18) and in a large study performed in general practice across Europe clinical diagnosis of pneumonia had a sensitivity of 0.29, a specificity of 0.99, positive predictive value of 0.57 and a negative predictive value of 0.96 (19). However, clinical features did not perform similarly in all patient groups such as the elderly and nursing home residents (20) and the initial Emergency Department diagnoses of pneumonia often turned out to be incorrect after further investigations (21).

1.1.4.2 Biomarkers

Biomarkers have been used in an attempt to improve the recognition of pneumonia, the most studied being C-reactive protein (CRP) and procalcitonin (PCT). In studies of CRP with and without clinical features of pneumonia sensitivity varied between 0.36-1.0 and specificity 0.52-0.96 for detecting radiographic pneumonia depending on the cut off of CRP used (22-24). If an infiltrate was present on the radiograph then these values changed to sensitivity 0.36-0.89 and specificity 0.17-0.91 (24). In another primary care study a CRP >20mg/l had a sensitivity of 0.73, specificity of 0.65, positive predictive value of 0.24 and negative predictive value of 0.94 to diagnose pneumonia in patients already suspected of having lower respiratory tract infections (25). Studies of PCT to diagnose pneumonia in primary care have shown sensitivities of 0.17-0.90, specificities of 0.59-1.0, positive predictive values of 0.24-1.0 and negative predictive values of 0.89-0.94 in the absence of radiology depending on the cut off levels used. If an infiltrate was already present on the CXR then these values changed to sensitivity 0.43-0.90 and specificity 0.39-0.87. In comparison blood cultures only had a sensitivity of 0.11 (24, 25).

1.1.4.3 Radiology

Many of these studies used radiological findings as confirmation of pneumonia, however, depending on the frequency of bacterial infection infiltrates on chest radiograph have been found to have a positive predictive value of only 0.46-0.85 (26) and lack sensitivity, with around 21% of radiographs being negative initially (27).

1.2 Ventilator Associated Pneumonia

Ventilator associated pneumonia (VAP) is defined as pneumonia occurring at least 48-72h after endotracheal intubation (28). It is associated with inflammation of the lung parenchyma secondary to infectious agents not present at the time of initiation of mechanical ventilation (MV)(29). VAP is a common nosocomial infection and causes a significant mortality and morbidity.

1.2.1 Pathology

The act of invasive ventilation, either as part of anaesthesia for surgery or for respiratory support, circumvents many of a patient's natural mechanisms of protecting the lungs from colonisation and infection. The endotracheal tube bypasses the vocal cords and the normal methods of gas humidification (30). Sedation leaves patients unable to cough and clear secretions and severe illness causes modulation in the immune system which can leave patients susceptible to infection. Pneumonia occurs when these barriers to infection are overcome and the normally sterile lungs become colonised with and inflamed secondary to pathogenic organisms.

VAP is thought to be predominantly caused by micro-aspiration of contaminated oropharyngeal fluid into the lungs. Contamination of mucosal surfaces and secretions with pathogenic bacteria is common in critical illness and increases with severity of disease (31). Secretions may pool above the

endotracheal cuff and can then be transmitted into the lung. The endotracheal tube can also serve as a reservoir of micro-organisms with a biofilm forming within hours of intubation (32). Much less commonly pneumonia may be caused by haematogenous spread of micro-organisms from a site distant to the lungs, from contiguous spread of disease or by inhalation of an infective aerosol.

1.2.2 Epidemiology

MV increases the risk of pneumonia by 3-7 times (33, 34). However, the reported incidence of VAP is variable depending on the ICU, patient population, diagnostic method and rates of antibiotic use. VAP rates may vary between 6% and up to nearly 40% in different groups, table 1.2.

Table 1.2. Reported frequencies of VAP in different ICU populations.

Study	Type of study	ICU	Frequency (%)	Rate/1000 Ventilator Days
<i>Langer, 1987 (35)</i>	Prospective	Mixed	38.2	-
<i>Fagon, 1989 (36)</i>	Prospective	Mixed	9	-
<i>Torres, 1990 (37)</i>	Prospective	Mixed	24	-
<i>Baker, 1996 (38)</i>	Prospective	Trauma	5.8	
<i>Long, 1996 (39)</i>	Retrospective	Medical	-	11.5
<i>Long, 1996 (39)</i>	Retrospective	Neurological	-	19.4
<i>Sirvent, 1997 (40)</i>	Prospective	Neurological	37	
<i>Cook, 1998 (41)</i>	Prospective	Mixed	17.5	14.8
<i>Leal-Noval, 2000 (42)</i>	Prospective	Cardiothoracic	6.5	-
<i>Rello, 2002 (43)</i>	Retrospective	Mixed	9.3	-
<i>Bouza, 2003 (44)</i>	Prospective	Cardiothoracic	7.9	34.5
<i>Rosenthal, 2003 (45)</i>	Prospective	Mixed	-	51
<i>Lizan-Garcia, 2006 (46)</i>	Prospective	Surgical	17.7	21
<i>Joseph, 2009 (47)</i>	Prospective	Mixed	18	22.9

Incidence of VAP may also be influenced by concomitant disease, with VAP rates increasing in patients suffering from ARDS to 37 -60% (48-50).

1.2.3 Risk Factors

Although duration of mechanical ventilation is one of the most significant risk factors for development of VAP (37, 44, 51) evidence suggests that after ten days of ventilation the incidence of

VAP decreases (33). Numerous other factors, table 1.3 have also been implicated as risk factors for VAP as outlined below.

Table 1.3. Risk Factors for VAP (29, 37, 41, 42, 44, 52-56)

Patient Factors	Intervention Factors
Impaired airway reflexes	Sedative agents
High APACHE II score	Cardiopulmonary resuscitation
Large volume gastric aspiration	Enteral nutrition
Chronic Obstructive Pulmonary Disease	Nasogastric tube
Postoperative cardiac failure	Transfusion of blood products
Central nervous system dysfunction	Aerosolized therapy
Trauma	Surgery
Burns	Re-intubation
	Stress ulcer prophylaxis
	Supine positioning
	Patient transfer
	Neuromuscular blocking agents

1.2.3.1 Surgery

Patients who have undergone surgery appear to be at higher risk for pneumonia than equivalent medical patients (51). Within surgery some patients may be more at risk than others. Cardiothoracic (57) and both burns and trauma (41, 53) patients have been independently found to have higher rates of VAP.

1.2.3.2 Stress Ulcer Prophylaxis and Positioning

Alkalisating gastric fluid has been shown to lead to gastric contamination with potentially pathogenic micro-organisms (58). A meta-analysis looking at H₂ antagonists found an increase in VAP (59) and a randomised controlled trial comparing feeding in the supine versus semi-recumbent position confirmed a significantly increased rate of VAP in those fed in the supine position (60).

1.2.3.3 Intubation

The presence of the endotracheal tube may act as a reservoir for pathogenic organisms and circumvent natural defence mechanisms. The need for re-intubation has been found to be an independent risk factor for VAP in a number of studies (37, 42, 61). Similarly transfer of patients out of the ICU, for example to the radiology department or to the operating theatre, has been associated with increased VAP rates (54), however, this may be a surrogate for patients who are sicker and require more intervention.

The role of tracheostomy in preventing VAP is unclear. Although both a randomised trial (62) and subsequent meta-analysis (63) found trends towards reduction in the rate of VAP neither proved statistically significant.

1.2.3.4 Antibiotics

The role of antibiotics in preventing VAP is unclear. A number of studies have found that prior administration of antibiotics to be an independent risk factor (42, 55) but in others antimicrobial agents have been found to have a protective effect (40, 52). In one study the previous use of antimicrobials proved to be a risk factor for mortality (64).

1.2.4 Aetiological Agents

The European Prevalence of Infection in Intensive Care Study found that on a single day nearly a third of ICU-acquired pneumonia was caused by *Staphylococcus Aureus*, closely followed by Pseudomonas species (65). Other organisms such as *E.Coli*, *Acinetobacter*, *Enterococci* and yeasts were much less common. *Haemophilus Influenza* has been found to cause VAP at around 10 days post onset of MV, commonly in those who have not received prior antimicrobial agents but is associated with a lower mortality than other causes (66).

Infection with resistant organisms is a significant problem. Vanhems *et al* found that risk factors for pneumonia caused by resistant organisms were a medical diagnosis, transfer from another ward, the presence of a colonised central venous line and longer length of hospital stay (67). Patients with VAP caused by Methicillin Resistant *Staphylococcus Aureus* (MRSA) are likely to have been ventilated for longer, have received prior antibiotics and corticosteroids and are more likely to suffer from chronic obstructive pulmonary disease (COPD) than those with the sensitive strain (68). MRSA is also more likely to be associated with bacteraemia, septic shock and has a higher mortality than that caused by sensitive staphylococci (68). Patients with head trauma, neurosurgery, ARDS and large volume pulmonary aspirate are predisposed to infection with *Acinetobacter* species (69).

1.2.5 Mortality, Morbidity and Health Care Costs

Estimates of mortality associated with VAP have ranged from 34-70% (42, 44, 45, 56). However, due to differences in diagnostic criteria, heterogeneity of patient populations and associated pathology it has been difficult to determine to what extent VAP is the cause of death. Pneumonia is associated with significant increases in hospital and ICU stay. Hospital stay can be increased by 10-20 days for patients with VAP (51).

Nosocomial pneumonia is recognised as one of the most costly hospital acquired infections (70, 71). Development of VAP significantly increases the cost of medical care by 1.5 (38) to 3 times (56) compared to patients who do not develop this complication.

1.2.6 Diagnosis

1.2.6.1 Clinical Features

Fagon and co-workers found that using clinical features, such as temperature, oxygenation, radiology, laboratory results and change in endotracheal secretions, clinicians only correctly diagnosed VAP 62% of the time (72). Leukocytosis, fever and quality of respiratory secretions have

all performed poorly when compared to histological specimens with sensitivities ranging from 46-77% and specificities of 42-58% (73).

A study examining post mortem specimens of lung tissue of patients with ARDS found a 29% misdiagnosis rate for pneumonia based on clinical parameters. Although fever, leucocytosis and growth of pathogens from sputum were more common in patients with pneumonia they were still present in 70-80% of those without. Response to antimicrobial therapy was misleading with more patients without pneumonia appearing to respond (74).

1.2.6.2 Radiology

Presence of infiltrates on the chest radiograph have a sensitivity of 92% but a specificity of only 33% (73) when compared to biopsy confirmed VAP. However, the presence of radiological infiltrates plus two of: leucocytosis, fever or purulent secretions had a sensitivity of 69% and a specificity of 75% (73). Comparison of specific radiographic findings with post mortem confirmation of VAP found that the presence of an air bronchogram had the best overall performance with a sensitivity of 83% and specificity of 58% (75) but alveolar infiltrates were the most sensitive finding (88%) and fissure abutment was the most specific (96%). However, no radiological finding had a positive predictive value of more than 68% for VAP.

1.2.6.3 Microbiology

A microbiological diagnosis of pneumonia is important in confirming clinical suspicion and in guiding antibiotic therapy. Specimens can be collected using a variety of techniques from tracheal aspirate (TA), bronchoalveolar lavage (BAL), protected specimen brushings (PSB) and mini-bronchoscopy. These methods have been found to have differing efficacies in the diagnosis of VAP.

A comparison of various microbiological sampling techniques against pathological specimens gave TA, protected bronchoalveolar lavage, BAL and PSB sensitivities of 69, 39, 77 and 62% respectively

and specificities of 92, 100, 58, 75% (73). Using post mortem histology as a gold standard Marquette *et al* found that TA, PSB and BAL had sensitivities of 56, 58 and 47% and associated specificities of 86, 89 and 100%. Use of staining to detect intracellular organisms from BAL samples was also associated with 100% specificity but a poor sensitivity of only 37% (76).

TA is often felt to have poor specificity for the diagnosis of VAP due to a tendency to detect airway colonisation. However, in a study comparing PSB, BAL and TA, quantitative culture of TA with a cut off between 10^5 and 10^6 Colony Forming Units (CFU)/ml had a sensitivity and specificity of around 70% (77, 78). However, BAL and PSB had greater specificities of 87 and 93%. TA was also found to have a better negative predictive value than PSB (72 vs 34%, $p < 0.05$) (78).

A randomised pilot study comparing BAL combined with PSB to TA to guide antibiotic decision making found no statistical difference in mortality or morbidity between the two methods. However, there was a trend towards higher mortality in the group undergoing invasive sampling (79). In another, non-randomised, trial invasive pulmonary investigation with BAL appeared to reduce mortality compared to a control group and the results of this investigation were found to significantly influence physician decision making (80). A meta-analysis of four randomised controlled trials found no overall difference in mortality between invasive and non-invasive diagnostic approaches but that invasive investigation consistently led to more frequent changes in antibiotic prescribing (81).

All sampling techniques pose technical challenges. If samples are not collected and handled correctly the diagnostic yield may be reduced. It is therefore important that for microbiological investigations to remain valid, stringent sampling methods must be adhered to (82).

1.2.6.4 Scoring Systems

Pugin *et al* developed a Clinical Pulmonary Infection Score (CPIS) for the diagnosis of VAP based on six clinical parameters, table 1.4, which gave a score from 0-12 (83). They found that a score of

greater than six correlated with a bacterial index of greater than five on both guided and blind BAL. A randomized study Singh *et al* used the CPIS score to guide antibiotic prescribing. They found a significant reduction in antibiotic prescribing without increase in mortality or length of ICU stay (84).

Table 1.4. Clinical Pulmonary Infection Score (83)

Clinical Feature	Score
Temperature (°C)	
36.5-38.4	0
38.5-38.9	1
≥39 ≤36	2
White Cell Count (mm⁻³)	
4,000-11,000	0
>11,000, <4,000	1
Band forms >500	+1
Radiology	
No infiltrate	0
Diffuse (Patchy) Infiltrate	1
Localised Infiltrate	2
Oxygenation (mmHg)	
PaO ₂ /FiO ₂ > 240 or ARDS	0
PaO ₂ /FiO ₂ ≤240	2
Secretions	
<14 of total secretions in 24h	0
≥14 of total secretions	1
Plus purulent secretions	+1
Microbiology	
Pathogenic bacteria cultured ≤ 1+ or no growth	0
Pathogenic bacteria cultured ≥ 1+	1
Gram stain ≥ +1 with same pathogenic organism	+1

The use of the CPIS score as a diagnostic tool has been debated. Fartoukh *et al* found that a modified CPIS score at baseline was only slightly better at predicting VAP than a strong clinical suspicion but that it could be improved with the addition of the gram stain result from either protected telescopic catheter or BAL sampling (85). The CPIS score was originally developed in medical ICU patients and concern has been raised that it may not be applicable in other patient groups. In some instances, for example in burn and trauma patients, the area under the receiver operating curve for the CPIS score has been less than 0.5 (86).

1.2.6.5 Biomarkers

Various biomarkers have been suggested to aid in the diagnosis of VAP including total bile acids, soluble triggering receptor expressed on myeloid cells (sTREM-1), C-reactive protein (CRP), procalcitonin (PCT), elastin fibres and endotoxin in BAL fluid. Of these, sTREM-1, CRP and PCT are probably best studied. sTREM-1 is a glycoprotein expressed on phagocytic cells which is up-regulated in bacterial infection. An initial study found sTREM-1 measured in BAL samples had a sensitivity of 96% and a specificity of 90% for pneumonia. However, in subsequent studies it has performed less well than a CPIS \leq 6 (87) and has been non-discriminative for VAP (88), possibly being influenced by prior antibiotic use. It has proved possible to measure sTREM-1 in exhaled breath condensate, although at lower concentrations than in BAL fluid, presenting a non-invasive means of measurement (89). However, in this study BAL levels still performed poorly as a diagnostic tool.

CRP, a protein manufactured in the liver that is elevated with inflammation, and PCT, a pro-hormone secreted into the serum from the C-cells of the thyroid in health and from other neuroendocrine tissues during inflammation, have both been measured in serum and BAL fluid as an aid to VAP diagnosis (90). In one study serum PCT performed better than CRP in separating VAP from non-VAP with a sensitivity of 100% (91). However, both CRP (92) and PCT are elevated in infection from any cause in the ICU limiting their specificity.

A randomised controlled trial using PCT to guide antibiotic therapy in lower respiratory tract infections found a reduction in antibiotic prescribing without an increase in adverse events (93) indicating a role in treatment decisions. However, as a diagnostic tool for VAP PCT is limited as it becomes elevated in a range of bacterial infections as well as non-bacterial inflammatory conditions (94).

It is therefore apparent that pneumonia is a major healthcare problem and that better diagnostic methods are required to better manage patients.

1.3 Metabonomics

Metabonomics is “the quantitative measurement over time of the metabolic responses of an individual or population to drug treatment or other intervention” such as a disease process (95). Spectroscopic techniques including nuclear magnetic resonance (NMR) spectroscopy and mass spectrometry (MS) have been used to determine the global metabolic profiles of numerous types of biological samples. Blood and urine are the most commonly analysed but any biological specimens such as tissue, cerebrospinal fluid or exhaled breath condensate (EBC) can be used (96-99). These methods have been used to evaluate numerous clinically significant conditions including trauma patients (100, 101), detection of acute kidney injury and monitoring of dialysis (102-104), diagnosis of subarachnoid haemorrhage (105), and acute lung injury (106).

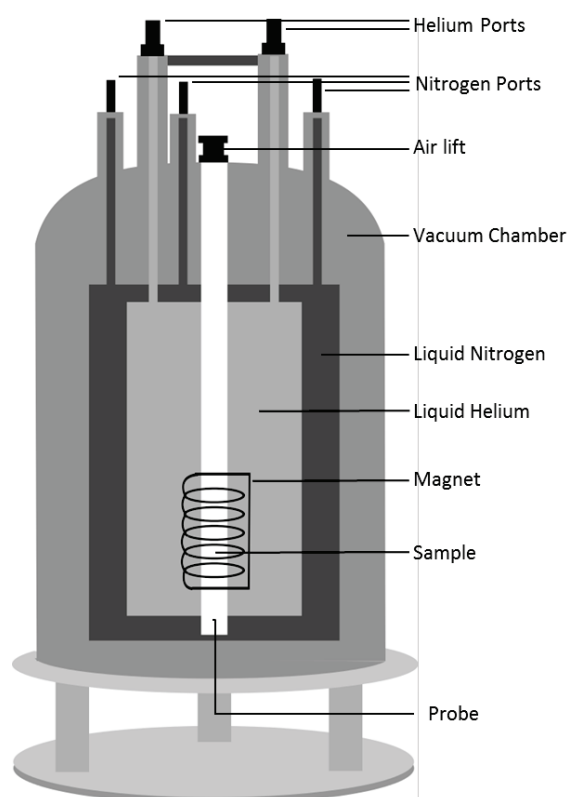
Metabonomic analysis is carried out using two broad analytical platforms, nuclear magnetic resonance spectroscopy and mass spectrometry. These two techniques each have their own strengths and weaknesses and together give complementary information. Data can be acquired that either provides global information collecting as much non-targeted metabolic information as possible, which is useful for initial biomarker discovery when there are no pre-conceived ideas regarding candidate markers, or can be targeted to obtain detailed information on a specific class of metabolites or metabolic processes.

1.3.1 ^1H Nuclear Magnetic Resonance Spectroscopy

NMR spectroscopy uses the magnetic properties of certain nuclei that possess spin, for example ^1H and ^{13}C . NMR spectrometers use superconductors to generate strong magnetic field, figure 1.1. A spinning charge placed in such a magnetic field produces two spin states – one up, aligned with the magnetic field, and one down, aligned against the magnetic field (107). The energy difference between the two spin states is proportional to the magnetic moment of the nuclei which is

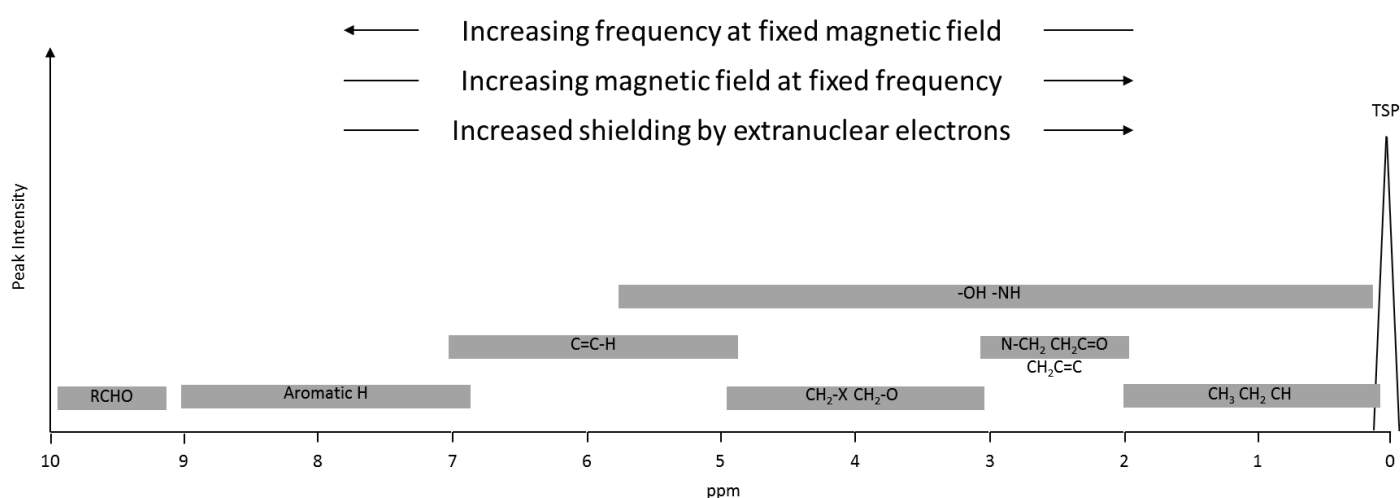
dependent on the local electron environment. When a sample containing these nuclei is excited with a radio frequency pulse, a free induction decay (FID) is produced. A Fourier transform is carried out on the FID to produce a frequency domain spectrum. Due to the low signal to noise ratio of a single FID several recordings are taken and an average taken. The resonance frequency of a given nucleus is dependent on the intermolecular magnetic field which is dependent on the local electron structure. When a magnetic field is applied, the electrons move in response to the field and generate local magnetic fields that oppose the larger, applied magnetic field, shielding the proton. The applied magnetic field then has to be altered to achieve resonance. Resonances are reported in relation to a reference signal, such as 3-(trimethyl-silyl) propionic acid (TSP), in order to account for magnetic fields of different strengths and these values are divided by the spectrometer frequency to give chemical shifts in parts per million (ppm).

Figure 1.1. Schematic diagram detailing the main components of an NMR spectrometer.



The chemical shifts are predictable due to the local electron shielding and give information about the structure of the molecule, figure 1.2. The magnitude or intensity of NMR resonance signals is displayed along the vertical axis of a spectrum, and is proportional to the concentration of the sample. However, of two substances with identical concentrations the stronger signal will be obtained from the one with the greater number of protons.

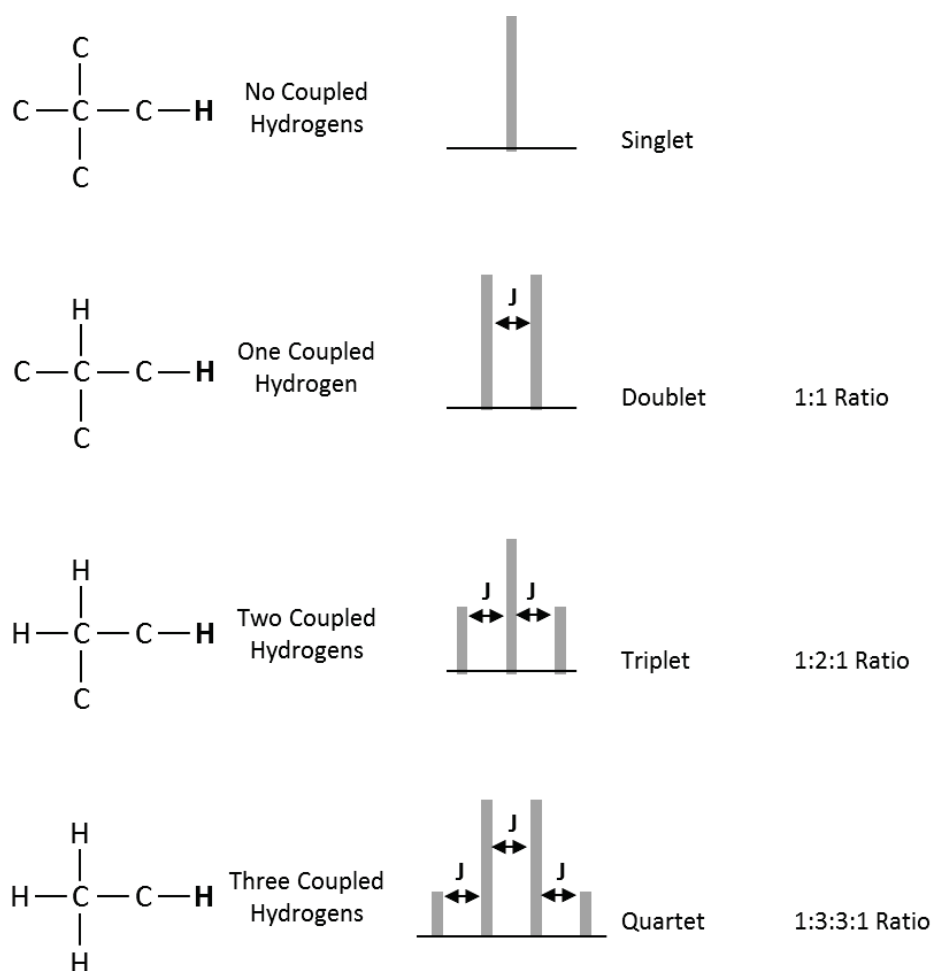
Figure 1.2. Proton chemical shift ranges in ppm. Common metabolite structural components with the typical spectral area they inhabit are shown (Adapted from (108))



As well as the chemical shift for a given proton, NMR spectroscopy also gives information regarding adjacent protons. Spin-spin interaction of adjacent protons results in the phenomenon known as J-coupling. If an atom under examination is influenced by a nearby nuclear spin, the observed nucleus responds to such influences, and its response is manifest in its resonance signal. Such influences are seen as splitting of the spectral peak, figure 1.3. Identical chemical environments have no spin-spin interaction and neither do those greater than three bonds away. Combining coupling and chemical shift gives information about the chemical environment of the nucleus and the number of surrounding nuclei, hence molecular structure can begin to be elucidated.

For the purposes of metabonomics ^1H NMR has several strengths. Little sample preparation is required, the technique is relatively non-destructive, quantitative, and non-invasive. Data obtained from NMR experiments is reproducible (109) and robust. Concentrations of metabolites are detectable down to micromole/l concentrations and analysis is relatively quick taking as little as 3-4 minutes per sample. Typically ^1H NMR spectra of urine contains thousands of narrow low molecular weight metabolites whereas serum and plasma contain a mixture of low and high molecular weight

Figure 1.3. Representation of J-coupling caused by adjacent protons. J represents the J-constant. The ratio of peaks is given for each of the multiplets, these follow the rules of Pascal's triangle (108).

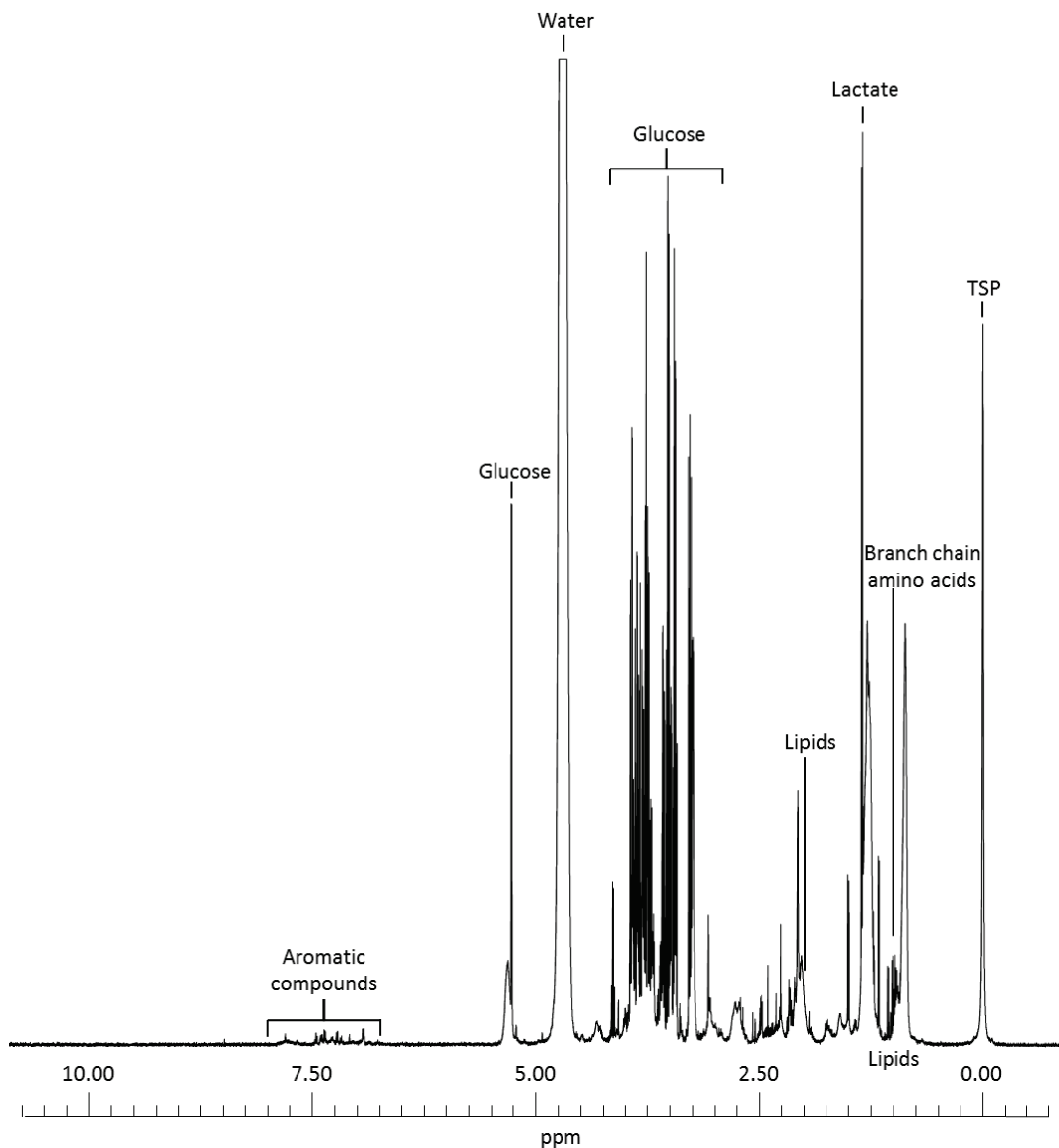


compounds, figure 1.4. Experimental pulse sequences can be chosen to selectively suppress particular spectral features, for example the Carr-Purcell-Meiboom-Gill (CPMG) sequence will suppress large

molecular weight metabolites revealing those of a smaller weight. Common to all experiments is the need to suppress the large water peak and this is achieved with a solvent suppression pulse sequence. Post-processing of NMR data requires spectral phasing to ensure all peaks project in the same direction, peak alignment to ensure that all peaks are correctly positioned and baseline correction to ensure a flat baseline prior to statistical analysis.

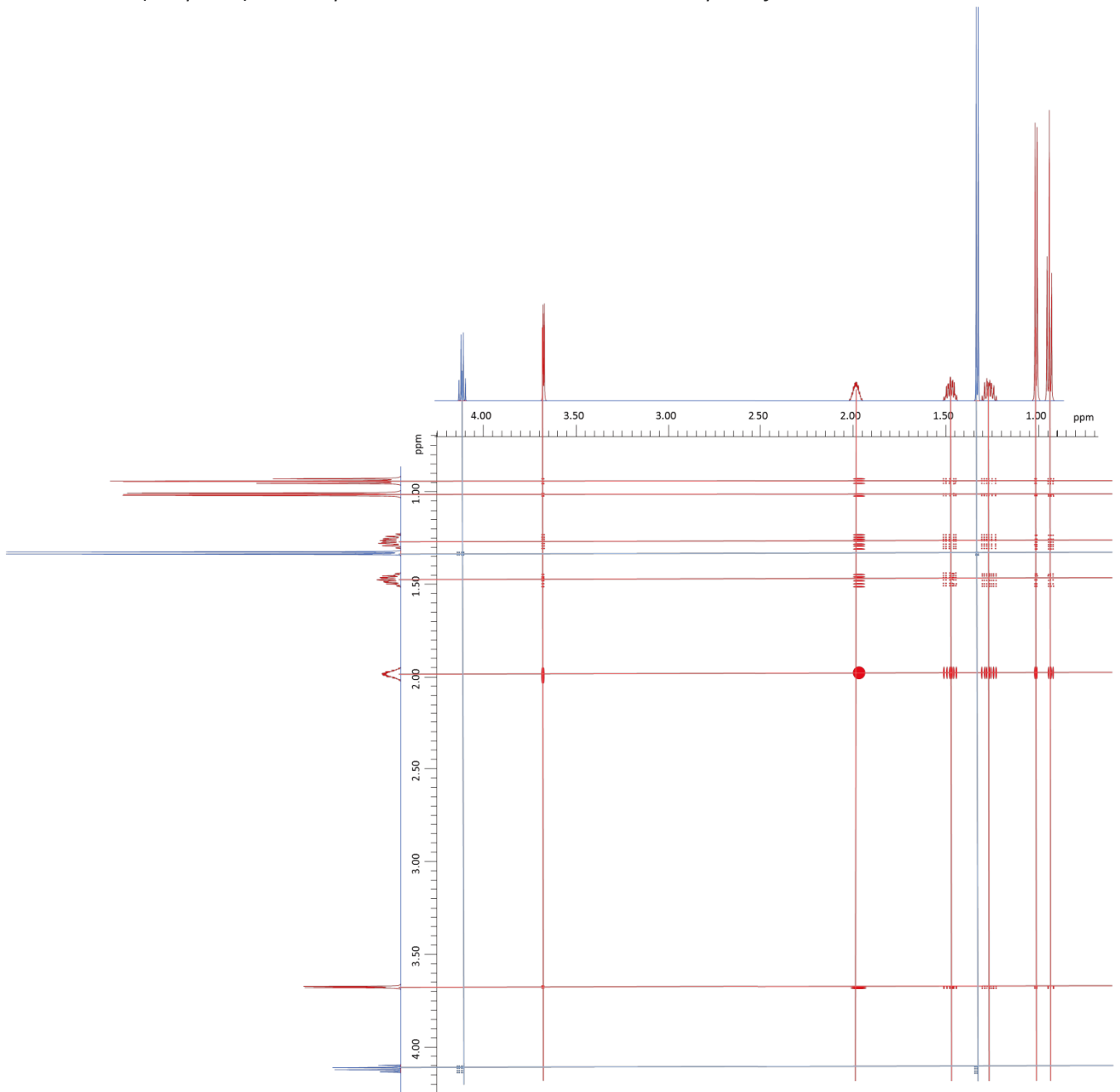
In addition to 1D experiments as outlined above, 2D experiments can be used to help determine metabolite structure. Examples include a 2D J-resolved experiment, which yields information on the

Figure 1.4. Example ^1H NMR spectrum obtained from a CPMG experiment on human serum.



multiplicity and coupling patterns of metabolites, correlation spectroscopy (COSY) and total correlation spectroscopy (TOCSY) experiments both of which provide spin–spin coupling connectivities, figure 1.5, giving information on which protons in a molecule are closely related (110, 111).

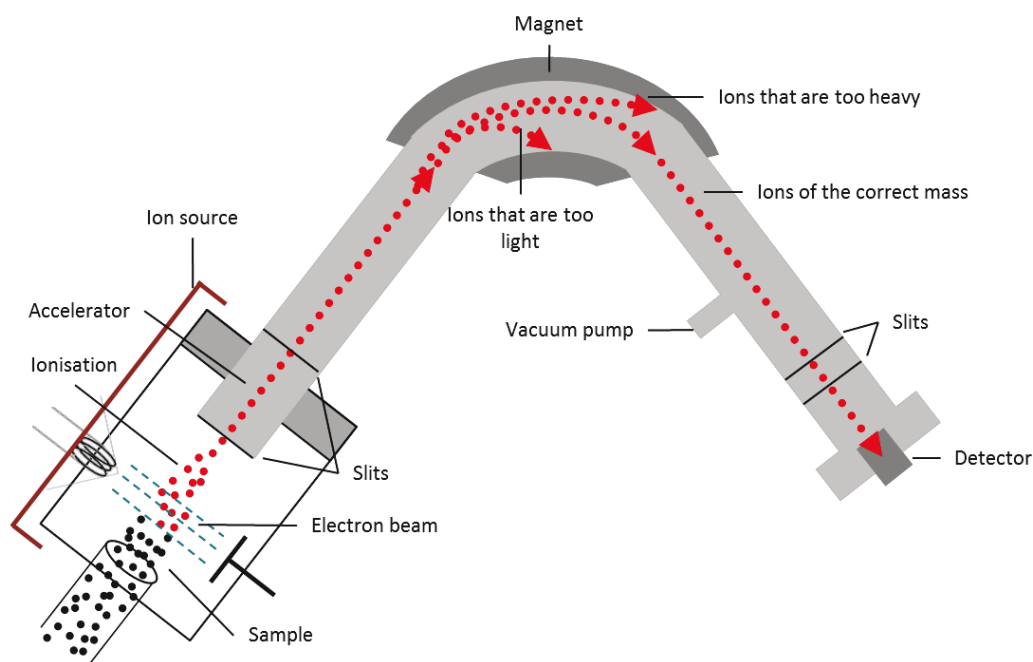
Figure 1.5. Illustration of a 2D Total Correlation Spectroscopy (TOCSY) experiment illustrating how it can be used to distinguish those peaks associated with lactate (blue peaks) and those associated with isoleucine (red peaks) in a complex mixture. Peaks that intersect are part of the same molecule.



1.3.2 Mass Spectrometry

Mass spectrometry (MS) is a technique that aims to identify metabolites within a sample based on the detection of the mass-charge ratio (m/z) of charged molecules or molecule fragments produced by the ionization of chemical compounds. Molecules in a sample are first vaporized before being ionized by being bombarded by either electrons or other ions. The molecule is thus broken into charged fragments which can be sorted based on their m/z ratio and detected by a device capable of detecting charged particles. Several techniques exist to separate and detect molecular fragments, an example is separation by accelerating ions and subjecting them to an electric or magnetic field, figure 1.6. The acquired data can be displayed as a spectrum of the relative abundances of the various particles of the same mass-charge ratio. The molecules in the sample can be identified through characteristic fragmentation patterns.

Figure 1.6. A schematic diagram of the component parts of a mass spectrometer.



In order to improve fragment separation mass spectrometry is often coupled to chromatographic techniques. Such techniques include gas chromatography-mass spectrometry (GC-MS), where a gas chromatogram is used to separate molecules in gaseous phase before they are fed into the ion source allowing ionisation and further separation. Liquid chromatography-mass spectrometry (LC-MS) and high performance liquid chromatography-mass spectrometry (HPLC-MS) similarly separates molecules in a sample in a liquid mobile phase using a liquid chromatogram using a combination of organic solvents prior to ionisation.

MS based platforms generally have the advantage of greater sensitivity compared to NMR, however, some substances such as sugars and amino acids are difficult to analyse with this method due to their polarity and lack of volatility (111). MS requires reasonably extensive sample preparation and, with long chromatographic times, can take longer to process than NMR. Also because of the need to vaporise and ionise the sample MS is a more destructive analytical technique than NMR.

1.3.3 Data Analysis

Analytical techniques used in metabonomics generate data sets that are unlike those produced in many other scientific areas. Whereas there would often be many more subjects than variables, metabonomics generally produces thousands of variables, several of which may correlate, and many may not be normally distributed. These features pose problems for regular statistical methods so analysis is generally performed using multivariate statistics. Many techniques exist within multivariate statistics but broadly speaking those used in chemometrics can be split into unsupervised tests, where no class information is given to the model. These are good at finding natural clustering within the data sets and at identifying outliers. Supervised tests, on the other hand, look for variation between predefined groups or classes and are able to build predictive models.

1.3.3.1 Principal Component Analysis

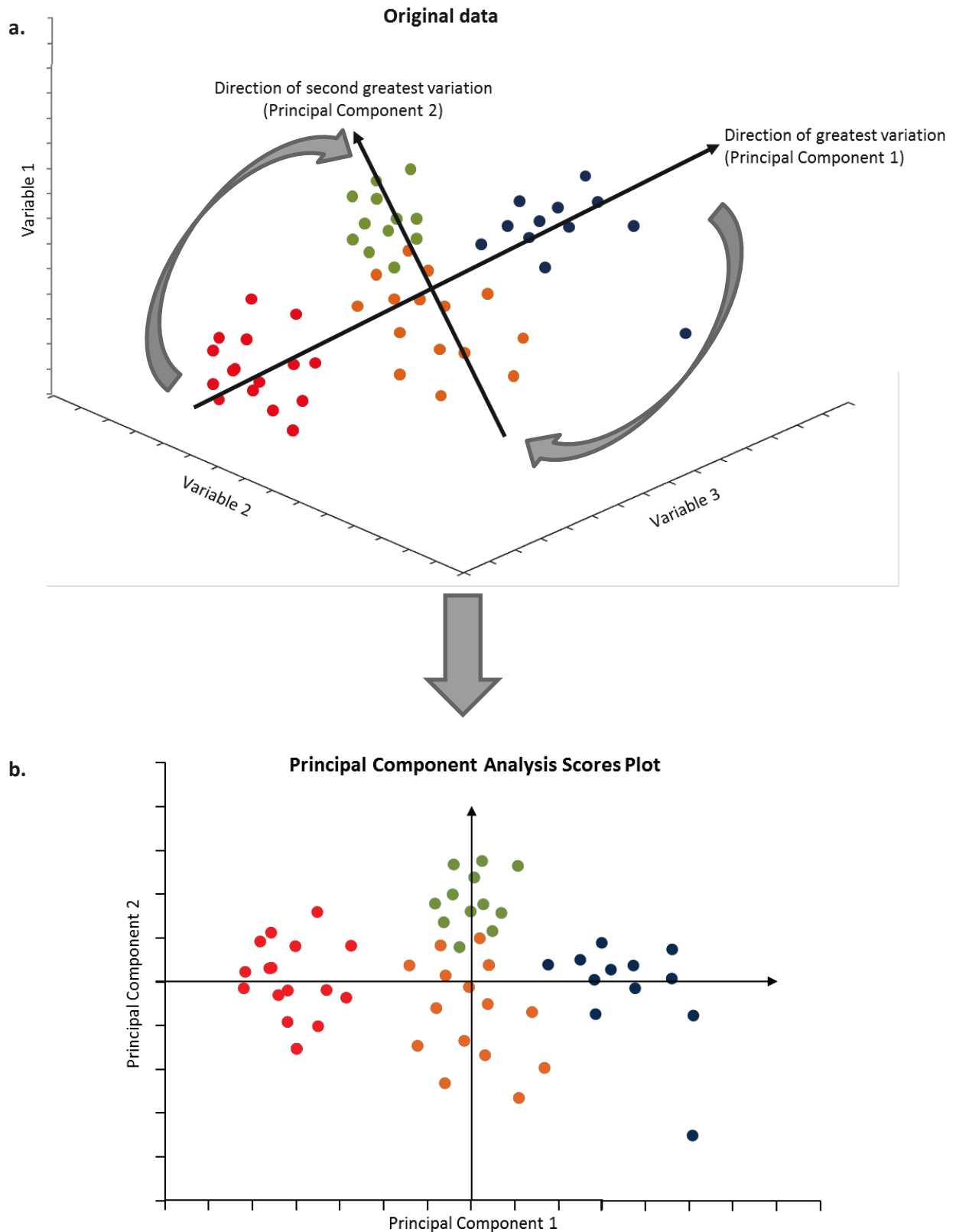
Principal Component Analysis (PCA) is the predominant method of unsupervised multivariate analysis used in metabonomics. It is generally concerned with elucidating the covariance structure of the data set by representing the data along new axes based on the direction of the maximum variation, so called principal components. Mathematically this is done by splitting the data into a set of eigenvectors, essentially directions of variation, and for each eigenvector an associated eigenvalue describes the magnitude of this variation. The first principal component is the eigenvector associated with the greatest eigenvalue and the second principal component will be that with the second largest value that is orthogonal to the first, figure 1.7. This method of analysis allows data reduction. Although an eigenvector exists for each variable in a data set some of these will contain very little variation and eigenvectors with low eigenvalues, which contain little information, are discarded. The data can then be re-displayed using the principal components as a new set of axes, giving a PCA scores plot, figure 1.7.

An approximation to the Student's t-test called the Hotelling's ellipse can be projected onto the PCA scores plot. This gives an indication of a 95% confidence interval within which 95% of observations should fall. Data points lying outside of this ellipse can be considered as strong outliers and can be examined in more detail.

1.3.3.2 Supervised Analysis

Supervised multivariate analysis is aimed at finding the variation in the data matrix that explains a predefined classification. One of the underlying methods of supervised analysis is partial least squares analysis (PLS). PLS determines the underlying relationship between two data matrices, X which contains the sample data and a second data matrix Y, containing dependent information, using a latent variable approach finding the fewest variables that account for the differences in the Y

Figure 1.7. Demonstration of how a multivariate set of data *a.* is converted into a Principal Component Analysis (PCA) scores plot *b.* by detecting the directions of greatest variation and converting these into a new set of axes.



matrix. Overall the goal is to predict Y from X. Where the Y data matrix contains classification data the process is called Partial Least Squared Discriminant Analysis (PLS-DA). Extensions of PLS and PLS-DA occur with both orthogonal partial least squared (OPLS) and orthogonal partial least squared discriminant analysis (OPLS-DA). These two techniques work in a similar fashion to their PLS counterparts. However, in these methods the variation in the X matrix is divided into that which explains data in the Y matrix and that which is orthogonal to it and does not explain the Y data. The data can be represented as one component that explains the between group variation and one orthogonal to it that explains within group variation. Although these extensions do not improve the predictivity of the models they aid analysis by improving both visualisation and diagnostics of the models.

In order to assess the predictive capacity of a model cross validation can be carried out. A number of methods exist to do this but a commonly utilized approach is to leave out every n^{th} row in the data matrix and build a model based on the remaining data. The remaining data can then be predicted by the model and the results compared to the expected outcome. This process can then be repeated until all of the data has been left out once. After cross validation it is possible to derive two descriptive metrics for the models. The first is known as the R^2Y which explains the amount of variation between the classification groups that is explained by the model. This value ranges from 0 to 1.0 with values approaching 1.0 explaining almost all of the variation in the model and lower values suggesting that much of the variation in the data is irrelevant or noise. The second value is the Q^2Y which describes the fraction of variation in the dependent variable, Y matrix, by the model. Again this can range from 0 to 1.0 and the higher the value the more predictive the model. The expected values of both R^2Y and Q^2Y are dependent on the type of data being analysed but in general should ideally be no more than 0.2 apart (112). For biological models a Q^2Y of 0.4 would equate to a reasonable model. However, the ideal way to test a model is to challenge it with a complete new set of data from a validation cohort of samples that have not been used to generate

the model in the first instance. From this set of data model statistics such as sensitivity, specificity and predictive values can be obtained.

In order to determine the variables that are important in separating two groups based on multivariate analysis the loading of each variable can be examined. The loading describes the correlation that a component has with the original variable, variables that are strongly correlated with the component have a loading close to 1.0 where as those that have an opposite effect have values closer to -1.0. Variables with loadings close to zero have no influence on the model.

1.3.3.3 Pre-processing

Prior to multivariate analysis data sets need to undergo several pre-processing steps. Mean centring is performed to ensure that the first component genuinely represents the direction of maximum variation as opposed to the mean vector. This is done by subtracting the mean from each variable and gives each variable a mean of zero. Multivariate analysis is very sensitive to scale. Variables that have a large magnitude tend to be associated with a large variance and would have a greater effect on the models than variables that are smaller with lower variance. Similarly if variables are measured in different units, for example heart rate in beats per minute and partial pressure of oxygen (PaO₂) in kPa, then the models would look very different to the same data analysed using a different measurement scale, for example where the PaO₂ is measured in mmHg. To alleviate these problems the data is often scaled so that each variable has the same unit variance.

1.4 Metabonomics of Sepsis and Pneumonia

A range of work has been carried out attempting to utilize metabonomic techniques to explore both sepsis and specific infections using cells, animals and human subjects with both NMR and MS, allowing over 500 metabolites and pathways to be implicated in infection. Work has been done using cell lines and culture media (113-119) allowing bacterial (114, 116, 117, 120) and Candida

species (119) to be identified with NMR. Specifically investigating cell lines infected with *Chlamydia Pneumonia* using several MS platforms found changes in amino acid and cholesterol synthesis (113) to be important in detecting the organism.

Several animal models have been used in an attempt to further understand the metabonomics of infection. Mice (115, 121-126), rats (127-132), horses (133) and primates (134) have all been used as models of various infections allowing biofluids including blood (121, 130), bronchoalveolar fluid (BALF) (128) and lymph (132) to be analysed as well as tissue including lung (124, 128), liver (124, 125), kidney (126) and spleen (124, 126). Infections as diffuse as cerebral malaria (126), peritonitis (128, 131) (127, 129), *E.coli* sepsis (134) and Gram positive and Gram negative infection (121) have been investigated. Metabolites including amino acids, those involved in energy and carbohydrate metabolism, fatty acids and those associated with mitochondrial dysfunction have all been identified in these animal models of infection.

A range of infections have also been explored in human subjects. The majority of work in humans involves clinical samples from subjects with a number of infections, however, humans have also been used to explore metabolic changes over time of a lipopolysaccharide induced sepsis model (135) which found alterations in fatty acid, amino acid and protein metabolism over a 24 hour period. A great deal of work has been done to look at urinary tract infection using NMR of urine samples (136-140) for a range of organisms including *E.coli* (137, 139) and Gram positive and negative infections (138) with an attempt to identify specific causative bacteria (139).

Several other specific infections have been studied including leprosy (141), cerebrospinal fluid analysis to distinguish various forms of meningitis and ventriculitis (142) and generic sepsis in both adults (143-146) and children (147, 148).

1.4.1 Pneumonia

A small amount of work has been carried out investigating pneumonia using metabonomics. Animal studies have found elevated lipoproteins, triglycerides, unsaturated and polyunsaturated fatty acids, ω -3 fatty acids, lactate and 3-hydroxybutyrate and reduced glucose levels in the plasma of rats infected with *Klebsiella Pneumoniae* compared to controls (149). Mice with pneumonia caused by *Staphylococcus Aureus* or *Streptococcus Pneumoniae* can be separated from control animals based on urine metabolic profiling (150). Viral pneumonia caused by *Influenza A* has been studied using MS finding several metabolites that were altered in infected animals, including the amino acids, valine, ornithine, and taurine and the eicosanoids PGF_{2a} and 20-ethyl-PGE₂ (123). A specific form of pneumonia, tuberculosis, has been examined using a murine model taking serum and tissue samples to successfully categorise infected and non-infected animals (124).

Work in humans has focused on community acquired pneumonia and tuberculosis. Studies in tuberculosis have found a combination of both classification metabolites and those associated with treatment (151, 152). A few studies exist examining more typical forms of pneumonia. A study using MS of plasma from children with pneumonia from Gambia found elevated uric acid, hypoxanthine, glutamic acid and L-tryptophan but reduced adenosine diphosphate levels. In this study, clustering based on sex was noted in the pneumonia group that was not seen in the controls suggesting potential differences in inflammatory responses between boys and girls (153). A study looking specifically at patients with *Streptococcus Pneumoniae* pneumonia found numerous urinary metabolites to separate cases from controls including citrate, succinate, 1-methylnicotinamide, several amino acids, glucose, lactate, acetone, carnitine, acetylcarnitine, hypoxanthine and acetate (154). This study also aimed to address several potential confounding factors associated with this type of investigation by comparing cases to several control groups such as those with other types of

lung disease, those with other types of pneumonia and those with other acute illnesses. In most cases multivariate statistical models provided reasonable prediction accuracy.

1.4.2 Critical Care

Work within critical care has focussed on the outcomes of patients with community acquired pneumonia (CAP) and sepsis (155). MS analysis of plasma found higher levels of bile acids, steroid hormone metabolites, markers of oxidative stress and nucleic acid metabolites in non-survivors, however, the statistical models based on these differences had only modest sensitivity with an area under the receiver operating curve (AUROC) of 0.67.

A common differential for VAP is acute lung injury (ALI) or ARDS and differentiation can be difficult. A metabonomic study of sepsis induced ALI and ARDS (106), in 13 patients with ALI or ARDS compared to 6 healthy controls, found differences in plasma levels of glutathione, adenosine, phosphatidylserine and sphingomyelin between case and controls and in another study using LC-MS of BALF several lipid metabolites increased and a component of surfactant decreased in BALF of those with ARDS (156). Other work in ICU patients has looked at predisposition to sepsis following trauma using NMR of plasma samples from 21 patients and identified valine, citrate, aspartate, allantoin and hydroxybutyrate as associated with the future development of sepsis (157). Looking at septic shock in adults on ICU glycerophospholipids and acetylcarnitines were elevated in 33 patients with sepsis when compared to 30 other patients with SIRS (146). Further exploration of sepsis on ICU used NMR techniques to predict mortality (145) in 37 intensive care patients compared to 20 controls and looked at sepsis in 137 children from different age groups admitted to critical care (148). In an attempt to explore ICU mortality (158) in adult ICU patients plasma samples were analysed with MS finding 31 metabolites associated with mortality most of which were elevated in those who died. These covered a range of metabolites including lipids, carbohydrates and amino

acids. Only six metabolites were greater in those who survived and these were all involved in the lipid synthesis pathway.

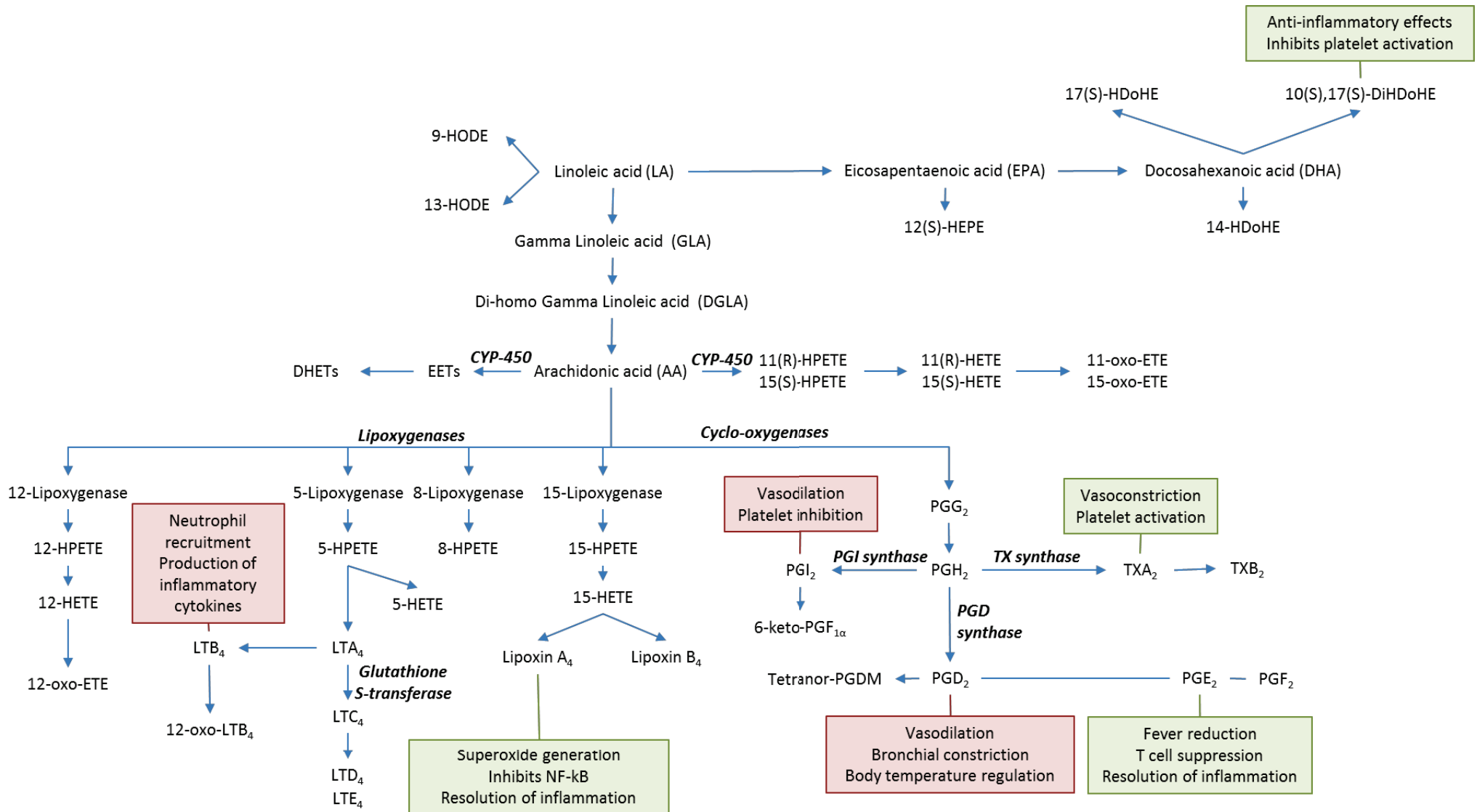
To date no work has been published using metabonomic methods to specifically focus on VAP or looking at methods for differentiating patients with pneumonia from similar critically unwell patients without pneumonia. Current work has often used healthy volunteers as controls for pneumonia cases. This approach has several disadvantages as healthy volunteers may be expected to be metabolically quite different from pneumonia patients compared to similar severely ill patients.

1.5 Oxylipins and Cytokines

Oxylipins are a family of molecules formed from the oxidation of fatty acids and the most well known of these are the eicosanoids, signalling molecules formed from the oxidation of 20-carbon fatty acids. Eicosanoids play an important role in mediating both inflammation and immunity and are predominantly derived from three fatty acids, arachidonic acid (AA), eicosapentanoic acid (EPA) and linoleic acid (LA). The derived eicosanoids can be subclassified, for example, prostaglandin analogs, thromboxanes, lipoxins and leukotrienes, figure 1.8. The effects of these mediators are varied and depend on the organ involved and the balance of mediators released but can have effects including vasodilation and vasoconstriction, bronchodilation and bronchoconstriction and release of other inflammatory mediators.

Cytokines are another broad range of small signalling proteins produced by a variety of cell types. They encompass interleukins (IL), interferons, tumour necrosis factor alpha (TNF α), colony stimulating factors and chemokines and are related to several of the adhesion molecules such as intracellular adhesion molecule 1 (ICAM-1). These mediators are generally produced from inflammatory cell lines including lymphocytes, monocytes, mast cells and natural killer cells and are

Figure 1.8. Scheme showing the origin of several eicosanoid and oxylipin species. Labels in bold-italics denote enzymes. Summary of function is given for some of the eicosanoid species. Red boxes denote predominantly inflammatory species and green boxes those with anti-inflammatory actions.



implicated in a range of pathology from infection and inflammation to malignancy. The interactions of cytokines and eicosanoids are complex and are interdependent and can have similar actions.

Eicosanoids such as the leukotrienes, especially leukotriene B₄ (LTB₄), are thought to be important in protecting the lungs from infection with actions including chemoattraction and leukocyte activation. LTB₄ may increase IL-6 levels (159) and has been associated with pulmonary complications following trauma (160). *Streptococcus Pneumonia* has been shown to be capable of inducing COX-2 expression, an enzyme crucial to eicosanoid production, within lung tissue in models of lung infection (161). Eicosanoids not only act as pro-inflammatory mediators but, substances such as the lipoxins, have been implicated in the resolution of pulmonary inflammation. Lipoxin A₄ can be generated in response to lung injury and has been found in the BALF of patients with pneumonia (162) and may inhibit LTB₄ mediated chemoattraction.

Cytokines are also known to play an important role in the pathology of pneumonia with circulating levels of pro-inflammatory cytokines, such as TNF α , interleukin-1 (IL-1), interleukin-6 (IL-6), interleukin-8 (IL-8), interleukin-12 (IL-12), and interferon gamma (IFN γ) having been found to be elevated in patients with pneumonia. A study looking at pneumonia (163) found higher levels of IL-6 and interleukin-10 (IL-10) in non-survivors compared to survivors and higher IL-6, IL-10 and TNF α levels in those pneumonia patients with severe sepsis compared to those without. The inflammatory response to CAP may not be the same throughout life and may alter with age, for example, IL-8 has shown a trend to be elevated at admission in older patients with CAP compared to those younger than 50yrs (164). In children IL-6, IL-8 and IL-10 levels were found to be higher, not only in septic patients compared to controls, but also in those septic patients who went on to develop nosocomial infections (165). Specific micro-organisms have also shown similar patterns of cytokine response (166) with Interleukin 4 (IL-4), IL-6 and IL-10 being higher in mycoplasma pneumonia than in

controls. Many of these mediators are produced locally, for example, IL-8, LTB₄, C4, D4, and E4 have been found at higher concentrations in the BALF of pneumonia patients compared to controls (167).

The diagnostic potential of cytokines or eicosanoids in pneumonia has been examined in a few studies and a smaller body of work exists applying a panel approach to measuring an array of inflammatory mediators. For example, one study aimed to diagnose tuberculosis using a multiplex cytokine assay measuring cytokines produced from stimulated peripheral blood mononuclear cells with IFN γ , interferon gamma inducible protein-10 (IP-10), monokine induced by interferon gamma (MIG), TNF α and IL-2 showing the most significant differences between patients with active pulmonary tuberculosis and healthy controls (168). In another study ARDS cases were separated into different phenotypic groups based on IL-6 and IL-8 levels combined with other biological and clinical data (169). No work exists combining a large profile of cytokines and eicosanoids into one model in an attempt to diagnose either pneumonia in patients admitted to critical care or VAP in those already ventilated on the ICU.

1.6 Breath Analysis

Formalised breath analysis is used widely in law enforcement and in some diagnostic clinical tests such as for *Helicobacter pylori*. Volatile organic compounds (VOCs) in breath give signatures that are familiar to us as odours associated with several diseases from the ketones associated with diabetic complications to the recognizable hepatic fetor.

Online metabolic profiling of exhaled breath using selected ion flow tube mass spectrometry (SIFT-MS) and gas chromatography mass spectrometry (GC-MS) (170-172) can be performed. Metabolites such as acetone, ammonia and methane have been quantified (173, 174) in healthy volunteers and the repeatability of the SIFT-MS technique has been demonstrated (175). Exhaled nitric oxide (NO)

has shown potential for detecting airway inflammation in asthma, COPD (176) and pneumonia (177) and carbon monoxide levels in breath have been found to increase in patients with sepsis (178).

Headspace gas analysis from a range of cultures has shown potential to detect of a range of micro-organisms (179-181) including cultures of BALF from patients with pneumonia (182). For example, *Pseudomonas* has been identified from cultures taken from patients with cystic fibrosis (183, 184) and breath from these patients has been analysed in an attempt to determine *Pseudomonas* colonisation status (185-187). Analysis of exhaled breath may therefore allow detection of specific causative organisms in pneumonia by differentiating metabolic profiles. Although some of the above work shows promise for breath analysis to be used to explore pneumonia no studies exist examining metabolic profiling of exhaled gaseous breath with regard to this disease. Specifically no work has been done regarding VAP.

It is possible to condense and collect the water vapour contained in breath, known as exhaled breath condensate (EBC). EBC is 99% evaporated water but also contains droplets of fluid from the airway linings allowing non-volatile compounds to be measured. EBC contains a number of substances including interleukins (188), leukotrienes (189) and sTREM (89). Hydrogen peroxide is one of the most studied substances from EBC and is elevated in many inflammatory condition including ARDS (190), asthma (191) and may correlate with treatment response in patients with cystic fibrosis (192). Isoprostanes have been noted to be increased in COPD (193), asthma (194) and ARDS (195) and EBC pH appears to decrease with lung inflammation in conditions such as bronchiectasis, COPD and lung injury (196, 197). In the field of pneumonia thiobarbituric acid and hydrogen peroxide have been seen to increase in CAP (198, 199).

1.6.1 Metabonomics of Breath Condensate – ¹H-NMR Spectroscopy

Small scale studies with EBC have used NMR analysis to distinguish stable from unstable patients with cystic fibrosis (200), asthmatics from healthy controls (201-203), to investigate smoking related

diseases (204) and examine the potential of salivary and disinfectant contamination, from reusable collection equipment, of EBC (205). Studies have made attempts at metabolite assignment (99, 200, 204, 205) identifying 26 compounds between them. As yet there is no experience of collecting EBC from ventilated patients for the purpose of metabolite analysis. As with the gaseous phase of breath the optimal methods for sample collection, processing and analysis are not known.

1.6.2 Metabonomics of Breath Condensate –Mass Spectrometry

With its greater sensitivity MS potentially has advantages over NMR spectroscopy for the analysis of EBC given the very low concentrations of metabolites within the fluid. Most work has focussed on specific markers or panels of markers with little work utilising MS as a profiling tool (206, 207). Many specific substances within EBC have been explored including glucose (208), urea (209, 210), volatile organic compounds (211, 212), aldehydes (213-216), isoprostanes (195, 217-226), markers of oxidative stress (218), cystinyl leukotrienes (218, 227, 228), leukotrienes (189, 227, 229-233), eicosanoids (234-239), 12-HETE (240), lysophosphatidic acid (241), asymmetric dimethylarginine (ADMA) (242, 243), adenosine (209), phenylalanine (209), lysine (244), tyrosine (245), hydroxyproline (245), proline (245), purines (246-249), metallic elements (250), 3-nitrotyrosine (245, 251-254), and proteins (255) using a number of MS methods including LC-MS (206-208, 218), Liquid Chromatography Tandem Mass Spectrometry (LC-MS/MS) (217, 241, 255), GC-MS (211) and Ultra Performance Liquid Chromatography Tandem Mass Spectrometry (UPLC-MS/MS) (227, 243).

The majority of work using MS has, again, focussed on relatively stable diseases in community patients including healthy subjects (215, 238, 256), asthma (189, 206, 218, 227, 232, 234-236, 239, 242, 248), COPD (216, 247, 250, 255), pulmonary fibrosis (223, 224, 241), cystic fibrosis (208, 209), pulmonary hypertension (211), bronchopulmonary dysplasia (207), pneumoconiosis (229), silicosis (221), asbestosis (226), Churg Strauss (240) and seasonal rhinitis(233). ARDS (195) has been studied in critically unwell patients. Almost all studies have been performed in spontaneously ventilating

patients with only two in those requiring mechanical ventilation (195, 210) one of which (210) did not investigate particular disease state and only looked at urea measurement. No studies have been carried out profiling EBC in patients with pneumonia either with or without the need for mechanical ventilation. EBC analysis is appealing for the diagnosis of pneumonia in ventilated patients as it is a non-invasive, easily obtained biofluid that directly samples from the site of pathology.

1.7 Hypothesis and Aims

1.7.1 Hypothesis

The application of metabolic and inflammatory profiling to biofluids including serum, urine and breath condensate obtained from patients ventilated on the Intensive Care Unit will aid the diagnosis of pneumonia and ventilator associated pneumonia.

1.7.2 Aims

The following aims will be addressed:

- *Can metabolic profiles of serum and urine be used to aid diagnosis of patients with pneumonia and VAP?*
- *To investigate the potential of using ¹H-NMR and MS as methods for analysing EBC collected from ventilated patients.*
- *Can metabolic profiling of EBC aid in the diagnosis of pneumonia and VAP?*
- *Can comparing metabolic profiles of breath condensate, serum and urine give an insight into local and global metabolic changes?*
- *Can a panel approach to the measurement of eicosanoids aid the diagnosis of both pneumonia and VAP?*
- *Can a panel approach to the measurement of cytokines aid the diagnosis of both pneumonia and VAP?*

- *Can combining eicosanoid and cytokine profiles into an 'inflammatory profile' improve the diagnostic potential of this approach?*
- *Can multivariate methods applied to routinely collected clinical data produce discriminant models to differentiate those with and without pneumonia?*
- *Can combining clinical data with profiling data from biofluids improve diagnostic potential of these approaches?*

Section II – Methodology

2. PROTOCOLS AND METHODS

2.1 Patient Recruitment.

All patients were recruited in line with the independent research ethics committee approval (REC 10/H0709/77). Adult patients (age >16yrs) were screened at both Charing Cross and St Mary's Hospitals, Imperial College Healthcare NHS Trust. Patients were eligible for recruitment if they fulfilled the following criteria:

1. Patients requiring intubation and ventilation who were expected to be ventilated for >48 hours
2. Patients who could be recruited within 48 hours of intubation
3. Patients fulfilling 2/4 of the criteria of the systemic inflammatory response syndrome (SIRS) as follows:
 - (1) Fever (>38⁰ C) or hypothermia (< 36⁰ C),
 - (2) Tachycardia (heart rate > 90 beats per minute),
 - (3) Tachypnoea (respiratory rate > 20 breaths per minute or PaCO₂ < 4.3 kPa) or need for mechanical ventilation,
 - (4) Abnormal leukocyte count (> 12,000 cells/mm³, < 4000 cells/mm³, or > 10% immature [band] forms).

Patients were excluded if the following criteria were met:

1. Refusal of assent from the patients next of kin
2. Pre-existent immunosuppression, either congenital or acquired
3. Use of granulocyte colony stimulating factor

Three groups of patients were recruited. The predominant group was a cohort of patients with isolated neurological pathology or brain injury (BI), such conditions included subarachnoid haemorrhage (SAH), isolated head injury, cerebrovascular accidents (CVA), isolated brain tumours and status epilepticus. Patients with disseminated pathology that may have effect on their lungs such as polytrauma or disseminated malignancy with cerebral metastasis were not recruited into this group. A second group of patients admitted with a primary diagnosis of pneumonia were recruited to act as a positive control group. Finally a, small, third group of patients was enrolled with a range of conditions who's samples could be used for method development.

2.1.1 Consent

As, by definition, patients recruited to the study were undergoing invasive ventilation it was not possible to obtain direct patient consent. Instead informed assent was obtained from the patient's personal consultee or where no such person existed a professional consultee caring for the patient but not directly involved in the study. All patients were followed up once mechanical ventilation had ceased and where patients regained capacity retrospective consent was obtained for involvement in the study.

2.1.2 Sample collection

The first set of biofluid samples, exhaled breath condensate, serum and urine, were obtained from recruited patients as soon as possible after personal consultee assent had been obtained. Subsequent samples were collected on alternate days until either four sets of samples had been obtained over the course of the first week or the patient no longer required Intensive Care.

2.1.2.1 Serum

All blood was drawn from indwelling vascular access. Where a patent arterial catheter was in place this source was used for sample collection, if no arterial access was available blood was drawn from

the central venous catheter. 5ml of blood was aspirated from the line to clear the saline flush prior to sample collection. Serum samples were collected into 10ml, red-topped Vacutainer® (New Jersey, USA) tubes containing a silicone clot activator. 10ml of blood were drawn into the tube from the indwelling catheter and placed directly on ice. Samples were left to clot for 30 minutes on ice in order to limit metabolic activity within the sample during clotting. Samples were then centrifuged at 1600g at room temperature for 10 minutes prior to being divided into 100-500µl aliquots. Aliquots were then kept frozen at -80°C before analysis. A clotting time of 30minutes was used to balance the time needed to allow the samples to clot adequately whilst minimising the time between sample collection and aliquots being frozen (110, 257).

After analysing the first samples it became apparent that in some aliquots clotting had continued during the freezing process leaving insufficient sample volume to run the required experiments. In order to improve the volume of serum obtained in samples collected latterly, a second red-topped Vacutainer was collected simultaneously. Whilst the first was processed as described above, the second was centrifuged for a further 5 minutes to improve clot and serum separation. This then provided two groups of paired samples, those centrifuged for 10 and those for 15 minutes. Where possible 10 minute samples were used for all analysis, however, where insufficient sample was obtained a 15 minute sample was substituted. Where possible a direct comparison of 10 to 15 minute samples was made where paired samples existed.

2.1.2.2 Urine

All urine samples were collected from indwelling urinary catheters. The catheter was clamped for 20-30min prior to sample collection to ensure a fresh sample was obtained. 5ml of urine was then aspirated from the side port of the catheter before being placed into a 10ml red-topped Vacutainer® (New Jersey, USA) tube. Immediately after collection collected samples were centrifuged at 1900g, at room temperature for ten minutes before being divided into aliquots of 600-700µl. All aliquots

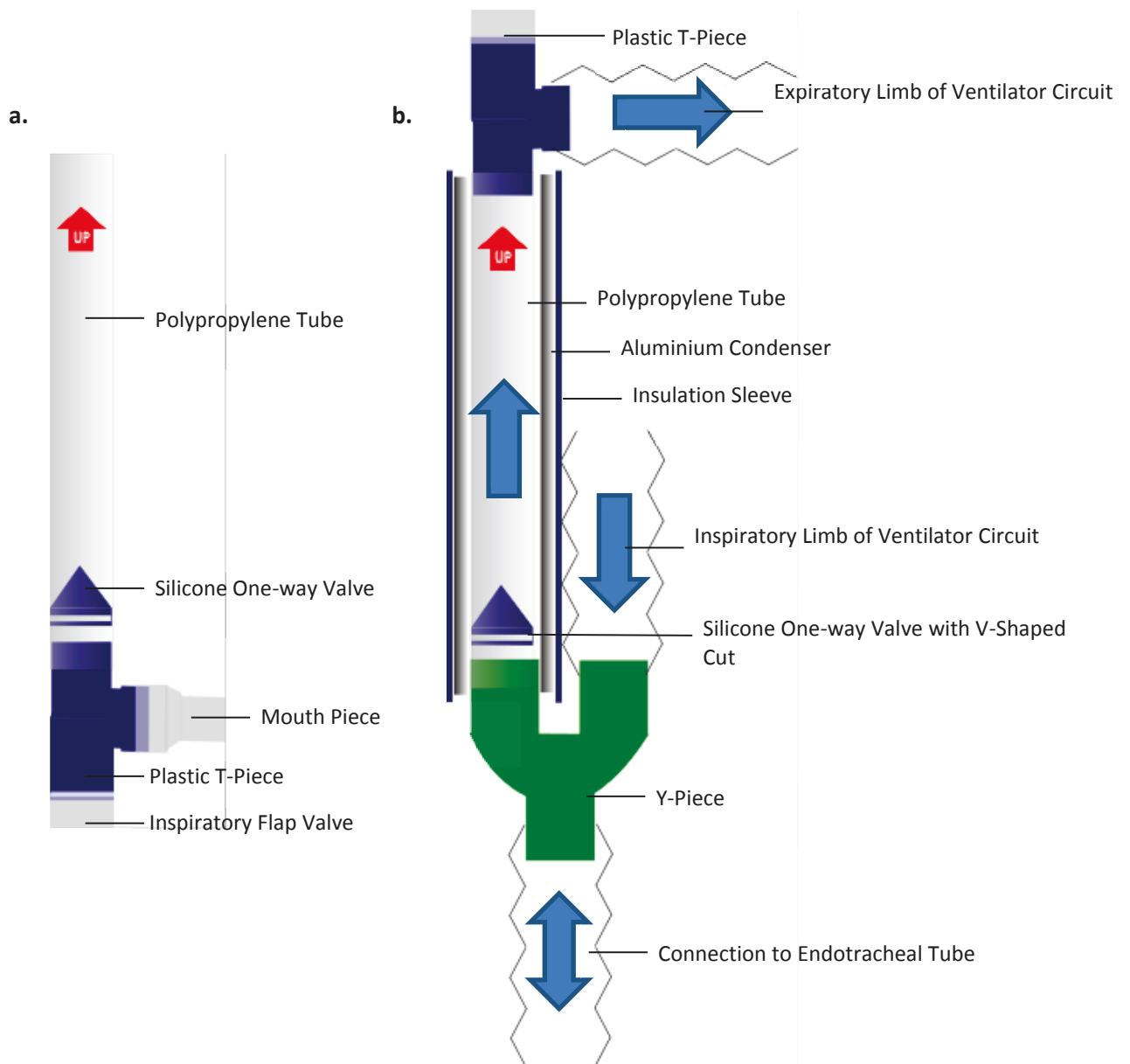
were immediately frozen at -80°C , the time between a samples collection and its placement in the freezer was kept to a minimum.

2.1.2.3 Exhaled Breath Condensate

Exhaled breath condensate (EBC) was collected using the commercially available RTube™ (Respiratory Research, USA) device. This device consisted of a single use polypropylene tube with a one-way silicone rubber valve, figure 2.1. For sample collection the disposable tube was covered with a re-useable aluminium tube which is otherwise kept at -80°C this acted as a condenser. The time between removing the condenser from the freezer and connecting the collection equipment to the ventilator circuit was kept to a minimum. To allow the aluminium tube to be handled a polyester/cotton insulator was used. The device is predominantly intended for sample collection from spontaneously breathing subjects and comes fitted with a mouth piece and one way inspiratory valve combined as a plastic T-piece. In order to fit the device into the ventilator circuit the mouth piece was removed and the plastic T-piece inverted and placed on in the top of the RTube™, figure 2.1. The rearranged equipment could then be placed into the expiratory limb of the ventilator circuit. In order to prevent excessive expiratory pressure a small v-shaped nick was made in the silicone valve using sterile scissors. The presence of the silicone valve ensured that only expiratory breath was being condensed.

EBC samples were collected by placing the collection equipment in the expiratory limb of the ventilator circuit for 15 minutes. One to two minutes prior to collection the heat and moisture exchange (HME) filter was removed. This ensured sufficient moisture content of the exhaled breath passing through the RTube™ to allow an adequate amount of condensate to be collected. During EBC collection patients underwent full monitoring of saturations, respiratory rate, end-tidal CO_2 , heart rate and blood pressure as well as the respiratory parameters being delivered by the

Figure 2.1 a. Components of the RTube™ device b. The RTube™ connected into the expiratory limb of the ventilator circuit



ventilator. This ensured the safety of sample collection and allowed collection to be terminated in case of patient instability. Prior to sample collection the ventilator settings were set by the physician responsible for the patient's care and these were unchanged during collection. A record was kept of all settings at the time of collection.

After 15 minutes of collection time the EBC was divided into aliquots by pushing the silicone valve up to the top of the collection tube using a solid aluminium plunger. Samples were divided into aliquots of 500µl and frozen immediately at -80°C.

2.1.3 Clinical Data Collection

A comprehensive set of clinical data was recorded for each day of a patients ICU stay. Data included all physiological variables, laboratory test results, radiology results, arterial blood gas results, microbiology results and administered drugs, fluid and feed, table 2.1. Data were collected at 8:00am every morning and covered the preceding 24h period. For all variables the minimum and maximum values were recorded for the 24h period.

2.1.4 Patient Follow Up

Whilst on ICU patients were followed up daily and following step down to the ward patients were followed up until discharge or death with significant events during their stay recorded.

2.2 Diagnosis of Pneumonia

2.2.1 Brain Injury Patients Developing Ventilator Associated Pneumonia

Patients from the brain injury group were followed up daily and a diagnosis of ventilator associated pneumonia was made based on Clinical Pulmonary Infection Scoring (CPIS) (83), table 2.2. In contrast

Table 2.1 Clinical data collected for all enrolled patients

Bedside Variables	Laboratory Variables	Drugs
Ventilator Settings		
Ventilator mode	White Blood Cell Count ($\times 10^9/L$)	All drugs administered over the preceding 24h with timings and doses
Peak end expiratory pressure (PEEP) (cmH_2O)	Haemoglobin (g/dl)	
FiO ₂	Platelet Count ($\times 10^9/L$)	All fluids given over the preceding 24h with timings and volumes
Respiratory rate set (breaths/min)	Haematocrit (%)	
Respiratory rate measured (breaths/min)	Prothrombin Time (s)	Type and volume of feed administered with timing
Set tidal volume (ml)	Activated Partial Thromboplastin Time (s)	
Expiratory tidal volume (ml)	Fibrinogen (g/L)	Blood products given with timing
Pressure support (cmH_2O)	Sodium (mmol/L)	
Pressure control (cmH_2O)	Potassium (mmol/L)	
Expiratory minute volume (L)	Creatinine ($\mu\text{mol/L}$)	
Peak airway pressure (cmH_2O)	Urea (mmol/L)	
Inspiratory:Expiratory ratio	Chloride (mmol/L)	
	Magnesium (mmol/L)	
Physiological Parameters		
Heart rate (beats/min)	C-Reactive Protein (mg/l)	
Systolic blood pressure (mmHg)	Alanine Transaminase (IU/L)	
Mean arterial pressure (mmHg)	Alkaline Phosphatase (IU/L)	
Diastolic blood pressure (mmHg)	Bilirubin ($\mu\text{mol/L}$)	
Oxygen saturations (%) with associated FiO ₂	Albumin (g/L)	
Glasgow Coma Scale	Corrected Calcium (mmol/L)	
Temperature ($^{\circ}\text{C}$)	Phosphate (mmol/L)	
Central Venous Pressure (CVP)(cmH_2O)	Microbiology Results	
Hourly urine output (ml/h)	Culture results from tracheal aspirates	
Total urine output over 24 hours (ml)	Culture results from blood cultures	
Total fluid input over 24 hours (ml)	Other microbiology specimens sent	
Total oral input over 24 hours (ml)		
Amount of tracheal secretions over 24h	Radiology Results	
Colour of tracheal secretions over 24h	Chest radiograph reports	
	Computed Tomography (CT) reports	
Blood Gas Parameters		
PaO ₂ :FiO ₂ ratio (kPa)		
PaCO ₂ (kPa)		
pH		
Bicarbonate (mmol/L)		
Base excess		
Lactate (mmol/L)		
Glucose (mmol/L)		

to the original published score this study gave a score of 0 to a temperature of 36.0-38.4 compared to 36.5-38.4 as published. This change was made as it was unclear what score temperatures of 36-36.5 should be given.

Table 2.2. Clinical Pulmonary Infection Score (CPIS) modified from Pugin et al, 1991 (83)

Clinical Feature	Score
Temperature (°C)	
36.0-38.4	0
38.5-38.9	1
≥39 ≤36	2
White Cell Count (mm⁻³)	
4,000-11,000	0
>11,000, <4,000	1
Band forms >500	+1
Radiology	
No infiltrate	0
Diffuse (Patchy) Infiltrate	1
Localised Infiltrate	2
Oxygenation (mmHg)	
PaO ₂ /FiO ₂ > 240 or ARDS	0
PaO ₂ /FiO ₂ ≤240	2
Secretions	
<14 of total secretions in 24h	0
≥14 of total secretions	1
Plus purulent secretions	+1
Microbiology	
Pathogenic bacteria cultured ≤ 1+ or no growth	0
Pathogenic bacteria cultured ≥ 1+	1
Gram stain ≥ +1 with same pathogenic organism	+1

Scores were calculated on a daily basis using clinical data from the preceding 24h. For variables that were not recorded on a daily basis such as radiology reports and microbiology data it was assumed that the last documented score remained true until there was documented change, for example new radiological findings or a newly positive or negative culture result. The CPIS gives a score ranging from 0-12 with a score ≥7 being taken to signify VAP. However, in our institution band form measurement and gram staining of tracheal secretions are not routinely performed limiting the score to 0-10, leaving patients with scores of five and six borderline for the diagnosis of VAP. To

account for this all scores ≥ 7 after 48h of ventilation were taken as confirmed diagnoses of VAP and those < 5 as definite controls, figure 2.2. Borderline cases with scores of five or six were assessed by an independent clinician and classified as cases or controls. Patients with high scores within the first 48h of ventilation, where there was also clinical suspicion were treated as cases of primary pneumonia and not VAP. Patients with a CPIS < 5 at the time of the first sample collection were considered free of infection and used as the control group, figure 2.2. Where any conflict existed between the CPIS score and the clinical judgement the clinical records were reviewed and a decision made regarding clinical grouping. Where this did not clarify the situation cases were passed to an independent assessor.

2.2.2 Pneumonia

Patients admitted for ventilation with a primary diagnosis of pneumonia were initially identified based on the clinical judgement of the physician with responsibility for their care. This was based on features from the history, clinical examination findings, laboratory tests and radiological investigations. However, as there is a recognised degree of intra-observer variability when making this diagnosis more objective criteria were required. The CPIS score was calculated for all patients felt to have pneumonia on admission to ICU and only those patients scoring ≥ 6 within 48h of the timing of the first sample of stay were taken as confirmed diagnoses. A lower CPIS target was accepted in this group due to difficulties obtaining certain clinical parameters, such as microbiological specimens when patients initially present to hospital compared to the ease of acquisition from an already intubated and ventilated patient. In order to be classified as a case of pneumonia there had to be both a clinical suspicion at the time of admission and a high enough CPIS, figure 2.3. Where any conflict existed between the CPIS score and the clinical judgement the clinical records were reviewed and a decision made regarding clinical grouping. Where this did not clarify the situation cases were passed to an independent assessor for classification.

Figure 2.2. Study classification pathway for patients admitted for ventilation with brain injuries.

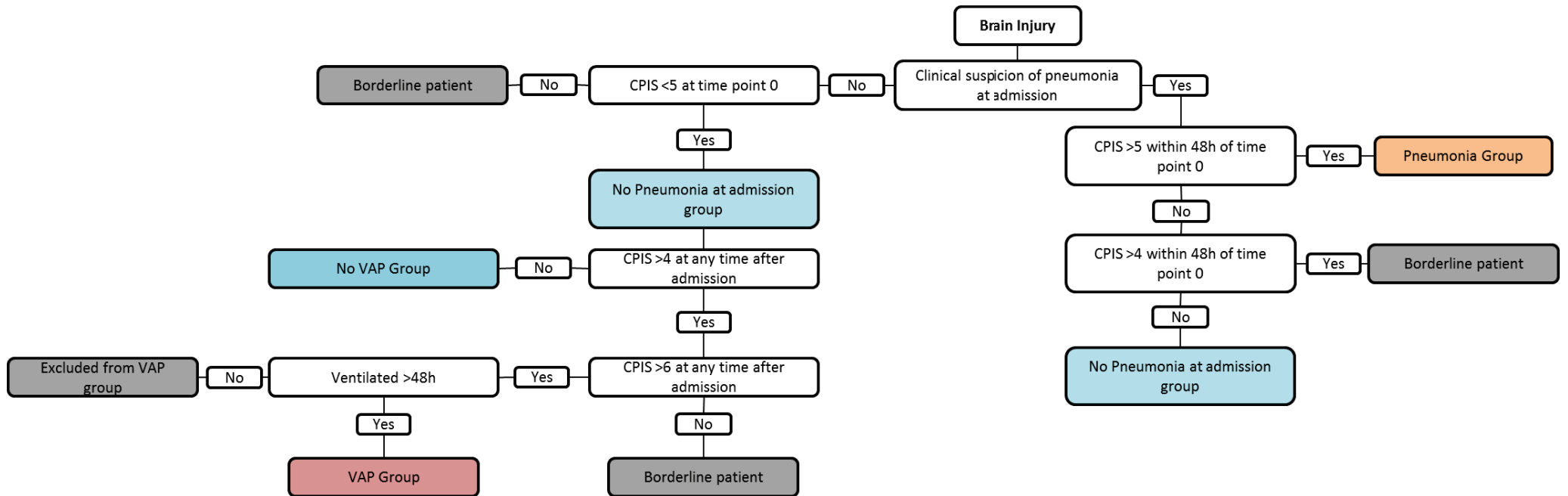
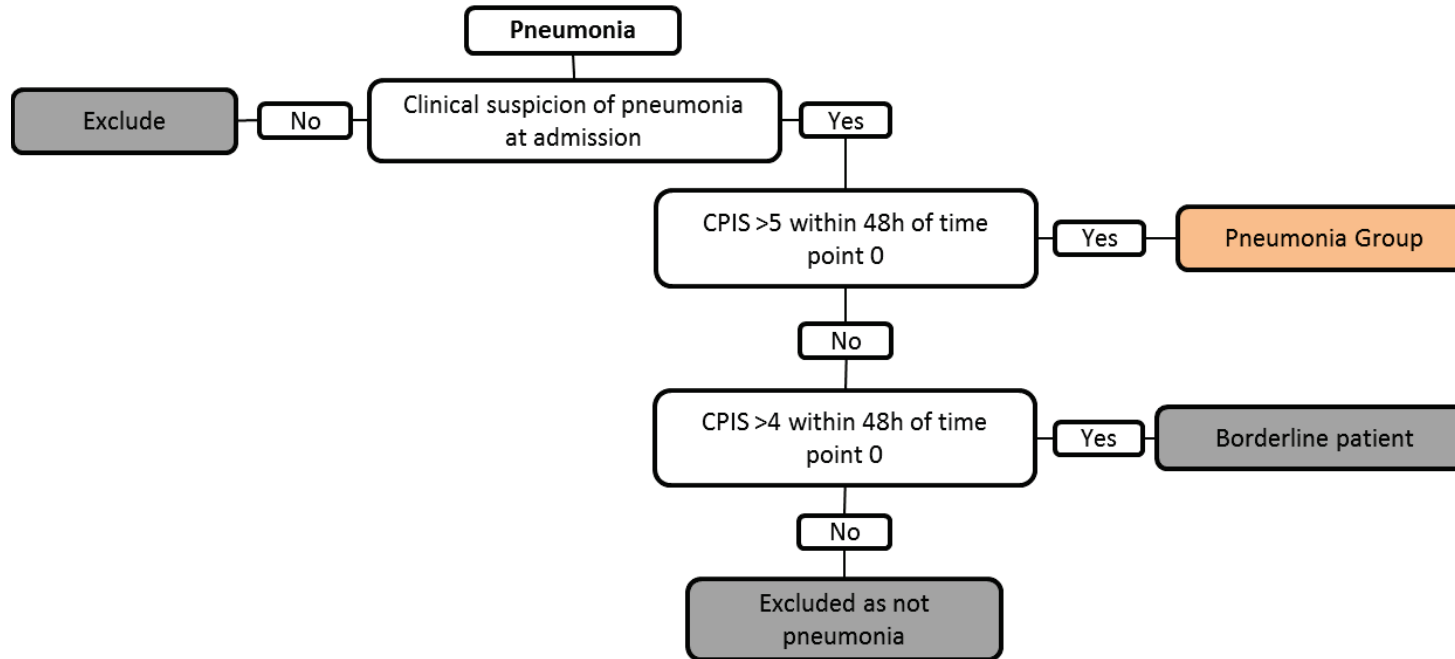


Figure 2.3 Study classification pathway for patients admitted for ventilation with a presumed diagnosis of pneumonia.



2.3 Specific Processing

Details of specific experimental assays used for each experiment are given in the relevant chapters. Nuclear Magnetic Resonance Spectroscopy for global metabolic profiling of serum and urine, chapter 3, targeted measurement of oxylipins using mass spectrometry and cytokine measurement using flow cytometry, chapter 4, and global metabolic profiling of breath condensate using mass spectrometry, chapter 5.

2.4 Statistical Analysis

Statistical analysis was performed using a combination of multivariate and univariate techniques. Routine data handling was performed in Excel 2010 (Microsoft, USA). Univariate statistical analysis was used to compare individual analytes and characteristics of included patients using SPSS version 22 (IBM, UK) and Excel 2010 (Microsoft, USA). The Student's t-test was used to compare continuous variables between groups of patients and Fisher's exact test to compare categorical variables. Normality of metabolite distributions was determined using Kolmogorov-Smirnov and Shapiro-Wilk tests of normality. Non-normally distributed analytes were compared using the Mann-Whitney U test. To control for the false discovery rate and limit the number of type I errors the Benjamini-Hochberg procedure was used when multiple univariate comparisons were made. A p-value of 0.05 or less was taken to represent statistical significance.

For much of the data there were far more variables than there were observations, making multivariate analysis an ideal way to evaluate the data. All multivariate analysis was performed using the SIMCA statistical package (Umetrics, Sweden). Initial exploration of data sets was performed with principal component analysis (PCA). PCA is an unsupervised method of multivariate analysis, meaning that during analysis the model has no prior knowledge of the observation classifications of interest and instead finds the largest directions of natural variation. It employs orthogonal

transformation of a data set of observations and correlated variables into a matrix of uncorrelated variables. The transformation is performed in such a way that the first set of variables, or component, demonstrates the largest variation from within the data and all subsequent components demonstrate the next greatest direction of variation in an orthogonal direction to the previous component. PCA was performed first on the data to look for natural separation of groups of observations that would either explain groups of clinical interest or detect clustering not overtly apparent in the data that may have affected further analysis. Data from PCA analysis were displayed on scores plots which plot two components of interest against each other. Data points on the scores plots were artificially coloured to represent groups of clinical interest, although these data were not used in construction of the models. PCA was also used to detect significant outliers. On the scores plots the Hotelling's ellipse represents a 5% confidence interval, a multivariate equivalent of Student's t-test, and observations lying outside of this were considered strong outliers which warranted further investigation to look for explanations for why an individual was an outlier. The amount of the total population variance explained by a PCA model is explained by the R^2X value of the model, this is expressed as a decimal with a model with an R^2X of 1.0 explaining all of the variance within a data set. The predictive value of the model is expressed as the Q^2X , again expressed as a decimal with values approaching 1.0 demonstrating the best prediction. In the case of PCA, the Q^2X value does not inform about class but only reflects the overall variance in the total dataset.

Supervised multivariate analysis using orthogonal partial least squared discriminant analysis (OPLS-DA) was used to generate models to optimally separate predefined groups. OPLS-DA is another form of multivariate analysis similar to PCA. However, in this analysis the model attempts to find variation in the original data set, X, that explains the clinical classifications represented in a second matrix, Y. OPLS-DA differs from partial least squared analysis discriminant analysis (PLS-DA) in that the data in the X-matrix is separated into that which predicts the Y data and that which is uninformative or

orthogonal to it, improving visualization of metabolites associated with clinical parameters. OPLS-DA models were cross validated using seven fold cross-validation using a “leave-one-out” methodology. This method uses every 7th observation as a validation set that is predicted by the model, the predicted values can then be compared to the actual classes. This is repeated until every observation has been left out once and once only. The cross validation allowed a value, Q^2Y , to be generated that estimated the predictive capacity of the model with a value of 1.0 representing a completely predictive model for sample class. The degree of variation in the original data set explained by the model is again given by R^2X with a value of 1.0 implying that all the variation is explained, on the other hand the amount of variation between the groups being compared explained by the model is given by R^2Y . To assess the reliability of the OPLS-DA models a cross-validated analysis of variance was used (CV-ANOVA) which analyses whether the model has significantly smaller cross validated predictive residuals than just the variation around the global average, as would be expected if the model was generate by chance. This test tests the hypothesis that the residuals of the model are those that would be obtained by chance, if no relationship existed, and acts as a test of significance of the Q^2Y (112).

The number of components in the OPLS-DA models were limited to being no more than half the number of samples in the smallest group used in the model and components were no longer added when they failed to improve the Q^2Y by 0.05 or more. Data from the OPLS-DA models were again displayed on scores plots with the first component plotted against the orthogonal component, data were displayed before and after cross-validation.

The ideal way to assess the predictive models is to challenge them with a new data set that has not been used to build the original model. Where there were sufficient samples from the patients categorised by the independent assessor these were used as a small test set, of around ten patients, to assess the predictive capacity of the models. When this was possible the unseen data were put

into the model and the classifications based on the model were compared with those from the assessor. Based on the number of agreements and disagreements the sensitivity, specificity, positive and negative predictive values of the models could be calculated.

In order to test whether the models were performing better than chance. Permutation testing was performed on a similar PLS-DA model to the OPLS-DA model in question. The Y variables were then randomly generated 20 times, in order to scramble the true class information, and a new PLS-DA model constructed for each permutation. The Q^2Y and R^2X could then be compared with those generated from the random models.

To identify analytes that were important in separating clinical groups a number of methods were employed. Firstly, when the number of analytes were relatively small the loadings plots for the model could be examined directly. The loadings plot plots the weight for each variable against axes representing the components of the relevant model. As such it looks similar to the scores plot but instead of each data point representing an observation they represent the analytes. The scores plots and loadings plots could be directly compared and the analytes at the extremes of each axis could be seen to be causing most of the separation in the equivalent direction on the scores plot.

Analytes were also assessed using the 's-plot'. The s-plot is used to visualize both the covariance and the correlation between the variables and the predictive score. Thus the most discriminant analytes will be associated with both a high correlation and covariance and will be at the extremes of the 'S'. Data that underwent univariate scaling did not produce the typical 'S' as the correlation and covariance showed a linear relationship. Similar to the s-plot, spectral data from NMR data were displayed on an s-line plot, or regression coefficient plot. Here the variables are plotted against the loading for that variable, giving the overall appearance of the original spectrum. However, instead of all of the spectral peaks pointing in the upward direction as seen in the original NMR data, the peaks are directed either upward or downward depending on the clinical group the metabolite

predominates in. The strength of the metabolite's importance in separating the two groups is given by colouring each peak based on the absolute correlation variable for that variable based on the clinical classification.

Where several analytes appeared to cause separation of a model the Variable Importance for the Projection (VIP) was used to help define those variable most important in the model. VIP is a parameter which summarizes the importance of the variables, it is a weighted sum of squares of the OPLS-DA weights, taking into account the amount of explained Y-variance in each dimension. Variables with large VIP, larger than 1, were considered the most important for explaining the classification (112).

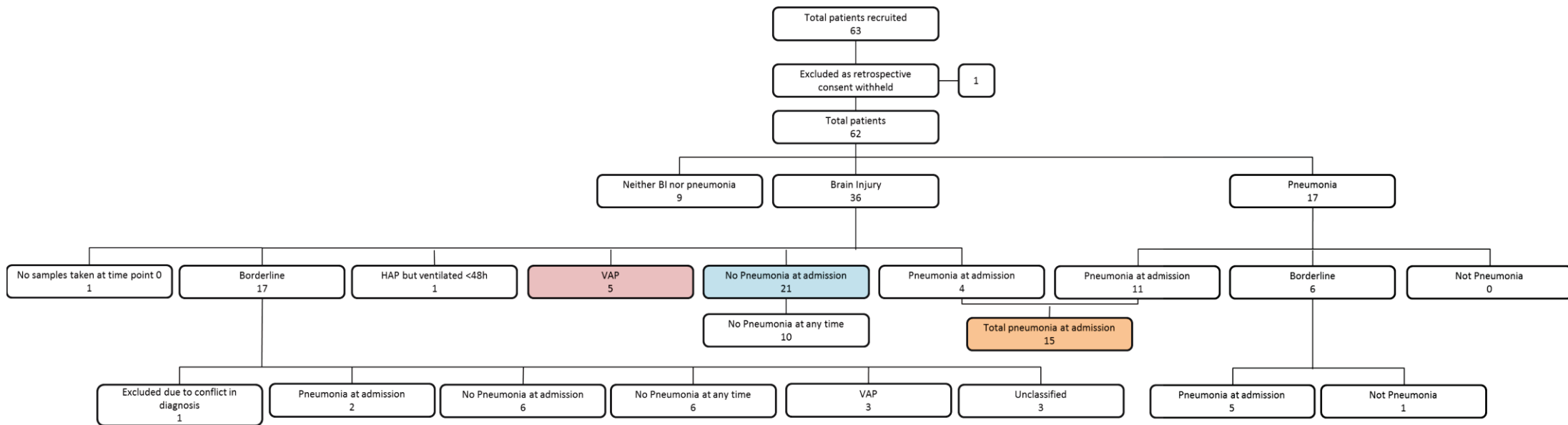
To aid the identification of metabolites in NMR data Statistical Total Correlation Spectroscopy (STOCSY) was used to correlate peaks of interest with other peaks in the spectrum using an in-house MatLab 2013 (MathWorks, Massachusetts, USA) script. This process correlates a selected peak with all other peaks in the spectrum. Peaks with the highest correlation are likely to be part of the same metabolite where as those with an intermediate correlation co-efficient are likely to be associated with the index peak but not within the same metabolite, for example as part of the same metabolic pathway.

2.5 Patient Details.

Sixty-three patients were recruited in total, figure 2.4. Of these one had to be excluded as the patient withheld retrospective consent. Of the remaining 62 patients nine had diagnoses other than brain injuries or pneumonia leaving a potential 36 brain injured and 17 pneumonia patients. Following the classifications described earlier four of the brain injured patients had pneumonia at the time the first sample was collected as did eleven of the pneumonia group, leaving 15 patients classified as having pneumonia at the time the first samples were collected. Classification of the brain injured patients found 21 had no suggestion of pneumonia when the first sample was taken, of which ten never developed signs of pneumonia. From this group of 21 patients the control group was drawn. Six of the brain injured patients developed pneumonia based on CPIS during their stay, five of these developed pneumonia after 48h of ventilation so were defined as VAP. One of the brain injured patients did not have samples taken at the first time point and was excluded from further analysis.

Seventeen brain injured patients were borderline for either a diagnosis on pneumonia at admission or for the development of VAP. Similarly six of the potential cases of pneumonia failed to be classified using the defined algorithm. These 22 patients were submitted to an independent assessor for further classification. When this was completed, seven patients were classified as having pneumonia at admission, two of whom had associated brain injuries, six of the brain injured patients were classified as not having pneumonia when the first sample was taken and 3 were felt to develop VAP. One patient was excluded from further analysis as they had initially been classified as not having pneumonia at admission but were submitted as a potential VAP but were felt to have had pneumonia at recruitment by the independent assessor. Due to this conflict they were excluded from further analysis.

Figure 2.4. Breakdown of recruited patients



Four of the recruited patients only had breath condensate collected as they had been co-enrolled into an interventional trial that precluded further urine or serum sample collection.

Initial statistical models were made based on the classifications based on the described algorithms. The patients independently classified were used to further explore the data and test the ability of the models to categorize patients.

The majority of the brain injured patients had suffered either a subarachnoid haemorrhage, or a haemorrhagic cerebrovascular accident, table 2.3. Of those patients initially classified as having pneumonia at enrolment, the majority were felt to have been at risk of aspiration, five had associated brain injuries and one had a pneumonia in the context of endocarditis, table 2.4.

Table 2.3 Causes of brain injury in the recruited patients.

Cause of Brain Injury	n
Status Epilepticus	4
Thrombotic CVA	6
Haemorrhagic CVA	10
Subarachnoid haemorrhage	12
Loss of consciousness	1
Subdural Haematoma	2
Motor Neurone Disease	1

Table 2.4 Causes of pneumonia in those with pneumonia at enrolment

Cause of Pneumonia	n
Community Acquired	2
Aspiration	8
Endocarditis	1
Empyema	2
Hospital Acquired	2
Associated with brain injury	5

The demographic details of the patients between the two groups based on the initial classification, table 2.5, were similar. The features that differentiated the groups were those that implied pulmonary infection. These included CPIS, C-reactive protein, $\text{FiO}_2\text{:PaO}_2$ ratio and the use of antibiotics. The organisms causing pneumonia in those admitted with pneumonia and those developing VAP can be seen in table 2.6.

Table 2.5. Clinical features of included patients based on initial classification. Continuous variables are given as mean and standard deviation and categorical variables as number and percentage. *p*-values presented in bold text relate to parameters that were significant at the $p < 0.05$ level. *P*-values given in demographic tables are not corrected for multiple comparisons.

	Pneumonia (P)	Brain Injury (BI)	p-value (BI vs P)	VAP	p-value (BI vs VAP)
n	15	21	-	5	-
Age (Mean +/- SD)	54.7±16.8	52.3±14.9	0.65	50.8±17.2	0.87
Sex, Number of males (%)	10 (67)	12 (57)	0.73	3 (60)	1.00
Ethnicity, number White European (%)	11 (73)	15 (71)	1.00	4 (80)	1.00
Outcome, Number alive (%)	10 (67)	16 (76)	0.71	3 (60)	0.59
APACHE II Score (Mean +/- SD)	19.7±5.8	17.0±6.0	0.18	17.8±9.4	0.86
SOFA Score (Mean +/- SD)	10.5±3.1	8.9±2.6	0.12	8.6±3.1	0.87
CPIS (Mean +/- SD)	5.9±1.1	2.1±1.4	<0.001	7.0±1.6	<0.01
Lowest WCC (10 ⁹ /L) (Mean +/- SD)	15.6±7.2	10.0±3.8	0.01	10.5±3.2	0.76
Highest WCC (10 ⁹ /L) (Mean +/- SD)	16.1±7.0	11.2±3.9	0.03	10.5±3.2	0.70
Lowest CRP (mg/L) (Mean +/- SD)	180.4±104.1	49.4±54.2	<0.001	116.7±28.2	<0.01
Highest CRP (mg/L)(Mean +/- SD)	196.3±95.8	62.0±52.5	<0.001	116.7±28.2	<0.01
Lowest Temperature (°C) (Mean +/- SD)	35.9±0.8	36.0±0.7	0.58	36.0±1.6	0.95
High Temperature (°C) (Mean +/- SD)	37.6±0.9	37.6±0.7	0.77	38.0±1.3	0.45
Lowest FiO2 (Mean +/- SD)	0.43±0.14	0.40±0.22	0.54	0.36±0.07	0.51
Lowest PaO2:FiO2 (Mean +/- SD)	24.4±9.2	41.8±15.5	<0.001	18.6±8.5	<0.001
Lowest MAP (mmHg) (Mean +/- SD)	70.7±10.2	74.0±11.3	0.36	71.0±12.4	0.64
Use of noradrenaline, N (%)	11 (73)	13 (62)	0.72	1 (20)	0.15
Use of antibiotics N (%)	15 (100)	10 (48)	<0.001	5 (100)	0.05
Enteral nutrition, N (%)	13 (87)	15 (71)	0.42	5 (100)	0.30

Table 2.6. Organisms causing pneumonia in those admitted with pneumonia and those developing VAP from the group of patients based on original classification. Organisms grown from sputum sampling. (*based on urine antigen testing.)

Admission Pneumonia		VAP	
Organism	n	Organism	n
<i>Morexella</i>	1	<i>S Aureus</i>	3
<i>Enterobacter</i>	1	<i>Klebsiella</i>	1
<i>Pseudomonas</i>	2	<i>Serratia</i>	1
<i>E. Coli</i>	1		
<i>Pneumococcus</i>	2		
<i>Morganella</i>	1		
<i>Legionella*</i>	1		
<i>Haemophilus</i>	1		
Mixed growth	1		
Nil	5		

Section III – Clinical Studies

3. ¹H-NMR ANALYSIS OF SERUM AND URINE

3.1 Summary

¹H-NMR spectroscopy has been used to analyse biofluids from patients with a range of conditions in order to employ a metabonomic approach to further understand the underlying pathology. Limited work has been done using this technique in either samples obtained from critically unwell patients or those with pneumonia. In this chapter ¹H-NMR spectroscopy was employed to analyse both serum and urine samples collected from patients admitted to intensive care with and without pneumonia. Analysis of serum samples demonstrated potential to differentiate these groups with performance being better for patients admitted with pneumonia than for those who developed VAP. Interesting metabolic differences were observed between the groups with lipids, amino acids and glycoproteins appearing to be important in separating the groups perhaps representing changes in energy metabolism. Analysis of urine was more challenging with metabolites being much more difficult to identify perhaps relating to the fact that intensive care patients receive a large number of drugs many of which are excreted intact or in part in the urine. Many of the peaks seen in the urine samples probably represented drugs and their metabolites limiting the ability to pursue the aim of this study which was to identify changes in innate metabolism. Overall serum seemed a much more robust biofluid to analyse when applying metabonomic methods to critical care patients and more specifically was a better method by which to identify those patients with pneumonia.

3.2 Background

Little work has been done characterising pneumonia using metabonomic techniques. Elevated levels of lipoproteins, triglycerides, unsaturated and polyunsaturated fatty acids, ω -3 fatty acids, lactate and 3-D-hydroxybutyrate and reduced glucose levels have been found in the plasma of rats infected with *Klebsiella Pneumoniae* compared to controls (149) and differentiation of mice with pneumonia

caused by *Staphylococcus Aureus* or *Streptococcus Pneumonia* from control animals has been observed via urine metabolic profiling (150). Similarly work using *Chlamydia Pneumoniae* infected cell lines (113) identified a number of metabolic pathways that were altered by including those involved in carbohydrate and lipid metabolism along with altered concentration of several amino acids.

Work in human subjects has predominantly focused on community acquired pneumonia. A small study using MS analysis of plasma and urine from Gambian children, using eleven cases of pneumonia and eleven controls, found elevated uric acid, hypoxanthine, glutamic acid and L-tryptophan but reduced adenosine diphosphate levels within plasma samples. In this study clustering based on sex was noted in the pneumonia group that was not seen in the controls suggesting differences in inflammatory responses between boys and girls (153). Another study looking at metabolic profiling of urine compared 47 patients with *Streptococcus Pneumoniae* pneumonia to 47 matched controls and found numerous urinary metabolites to separate the groups including citrate, succinate, 1-methylnicotinamide, several amino acids, glucose, lactate, acetone, carnitine, acetylcarnitine, hypoxanthine and acetate (154). This study attempted to address several potential confounding factors associated with this type of investigation by comparing cases to several control groups such as those with other types of lung disease, those with other types of pneumonia and those with other acute illnesses. In most cases multivariate statistical models provided reasonable prediction accuracy. This study also attempted to look at the metabolic trajectory of patients with pneumonia by taking serial urine samples and looking at the change in metabolic profiles over time. Work has not been restricted to bacterial infection, a study using UPLC-MS analysis of serum (258) compared samples taken during acute infection with *Influenza A* with those taken after recovery and found a number of biomarkers associated with viral infection many of which were inflammatory molecules such as prostaglandins and leukotrienes as well as a number of amino acids.

Within critical care work has focussed on outcomes of patients with community acquired pneumonia (CAP) and sepsis (155). MS analysis of plasma, from 15 patients who died matched to the same number of survivors, found higher levels of bile acids, steroid hormone metabolites, markers of oxidative stress and nucleic acid metabolites in non-survivors, however, the statistical models based on these differences had only modest sensitivity with an area under the receiver operating curve (AUROC) of 0.67 which is less than that expected from the APACHE II scoring. From these studies only one (154) has attempted to look at the changes in metabolic trajectories over time.

It is often difficult to distinguish VAP from acute lung injury (ALI) or acute respiratory distress syndrome (ARDS). A metabonomic study of sepsis induced ALI and ARDS (106) found differences in plasma levels of glutathione, adenosine, phosphatidylserine and sphingomyelin compared to healthy controls.

To date no work has been done using metabonomic methods specifically focusing on VAP or looking at methods for differentiating patients with pneumonia from similar critically unwell patients without pneumonia. Healthy volunteers have often been used as controls for pneumonia cases in the literature. This approach has several disadvantages as healthy controls may be expected to be metabolically much further away from pneumonia patients than similar severely ill patients. In this study an attempt was made to overcome this problem by using a control group consisting of patients similarly ventilated on ICU without pneumonia or infection.

3.3 Aims

The overall aim of this study was to use metabonomic techniques to attempt to improve the diagnosis of pneumonia in patients requiring ventilation, specifically those going on to develop VAP.

The following questions were addressed:

1. *Can metabolic profiles of serum and urine be used to aid diagnosis in patients with pneumonia and VAP?*
2. *Can comparing metabolic profiles of serum and urine give an insight into local and global metabolic changes?*

3.4 Protocols

3.4.1 Patient Recruitment and Sample Collection

Patients were recruited and serum samples taken as described in chapter 2. Patients were defined as either having pneumonia or a brain injury as described earlier. All patients were followed up over time and those brain injured patients developing VAP were defined based on CPIS scoring, for a breakdown of the CPIS score used see chapter 2. Patients with borderline scores were assessed and classified as VAP or no VAP by an independent assessor.

3.4.2 Sample Processing

All samples were transported between sites on ice if preparation was to be done immediately or on dry ice and placed directly into a -80°C freezer if preparation was to be carried out at a later date. Samples were allowed to thaw at room temperature before further preparation.

3.4.2.1 Serum

A volume of 300 µL of serum was mixed with 300 µL of H₂O:D₂O buffer containing 1.5 M of KH₂PO₄, TSP and NaN₃ at pH 7.4. Samples were vortexed and centrifuged at 12000 g for five minutes to remove solid material. 550 µL of the supernatant was placed into 5 mm NMR tubes and immediately loaded onto a refrigerated SampleJet robot (Bruker Corporation, Germany) and kept at 5°C until measurement. All measurements were carried out within 24h of sample preparation.

3.4.2.2 Urine

A volume of 540 μL of urine where mixed with 60 μL of D_2O buffer containing 1.5 M of KH_2PO_4 , TSP and NaN_3 at pH 7.4. Samples were vortexed and centrifuged at 12000g for five minutes to remove solid material. 550 μL of the supernatant was placed into 5 mm NMR tubes and immediately loaded onto a refrigerated SampleJet robot (Bruker Corporation, Germany) and kept at 5°C until measurement. All measurements were carried out within 24h of sample preparation.

3.4.3 ^1H -NMR 1D Experimental Data Acquisition

All ^1H -NMR experiments were performed using a Bruker Avance III 600 spectrometer working at 14.1 T equipped with a BBO probe.

3.4.3.1 Serum

^1H -NMR spectra of serum samples were collected at a constant temperature of 310K using the relaxation edited Carr-Purcell-Meiboom-Gill (CPMG) pulse sequence. This allows low molecular weight species to be detected by eliminating signals from proteins. A total of 32 free induction decays (FID) were acquired for each experiment in 96 K data points using a 20 ppm spectral width centred at 4.75 ppm. The relaxation delay was set at 4 s and a water pre-saturation pulse was applied during this period to cancel the water signal. The receiver gain was kept constant at a value of 90.5. All experimental acquisition was automated and samples were held in the spectrometer for five minutes before data acquisition to allow temperature equilibration. For each sample a standard 1D pulse sequence using the first part of a Nuclear Overhauser Effect pulse sequence to achieve presaturation of the water peak (110), and J-resolved 2D experiments were also performed using the same parameters as above.

To aid metabolite identification further 2D experiments were carried out on selected samples. Correlation Spectroscopy (COSY), to demonstrate proton spins that are directly coupled to

each other, and Total Correlation Spectroscopy (TOCSY), to demonstrate coupled protons within 6 bonds in a molecule, experiments were performed. For COSY experiments a 12 ppm spectral width was used with a relaxation delay set at 1.2s during which a water pre-saturation pulse was applied to cancel the water signal. For TOCSY experiments a 12 ppm spectral width was used with a relaxation delay set at 2.0s during which a water pre-saturation pulse was applied to cancel the water signal.

3.4.3.2 Urine

A standard one-dimensional experiment using the first increment of the NOESY pulse sequence to achieve pre-saturation of the water resonance (110) and a 2D J-resolved experiment were run for all samples in automation at a constant temperature of 300 K. 32 FIDs were accumulated for each experiment in 64 K data points using a 20 ppm spectral width centred at 4.75ppm. The relaxation delay was set at 4s and a water pre-saturation pulse was applied during this period to cancel the water signal. The receiver gain was kept constant at a value of 90.5. All experimental acquisition was automated and samples were held in the spectrometer for five minutes before data acquisition to allow temperature equilibration.

3.4.4 Pre-Processing

The FID values were multiplied by an exponential function equivalent to a 0.3Hz line broadening factor before Fourier transformation. The resulting spectra were subject to automated phasing, to ensure all spectral peaks were directed upwards, and baseline correction, to ensure the baseline of all spectra was set to 0, using TopSpin 3.2 (Bruker Corporation, Germany). Where necessary manual correction to the pre-processing was performed using TopSpin 3.2 (Bruker Corporation, Germany).

Spectra were imported into MatLab 2013 (MathWorks, Massachusetts, USA) using in-house scripts for all pre-processing steps. Spectra from serum samples were calibrated to the α -glucose signal at

5.23ppm and the spectra from urine samples to TSP at 0ppm. For all spectra the region from 0.1-10ppm, to exclude the peak due to TSP, was divided into approximately 40,000, serum, or 34,000, urine, data points. The water signal region (4.5-4.85ppm, serum and 4.72-4.84ppm, urine) for all spectra and the signals due to urea in urine spectra (5.65-6.0ppm) were removed prior to further processing. All samples underwent probabilistic quotient (median fold) normalisation (259), which is typically used for pre-processing of human urine samples. Urine spectra also underwent a further step of automated peak alignment using an in-house statistical algorithm to improve alignment of peaks from one spectrum to another.

3.4.5 Statistical Analysis

Prior to multivariate analysis all spectral data were scaled to unit variance. By standardising the variance of variables this attempts to take into account the potential influence on multivariate models of analytes with naturally higher concentrations that tend to be associated with higher variance and allows variables with generally lower values to be given similar weight within the model. Multivariate statistics were used to analyse the data. Initial exploration with principal component analysis (PCA) was performed to look for natural clustering and to detect outliers before supervised multivariate analysis using orthogonal partial least squared discriminant analysis (OPLS-DA) was used to generate models to optimally separate predefined groups. OPLS-DA models were cross validated using seven fold cross-validation using a "leave-one-out" methodology. Important metabolites in each model were identified by examining the loadings associated with each model and the most important metabolites were selected by picking those associated with the highest correlation coefficients for each model. All multivariate analysis was performed using the SIMCA 13.0 statistical package (Umetrics, Sweden). Further discussion of multivariate techniques can be found in chapter 2.

3.4.5 Metabolite Identification

Metabolites recognised as being important in the multivariate models were identified using a combination of techniques. Initially Statistical Total Correlation Spectroscopy (STOCSY) using an in-house script MatLab 2013 (MathWorks, Massachusetts, USA) was used to look for peak correlation within the acquired spectra. Further metabolite structure could be confirmed using a combination of 2D experiments, J-Res, COSY and TOCSY, performed on selected samples. Metabolites were then found in the SBASE data base using AMIX 3.9.11 software (Bruker BioSpin) or in published literature.

3.5 Results

3.5.1 Patients

Thirty three patients, that fulfilled the criteria defined in chapter 2, had either adequate serum or urine samples or both for $^1\text{H-NMR}$ analysis. Of those with serum samples, 12 had pneumonia on admission and 21 had brain injuries with no suggestion of pneumonia when the first serum sample was taken. Of those with urine samples 13 had pneumonia and 20 brain injuries when the first samples were taken. The discrepancy in the number of cases and controls between the serum and urine reflects differences in the samples available from the patients recruited. Five brain injured patients went on to develop VAP based on CPIS scoring. As previously described in chapter 2, patients with borderline CPIS scores were reviewed by an independent clinical assessor and classified as non-infected, pneumonia or VAP based on clinical course. Based on this assessment a further five brain injured patients were classified as not having pneumonia on admission, four patients were defined as pneumonia and two as VAP. All initial comparisons were made with the original grouping of patients based on CPIS. Clinical features of these patients can be seen in table 3.1.

Table 3.1. Clinical features of included patients with a) serum and b) urine for NMR analysis. Continuous variables are given as mean and standard deviation and categorical variables as number and percentage. P-values presented in bold text relate to parameters that were significant at the $p < 0.05$ level. The clinical parameters compared were taken from the 24h prior to 8:00 am on the day of sampling, for the pneumonia and brain injured patients this was time point 0 and for cases of VAP this was the 24h prior to the sample taken soonest after the onset of VAP.

a.

	Pneumonia (P)	Brain Injury (BI)	p-value (BI vs P)	VAP	p-value (BI vs VAP)
N	12	21	-	5	-
Age (Mean +/- SD)	53.5±17.2	52.3±14.9	0.84	50.8±17.2	0.87
Sex, Number of males (%)	9 (75)	12 (57.1)	0.46	3 (60.0)	1.00
Ethnicity, number White European (%)	8 (66.7)	15 (71.4)	1.00	4 (80.0)	1.00
Outcome, Number alive (%)	7 (58.3)	16 (76.2)	0.43	3 (60.0)	0.59
APACHE II Score (Mean +/- SD)	19.8±6.5	17.0±6.0	0.22	17.8±9.4	0.86
SOFA Score (Mean +/- SD)	10.1±3.3	8.9±2.6	0.29	8.6±3.1	0.87
CPIS (Mean +/- SD)	5.8±1.1	2.14±1.4	<0.001	7±1.6	<0.01
Lowest WCC ($10^9/L$) (Mean +/- SD)	15.8±7.9	10.0±3.8	0.03	10.5±3.2	0.76
Highest WCC ($10^9/L$) (Mean +/- SD)	16.4±7.6	11.2±3.9	0.04	10.5±3.2	0.70
Lowest CRP (mg/L) (Mean +/- SD)	154.5±94.0	49.4±54.2	<0.01	116.7±28.2	<0.01
Highest CRP (mg/L) (Mean +/- SD)	174.4±87.9	62.0±52.5	<0.01	116.7±28.2	<0.01
Lowest Temperature (°C) (Mean +/- SD)	35.7±0.8	36.0±0.7	0.30	36.0±1.6	0.95
High Temperature (°C) (Mean +/- SD)	37.7±1.0	37.6±0.7	0.67	38.0±1.3	0.45
Lowest FiO ₂ (Mean +/- SD)	0.45±0.2	0.39±0.2	0.42	0.36±0.1	0.51
Lowest PaO ₂ :FiO ₂ (Mean +/- SD)	24.9±9.5	41.8±15.5	<0.001	18.6±8.5	<0.001
Lowest MAP (mmHg) (Mean +/- SD)	72.7±10.2	74.0±11.3	0.72	71.0±12.4	0.64
Use of noradrenaline, N (%)	8 (66.7)	13 (61.9)	1.00	1(20.0)	0.15
Use of antibiotics N (%)	12 (100)	10 (47.6)	<0.01	5 (100)	0.05
Enteral nutrition, N (%)	11 (91.7)	15 (71.4)	0.22	5 (100)	0.298
Time to sampling from start of ventilation (h) (Mean +/- SD)	44.3±10.1	40.1±16.9	0.37	143.4±44.9	<0.01
Time of day of sample, Number taken in the morning (%)	8(66.7)	13 (61.9)	1.00	5 (100)	0.28

b.

	Pneumonia (P)	Brain Injury (BI)	p-value (BI vs P)	VAP	p-value (BI vs VAP)
N	13	20	-	5	-
Age (Mean +/- SD)	53.5±16.5	53.6±13.9	0.98	50.8±17.2	0.75
Sex, Number of males (%)	9 (69.2)	11 (55)	0.49	3 (60.0)	1.00
Ethnicity, number White European (%)	9 (69.2)	15 (75)	1.0	4 (80.0)	1.00
Outcome, Number alive (%)	8 (61.5)	15 (75)	0.46	3 (60.0)	0.60
APACHE II Score (Mean +/- SD)	19.6±6.3	16.9±6.1	0.22	17.8±9.4	0.84
SOFA Score (Mean +/- SD)	10.2±3.2	8.8±2.7	0.20	8.6±3.1	0.92
CPIS (Mean +/- SD)	5.8±1.0	2.2±1.4	<0.001	7.0±1.6	<0.01
Lowest WCC (10 ⁹ /L) (Mean +/- SD)	15.8±7.5	9.8±3.8	0.02	10.5±3.2	0.65
Highest WCC (10 ⁹ /L) (Mean +/- SD)	16.4±7.3	11.0±3.9	0.03	10.5±3.2	0.78
Lowest CRP (mg/L) (Mean +/- SD)	165.7±98.7	48.6±55.5	<0.01	116.7±28.2	<0.01
Highest CRP (mg/L)(Mean +/- SD)	184.1±91.3	61.8±53.8	<0.001	116.7±28.2	<0.01
Lowest Temperature (°C) (Mean +/- SD)	35.8±0.8	36.0±0.7	0.46	36.0±1.6	0.95
High Temperature (°C) (Mean +/- SD)	37.7±1.0	37.6±0.7	0.70	38.0±1.3	0.47
Lowest FiO2 (Mean +/- SD)	0.44±0.1	0.40±0.2	0.57	0.36±0.1	0.42
Lowest PaO2:FiO2 (Mean +/- SD)	24.0±9.7	41.4±15.7	<0.001	18.6±8.5	<0.001
Lowest MAP (mmHg) (Mean +/- SD)	71.7±10.4	74.0±11.6	0.56	71±12.4	0.64
Use of noradrenaline, N (%)	9 (69.2)	12 (60)	0.72	1 (20.0)	0.16
Use of antibiotics N (%)	13 (100)	9 (45)	<0.01	5 (100)	0.05
Enteral nutrition, N (%)	12 (92.3)	14 (70)	0.2	5 (100)	0.29
Time to sampling from start of ventilation (h) (Mean +/- SD)	43.5±11.4	40.8±17.3	0.59	144.6±45.4	<0.001
Time of day of sample, Number taken in the morning (%)	5 (39)	9 (45)	1.00	5 (100)	0.046

Patients were similar across the groups with respect to their demographic details. Features that identified the pneumonia and VAP groups from those with brain injuries included markers of infection such as CRP, white cell count, use of antibiotics and the higher oxygen requirement as would be expected in patients with pulmonary infection.

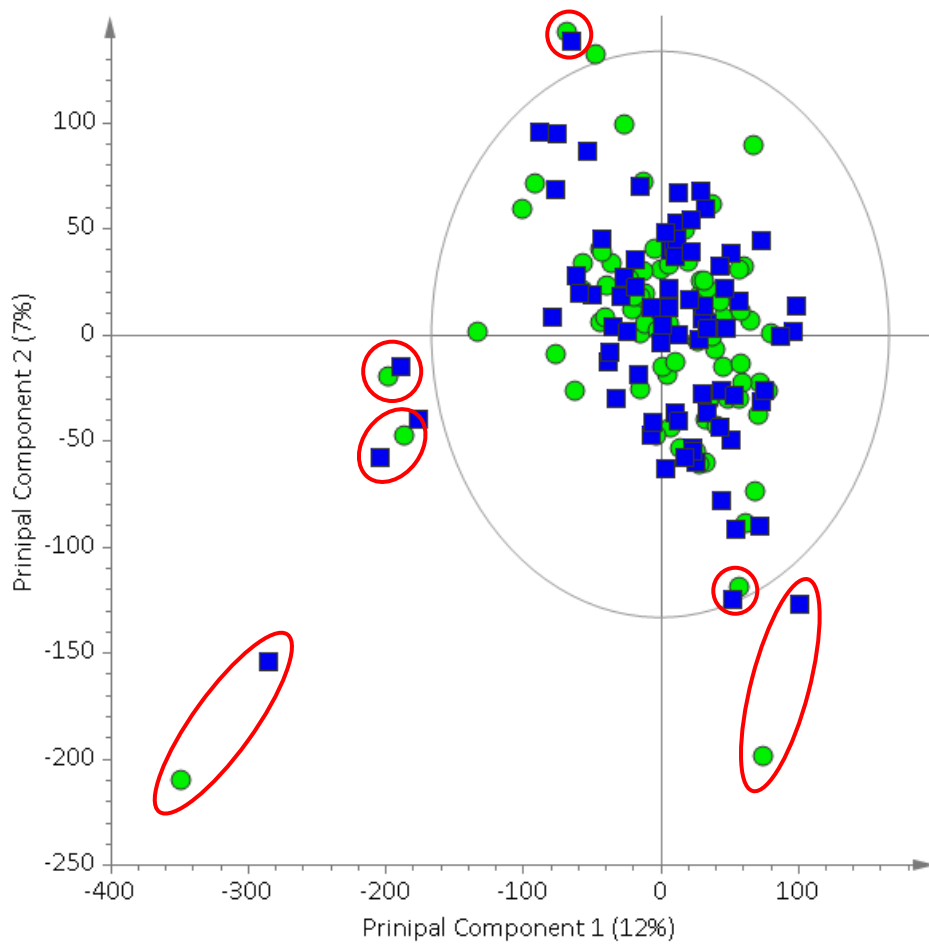
3.5.2 Serum

3.5.2.1 10 Minutes vs 15 Minutes of Centrifugation

Whilst processing the first batch of serum samples collected from this critically ill population it became apparent that some of the stored aliquots contained substantial amounts of clot when thawed providing insufficient serum for NMR analysis. In order to prevent further loss of data from the 30th patient recruited serum samples were collected in duplicate, one centrifuged for the standard 10 minutes and a second sample collected simultaneously that was centrifuged for an extra 5 minutes to try to provide a greater volume of supernatant that could be used if the 10 minute sample proved inadequate.

In order to ensure that there were no systematic differences between those samples that were centrifuged for 15 minutes compared to those that had the original 10 minutes a PCA was constructed for all patients who had paired samples spun for both lengths of time, figure 3.1. This demonstrated that there was no natural clustering of samples from the two groups with samples from the same patient and time point generally lying close together. It was not possible to construct an OPLS-DA model to differentiate the two groups as the Q^2Y remained negative (R^2Y 0.62 Q^2Y -0.77). The results of this analysis suggested that the use of aliquots centrifuged for 15 minutes alongside those that were centrifuged for 10 minutes would be possible when a 10 minute duration provided insufficient serum for analysis for a given patient.

Figure 3.1 PCA scores plot comparing serum samples centrifuges for 10minutes vs 15 minutes prior to freezing, paired samples only (R^2X 0.48, Q^2X 0.32). Green circles – 10 minutes in the centrifuge, blue squares – 15 minutes in the centrifuge, red rings indicate examples of paired samples. It is not possible to form an OPLS-DA model to separate the two groups (R^2Y 0.62, Q^2Y -0.77).



3.5.2.2 Brain Injury vs Pneumonia

The 21 patients who had no evidence of pneumonia based on CPIS when the first serum sample was taken were compared to the 12 patients who had pneumonia at the time of sampling. Initial PCA showed that there were two patients from the brain injured group who were outliers as defined as lying outside of the Hotelling's ellipse (multivariate approximation to the 95% confidence interval derived for the Students' t test), figure 3.2. Of these two patients one was a more extreme outlier than the other which sat near the ellipse. When the raw spectra of these two samples were examined there were no technical differences that could be seen leading to them being outliers. The predominant differences between these samples and the others were that the furthest outlier, at the extreme left of the plot, demonstrated high levels of the ketone bodies, 3-hydroxybutyric acid and acetoacetic acid, that were not seen in the other patients, figure 3.3. These findings fit clinically with the presentation of this patient who had been drinking heavily before attending hospital after a fall and head injury and in whom it took some time to establish feeding. When all of the samples from this patient were examined over time the levels of ketone bodies could be seen to fall as feeding was established. The second outlying spectrum was associated with some broad signals in the 5.75-5.38 ppm region that are yet to be identified as well as pronounced glucose and mannitol peaks. This patient was given mannitol prior to enrolment for control of intracranial pressure. As there were no gross technical reasons for these samples to be outliers they have been kept in all further analysis.

If the third and fourth components of this model were examined some separation between the two groups (pneumonia vs brain injury) could be seen along the third component although there remained a large degree of overlap, as is expected with human populations subject to a high degree of genetic and environmental diversity.

Figure 3.2 PCA scores plot comparing samples taken from patients with brain injuries, blue circles, and patients with pneumonia, red squares, at the start of ventilation ($R^2 \times 0.31$ $Q^2 \times 0.05$). The ellipse represents Hotelling's T^2 at $p=0.05$ a) first and second components showing no natural separation between the two groups in either component, two of the brain injured patients are outliers as demonstrated by lying outside the Hotelling's ellipse, numbered, b) some separation can be seen between the groups when the second and third components are examined, the majority of the separation is along component 3, y-axis.

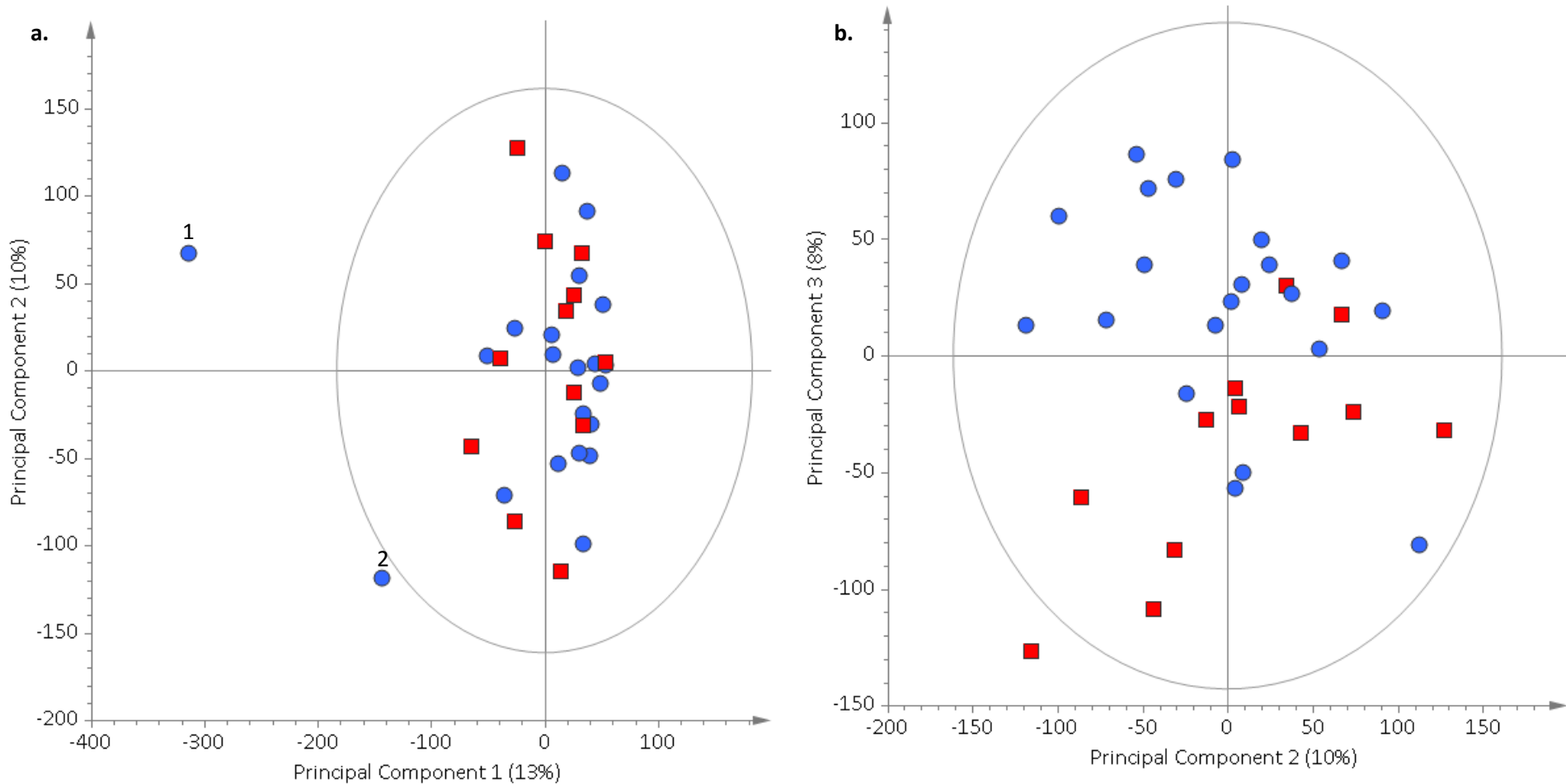


Figure 3.3. Comparison of outlying spectra, blue (patient 1 from figure 3.2) and black (patient 2 from figure 3.2) with representative spectrum from the rest of the group, green, important metabolites are labelled. Only the portion of the spectra with important metabolites is shown.

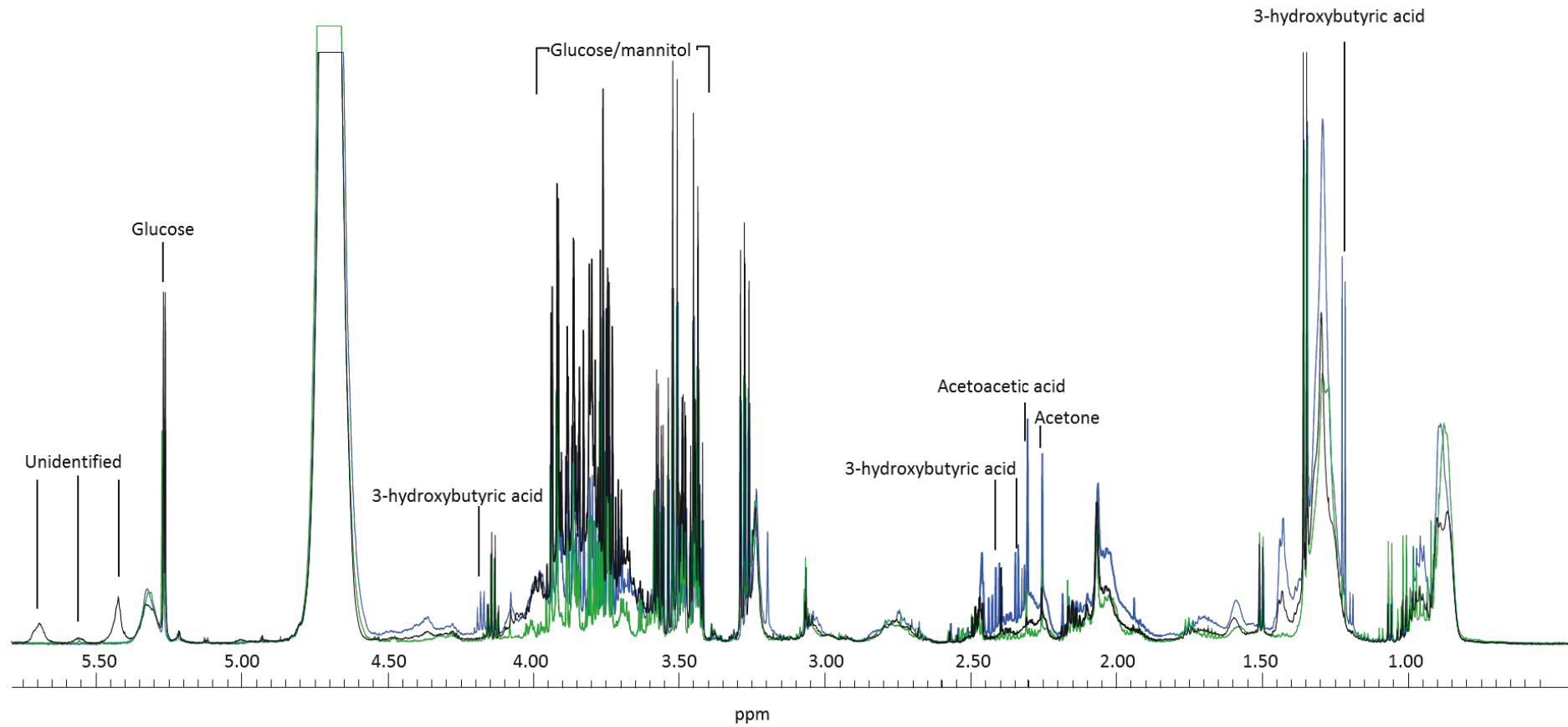
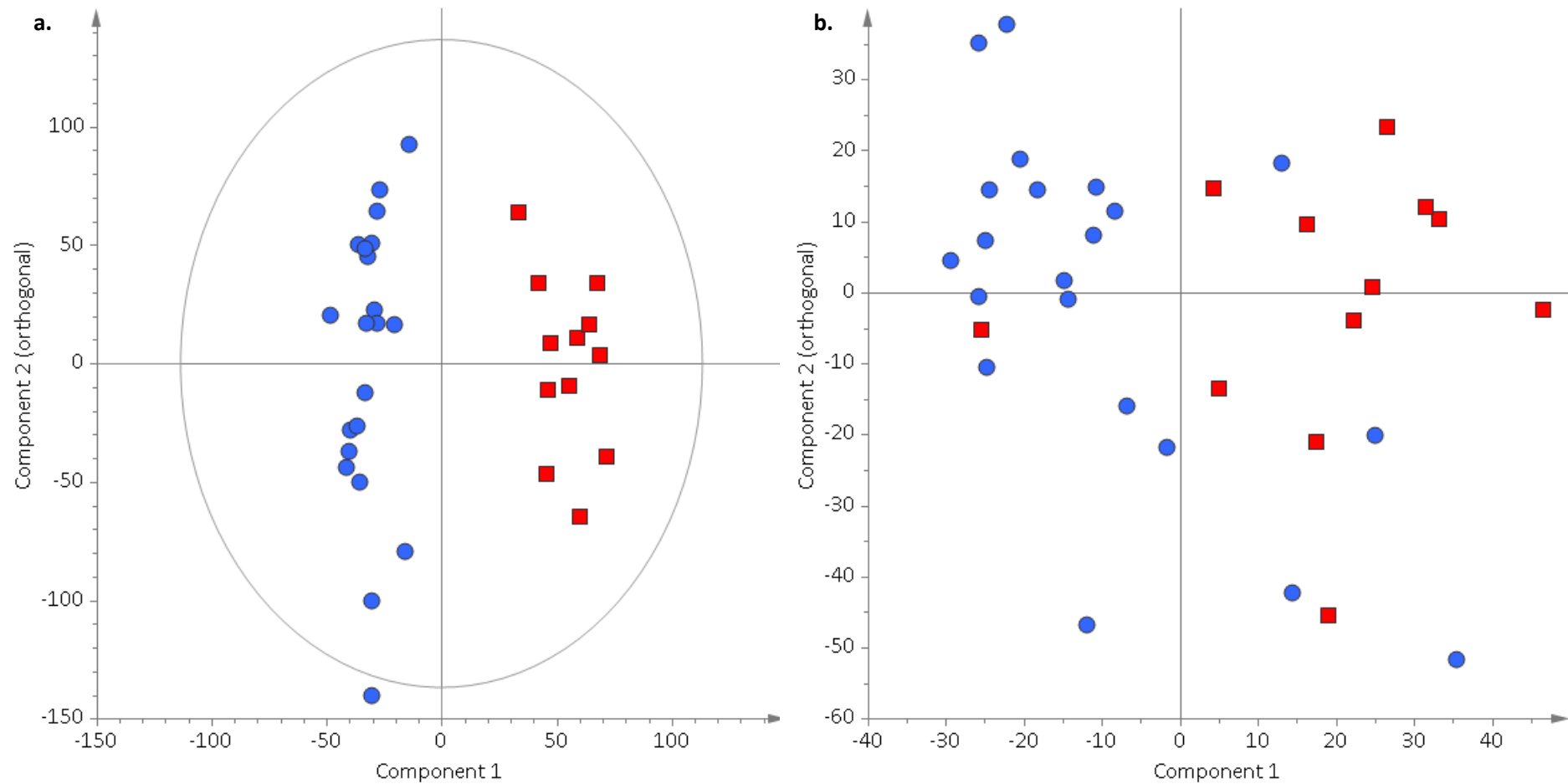


Figure 3.4. OPLS-DA model with one orthogonal component comparing patients admitted with brain injuries, blue circles, to those with pneumonia, red squares, at the start of ventilation (R^2Y 0.95 Q^2Y 0.37 $p=0.01$) a) before and b) after cross validation. Before cross validation the groups can be seen to be separated with pneumonia samples separated in the positive direction along the first component. After cross validation this separation is less with several samples crossing between groups.



Supervised models with OPLS-DA (R^2Y 0.95 Q^2Y 0.37 $p=$ 0.01), figure 3.4, and a PLS-DA (R^2Y 1.0 Q^2Y 0.78) could be built to separate the two groups of patients. However, the PLS-DA model required four components in order to achieve this level of predictive capacity, reflecting the extreme variation in this dataset. After cross validation of the OPLS-DA model several patients could be seen to move between the groups. One pneumonia patient was misclassified as a brain injury after cross validation. Interestingly although this patient had features of pneumonia on admission with chest x-ray changes, a high white cell count, *pneumococcus* isolated from the sputum and an initially high oxygen requirements they showed a rapid clinical improvement and were extubated rapidly. Four of the 21 brain injured patients were misclassified as pneumonia. Of these one went on to develop VAP as defined by CPIS, one did not develop a CPIS high enough to define VAP but was classified as such by an independent assessor and two never showed evidence of VAP, although one of them had an *acinetobacter* species isolated from their sputum.

When the model was validated with the nine patients that had samples taken at the first time point who initially had borderline CPIS and were classified by an independent assessor the model had a sensitivity of 0.5, specificity of 1.0, positive predictive value of 1.0 and a negative predictive value of 0.71. The metabolites identified as being important in causing the separation in this model can be seen in figure 3.5 and 3.6. Many of the metabolites that seem to be important in this comparison appear to be lipid species along with contribution from the amino acids phenylalanine and alanine and also formate.

If only those brain injured patients who did not go on to develop VAP were considered as a comparison group to those with pneumonia at the time of sampling the OPLS-DA model did not improve (R^2Y 0.96 Q^2Y 0.32 $p=$ 0.11) and if validated with the independently assessed patients there were no improvements in the model summary statistics, sensitivity 0.75, specificity 0.6, positive predictive value 0.6 and negative predictive value 0.75. Within this model the same metabolites

Figure 3.5. OPLS-DA regression coefficient plot coloured according to the correlation between the metabolic NMR data and the class information relating to supervised multivariate statistical analyses from figure 3.4. Metabolites dominating in the pneumonia group deflect upwards and in brain injuries downwards. The strength of the correlation of metabolites to this model is given by the intensity of the colour of the peak with red representing the strongest correlation and dark blue no correlation. Figure 3.6 zooms in on important areas of the spectrum with important metabolites labelled.

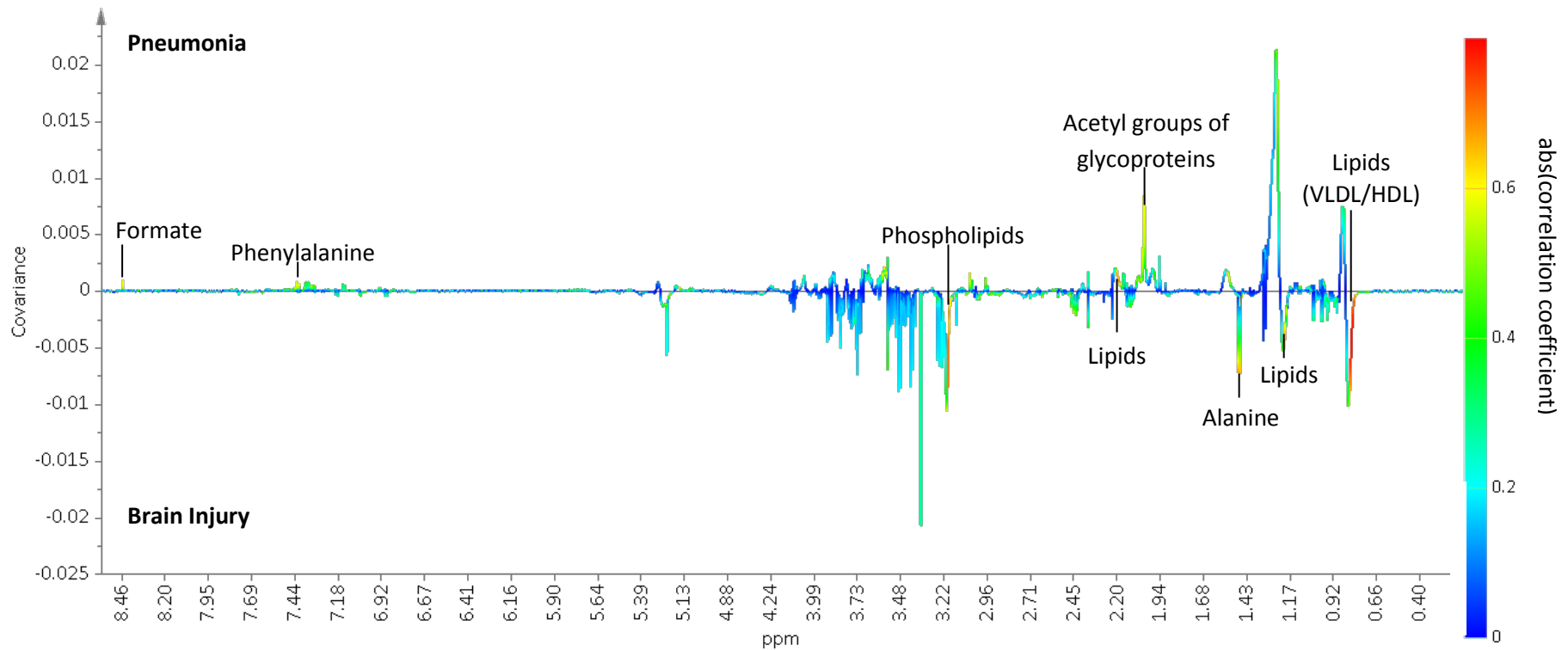
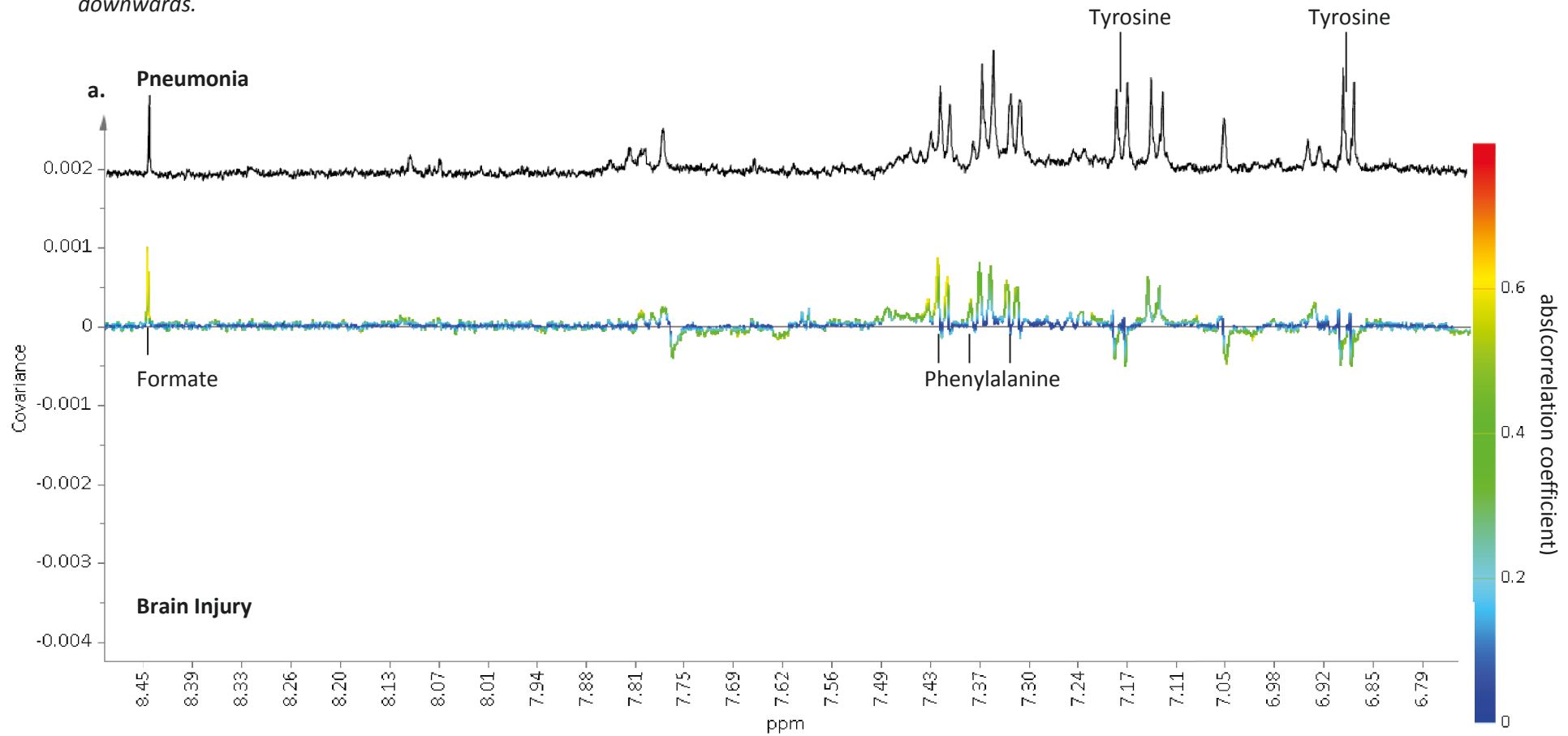
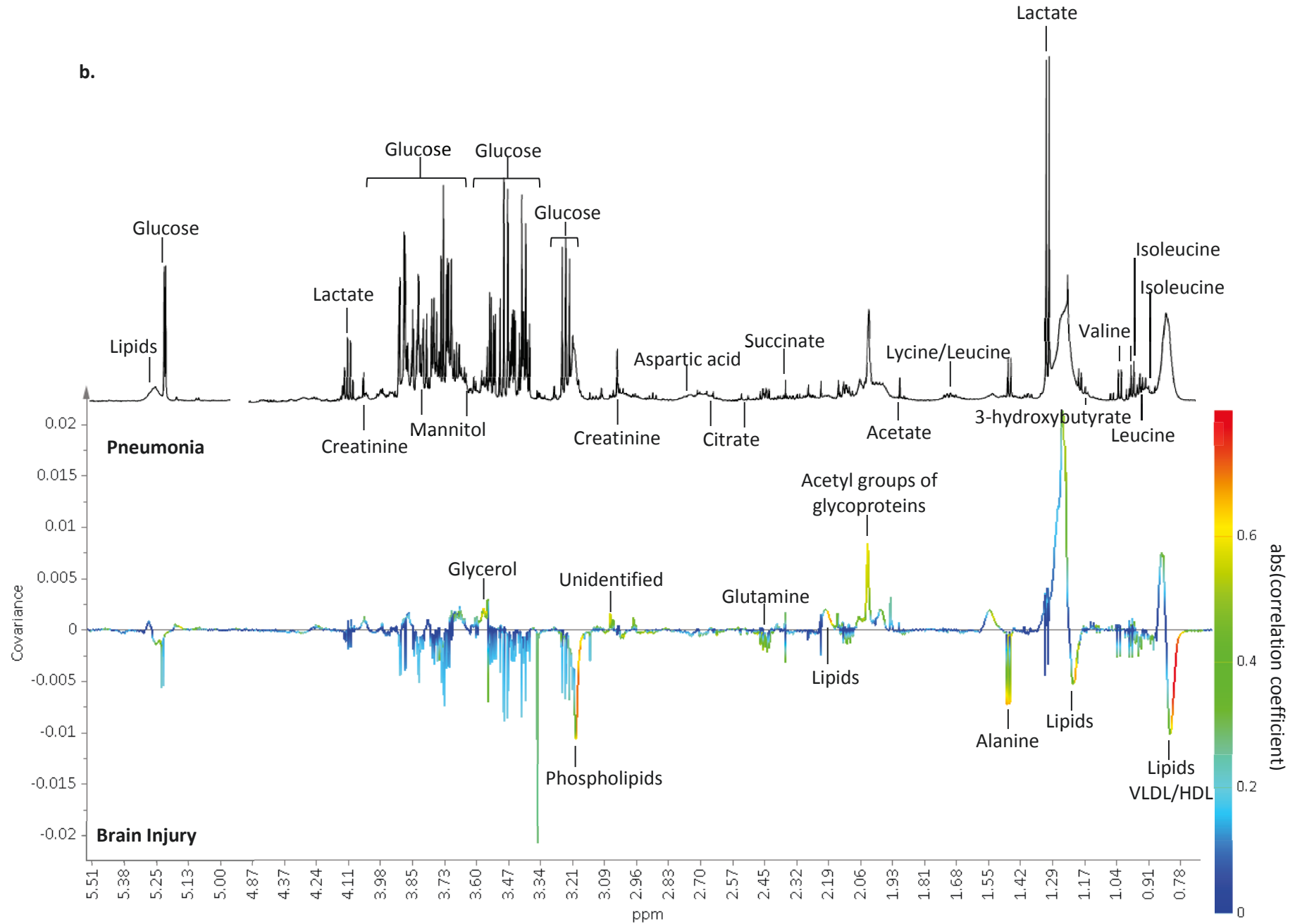


Figure 3.6 Close up portions of the regression co-efficient plot shown with reference spectrum with important metabolites labelled. a. Low field spectral region. b. High field spectral region. The water peak has been removed. The top spectra in black is a representative serum spectrum for a CPMG experiment and the lower figure is the OPLS-DA regression coefficient plot coloured according to the correlation between the metabolic NMR data and the class information relating to the OPLS-DA model from figure 3.4. Metabolites dominating in the pneumonia group deflect upwards and in brain injuries downwards.





caused most of the separation as with the previous model taking all brain injured patients with lipid species, alanine and formate seeming to be of greatest importance.

3.5.2.3 Brain Injury vs VAP

When a three component PCA (R^2X 0.34 Q^2X 0.04) was constructed to explore the comparison of the 21 patients with brain injury but no evidence of pneumonia to the samples taken from the five patients who developed VAP at the time that the infection developed no clear separation could be seen along any components. The same patients whose samples were outliers in the previous PCA models remained similarly placed. An OPLS-DA model with one orthogonal component (R^2Y 0.94, Q^2Y 0.07, $p=0.8$), figure 3.7, had only a very limited ability to separate those with VAP from brain injuries at the time point of admission. After cross validation several brain injured patients were miss-classified as VAP including the same brain injured patients that were miss-classified as Pneumonia in the earlier model comparing brain injuries to pneumonia. The VAP patient that most closely approached the brain injury group was the earliest to be diagnosed with VAP out of the five patients. The sample used for this patient was taken as the CPIS was rising as the peak CPIS occurred on a time point in an interval between the 48hly samples, perhaps missing the peak of the metabolic changes associated with VAP. When this model was used to classify the next sample taken from this patient it falls well within the VAP group suggesting metabolic changes are developing in the initial sample.

When only brain injured patients who did not go on to develop infection were taken as the control group the predictive capacity from cross validation improved to a Q^2Y of 0.16 (R^2Y 0.98, Q^2Y 0.16, $p=0.70$). Similarly, when a larger group of patients was taken that combined the original patients classified via CPIS with those classified by an independent clinical assessor the model also marginally improved (R^2Y 0.94, Q^2Y 0.27, $p=0.055$) when all brain injured patients were taken and to a greater degree when only those without infection at the first time point were taken (R^2Y 1.0, Q^2Y 0.53,

Figure 3.7 OPLS-DA model with one orthogonal components comparing serum from patients admitted with brain injuries at the start of ventilation, blue circles, to serum from those who developed VAP at the time infection developed, green triangles, (R^2Y 0.94, Q^2Y 0.07, $p=0.8$) a) before and b) after cross validation. Before cross validation the groups can be seen to be separated with VAP samples distributed in the positive direction along the first component. After cross validation this separation is less with several samples crossing between groups.

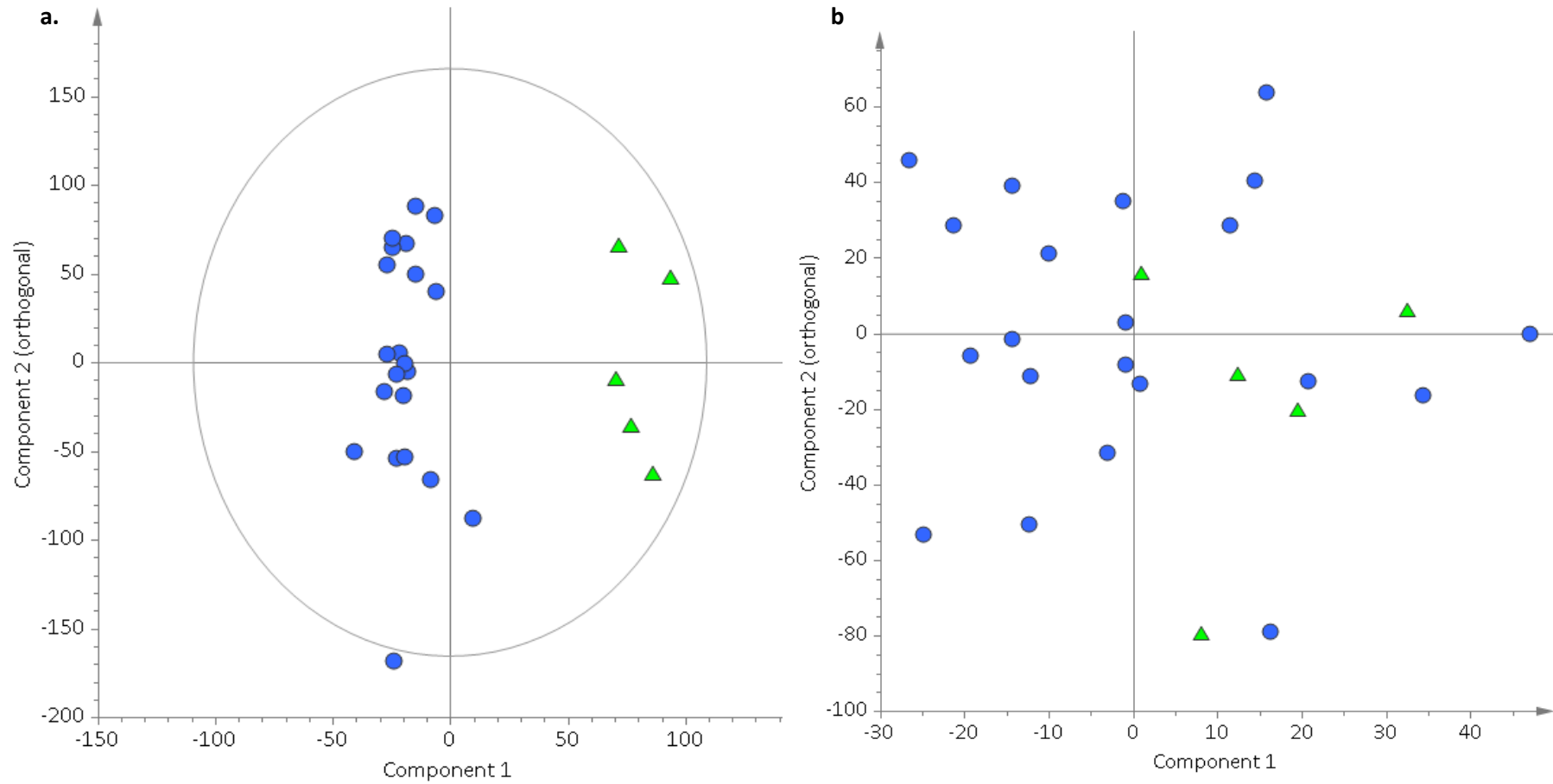
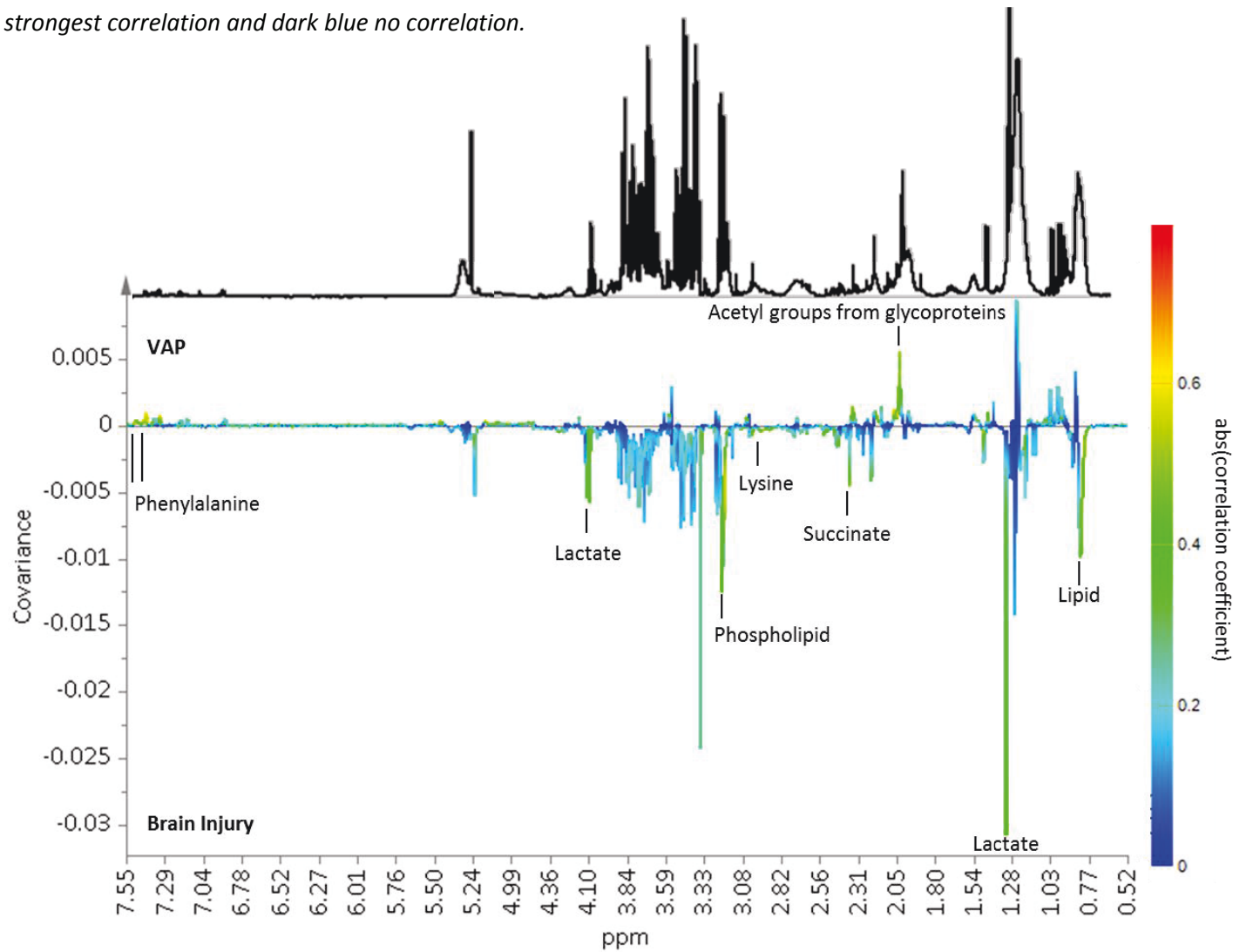


Figure 3.8. OPLS-DA regression coefficient plot, shown with a reference spectrum, coloured according to the correlation between the metabolic NMR data and the class information relating to supervised multivariate statistical analyses from figure 3.7. Metabolites dominating in the VAP group deflect upwards and in brain injuries downwards. The strength of the correlation of metabolites to this model is given by the intensity of the colour of the peak with red representing the strongest correlation and dark blue no correlation.



p=0.37). However, the metabolites causing separation between brain injured patients with VAP and those at admission were similar between all of the above comparisons, figure 3.8, with lipids, glycoproteins and some amino acids such as phenylalanine leading to the separation between groups.

3.5.2.4 Time Course

As any metabolic changes seen when samples taken from patients with brain injuries at the start of ventilation were compared to those when VAP developed could have been related to the length of stay on intensive care as opposed to the development of infection further analysis was performed on sequential time points from the brain injured patients who did not go on to develop VAP. When OPLS-DA was used to compare the first time point to the fourth time point some, although limited, separation was seen when both the original groups based on CPIS (R^2Y 0.98, Q^2Y 0.11, $p=0.82$) and combined groups including the independently classified patients (R^2Y 0.99, Q^2Y 0.09, $p=0.96$) were used, although in neither case did the models reach statistical significance, possibly due to the small group sizes in these comparisons. Although few of the metabolites had a particularly strong correlation in these models, figure 3.9, there was a trend for phenylalanine and acetyl groups from glycoproteins to increase over time and glucose, citrate, and glutamine to decrease. When the first time point was compared to either time point two or three, the metabolic changes were less marked suggesting that the changes seen between time point one and four were gradual over the course of the ICU stay and did not happen rapidly, for example after treatment was commenced.

When the patients admitted with pneumonia were examined over the course of their stay an OPLS-DA model with only one component (R^2Y 0.70, Q^2Y 0.10, $p=0.44$) comparing the first time point to the last time point demonstrated that there were strongly correlated changes in lipid signals over time with all lipid regions tending to increase with glucose, again, showing a tendency to fall, figure

Figure 3.9. OPLS-DA regression coefficient plot, shown with an example spectrum, coloured according to the correlation between the metabolic NMR data and the class information relating to supervised multivariate statistical analyses comparing patients admitted with brain injuries at the first time point and the fourth. Metabolites dominating in the fourth time point ($n=5$) deflect upwards and in the first ($n=12$) downwards. The strength of the correlation of metabolites to this model is given by the intensity of the colour of the peak with red representing the strongest correlation and dark blue no correlation.

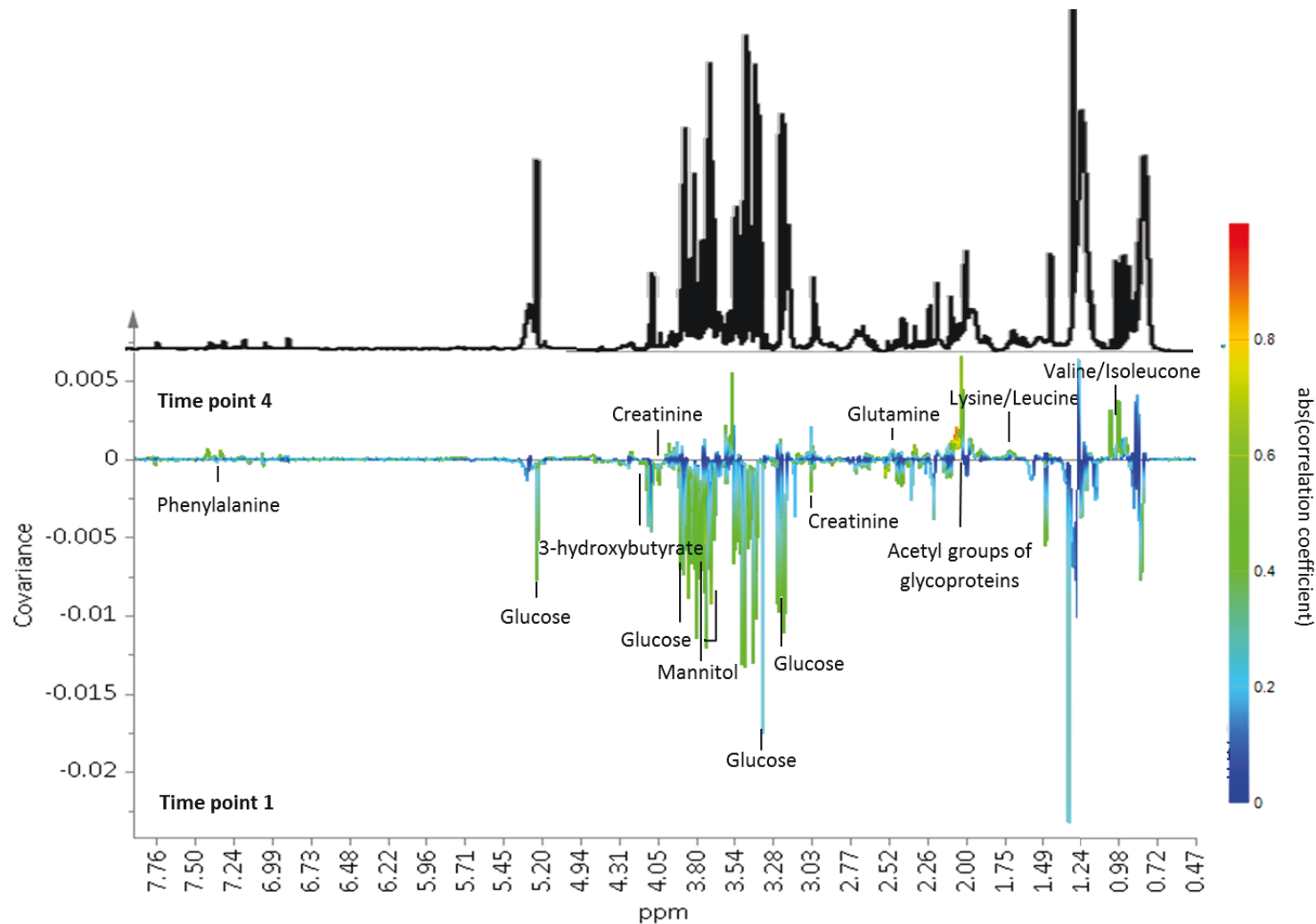
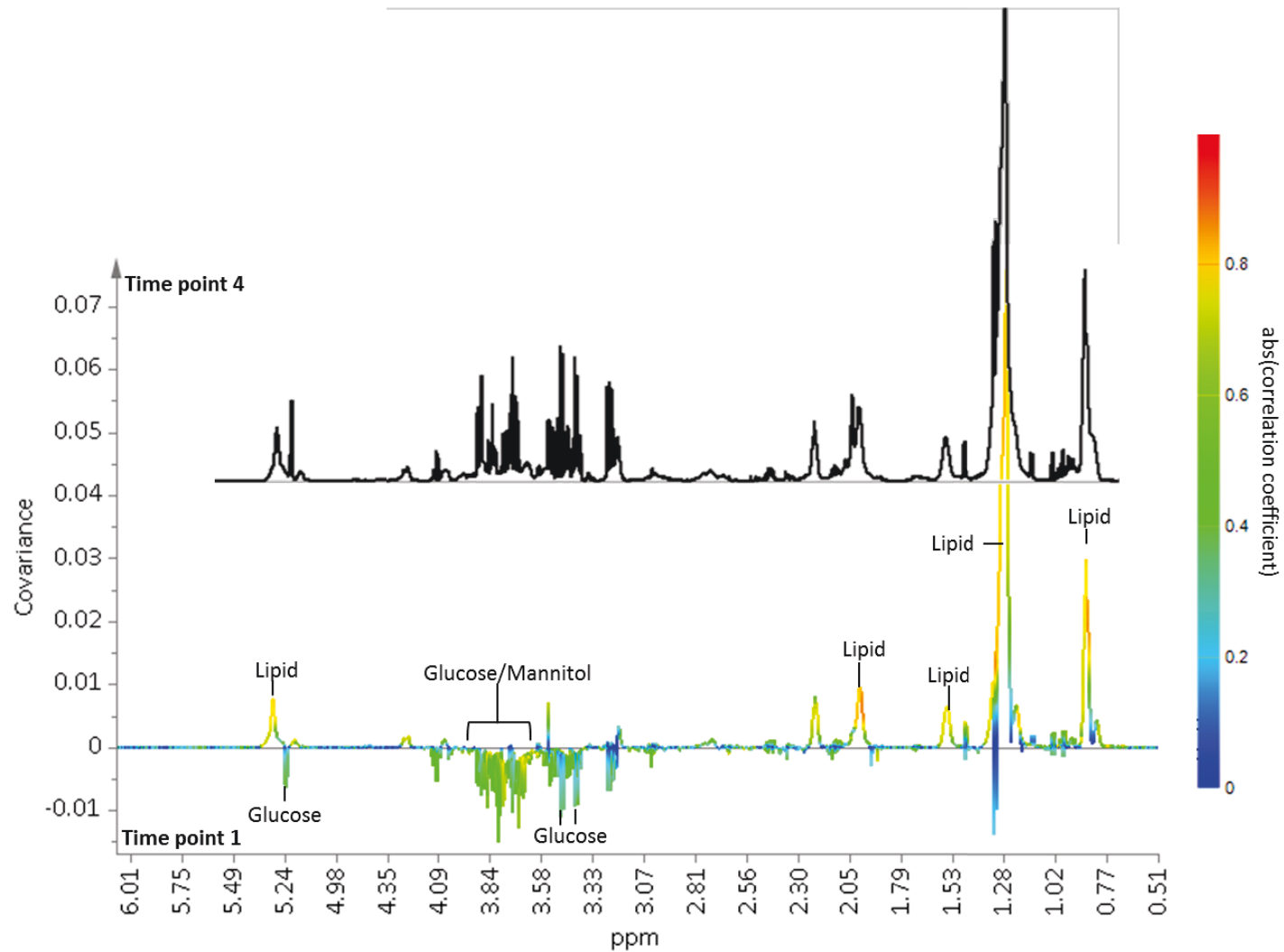


Figure 3.10. OPLS-DA regression coefficient plot, shown with an example spectrum, coloured according to the correlation between the metabolic NMR data and the class information relating to supervised multivariate statistical analyses comparing patients admitted with pneumonia at the first time point and the fourth. Metabolites dominating in the fourth time point ($n=6$) deflect upwards and in the first ($n=11$) downwards. The strength of the correlation of metabolites to this model is given by the intensity of the colour of the peak with red representing the strongest correlation and dark blue no correlation.



3.10. However, when only paired samples, those patients who had samples from both time point one and four, were used the strength of the correlation of the lipid signals diminished although the trends remained. Although the correlation was not as strong in this cohort of patients, phenylalanine appeared to reduce over time in contrast to the trend seen in the brain injured patients. If the fourth time point samples from brain injured patients were compared to the same time points from patients with pneumonia an OPLS-DA model (R^2Y 0.99, Q^2Y 0.20, $p=0.81$) demonstrated that at this time during ICU stay lipids tended to be higher within the pneumonia patients compared to those with brain injuries.

When the fourth time point from brain injured patients who did not develop VAP was compared to the time point where VAP developed in the infected patients it was not possible to construct an OPLS-DA model that would separate the groups (R^2Y 0.93, Q^2Y -0.38). However, if the combined group of patients, including those classified by an independent assessor, was used a positive Q^2 was obtained (R^2Y 1.0, Q^2Y 0.28, $p=0.73$). In this model, figure 3.11, few metabolites had a co-efficient of correlation much above 0.5. Those metabolites that were most strongly correlated with one or other disease class were phenylalanine which remained higher in the VAP group and glucose and alanine which were higher in those that did not go on to develop VAP.

Using the original group based on CPIS or the combined group using the independently classified patients it was not possible to build an OPLS-DA model that would distinguish the time that VAP developed from the first sample taken when these patients were admitted to intensive care with the Q^2 never being positive (R^2Y 0.92, Q^2Y -0.10).

Figure 3.11. OPLS-DA regression coefficient plot, shown with an example spectrum, coloured according to the correlation between the metabolic NMR data and the class information relating to supervised multivariate statistical analyses comparing patients admitted with brain injuries who did not go on to develop pneumonia at time point four to the time point that VAP developed in those that developed infection. Metabolites dominating in the VAP group ($n=7$) deflect downwards and those without ($n=6$) upwards. The strength of the correlation of metabolites to this model is given by the intensity of the colour of the peak with red representing the strongest correlation and dark blue no correlation.

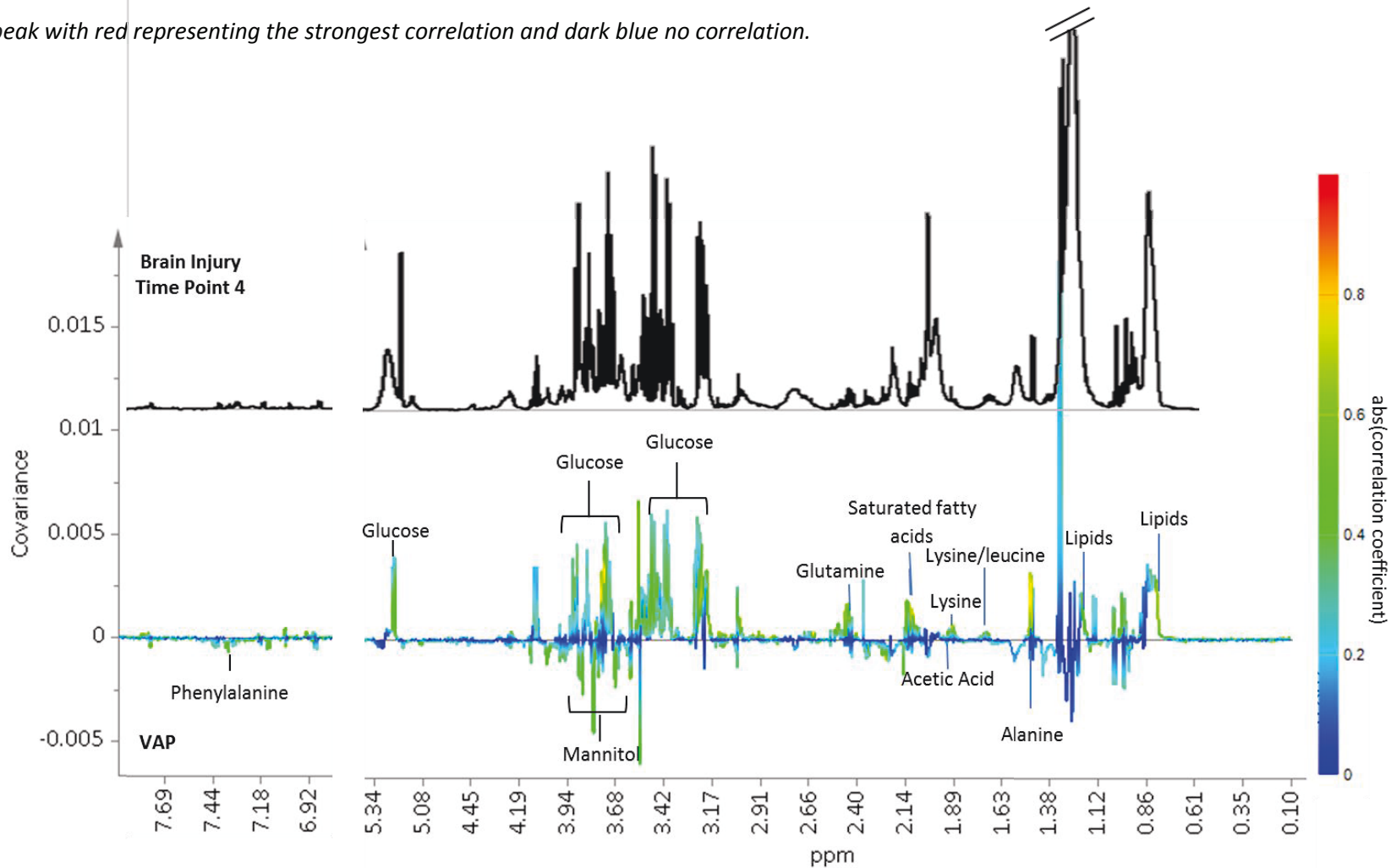


Figure 3.12 One component PCA analysis comparing urine samples taken from patients with brain injuries, blue circles, and patients with pneumonia, red squares, at the start of ventilation ($R^2 \times 0.19$ $Q^2 \times 0.06$). The first component is given on the y-axis against the sample number, x-axis. Three outliers can be identified, two from the brain injury group and one from the pneumonia group as can be seen with the three points lying below the 2 SD line. No clear class-related separation can be seen along the first component of the remainder of the samples.

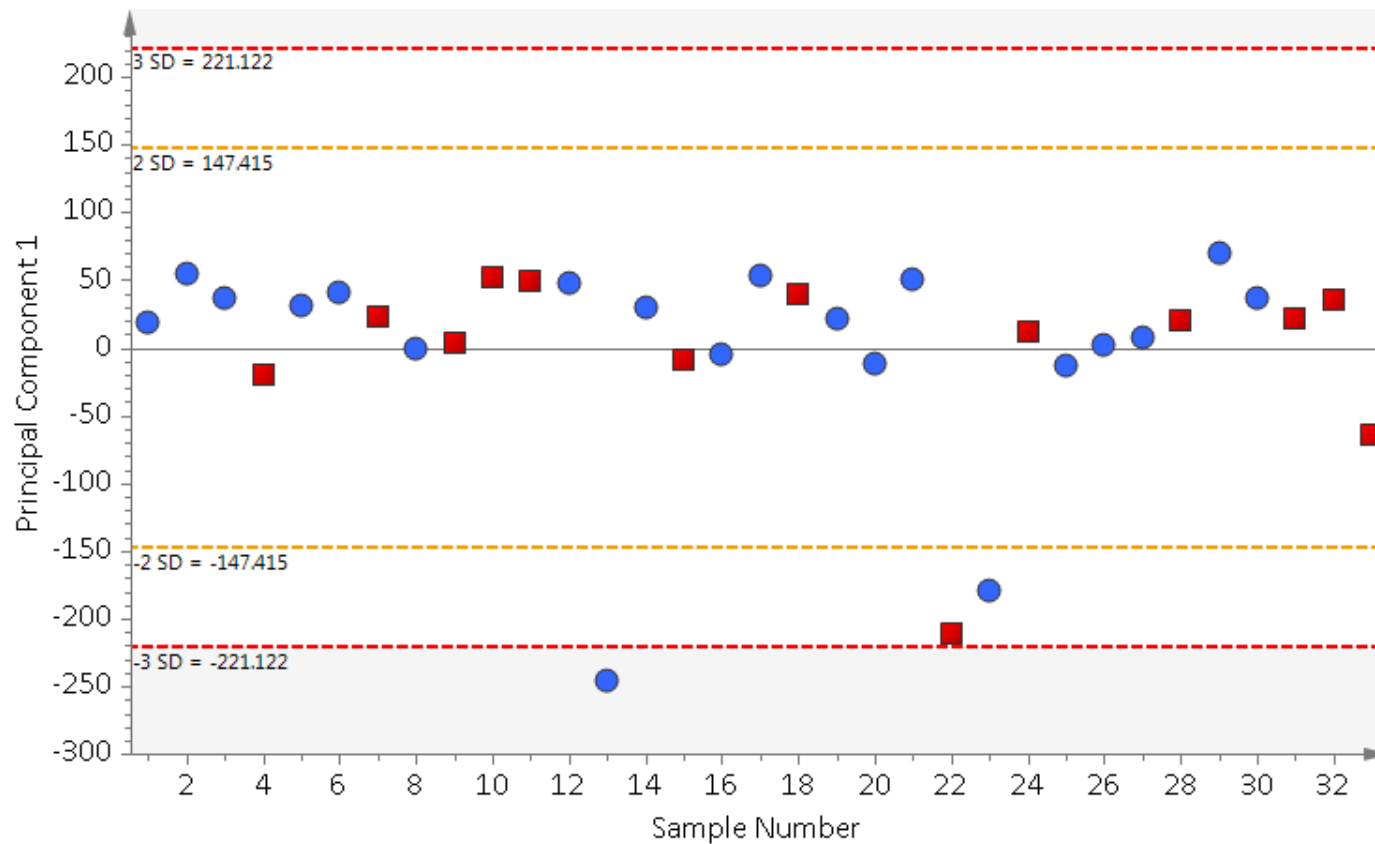
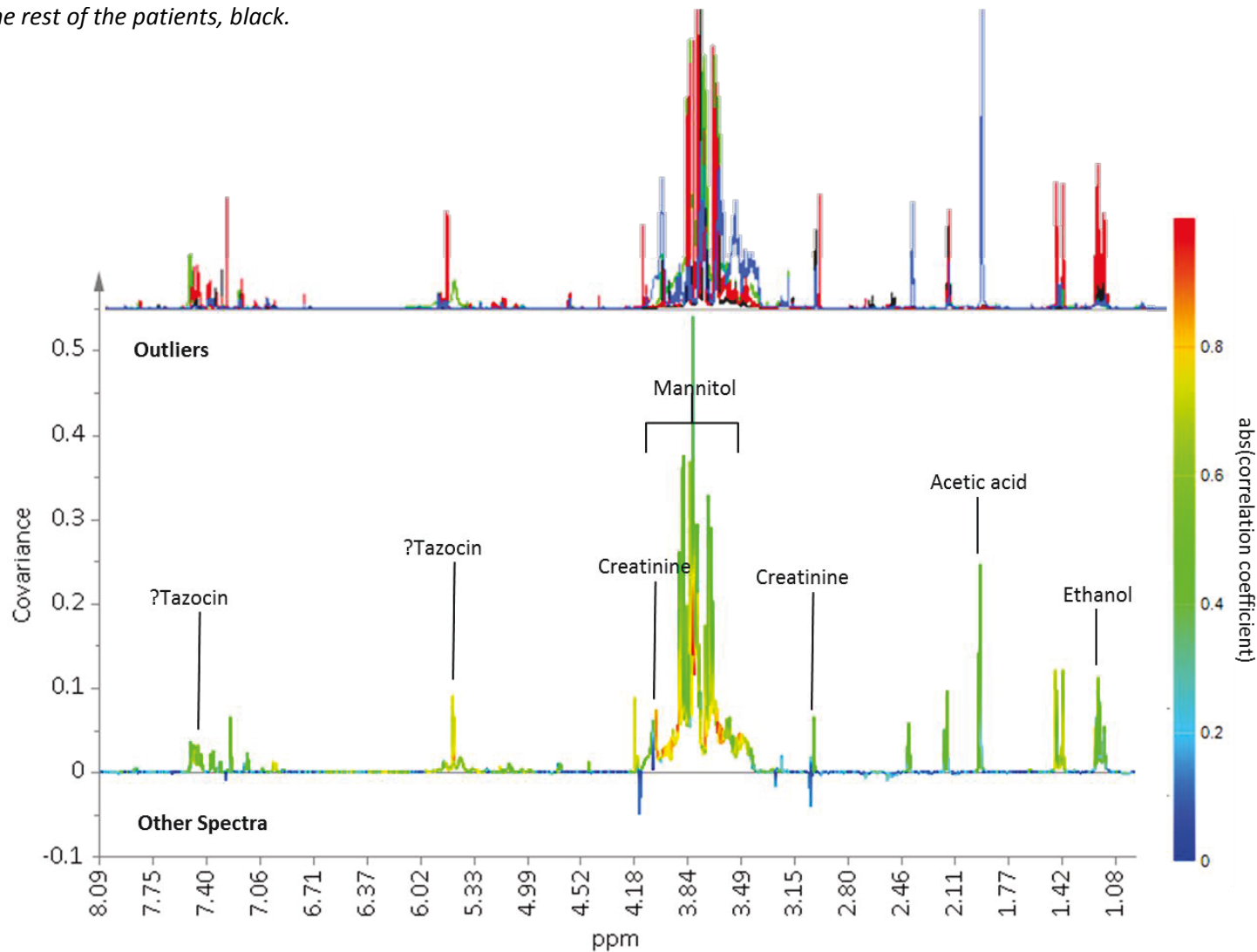


Figure 3.13. OPLS-DA regression coefficient plot coloured according to the correlation between the metabolic NMR data and the class information relating to supervised multivariate statistical analyses comparing the three outliers from figure 3.12 with the rest of the patients. Metabolites dominating in the outliers deflect upwards. The strength of the correlation of metabolites to this model is given by the intensity of the colour of the peak with red representing the strongest correlation and dark blue no correlation. The spectra from the outliers are given for comparison, blue, red and green along with a representative spectrum from the rest of the patients, black.



3.5.3 Urine

3.5.3.1 Brain Injury vs Pneumonia

Initial comparison, with PCA, of the 20 brain injured patients with the 13 pneumonia patients who had urine samples taken at the first time point following the onset of ventilation demonstrated three outliers, figure 3.12. When these outliers were examined, figure 3.13, no clear technical differences could be seen leading to these samples being outliers. Instead there seemed to be differences in both the presence of some metabolites and the quantities of others. As there were no technical reasons to omit these patients they were included in further analysis.

When an OPLS-DA model was made of this data, figure 3.14, (R^2Y 0.83, Q^2Y 0.37, $p=0.009$) it had a sensitivity of 0.75, specificity of 0.8, positive predictive value of 0.75 and negative predictive value of 0.8 after validation with the independently classified patients, four with pneumonia and five with brain injuries. If only those patients who did not go on to develop VAP were used the model had a similar performance (R^2Y 0.92, Q^2Y 0.45, $p=0.08$) at cross-validation. In case the outliers identified in the PCA were exerting a disproportional effect on the model it was repeated excluding these three patients. With this model the general pattern remained the same with similar model statistics (R^2Y 0.97 Q^2Y , 0.33, $p=0.13$).

The metabolites that caused the majority of the separation, figure 3.15, were more difficult to characterise than in the serum models due to marked heterogeneity of the urine samples. Of those metabolites identified creatinine excretion appeared higher in the brain injury group. When the clinical data was examined, although there was no significant difference between the two groups, there is a trend to the serum creatinine to be higher in the pneumonia patients (91.9 ± 71.5 vs 74.3 ± 22.6 $\mu\text{mol/l}$, $p=0.33$) with similar average hourly urine output within the 24h prior to sampling (113.3 ± 59.0 vs 130.4 ± 99.9 ml/h , $p=0.55$). This data may represent a lower creatinine clearance

Figure 3.14 OPLS-DA model with one orthogonal components comparing urine from patients admitted with brain injuries at the start of ventilation, blue circles, to urine from those with pneumonia, red squares, (R^2Y 0.83 Q^2Y 0.37 $p=0.009$) a. before and b. after cross validation. Before cross validation the groups can be seen to be separated with pneumonia samples distributed in the positive direction along the first component, even before cross validation one of the brain injury patients can be seen to fall within the pneumonia group. One of the pneumonia samples can be seen to be on outlier along the orthogonal component, y-axis. After cross validation this separation is less with several samples crossing between groups, especially with brain injured patients being miss-classified as pneumonia.

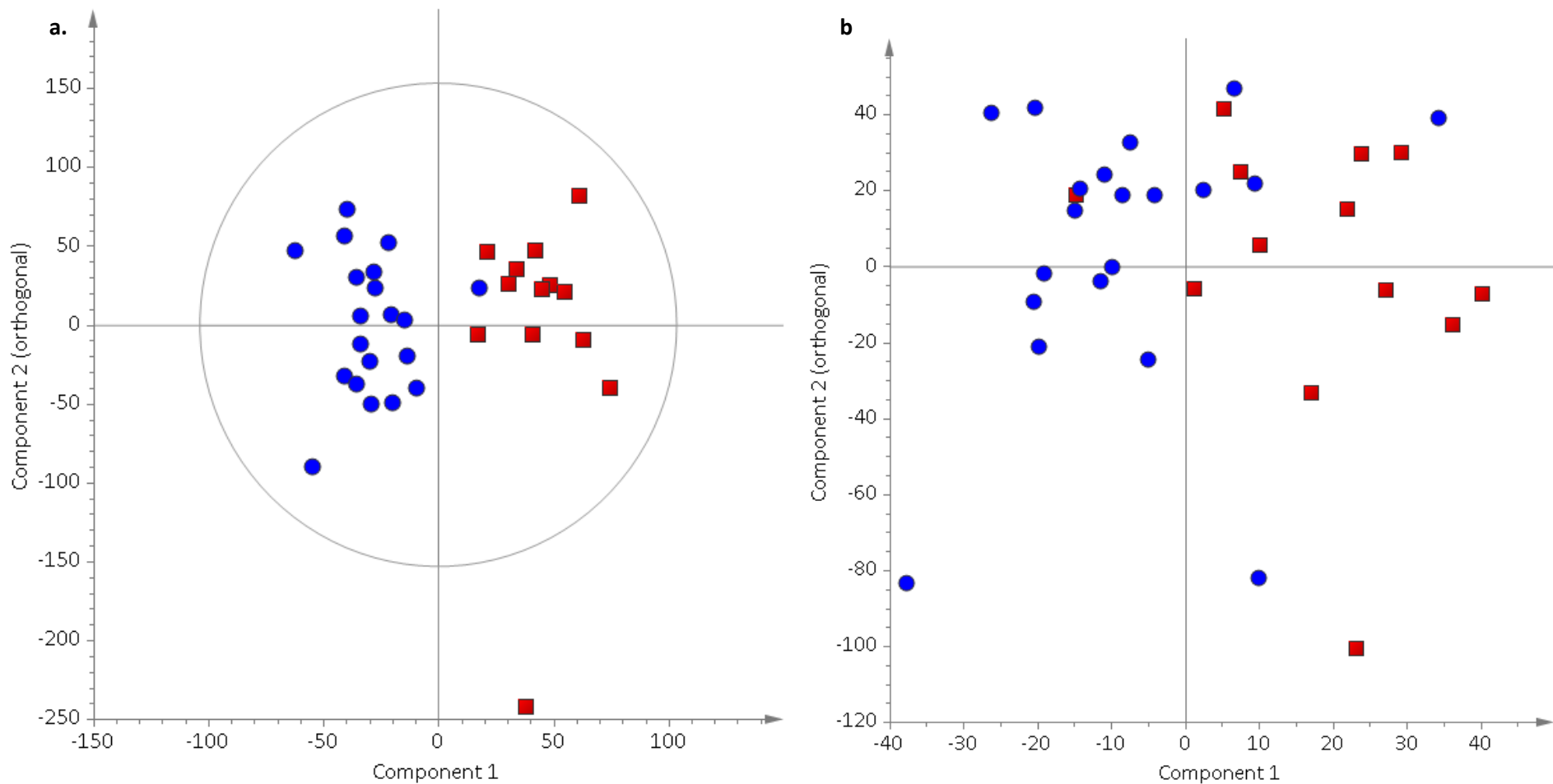
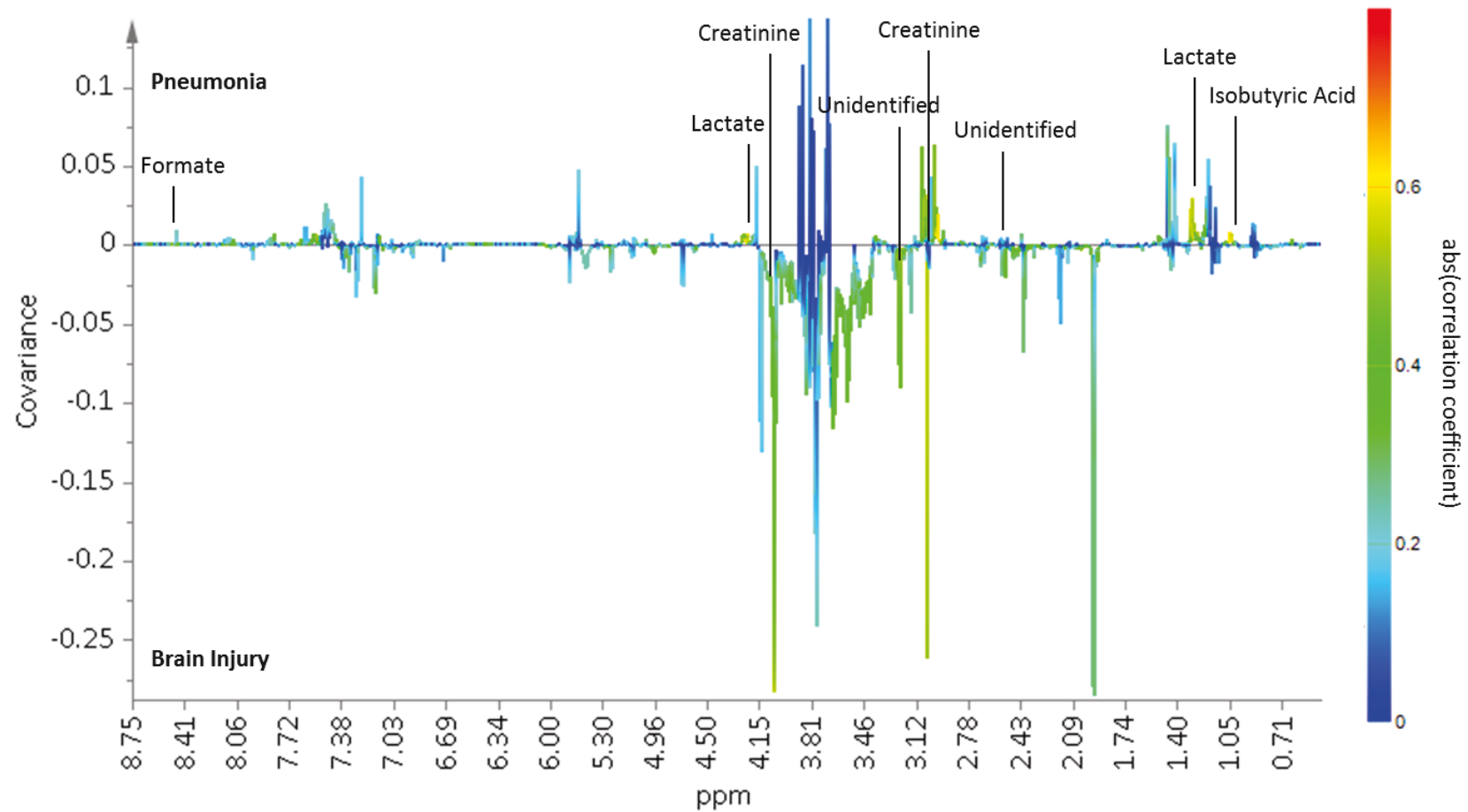


Figure 3.15. OPLS-DA regression coefficient plot coloured according to the correlation between the urine metabolic NMR data and the class information relating to supervised multivariate statistical analysis, figure 3.14, comparing the patients with brain injuries to those with pneumonia. Metabolites dominating in the pneumonia group deflect upward and those in the brain injured patients downwards. The strength of the correlation of metabolites to this model is given by the intensity of the colour of the peak with red representing the strongest correlation and dark blue no correlation.



associated with pneumonia and infection. Also when serum levels of lactate close to the time of sampling were compared there was no significant difference between the groups (1.43 ± 0.91 vs 1.26 ± 0.50 mmol/l, $p=0.54$).

3.5.3.2 Brain Injury vs VAP

PCA of the urine samples taken from the brain injured patients at the point of admission to ICU and those taken at the time that VAP developed (R^2X 0.311, Q^2X 0.02) demonstrated the same outliers as when the brain injured patients were compared to those with pneumonia but with no clear separation of the samples into groups. OPLS-DA was also unable to separate the two groups (R^2Y 0.61, Q^2Y -0.08) even if a combined patient group was used (R^2Y 0.51, Q^2Y -0.09). However, if only those patients who did not get VAP were used as controls the Q^2 of the model improved (R^2Y 0.90, Q^2Y 0.33, $p=0.31$). When the metabolites causing separation in this model were examined very few had strong correlations with either group and those that did appeared to be present in only one or two of the samples analysed. This indicated the impact on the model that a few metabolites may have if present in large quantities in a few samples. The fact that these metabolites were not universally present raised the possibility that they may arise from an exogenous source such as drugs that were not universally administered to all patients or that were metabolised differently in different patients producing differing metabolic profiles.

3.5.3.3 Time Course

When the urine samples collected at the first time point, $n=11$ from those patients with brain injuries who did not develop VAP were compared to those from the fourth time point, $n=5$, using OPLS-DA (R^2Y 0.91, Q^2Y 0.31, $p=0.36$), figure 3.16, the metabolites that could be identified that seemed to separate the two groups were often related to medication metabolites such as paracetamol-glucuronide and mannitol. The metabolic changes observed seemed to be gradual as it

Figure 3.16. OPLS-DA regression coefficient plot coloured according to the correlation between the metabolic NMR data and the class information relating to supervised multivariate statistical analysis, comparing urine samples from the patients with brain injuries who do not develop VAP at time point 1 and 4. Metabolites dominating at the first time point deflect downwards and those at the fourth upwards. The strength of the correlation of metabolites to this model is given by the intensity of the colour of the peak with red representing the strongest correlation and dark blue no correlation.

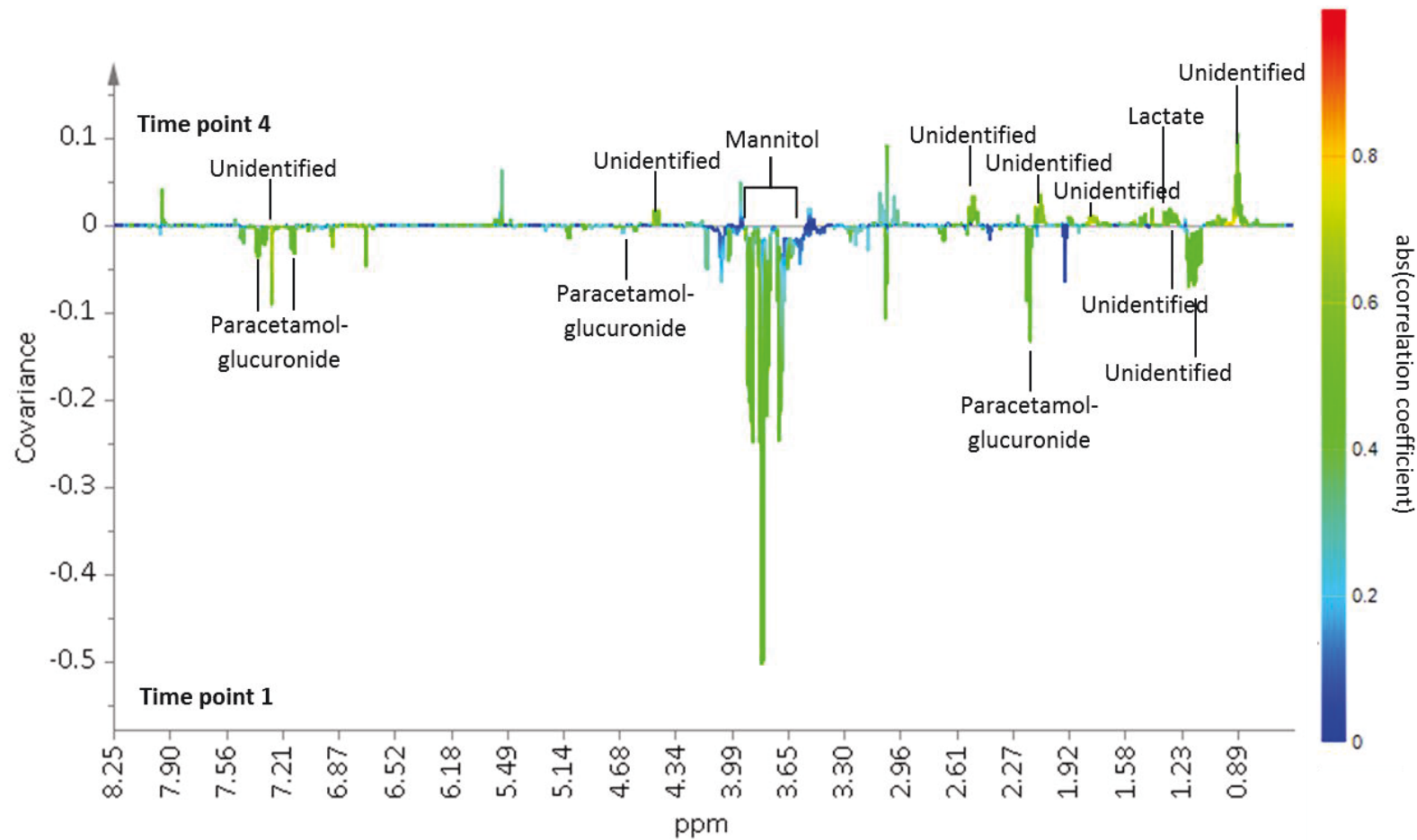
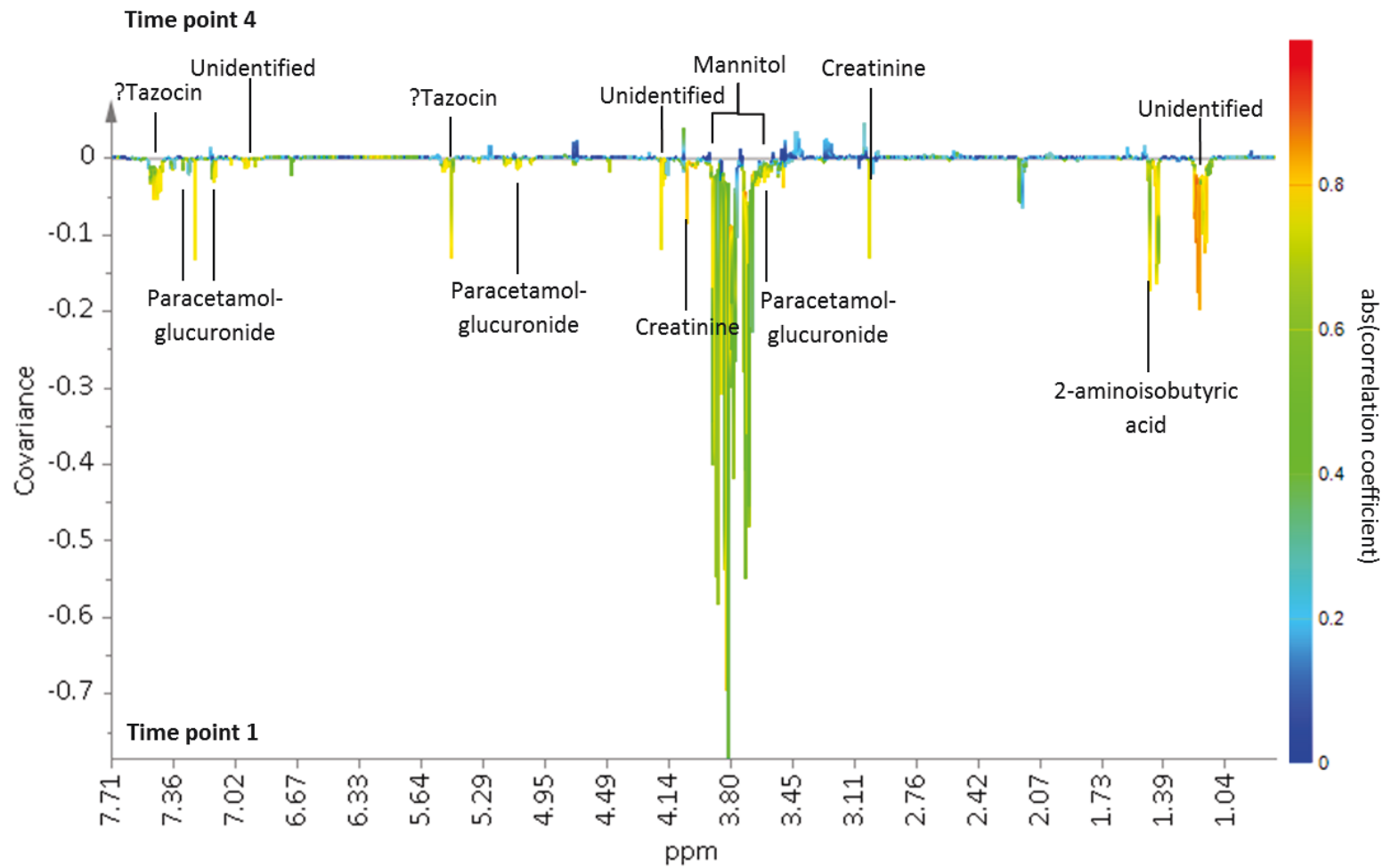


Figure 3.17. OPLS-DA regression coefficient plot coloured according to the correlation between the metabolic NMR data and the class information relating to supervised multivariate statistical analysis, comparing urine samples from the patients with pneumonia at time point 1 and 4. Metabolites dominating at the first time point deflect downwards and those at the fourth upwards. The strength of the correlation of metabolites to this model is given by the intensity of the colour of the peak with red representing the strongest correlation and dark blue no correlation.

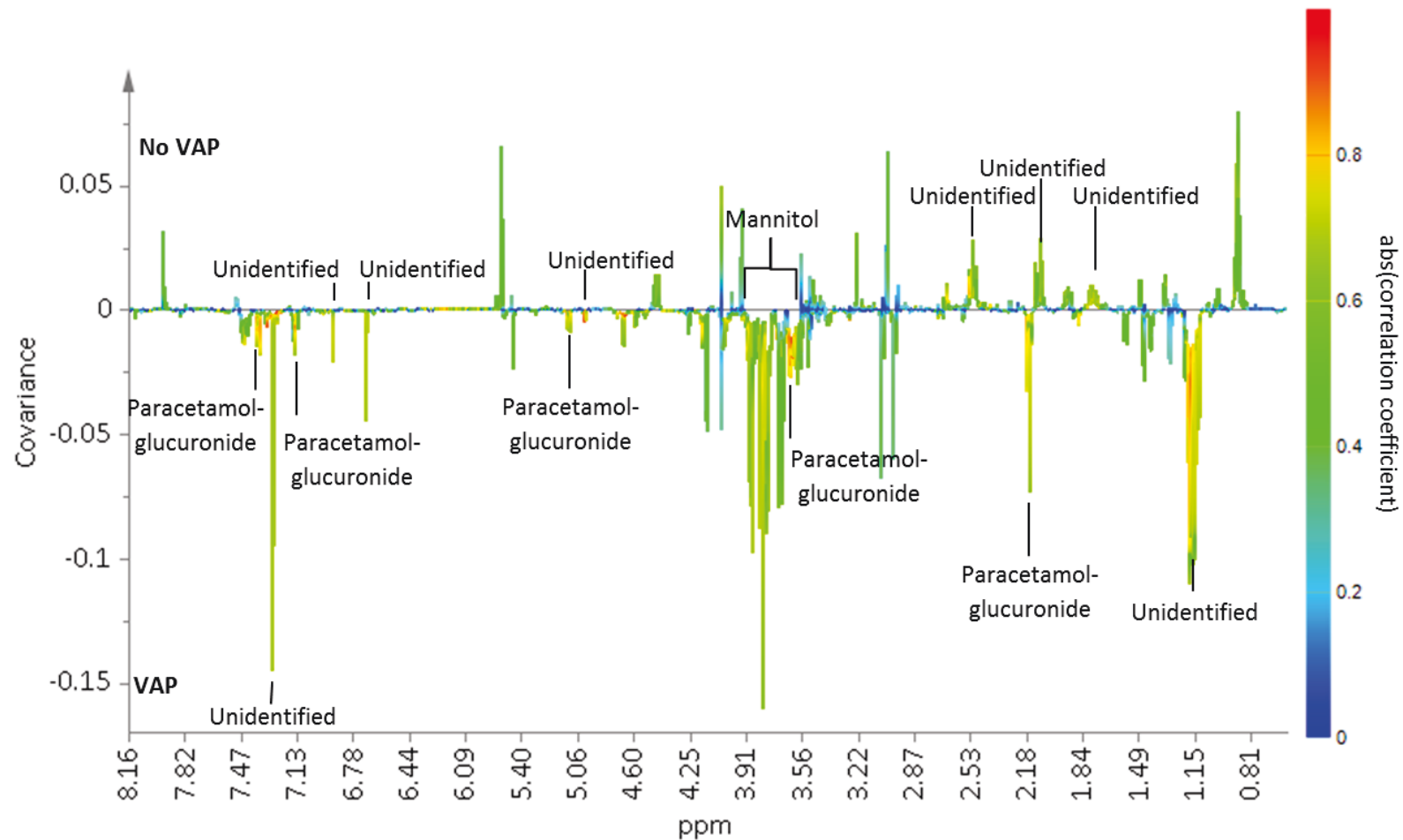


was not possible to build predictive models to separate time point one from either time point two or three. When the same comparison, of time point one and four, was made for the patients who were admitted with pneumonia (R^2Y 0.47, Q^2Y 0.02, $p=0.82$) the model had only a minimal predictive capacity. However, the metabolites associated with this model had much stronger correlations with the groups, figure 3.17. Several metabolites were strongly associated with time point one, however, of those that were identifiable several appeared to be drugs or their metabolites. The fact that many of the peaks were not clearly identifiable when compared to metabolites contained within the database may imply that they were also related to drug metabolism and not naturally occurring metabolites.

When the urine samples taken when brain injured patients developed VAP were compared to samples taken at a similar time from those who did not go on to develop infection an OPLS-DA could be constructed (R^2Y 0.74, Q^2Y 0.29, $p=0.30$), figure 3.18, with a number of strongly associated metabolites. If the combined group of patients was used to construct the model the Q^2Y rapidly diminished (R^2Y 0.61, Q^2Y 0.04, $p=0.78$) although the pattern of metabolite changes appeared similar warranting further investigation of the potential of these metabolite as classifiers. However, as with the previous models the metabolites in question were difficult to identify and some of them appeared to be related to drug metabolites.

Looking only at the brain injured patients who developed VAP during their stay, an OPLS-DA model based on the original group was unable to differentiate the time that VAP developed from the initial time point after admission (R^2Y 0.87, Q^2Y -0.12). If, however, the combined group was used the Q^2Y improved (R^2Y 0.55, Q^2Y 0.10, $p=0.49$) although the spectral region most strongly associated with this model was that associated with mannitol suggesting that we were not seeing genuine differences due to disease but associated treatments.

Figure 3.18. OPLS-DA regression coefficient plot coloured according to the correlation between the metabolic NMR data and the class information relating to supervised multivariate statistical analysis, comparing urine samples from the patients with brain injuries who do not develop VAP at time point 4 with the time point that VAP develops in those that do. Metabolites dominating in the VAP group deflect downwards and those in those without VAP upwards. The strength of the correlation of metabolites to this model is given by the intensity of the colour of the peak with red representing the strongest correlation and dark blue no correlation.



3.5.3.4 Treatment Effect

As illustrated in the last examples, the fact that many drugs are excreted via the urine risked these models showing effects based, not on differences due to pathology, but due to the effects of treatments that may be more common in one or more of the groups.

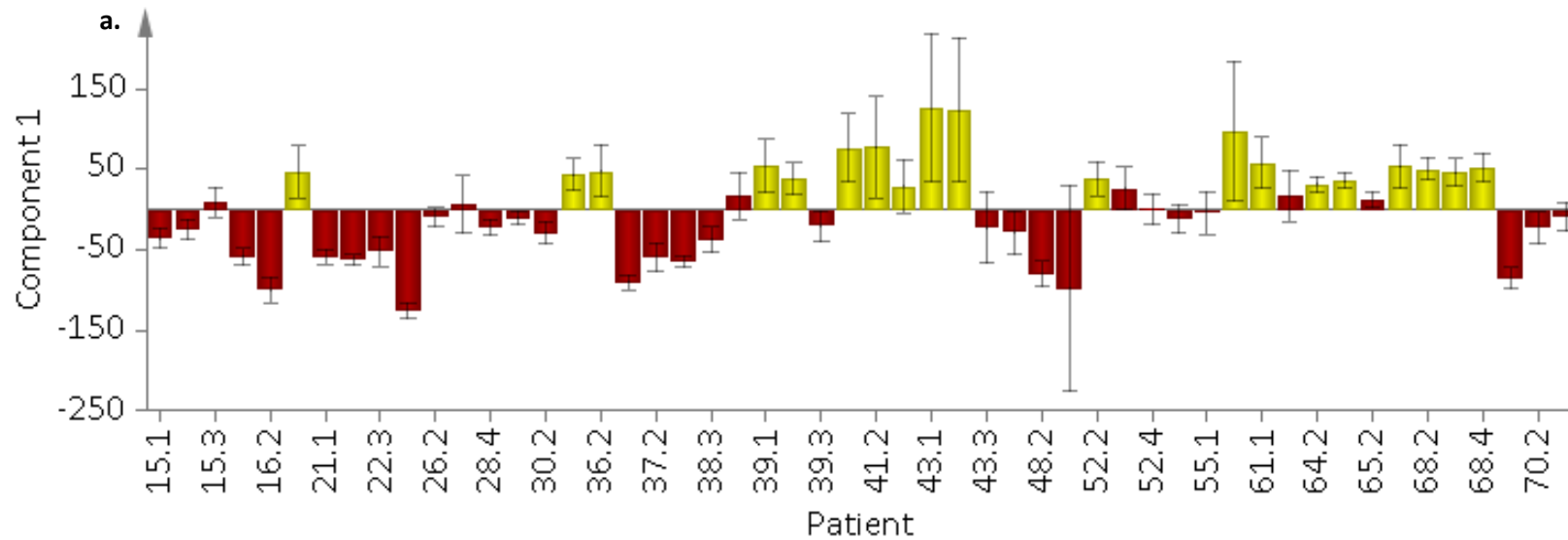
In an attempt to address this problem a correlation matrix was constructed to correlate the samples taken whilst patients were on each documented drug with the urine ^1H NMR spectra. This allowed peaks that seemed important in discriminant models to be correlated with drug data to try to establish if they were potentially related to treatment as opposed to disease.

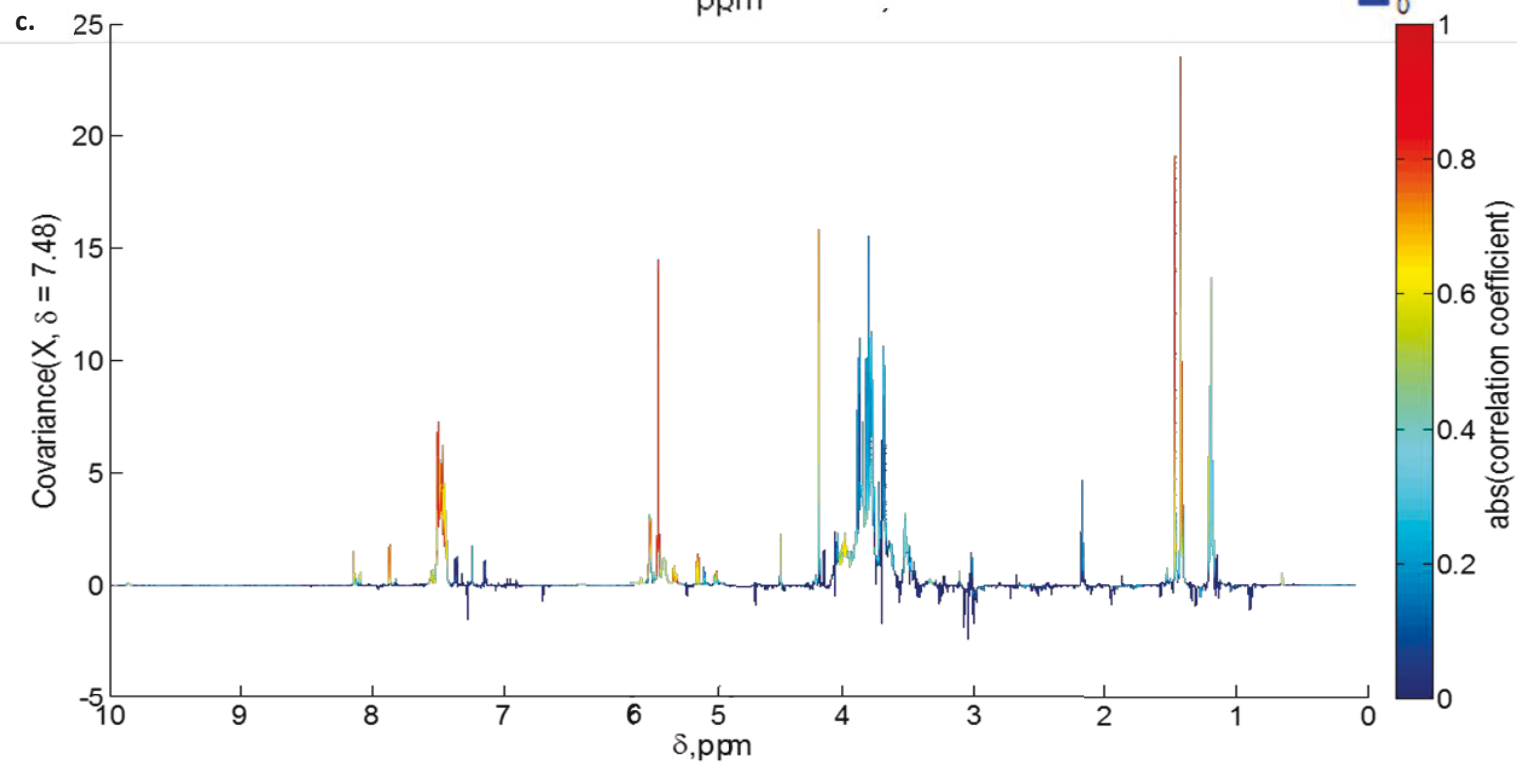
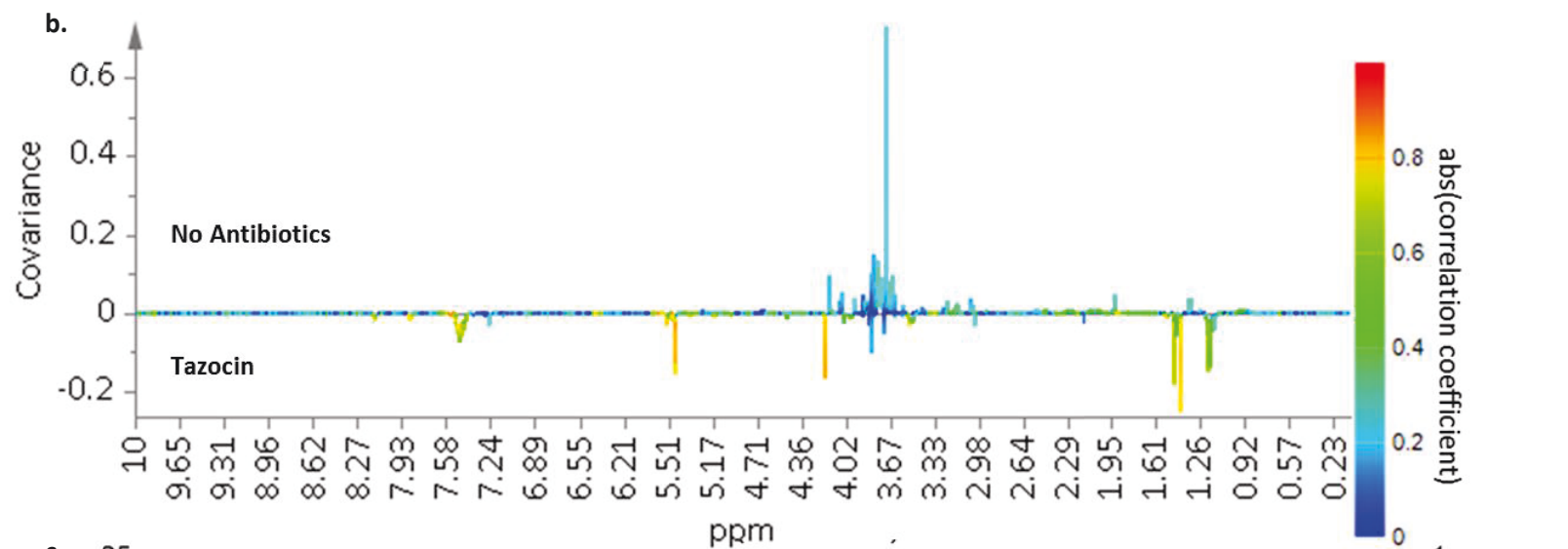
Also the rates of drug use in each group were compared. OPLS-DA models were constructed comparing samples taken whilst patients were on a given drug with those taken in the absence of the drug for drugs where there was a difference of more than 20% in the use of a drug between groups of clinical interest. Where discriminant models could be built loadings from these models were inspected in an attempt to identify metabolites that were associated with a given drug, figure 3.19. Since the number of drugs collectively given to these patients exceeded 220 then detailed assignment of all drugs and their urinary metabolites was not practical.

Spectral features that appeared to be commonly connected to particular drugs or that were found by database searching, such as mannitol, that appeared important in comparisons that had previously been made could then be digitally removed from the spectra and the models reconstructed.

If the OLS-DA model comparing patients with brain injuries and pneumonia was reconstructed with the peaks from mannitol and those that were associated with both Tazocin and Meropenem use removed the overall Q^2Y remained similar (R^2Y 0.87, Q^2Y 0.33, $p=0.02$) to the model produced

Figure 3.19. OPLS-DA, with one component, (R^2Y 0.63, Q^2Y 0.50, $p < 0.001$) comparing metabolic NMR data from urine samples from patients receiving the antibiotic tazocin, red bars, with those not on antibiotics, yellow bars. a. Scores plot for the comparison with b. the regression coefficient plot for the OPLS-DA model with those peaks deflected downwards representing those more abundant in patients receiving tazocin, the colour of the peaks representing the strength of the association. c. STOCSY regression co-efficient plot showing the statistical correlation of the peak at 7.48ppm with all other peaks in the spectra, across all urine samples. The strength of correlation is given by the colour of the peaks. The most strongly correlated peaks coincide with those discriminating patients receiving tazocin in figure 3.19b.





earlier. Examining the loading of this model suggested that creatinine excretion remained higher in the brain injured group whilst lactate excretion was higher in the pneumonia group.

3.6 Discussion

The data in this chapter examine the ability of ^1H NMR spectroscopy of serum and urine from patients on intensive care to differentiate patients with and without pneumonia. Previously there has been limited work focussing on ^1H NMR spectroscopy of biofluids from critically unwell patients. Specifically a limited number of studies have explored metabolic profiles of urine (260, 261) with a slightly greater number of studies examining blood, either serum or plasma, (100, 101, 145, 148, 157, 262-264) with one focussing on a paediatric population (148).

Models based on serum data have a moderate ability to differentiate pneumonia from brain injury at the first time point after enrolment. Several of the metabolites seen to be causing separation between patients with and without pneumonia appear to be lipid species. This is in keeping with animal work done looking at *Klebsiella pneumoniae* infection (149) where lipids were found to be elevated in infected animals' plasma. Similarly in an animal model of *Chlamydia Pneumonia* (265) alterations in lipid profiles were found to be induced after inoculation of mice with the infecting organism, specifically acute and transient reduction in cholesterol levels. More generally lipids play an important role in sepsis with fatty acids being elevated in non-survivors (266). Other forms of inflammation are also associated with alteration in lipid profiles, experimental administration of endotoxin to human subjects has been seen to induce secretory phospholipase A2 and alter high density lipoprotein (HDL) composition (267). Within critical care populations alterations in circulating lipids have been seen to differentiate chronic from acute liver failure (262) and higher cholesterol levels have been associated with survival in heart failure (263). An animal model of ventilator associated lung injury found that using MS analysis of serum lipids distinct lipid profiles could be found for animals with and without lung injury (268). In a Swiss observational study patients with

bacterial CAP had lower total, HDL and low density lipoprotein (LDL) cholesterol and higher triglyceride concentrations than those without bacterial CAP (269) and similar changes in cholesterol were found in a Turkish study that compared patients with CAP to controls (270) with negative correlation being seen between cholesterol levels and the extent of radiographic pneumonia. Within this study a similar trend was seen with HDL levels being lower in those with pneumonia than in those with brain injuries. Total and HDL cholesterol and apolipoproteins A1 and B were reduced in the acute infective process in another observational study (271) with triglyceride levels increasing in those with atypical bacterial pneumonia. In children with complicated pneumonia apolipoprotein A levels have also been seen to fall in acute infection (272). In chronic *Chlamydia Pneumonia* infection (273) triglyceride levels have been seen to rise and HDL cholesterol levels fall in comparison to uninfected individuals.

Of course changes in the lipid profiles may not entirely be related to one of the groups having the presence of infection, it may be that alterations to serum lipids may tell us something about those patients who have sustained brain injuries. In one small study apolipoprotein A4, amongst several proteins, was found to be reduced in those patients with subarachnoid haemorrhage who went on to develop vasospasm (274) and in another it has been suggested that first degree relatives of patients with aneurysmal subarachnoid haemorrhage who have elevated lipoprotein A need further follow up due to the increased risk of aneurism formation (275). Across a group of patients with cerebrovascular disease of differing aetiologies total and LDL cholesterol were higher than in the serum of controls where as HDL cholesterol decreased (276) but in a large observational study neither levels of cholesterol nor triglycerides were associated with the risk of aneurysmal subarachnoid haemorrhage (277) and in a Japanese case control study both HDL cholesterol and triglycerides were found to be lower in patients with subarachnoid haemorrhage (278). No significant risk was associated with HDL cholesterol, triglycerides, lipoprotein or apoprotein A1

when relatives of patients with subarachnoid haemorrhage were screened for the presence of aneurysms (279).

Lipids may be elevated in the critically ill for a number of reasons. Not only do they provide a readily available source of energy but they may also have a role in regulating the immune response, for example they may have a protective effect by binding endotoxin (149, 280).

I also found that formate appeared elevated in those patients with pneumonia. Although formate has not previously been noted as a metabolite associated with pneumonia work it has been seen to be reduced in experimental models of sepsis (128, 129). At present it is unclear why there may be differences in the levels of formate in our pneumonia patients and in sepsis models, however, it may reflect differences in its oxidation to carbon dioxide in the two groups. Differences may exist between animal models and the way in which formate is metabolised in critically unwell human subjects. It may also be the case that these animal models of septic shock are not comparable with the pneumonia population, many of which had infection and sepsis but not severe sepsis or septic shock.

The other metabolites that discriminated patients with pneumonia from those with brain injuries were amino acids, especially phenylalanine, alanine and glutamine with the latter two being reduced in the pneumonia population and phenylalanine being increased. Phenylalanine has also been seen to be elevated in critically ill patients with acute compared to chronic liver failure (262) and both adults (145, 281) and children (148) with sepsis. Phenylalanine may be elevated in inflammatory conditions for a number of reasons. There may be a reduction in the conversion of phenylalanine to tyrosine, for example because of an increase in oxidative stress (282) or as a direct result of immune activation (283, 284). Alterations in the catabolism of skeletal muscle and the subsequent release of amino acids into the serum may also be responsible for differences in phenylalanine concentration in different conditions (284).

Although alanine has been seen to be increased in an animal model of sepsis (128) levels in adults with sepsis have been seen to be reduced as with the pneumonia patients in this study (145, 281) as they have in older children with SIRS (148). Similarly glutamine levels have been found to similarly reduce in both children (148) and adults (281) with sepsis in a similar fashion to these pneumonia patients. These changes may reflect alterations in nutritional status in these conditions or the alteration in the release of amino acids from muscle proteins.

Comparison of this data to the limited amount of work that has been carried out using profiling of serum in pneumonia finds a number of differences. Work in *Influenza A* (258) found mainly inflammatory molecules such as prostaglandins and leukotrienes as well as a number of amino acids in samples taken prior to recovery. Similarly MS analysis of plasma from children with pneumonia in Africa (153) found elevated uric acid, hypoxanthine and glutamic acid levels with decreases in ADP and L-tryptophan. Finally data from a group of patients on ICU (155) with sepsis associated with community acquired pneumonia showed higher levels of bile acids, metabolites of steroid metabolism and those related to oxidative stress in non-survivors. The differences in these studies compared to the current data may be for a number of reasons. Some differences may arise from alterations in the metabolic response to viral infection compared to bacterial pneumonia, the differences between studies looking at single causative agents compared to multiple agents as in this work or general differences in study populations such as the differences between comparing survivors to non-survivors compared to comparisons of infected with non-infected Individuals. All of the above studies used MS based platforms where as we used NMR. Not all metabolites are detected by NMR so a future step in the metabonomic assessment of patients in critical care with pneumonia would be to apply an MS based profiling methodology to extend the number of metabolites detected.

Although the models attempting to differentiate patients who developed VAP from those with brain injuries were not able to discriminate infected from non-infected patients as well as the models exploring patients admitted with pneumonia some of the metabolic changes were similar. Phenylalanine and phospholipids were again discriminators in the infected group and some lipid species were more dominant in the non-infected group. Within this comparison other metabolites that have a closer association with energy metabolism such as lactate and succinate seemed to be important. The differences in metabolic response to pneumonia at admission and to VAP can be explained in a number of ways. Firstly patients admitted with pneumonia may have been unwell in the community for a variable amount of time prior to admission to the intensive care unit potentially resulting in significant differences in their underlying nutritional state when compared to the brain injury patients. However, the patients with VAP were all derived from a group of brain injured patients who had been on the intensive care unit for roughly similar periods of time prior to infection during which time feeding regimens were established. Similarly it is possible that the metabolic 'snapshots' of the two types of infection occur at different times during the pathological process. Those admitted with pneumonia may have been at a later stage in their disease when the first sample was taken due to delays caused by recruitment and obtaining consent. These delays were not present for the samples taken from patients developing VAP as they had all been recruited as brain injured patients prior to the development of infection. Finally it is well known that organisms causing VAP are different from those causing pneumonia in the community and it is entirely possible that the differences in micro-organisms lead to differences in metabolic response.

Some interesting differences were seen when the first time point from patients with brain injuries was compared to the fourth in those who did not go on to develop VAP. Over time glucose, mannitol, creatinine and 3-hydroxybutyrate levels fell. These changes may represent treatment effect such as glycaemic control using intravenous insulin, the use of mannitol to treat raised intracranial pressure or its presence within several other drugs such as intravenous paracetamol, the

reduction of ketosis by the introduction of feed and the normalisation of renal function with adequate hydration. Several amino acids were seen to increase over time including phenylalanine, glutamine, lysine, leucine, valine and isoleucine. Such effects may be related to release from skeletal muscle or from the constituents of feed. Importantly other than the increase in phenylalanine over time the other metabolic changes seen with time were different to those seen in the patients who develop VAP suggesting that these changes may be disease related and not a feature of prolonged ICU stay.

Interestingly the metabolic changes seen over time for patients admitted with pneumonia were quite different to those seen in brain injured patients. Although there was a similar reduction in glucose and mannitol over time there was an increase in several lipid species not seen in the brain injured group. This could be explained by the fact that the patients with pneumonia were more likely to have undergone a period of reduced oral intake prior to admission and with the establishment of feed, lipid levels could be replenished. Another explanation may be differences in the trajectory of inflammatory mediators between the two groups.

Although models could be built using data from urine samples to differentiate pneumonia from brain injured patients metabolite identification within urine samples was much more difficult than for serum samples which may be reflected in the limited number of studies published using this biofluid in similar populations. Spectra obtained from urine were much more heterogeneous than those recorded in serum with several metabolites only appearing in a few urine samples where as in serum almost all metabolites were consistently present, although in differing concentrations. There are a number of possible explanations for the variability of metabolic spectra from urine. Firstly patients requiring critical care have a heavy burden of therapeutic drug use that quite easily exceeds medication use in other patient populations and animal models of disease studied previously. Within our population over 200 types of drug, fluid, blood product and feed were used with patients

receiving between five and 34 of these at any time point. Clearly, although some of these drugs will have a tendency to be co-administered, the potential number of combinations of drugs is enormous. Many of these drugs are either excreted unchanged in the urine or have urinary metabolites. The metabolism of these drugs may also be altered by a patient's clinical condition such as the presence of organ dysfunction, especially renal and liver failure, or the presence of other co-administered drugs that either interact directly or cause alterations in metabolism, for example by up or down regulating hepatic enzymes. As such it is easy to imagine that many of the peaks seen within urine spectra actually represent drugs and their metabolites and these may differ from patient to patient for any given drug depending on their clinical situation. One of the studies investigating metabolic profiles of urine samples obtained from critically unwell patients has also remarked on the presence of drug signals in their samples (260). Urine concentration also varies widely between patients, especially when there may be a degree of renal impairment. An attempt to address this problem was made by normalising the spectra, however, without a substance of known fixed concentration the ability to completely account for variation in concentration is impossible. Misrepresentation of the concentration of individual metabolites with respect to overall urine concentration may have a significant impact on the ability of an individual metabolite to act as a differentiating substance.

Because of the greater variability of urine samples, for example because of the greater variation in urinary pH, natural peak alignment from spectra to spectra was not as good as for serum. This made it necessary to implement a further peak alignment step using a mathematical algorithm. However, although this step improved overall peak alignment it had the potential to miss-align peaks that were in fact from different substances that happened to occur in similar spectral regions reducing the ability of these peaks to act as discriminating metabolites.

For these reasons it was difficult to assess the multivariate models generated from urine data and the large number of unidentified metabolites raises the strong possibility that the ability of models

to discriminate groups was driven, not by genuine disease related metabolic changes, but by treatment effects and drug metabolites.

Much of the previous work exploring the metabonomics of pneumonia has been done using urine specimens. However, in this study population none of the same discriminant metabolites were found but this may reflect the very different populations under investigation. Metabolic analysis of urine in critical care patients poses many challenges that are potentially not a problem in patients in the community, for example differences in drug use and presence of organ dysfunction.

The current work was limited as there are only a small number of patients in each group, especially when time courses and VAP were being considered. This may explain why for several of the models the p-values are non-significant despite good Q^2Y metrics. However, despite the small number of subjects the two groups were well matched for most baseline characteristics. These similarities limited the influence of confounding features on these models. The only significantly different features were those that are considered when making a diagnosis of pneumonia such as oxygenation, CRP and CPIS. Interestingly haemodynamic parameters, temperature and white cell count were also similar between groups.

The diagnostic method for pneumonia in this sample was based on the treating consultant's opinion of the underlying disease process refined by the CPIS score. However, in the absence of a gold standard by which to make the diagnosis this technique provided a refined group where borderline cases should have been excluded perhaps leading to some genuine cases being excluded.

With the NMR methodology used it is difficult to identify specific lipids and establish which lipid species were responsible for group separation making more specific conclusions regarding the role of lipids difficult. This could be pursued further with the application of Liquid Chromatography – Mass Spectrometry lipidomic analysis. The present data is promising in demonstrating that

metabonomic analysis of serum of critically ill patients has the ability to differentiate two clinical groups, with and without pneumonia.

3.7 Conclusion

^1H NMR analysis of serum from critically unwell patients showed an ability to differentiate those with pneumonia at admission from those without with a good degree of specificity. These techniques may also be beneficial in determining those patients who go on to develop VAP from a cohort of patients with brain injuries. The metabolites that differentiated the groups were predominantly lipids and amino acids with subtle differences in the metabolic profiles between those admitted with pneumonia and those who developed VAP.

Conclusions that could be drawn from the analysis of urine samples from patients on intensive care were much more limited. Although models often appeared to have good predictive capacity the heterogeneity of these samples made metabolite identification difficult and raised the concern that much of what was seen related to metabolites of the large number of drugs used in critical care and not to genuine disease differences.

4. SERUM INFLAMMASOME PROFILING

4.1 Summary

Both eicosanoids and cytokines have been explored in some detail with regard to their involvement in the pathogenesis of a range of inflammatory conditions and sepsis. Limited work has been carried out using profiling techniques of either set of mediators alone or in combination to assist in diagnosis. This chapter explores profiling 'the inflammasome', a panel of eicosanoids measured with mass spectrometry and cytokines measured with flow cytometry to distinguish patients admitted for ventilation with pneumonia from those with brain injuries and also those patients developing ventilator associated pneumonia (VAP) from within those with brain injuries. Both eicosanoid and cytokine profiles independently showed some ability to separate pneumonia from brain injury, however, this ability was much less when VAP was considered. By combining both cytokine and eicosanoid profiles the ability to separate patients with VAP from patients with brain injury could be improved indicating the merit of combining metrics from different biological classes. Differentiation of VAP was best when equivalent time points post onset of ventilation from patients without VAP were considered. Inflammatory mediators identified as causing separation between the groups demonstrated biological plausibility based on previous published work.

4.2 Background

Eicosanoids, signalling molecules formed from the oxidation of 20-carbon fatty acids, and cytokines, a broad range of small signalling proteins produced in a variety of cell types, have both been implicated in the pathology of many important diseases ranging from autoimmune conditions such as asthma and rheumatoid arthritis to malignancy and sepsis.

A range of animal studies and clinical observational studies have been performed to investigate the role of cytokines in pneumonia. Circulating levels of pro-inflammatory cytokines, such as tumour

necrosis factor alpha (TNF α), interleukin-1 (IL-1), interleukin-6 (IL-6), interleukin-8 (IL-8), interleukin-12 (IL-12), and interferon gamma (IFN γ) have often been found to be elevated in patients with community acquired pneumonia (CAP). For example, a study looking at nearly 2000 patients with pneumonia (163) found higher levels of IL-6, IL-10 and TNF α in those CAP patients with severe sepsis compared to those without, and higher IL-6 and IL-10 levels in non-survivors compared to survivors. In a paediatric population IL-6, IL-8 and IL-10 levels were found to be higher, not only in septic patients compared to controls, but also in those septic patients who went on to develop nosocomial infections than those who did not (165). Specific micro-organisms, such as mycoplasma, have also shown similar patterns of cytokine response (166) with IL-4, IL-6 and IL-10 being higher in mycoplasma pneumonia than in controls with levels improving over time. The inflammatory response to CAP may not be the same throughout life and may alter with age, for example, IL-8 has shown a trend to be elevated at admission in older patients with CAP compared to those younger than 50yrs (164).

A smaller body of work exists looking at the role that fatty acids and their metabolites, eicosanoids, have in the pathophysiology of pneumonia. *Streptococcus Pneumoniae*, a common cause of pneumonia, has been shown in models of lung infection to be capable of inducing COX-2 expression within lung tissue (161). Specific molecules such as the leukotrienes, especially leukotriene B4 (LTB4), are thought to be important in protecting the lungs from infection. LTB4 is important in chemoattraction and leukocyte activation and may act to increase IL-6 levels (159). Specifically LTB4 has been associated with pulmonary complications following trauma (160). Other fatty acid metabolites, such as the lipoxins, have been implicated in the resolution of pulmonary inflammation. Lipoxin A4 can be generated in response to lung injury and has been found in the bronchoalveolar lavage (BAL) fluid of patients with several pulmonary diseases including pneumonia (162). One proposed mechanism of action of Lipoxin A4 is to inhibit LTB4 mediated chemoattraction.

Much of the work looking at these inflammatory molecules has focused on local production within the alveoli and lung tissue by looking at BAL fluid and exhaled breath condensate (EBC) levels. For example IL-8, LTB₄, C₄, D₄, and E₄ have been seen to be at higher concentrations in the BAL fluid of pneumonia patients in whom organisms could be detected compared to controls (167). When work has been carried out looking at systemic levels of these mediators often only a few mediators are measured at a time and usually with a view to looking at mechanistic elements.

A limited amount of work has been carried out looking at the diagnostic potential of cytokines or eicosanoids in pneumonia and a smaller amount of work exists trying to apply a panel approach to measuring an array of these inflammatory mediators. One study used a multiplex cytokine assay to attempt to diagnose tuberculosis by measuring cytokines produced from stimulated peripheral blood mononuclear cells and found IFN γ , interferon gamma inducible protein-10 (IP-10), monokine induced by interferon gamma (MIG), TNF α and IL-2 showed the most significant differences between active pulmonary tuberculosis patients and healthy controls (168). In another study measurement of IL-6 and IL-8 were used in conjunction with other biological and clinical data to attempt to classify ARDS cases into groups based on different phenotypes (169).

In this chapter I outline a strategy for using a panel approach to measuring both metabolites of fatty acid metabolism, eicosanoids, cytokines and adhesion molecules to aid the diagnosis of both pneumonia and VAP.

4.3 Aims

The overall aim of this study was to use profiling techniques on a combination of inflammatory mediators including eicosanoids, cytokine and soluble adhesion molecules, here called the 'inflammasome', to attempt to improve the diagnosis of pneumonia in patients requiring ventilation, specifically those going on to develop VAP. The following questions were addressed:

1. *Can measuring a panel of eicosanoids improve the diagnosis for both pneumonia and VAP in ventilated patients on the Intensive Care Unit?*
2. *Can measuring a panel of cytokines improve the diagnosis for both pneumonia and VAP in ventilated patients on the Intensive Care Unit?*
3. *Can combining these methods improve the diagnostic potential of this approach?*

4.4 Protocols

4.4.1 Patient Recruitment and Sample Collection

Patients were recruited and serum samples taken as described in chapter 2. Patients were defined as either having pneumonia or a brain injury as described earlier. All patients were followed up over time and those brain injured patients developing VAP were identified based on CPIS scoring. For a breakdown of the CPIS see chapter 2. Patients with borderline scores were assessed and classified by an independent assessor.

4.4.2 Eicosanoid Measurement

Serum eicosanoid levels were measured using liquid chromatography coupled to tandem mass spectrometric detection (LC-MS/MS) using a targeted method developed internally for the Division of Computational and Systems Medicine of Imperial College London in collaboration with Arnaud Wolfer. It was designed to quantify 48 eicosanoids by using solid phase extraction of the analytes from complex biological matrices such as serum or plasma. The analytes were subsequently eluted in a small amount of organic solvent, followed by a chromatographic run optimized to separate all metabolites. Following negative electrospray ionization the analytes were selected by m/z , underwent collision and the most selective and quantitative product ions were again selected to be scanned by the detector.

4.4.2.1 Isotopically Labelled Internal Standards (IS)

Multiple extraction steps introduce variability in analyte recovery post sample preparation, with losses of 50% or more depending on metabolite and sample-specific matrix content. In order to compensate for variation resulting from the sample preparation steps, seven deuterated internal standards (IS), covering each chemical family, were spiked in the serum samples prior to extraction.

Seven deuterated internal standard solutions were combined into a single glass vial to give final concentrations of 2ng/ μ L of each. This stock solution was then further diluted into a working solution at a concentration of 300pg/ μ L with the addition of methanol and water reaching a final solvent ratio of 1:1. All standards were stored at -80°C prior to use.

4.4.2.1 Standard Mixtures

48 commercial solutions were used to generate standard solutions. 20 μ L of each eicosanoid was added to a single vial and the total volume adjusted to a final volume of 1ml with the addition of methanol to give a final concentration of 2ng/ μ L for each.

Serial dilutions of this standard mixture were then prepared using a 1:1 water to methanol ratio to give a thirteen point standard curve ranging from 1-10000pg/ μ L for free fatty acids and 0.1-1000pg/ μ L for eicosanoids. A zero sample was also prepared containing only internal standards. 100 μ L of each concentration on the calibration curve was added to a separate well on a new collection plate and 20 μ L of labelled internal standard was added to each. Blank samples were also prepared comprised of 120 μ L water/methanol with no internal standards. Once prepared the plate containing the calibration curve was stored at 4°C in the Sample Manager of the mass spectrometer.

4.4.2.3 Sample Preparation

Serum specimens were transported on ice prior to analysis and allowed to thaw at room temperature. Prior to preparation samples were randomised and prepared in this new order and blinded to any clinical information.

Samples were prepared in a 350 μ L 96-well collection plate (Waters, Manchester, UK), the preparation plate. 100 μ L of sample was placed in the relevant well and 20 μ L of IS at 300pg/ μ L were added to each well. The total volume in each well was made up to 150 μ L with the addition of 30 μ L of 2% formic acid solution in water to break small molecule-protein binding by acidification of the sample. The plate was then capped and gently mixed.

4.4.2.4 Solid Phase Extraction

Solid phase extraction was carried out using an Oasis Max Solid Phase Extraction (SPE) μ Elution plate (Waters, Manchester, UK). The plate was conditioned by addition of 200 μ L Methanol to each well. The wells were then dried with the use of a vacuum at 3" Hg until dryness was achieved. Liquid was collected into a 3ml 96-well 'waste plate' (Waters, Manchester, UK). 200 μ L of high purity, mass spectrometry grade, water was then added to equilibrate the sorbent and the wells were again dried by application of a vacuum at 5" Hg.

The samples were then loaded into the SPE plate, limiting the time between sorbent equilibration and sample loading to preserve the sorbent quality. 50 μ L of 1:1 water to methanol solution were added to each well of the preparation plate which was capped and mixed before being transferred into the SPE plate. The vacuum was applied to the SPE plate at 3" Hg being increased to 5" Hg as needed until the wells of the SPE plate were empty, ensuring sufficient time for contact between the sample and the sorbent allowing retention of the analytes.

The plate was washed with 200 μ L of 2% ammonium hydroxide to break the hydrogen bonds between the eicosanoids and proteins. 5" Hg vacuum was then applied until the wells were dry.

A further wash with 200 μ L 1:1 water to acetonitrile solution was applied to each well, to break hydrophobic bonding between proteins and the sorbent, and the plate was dried by applying a vacuum of 5" Hg.

The 'waste plate' was then removed from the SPE device and replaced with a 350 μ L 96-well collection plate (Waters, Manchester, UK). The analytes were eluted by the addition of 25 μ L of methanol and 2% formic acid. The vacuum was applied at 3" Hg followed by 10-15" Hg for one minute. This step was repeated a further three times leaving approximately 100 μ L in the collection plate.

The collection plate was removed from the SPE device and capped. The elution fraction was allowed to evaporate over approximately 2h by the application of a vacuum at 15" Hg. Once the extract was dry they were reconstituted with 100 μ L of 1:1 water to methanol solution. Following reconstitution plates were stored at 4°C in the Sample Manager of the mass spectrometer.

4.4.2.5 Ultra Performance Liquid Chromatography (UPLC) and Mass Spectrometry

Chromatographic analysis was performed using an Acquity UPLC system (Waters, Manchester, UK).

Prepared samples and standards were injected onto a HSS T3 UPLC column (100 mm \times 1 mm, 1.8 μ m) (Waters, Manchester, UK) at 40 °C with a flow rate of 140 μ L/min. The mobile phase A consisted of water and 0.1% formic acid and mobile phase B acetonitrile and 0.1% formic acid. The injection volume was 5 μ L.

After separation by UPLC, mass spectrometry was performed using a Xevo TQ-S triple quadrupole mass spectrometer (Waters, Manchester, UK). In negative ion mode, MS parameters were as follows: capillary voltage was set at 2.5 kV, cone voltage was set between 10-40 V depending on the

analyte being measured, source temperature 150°C, desolvation temperature 500 °C, desolvation gas flow 900 L/h and cone gas flow 150 L/h. All data were collected using MassLynx software (Waters, Manchester, UK)

4.4.2.6 Data Pre-processing

The same data preprocessing was applied to each 96-well plate and its corresponding calibration curves. Peaks were determined and peak area integrated using TargetLynx software (Waters, Manchester, UK). All peaks were inspected manually and corrected where necessary. The IS response factors were calculated and the analyte peaks were corrected for variation in extraction yields depending on the eicosanoid class. For each standard the concentration-response equation was established by least-square linear regression of the calibration curve. The calibration curves were constructed using the following rules:

- The response of the lowest concentration point (LLOQ) must be at least 5 times the response of the equivalent noise area.
- The measured concentration of standard must be 85-115% of the nominal value or 80-120% if at the lower limit of quantification.
- At least six standard points should meet these criteria and define the range of linearity between the lowest and upper limits of quantification.

Finally, sample concentrations were back-calculated from the constructed calibrations curves for each analyte.

4.4.3 Cytokine Measurement

A panel of 20 human inflammatory cytokines and soluble adhesion molecules were measured using the commercially available 20plex FlowCytomix™ kit (eBioscience, San Diego, USA). The kit allowed

20 cytokines to be measured using flow cytometry by utilising two bead populations of differing sizes (population A 5µm, population B 4µm.) Each population of beads had several sub-populations (size A – 11 subpopulations, size B – 9 subpopulations) each with a dedicated cytokine specific antibody and a different intensity of an internal fluorescent dye that excited in the far red (700nm) with an Argon laser. This allowed the 20 cytokines to be identified based on bead size and intrinsic fluorescence intensity, using a single fluorescence channel. All chemicals used were provided with the kits (eBioscience, San Diego, USA).

4.4.3.1 Assay Buffer

A 1x concentration of assay buffer was prepared from the 10x concentration of assay buffer provided with the kits consisting of phosphate buffered saline (PBS) containing 10% N,O-bis(trimethylsilyl)acetamide (BSA) by the addition of distilled water.

4.4.3.2 Sample Preparation

Serum samples were randomised prior to cytokine measurement to limit any batch effect that may confound the experimental design. Samples were transported on ice and allowed to thaw at room temperature prior to cytokine measurement. The time between samples being removed from the -80°C freezer and thawing was kept to a minimum and was approximately 30 minutes. All samples were run in duplicate.

4.4.3.3 Standard Curves

A lyophilized standard mixture of cytokines was included in the kit for preparing a standard curve for each cytokine. The standards were spun down for a few seconds in a microcentrifuge before being reconstituted in 1x assay buffer to give the concentrations detailed in table 4.1.

Table 4.1. Concentrations of cytokine standards on reconstitution per bead population.

Bead size A		Bead size B	
Standard	Concentration upon reconstitution	Standard	Concentration upon reconstitution
G-CSF	25000 pg/ml	E-Selectin	3000 ng/ml
ICAM-1	4000 ng/ml	IFN α	20000 pg/ml
IFN γ	20000 pg/ml	IL-1 α	1000 pg/ml
IL-6	20000 pg/ml	IL-1 β	20000 pg/ml
IL-8	10000 pg/ml	IL-4	20000 pg/ml
IL-10	20000 pg/ml	IL-13	20000 pg/ml
IL12p70	20000 pg/ml	IL-17A	10000 pg/ml
LAP	1500 ng/ml	IP-10	12500 pg/ml
MCP-1	30000 pg/ml	TNF α	20000 pg/ml
MIP1 α	10000 pg/ml		
MIP1 β	3000 pg/ml		

A series of seven declining concentrations of these standards were prepared using serial dilution. 50 μ L of the reconstituted standard was added to 100 μ L of assay buffer and mixed. 50 μ L of this mixture was then added to a further 100 μ L assay buffer and this process was repeated until there were seven solutions of diminishing concentration.

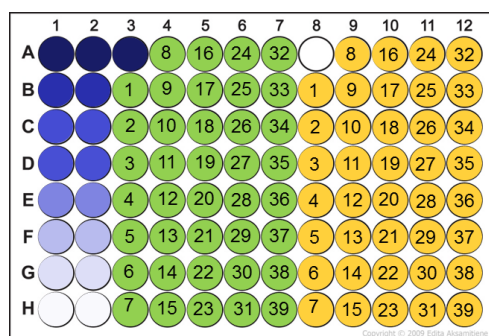
4.4.3.4 Fluorescent Beads

For each 96 well plate the provided bead mixture was vortexed for five seconds and mixed by repeated pipetting prior to transferring 1500 μ L into two Eppendorf tubes. These were centrifuged at 3000g for 5 minutes. The excess liquid was removed and the beads reconstituted to a total volume of 3000 μ L with the reagent dilution buffer provided in the kit. The resulting solution was vortexed for five seconds prior to use.

4.4.3.5 Preparation of Plates

Beads for flow cytometry were prepared in a 96-well filter plate prior to transfer to flow cytometry tubes. The wells of the plate were pre-wetted with the addition of 50 μ L of assay buffer to each well. The buffer was removed using a vacuum manifold until no fluid remained in the wells. 25 μ L of standard mixtures one to seven were added to the first and second columns, figure 4.1, and 25 μ L of assay buffer was added to the final well of each column as a blank. 25 μ L of sample were added to the remaining wells, each sample being run in duplicate. 25 μ L of bead mixture was then added to each well, including the blanks, followed by 25 μ L of biotin-conjugate antibody mixture. The biotin conjugated mixture contained specific antibodies that bound to the cytokines bound to the beads. The plate was then covered with adhesive film and incubated at room temperature for 2h on a plate shaker at 250rpm. The plate was protected from light with aluminium foil.

Figure 4.1. Schematic diagram illustrating the layout of the 96-well plate for sample preparation for flow cytometry. (1A-G first set of standard concentrations, 2A-G, second set of standard concentrations, H1, H2 blanks, A3 set up beads, green numbered wells represent samples and their duplicates in yellow).



After incubation the adhesive film was removed and the wells emptied using the vacuum manifold. The wells were washed by the addition of 100 μ L of assay buffer to each and emptied with the vacuum manifold. This step was performed twice.

100µL assay buffer and 50µL of streptavidin-PE solution were added to each well before covering and incubation at room temperature for one hour on a plate shaker at 250rpm. The plate was protected from light with aluminium foil. This incubation step allowed the streptavidin to bind to the biotin added in the previous step providing a fluorescent signal to allow cytokine quantification.

After incubation the wells were emptied on the vacuum manifold and the wells washed twice with 100µL of assay buffer as before.

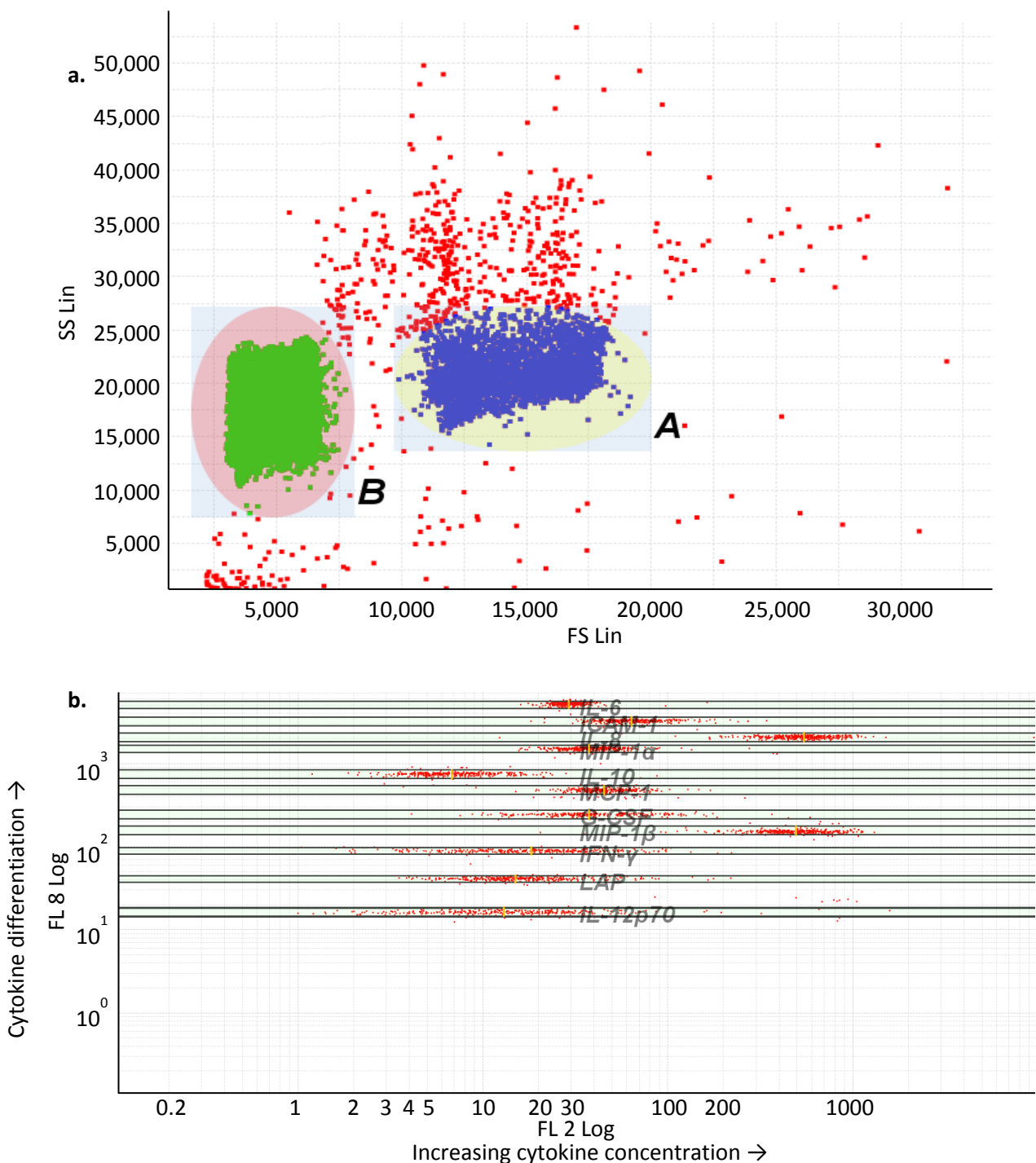
Finally 200µL of assay buffer were added to each well and mixed by repeated aspiration with a micropipette. This volume was transferred to tubes ready for measurement on the flow cytometer and the volume made up to 500µL with the addition of 300µL assay buffer. The tubes were covered in aluminium foil to protect them from light and kept at 4°C overnight prior to data acquisition.

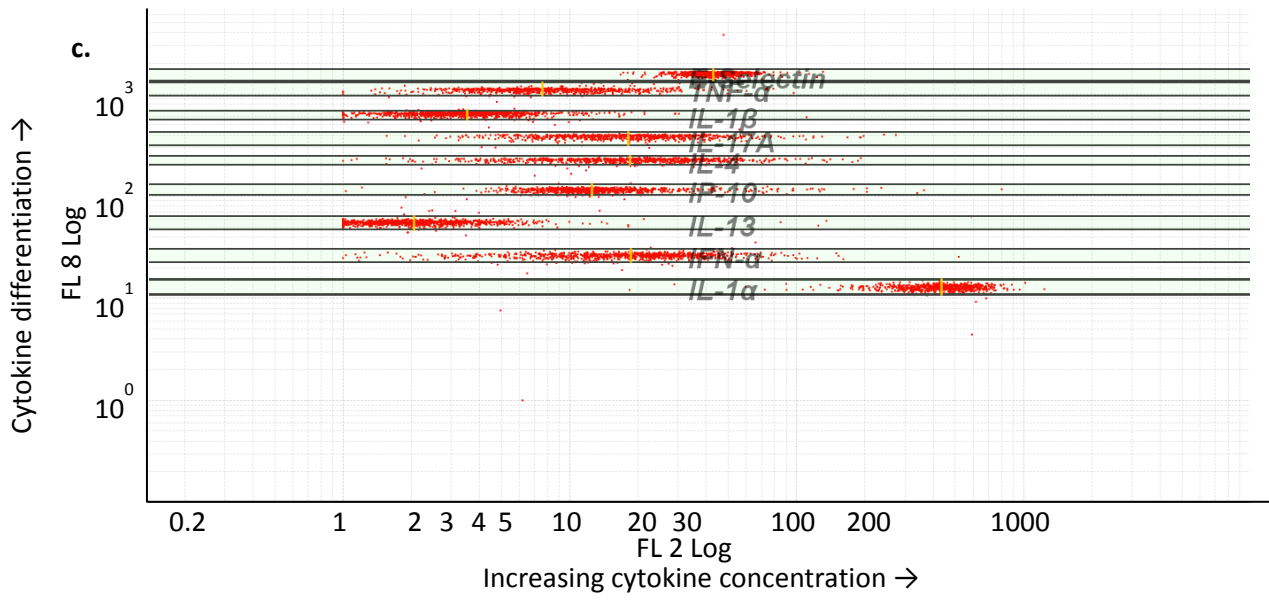
4.4.3.6 *Flow Cytometry*

Data were acquired on a CyAn flow cytometer (Beckman Coulter, Brea, USA). The forward scatter (FS) and side scatter (SS) were adjusted to allow the two bead populations to be discriminated on size, figure 4.2. Two gated regions were then created based on the two populations of beads. For each region fluorescence was detected at 595nm for Phycoerythrin (PE) emission (x-axis) to quantify cytokine concentrations and 700nm (y-axis) to separated cytokine specific bead populations. Voltage of the PE emission was adjusted to ensure that the beads with the highest standard cytokine concentrations touched the right side of the plot. Voltage of the far red emission was adjusted to give clear separation of the individual cytokines.

The total number of events counted was defined so that there would be approximately 300 gated events per analyte. After cytometer set up samples were run in sequential order and the generated files saved.

Figure 4.2. Representative plots from the flow cytometer demonstrating how the cytokines were identified and quantified. a) differentiation of the two bead populations based on size measured with forward scatter (FS, x-axis) and side scatter (SS, y-axis): each dot represents an individual bead, Beads marked A 5 μ m diameter, B 4 μ m diameter. b, c) Fluorescence channels for the two populations of cells, b) population A and c) population B. Far red emission (FL 8 Log) is shown on the y-axis and discriminates individual cytokines based on fluorescence intensity. PE emission (FL 2 Log), on the x-axis, measures cytokine concentration with higher intensity representing higher concentration.





4.4.3.7 Data Pre-processing

Data files were exported into FlowCytomix Pro™ software (eBioscience, San Diego, USA) for initial analysis. The software generated standard curves based on the average of the two sets of standard cytokine concentrations run on each plate. For each curve the software provided an estimate of the goodness of fit to the data points. Points were only removed from the curves on the rare occasions when there was clearly an outlier, with a point lying above or below the next point higher or lower on the curve. This was only required in a few instances.

Cytokine concentrations were calculated by comparing the mean fluorescence intensity (MFI) of each sample corrected for the MFI of the blank sample to the standard curve.

All duplicates were examined and where clear discrepancy existed in cytokine concentrations between a sample and its duplicate the sample was re-analysed. Similarly samples that saturated the concentration curves were rerun using a ten-fold dilution and concentrations calculated from this result. Where the calculated concentration failed to exceed the concentration curve, the average was taken from the repeated value and the upper limit of quantification from the standard curve.

Further statistical analysis was carried out using the mean of the cytokine concentrations calculated for each sample and its duplicate. Where a sample was re-run the average was taken of the rerun pair when these provided concentrations that were consistent.

4.4.3 Statistical Analysis

Routine data handling was performed in Excel (Microsoft, USA). Prior to multivariate analysis all mediator concentrations were scaled to unit variance. Standardising the variance of variables attempts to take into account the potentially enhanced influence on multivariate models of analytes with naturally higher concentrations that tend to be associated with higher variance and allows variables with generally lower values to be given similar weight within the model. Multivariate

statistics were used to analyse the data. Initial exploration with principal component analysis (PCA) was performed to look for natural clustering and to detect outliers before supervised multivariate analysis using orthogonal partial least squared discriminant analysis (OPLS-DA) was used to generate models to optimally separate predefined groups. OPLS-DA models were cross validated using seven fold cross-validation using a “leave-one-out” methodology. Permutation testing was used to evaluate equivalent partial least squared discriminant analysis PLS-DA models. Important metabolites in each model were identified by examining the loadings associated with each model and the most important metabolites were selected by picking those that had a Variable Importance for the Projection (VIP) of greater than 1.0 (112). All multivariate analysis was performed using the SIMCA statistical package (Umetrics, Sweden). Further discussion of multivariate techniques can be found in chapter 2.

Univariate statistical analysis was used to compare individual mediators and characteristics of included patients using SPSS (IBM, UK) and Excel (Microsoft, USA). Student’s T-test was used to compare continuous variables between groups of patients and Fisher’s exact test to compare categorical variables. Normality of metabolite distributions was determined using Kolmogorov-Smirnov and Shapiro-Wilk tests of normality. Non-normally distributed metabolites were compared using the Mann-Whitney U test and concentrations are given as median and interquartile range. To account for multiple comparisons the Benjamini-Hochberg procedure was used to control the false discovery rate. A p-value of 0.05 or less was taken to represent statistical significance.

4.5 Results

4.5.1 Patients

Thirty four patients, that fulfilled the criteria defined in chapter 2, had eicosanoids and cytokines measured in their serum. Of these 13 had pneumonia on admission and 21 had brain injuries with no

suggestion of pneumonia when the first serum samples were taken. Five brain injured patients went on to develop VAP based on CPIS scoring. Clinical features of these patients can be seen in table 4.2. As previously described in chapter 2, patients with borderline CPIS scores were reviewed by an independent clinical assessor and classified as non-infected, pneumonia or VAP based on clinical course. Based on this assessment a further six brain injured patients were classified as not having pneumonia on admission, five were defined as pneumonia and three as VAP. All initial comparisons were made with the original grouping of patients based on CPIS.

Patients were similar across the groups with respect to their demographic details. Features that identified the pneumonia and VAP groups from those with brain injuries included markers of infection such as CRP, use of antibiotics and the higher oxygen requirement as would be expected in patients with pulmonary infection.

Table 4.2. Clinical features of included patients. Continuous variables are given as mean and standard deviation and categorical variables as number and percentage. P-values presented in bold text relate to parameters that were significant at the $p < 0.05$ level. The clinical parameters compared were taken from the 24h prior to 8:00 am on the day of sampling, for the pneumonia and brain injured patients this was time point 0 and for cases of VAP this was the 24h prior to the sample taken soonest after the onset of VAP.

	Pneumonia (P)	Brain Injury (BI)	p-value (BI vs P)	VAP	p-value (BI vs VAP)
N	13	21	-	5	-
Age (Mean +/- SD)	53.5±16.5	52.3±14.9	0.84	50.8±17.2	0.87
Sex, Number of males (%)	9 (69.2)	12 (57.1)	0.72	3.0 (60.0)	1.00
Ethnicity, number White European (%)	9 (69.2)	15 (71.4)	1.00	4.0 (80.0)	1.00
Outcome, Number alive (%)	8 (61.5)	16 (76.2)	0.45	3.0 (60.0)	0.59
APACHE II Score (Mean +/- SD)	19.6±6.3	17.0±6.0	0.23	17.8±9.4	0.86
SOFA Score (Mean +/- SD)	10.2±3.2	8.9±2.6	0.23	8.6±3.1	0.87
CPIS (Mean +/- SD)	5.8±1.0	2.1±1.4	<0.001	7.0±1.58	<0.01
Lowest WCC (10⁹/L) (Mean +/- SD)	15.8±7.5	10.0±3.8	0.02	10.5±3.2	0.76
Highest WCC (10⁹/L) (Mean +/- SD)	16.4±7.3	11.2±3.9	0.03	10.5±3.2	0.70
Lowest CRP (mg/L) (Mean +/- SD)	165.7±98.7	49.4±54.2	<0.01	116.7±28.2	<0.01
Highest CRP (mg/L)(Mean +/- SD)	184.1±913	62.0±52.5	<0.001	116.7±28.2	<0.01
Lowest Temperature (°C) (Mean +/- SD)	35.8±0.83	36.0±0.68	0.45	36.0±1.6	0.95
High Temperature (°C) (Mean +/- SD)	37.7±0.96	37.6±0.68	0.65	38.0±1.3	0.45
Lowest FiO₂ (Mean +/- SD)	0.4±0.15	0.4±0.22	0.47	0.4±0.1	0.51
Lowest PaO₂:FiO₂ (Mean +/- SD)	24.0±9.7	41.8±15.5	<0.001	18.6±8.5	<0.001
Lowest MAP (mmHg) (Mean +/- SD)	71.7±10.4	74.0±11.3	0.54	71.0±12.4	0.65
Use of noradrenaline, N (%)	9 (69.2)	13 (61.9)	0.73	1.0 (20.0)	0.15
Use of antibiotics N (%)	13 (100)	10 (47.6)	<0.01	5.0 (100)	0.05
Enteral nutrition, N (%)	12 (92.3)	15 (71.4)	0.21	5.0 (100)	0.3
Time to sampling from start of ventilation (h) (Mean +/- SD)	42.7±11.5	40.1±16.9	0.61	143.4±44.9	<0.01
Time of day of sample, Number taken in the morning (%)	8 (61.5)	13 (61.9)	1.0	5.0 (100)	0.28

4.5.2 Eicosanoids

Of the 48 eicosanoids measured there were 17 where levels were below the lower limit of quantification in all samples, table 4.3. These were omitted from any further analysis. This left 31 quantifiable eicosanoids.

Table 4.3. The 31 quantified eicosanoids and the 17 that were unquantifiable.

Measured Eicosanoids	Unquantifiable Eicosanoids
C18:2 (LA)	tetranor-PGEM
C20:3 (DGLA)	tetranor-PGFM
C20:4 (AA)	15(S)-HEPE
C20:5 (EPA)	5,6-EET
C22:6 (DHA)	8,9-EET
9(S)-HODE	11,12-EET
13(S)-HODE	14,15-EET
tetranor-PGDM	5-oxo-ETE
12(S)-HEPE	LTD4
5(S)-HETE	LTE4
8(S)-HETE	PGD2
11(R)-HETE	PGF2alpha
12(R)-HETE	8-iso-PGF2alpha
15(S)-HETE	15dPGJ2
16(R)-HETE	11-dehydro TXB2
5,6-DHET	Resolvin D1
8,9-DHET	Resolvin D2
11,12-DHET	
14,15-DHET	
12-oxo-ETE	
14-HDoHE	
17(S)-HDoHE	
10(S),17(S)-DiHDoHE	
LTB4	
12-oxo-LTB4	
LTC4	
PGE2	
Lipoxin A4	
Lipoxin B4	
6-keto-PGF1alpha	
TXB2	

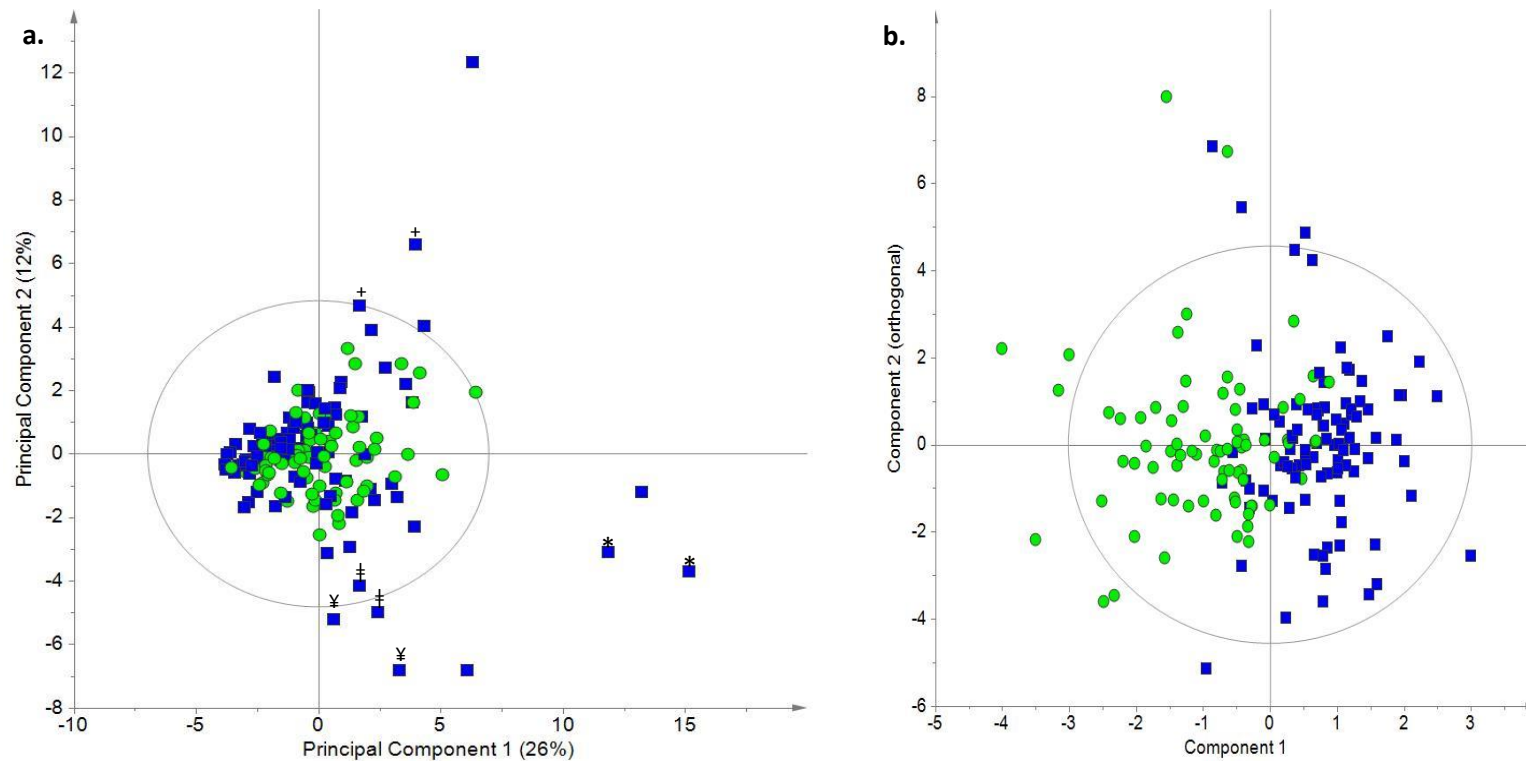
4.5.2.1 Evaluation of Batch Effect

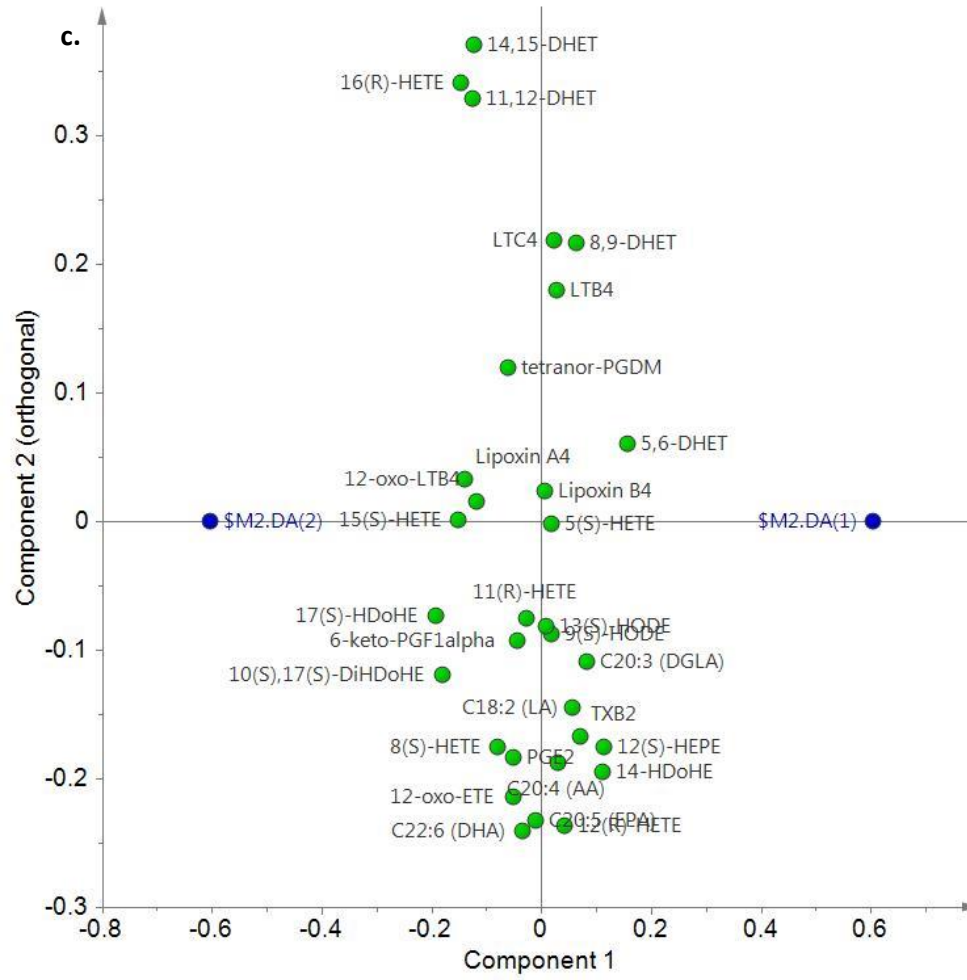
All eicosanoid measurements were carried out over a period of two days in two runs. PCA was used to evaluate the presence of any batch effect, figure 4.3. Most of the samples from both batches clustered together in the PCA scores plot, although the outliers appear to all arise from the first batch. On closer examination many of these appear to be due to patient factors as samples taken from the same patient appear together on the plot, regardless of the day of analysis. Although it is possible to construct an OPLS-DA model (R^2Y 0.50, Q^2Y 0.37, $p < 0.001$) to separate samples based on batch, there is a great deal of overlap of the two groups even before cross-validation has been applied, suggesting that batch effect, although present, was very small. The eicosanoids most susceptible to batch effect were 17(S)-HDoHE, 11,12-DHET, 12(S)-HEPE, 16(R)-HETE, 10(S),17(S)-DiHDoHE, 14-HDoHE, Lipoxin A4, 15(S)-HETE, TXB2, 14,15-DHET, 5,6-DHET, LA, 12-oxo-LTB4, 12(R)-HETE, 8(S)-HETE, and AA. In an attempt to establish the degree of effect that batch had on the overall variation within the samples the R^2X of the model was examined. Whereas the R^2Y metric quantifies the amount of variation explained by the model between the classification groups the R^2X quantifies the total amount of variation explained by the model across all samples. In this case although the OPLS-DA model was able to explain roughly 50% of the variation between the two batches (R^2Y 0.5) and was moderately predictive (Q^2Y 0.37) the total amount of variation across all samples explained was small at only 16% (R^2X 0.16) implying that the batch effect had only a small effect on the overall variation between samples. In order to examine batch more closely the clinical comparisons described below were also re-examined to assess for batch effect.

4.5.2.2 Brain Injury vs. Pneumonia

Initial comparison using PCA of the 13 patients with pneumonia at the start of invasive ventilation with the 21 brain injured patients who demonstrated no evidence of pneumonia when ventilation

Figure 4.3 a. Three component PCA scores plot (R^2X 0.49 Q^2Y 0.25), showing components 1 and 2. Samples are coloured according to batch, run 1 - blue squares, run 2 - green circles, samples marked with the same symbols arise from the same patient at different time points. The inability of this unsupervised model to find natural separation between the two batches implies minimal batch effect and that most of the variation between samples is due to factors other than batch. b. OPLS-DA model (R^2Y 0.50, Q^2Y 0.37, $p < 0.001$) with one component and one orthogonal component, shown prior to cross-validation, comparing samples from run 1, blue squares, to those from run 2, green circles. Samples to the far left and right of the plot show the greatest difference when variation based on batch effect is actively explored, the overlapping samples in the middle demonstrate least difference. c. Loading plot for the OPLS-DA model demonstrating the eicosanoids causing the most separation in the OPLS-DA model. Eicosanoids distributed at the extremes of the x-axis are responsible for most variation in the first component, x-axis, of the OPLS-DA model and those at the extremes of the y-axis are responsible for most variation in the orthogonal component.





was commenced showed no innate ability to separate these groups based on the presence or absence of pneumonia, figure 4.4. However, there appeared to be some distinct groupings or clusters within the data distribution. The group of four brain injured patients in the upper right quadrant of the plot had a dominance of almost all fatty acids and their subsequent eicosanoid metabolites whereas the bulk of the patients on the left showed a dominance of 6-keto-PGF1 α , LTC4, 12-oxo-LTB4 and Lipoxin B4. The three patients in the lower right quadrant differentiated from the main cluster by the presence of higher levels of TXB2, 11(R)-HETE, 12(R)-HETE, 8(S)-HETE, PGE2, 12(S)-HEPE, 12-oxo-ETE, 15(S)-HETE, tetranor-PGDM and 14-HDoHE. Comparison of these groups with clinical data showed no clear clinical explanation for this grouping. There was no differentiation based on the underlying pathology, the use of drugs known to alter eicosanoid metabolism or the development of later infection.

Use of OPLS-DA, figure 4.5, enabled a model to be constructed with R^2Y 0.68, Q^2Y 0.40, $p=0.02$. Examination of the loadings for the model showed a predominance of fatty acids, particularly DHA, EPA, AA and LA, in the brain injury group along with the metabolites 6-keto-PGF1 α , 5,6-DHET, 9(S)-HODE, 13(S)-HODE, 10(S),17(S)-DiHDoHE and 5(S)-HETE. Lipoxin B4 and tetranor-PGDM were more abundant within the pneumonia group. Testing this model with the set of 11 patients with borderline scores, that were reclassified blindly by an independent clinician, demonstrated the model to have a sensitivity of 0.60, a specificity of 0.67, a positive predictive value of 0.6 and a negative predictive value of 0.67. When the same subgroup of patients was used to construct a batch model only a much less predictive model could be made (R^2Y 0.52, Q^2Y 0.15, $p=0.30$) with less of the overall variation described by the batch model compared to the disease classification model (R^2X 0.42 vs 0.55) implying that disease group had a greater impact on inter sample variation than the batch effect.

Figure 4.4. a. Three component PCA model (R^2X 0.62, Q^2X 0.25), showing components 1 and 2, comparing samples taken at the first time point from patients admitted with pneumonia (red squares) to those admitted with brain injuries with no evidence of pneumonia when the first sample was taken (blue circles). No overall natural separation between pneumonia and brain injured patients is seen, however a group of brain injured patients seem to separate out into the right side of the plot, along the first component, and two patients with pneumonia separate from the main group along the second component. b. Loadings plot for the PCA model demonstrating the eicosanoids causing the most separation in the model. Eicosanoids distributed at the extremes of the x-axis are responsible for most variation in the first component, x-axis, and those at the extremes of the y-axis are responsible for most variation in the second component, y axis, of the PCA model.

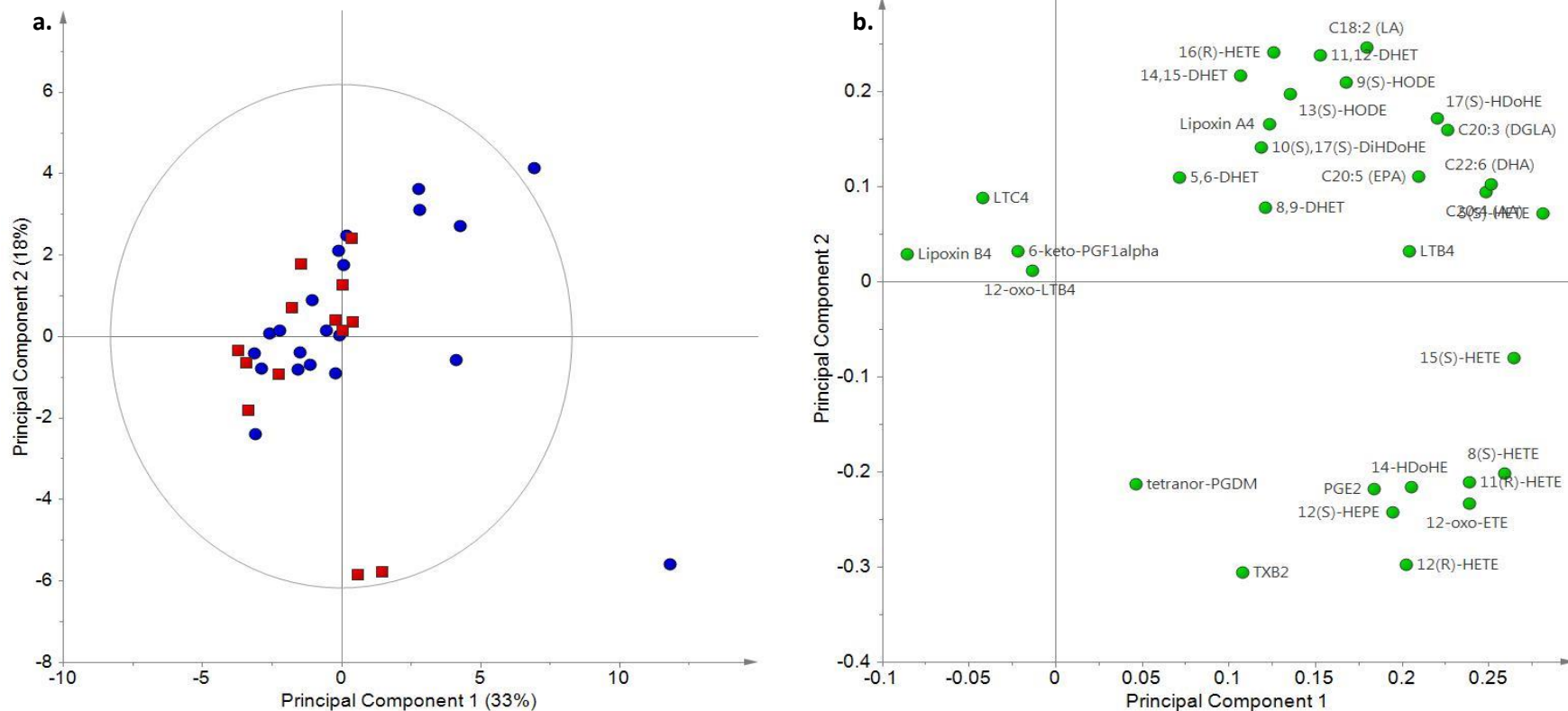
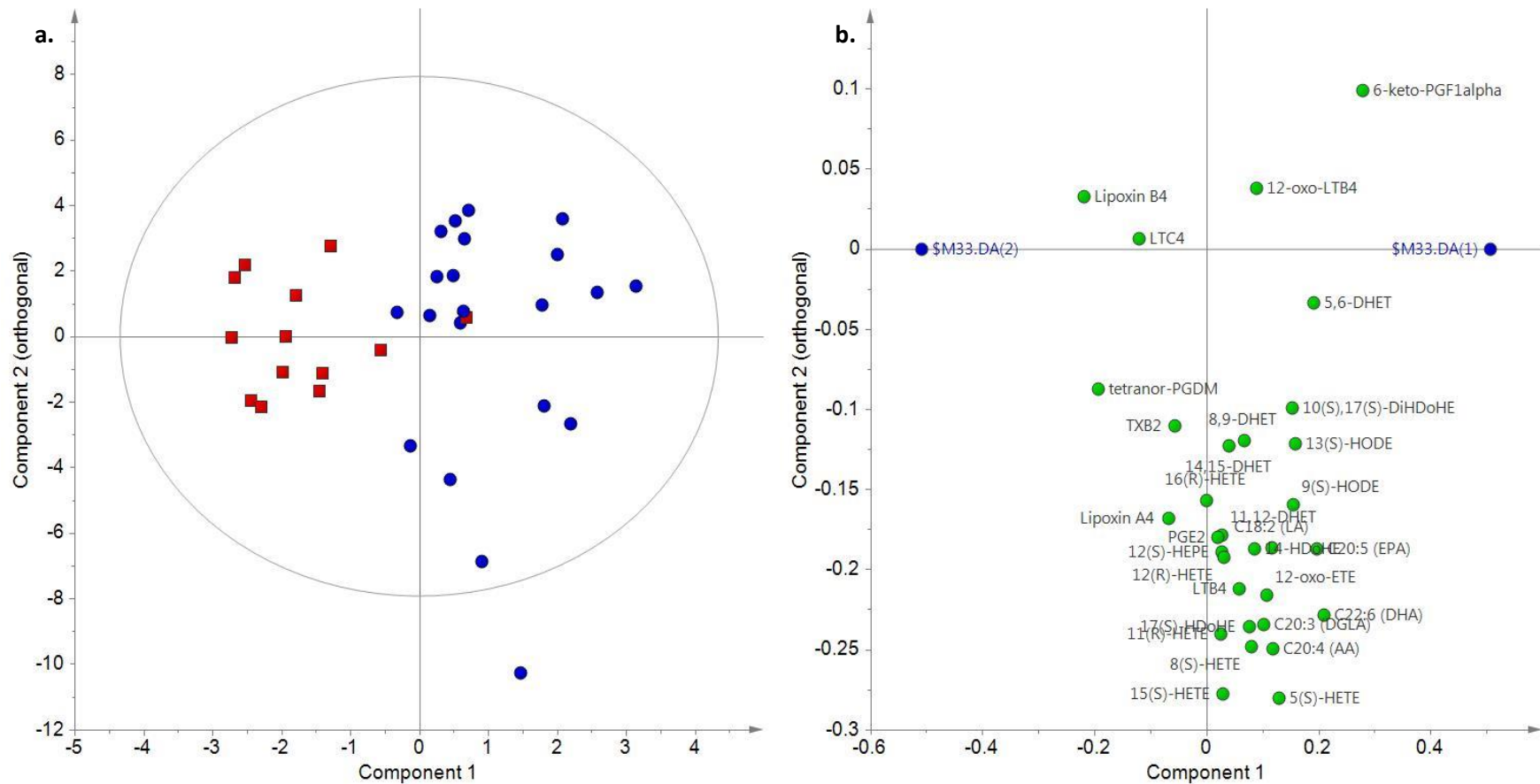


Figure 4.5 a. OPLS-DA scores plot from a model with one aligned and two orthogonal components, showing the aligned vs. the first orthogonal component, before cross validation, (R^2X 0.68 Q^2Y 0.40, $p=0.02$) based on eicosanoid analysis from samples taken at the first time point from patients admitted with pneumonia (red squares) to those admitted with brain injuries with no evidence of pneumonia when the first sample was taken (blue circles). Distribution along the x-axis shows the degree of separation of the two groups along the first component. b. Loadings plot for the OPLS-DA model demonstrating the eicosanoids causing the most separation in the model. Eicosanoids distributed at the extremes of the x-axis are responsible for most variation in the first component, x-axis, of the OPLS-DA model and those at the extremes of the y axis are responsible for most variation in the orthogonal component.



4.5.2.3 Brain Injury vs VAP

Comparison of serum samples taken from the 21 patients with brain injury without infection at the time of ventilation to the samples taken from the five brain injured patients who developed VAP based on CPIS scores at the time pneumonia developed failed to demonstrate separation on PCA. OPLS-DA modelling had no predictive capacity with a negative Q^2Y (R^2Y 0.36 Q^2Y -0.06). Models failed to have any predictive capacity even when VAP was compared to only samples from those brain injured patients who did not go on to develop VAP (R^2Y 0.56 Q^2Y -0.25), their own first time point (R^2Y 0.29 Q^2Y 0.01) or a larger group including the patients assessed by an independent assessor (R^2Y 0.23 Q^2Y -0.16). Some of this lack of predictivity may have related to batch effect. When a batch effect model was made from the subgroup of brain injured and VAP patients a more predictive model could be made (R^2Y 0.59, Q^2Y 0.35, $p=0.05$) and explained a greater proportion of population variation (R^2X 0.47 vs 0.15). This may have been because of the small number of VAP patients, especially if they had a tendency to be randomised to one of the batches.

4.5.3 Cytokines

4.5.3.1 Evaluation of Batch Effect

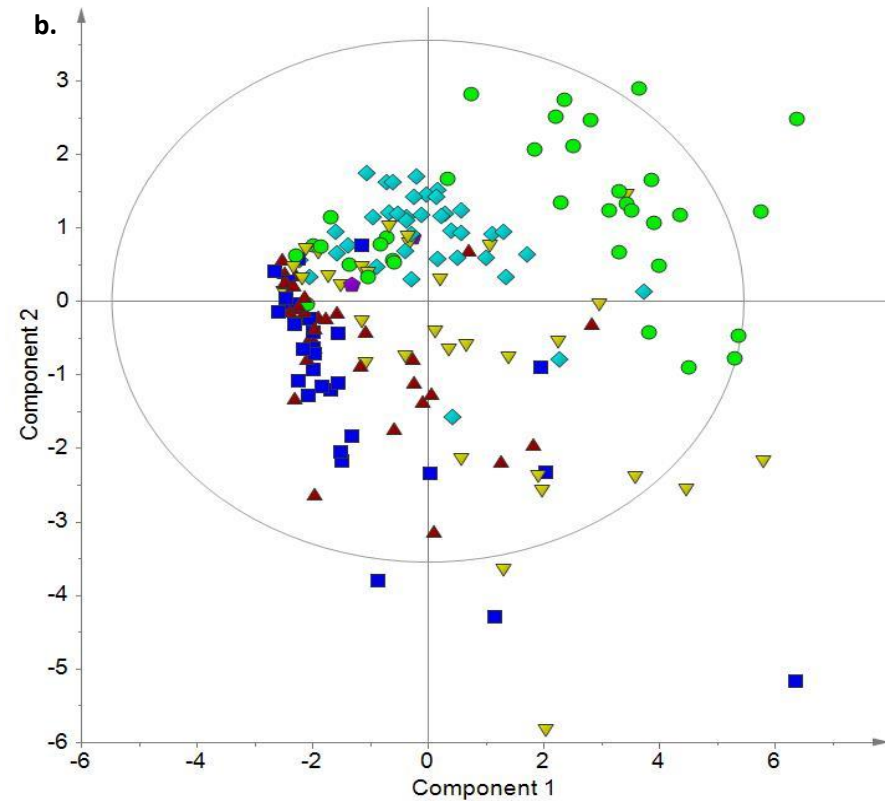
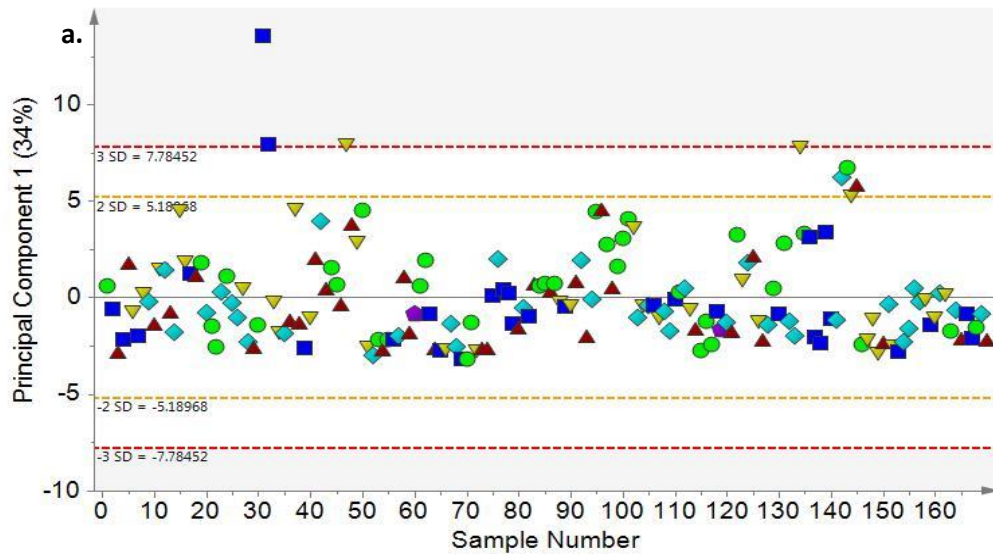
Cytokine measurement was performed in six batches due to the length of the protocol. In order to assess for batch effect PCA was performed and each sample was coloured based on the day on which it was run. One patient's samples were excluded from this analysis due to cytokine levels that were far in excess of the maximum values of many of the standard curves, even after rerunning the samples at a 40 fold dilution. This patient was found to have a lymphoma after enrolment to the study, this diagnosis possibly accounts for the pronounced cytokine levels. Interestingly this patient was not an outlier when only eicosanoids were considered, possibly a consequence of the difference in site of production of cytokines and eicosanoids in relation to lymphoma or the differing timescales

of production of the two types of mediators. This patient's samples were excluded from all other comparisons. The PCA, figure 4.6, shows no natural separation based on sample batch and individual patients' time points tended to cluster together, even when run on different days, suggesting inter-patient variability was greater than either that caused by batch effect or that from time point to time point. A two component OPLS-DA model (R^2Y 0.14 Q^2Y 0.08, $p < 0.001$) could be constructed to try to differentiate the batches. The biggest difference appeared to be between batch 2 and 5, examination of the loadings suggested most of this difference was accounted for by the levels of IL-10 and IL-12p70. However, when the R^2X of this model was explored the batch model explained 58% of the variation across all samples suggesting that batch may be an important contributor to this data.

4.5.3.2 Brain Injury vs Pneumonia

Comparison of the 13 patients with pneumonia on admission to those 21 with brain injuries, without infection, via PCA (R^2X 0.46 Q^2X 0.23) failed to show any natural groupings but with outliers all coming from the pneumonia group, the outliers were associated with elevated levels of almost all cytokines compared to the non-outliers suggesting a generalised increase in inflammatory activity. Supervised analysis with a single component OPLS-DA model (R^2Y 0.18, Q^2Y 0.11, $p = 0.17$), figure 4.7, only had a low ability on cross validation to discriminate the two groups. Assessment of the model with a test set of patients based on the borderline group of patients independently assessed only produced a sensitivity 0.6, specificity 0.67 positive predictive value of 0.6 and negative predictive value of 0.67, similar to those from the eicosanoid only model. All cytokines other than IL-8 and IL-1 α had a tendency to increase in the pneumonia patients, the most important cytokines, based on a VIP score of >1.0 , in this model were ICAM-1, E-selectin, IP-10, MCP-1, IL-13, and TNF α . When this subgroup was used to construct a batch model it was impossible to build an OPLS-DA model with a +ve Q^2Y suggesting that within this group the effects of batch were limited and those of the disease

Figure 4.6. a. Single component PCA (R^2X 0.34 Q^2Y 0.25) of all cytokine batches (run 1: red triangles, run 2: green circles, run 3: yellow inverted triangles, run 4: cyan diamonds, run 5: blue squares, run 6: purple pentagons) showing samples clustering by patient along the first component, direction axis, with no batch predominance as shown by the degree of overlap of the six batches. b. Two component supervised OPLS-DA model (R^2Y 0.21 Q^2Y 0.11, $p < 0.001$) before cross validation showing that the greatest difference is between batches 2 and 5, with this difference being driven by IL-10 and IL12p70 being more predominant in batch 2 as shown on the loadings plot, c. The loadings plot demonstrates the cytokines causing the separation in the OPLS-DA model. The cytokines at the extremes of the x and y-axes are responsible for the most separation in the same respective directions in the OPLS-DA model.



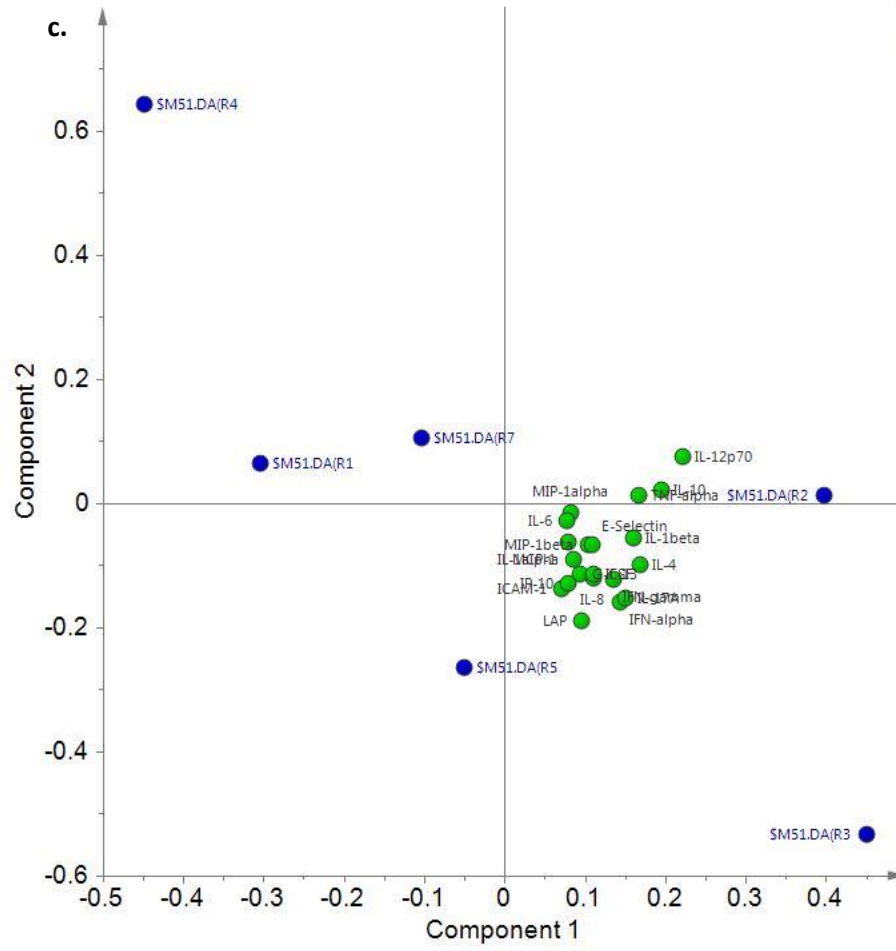
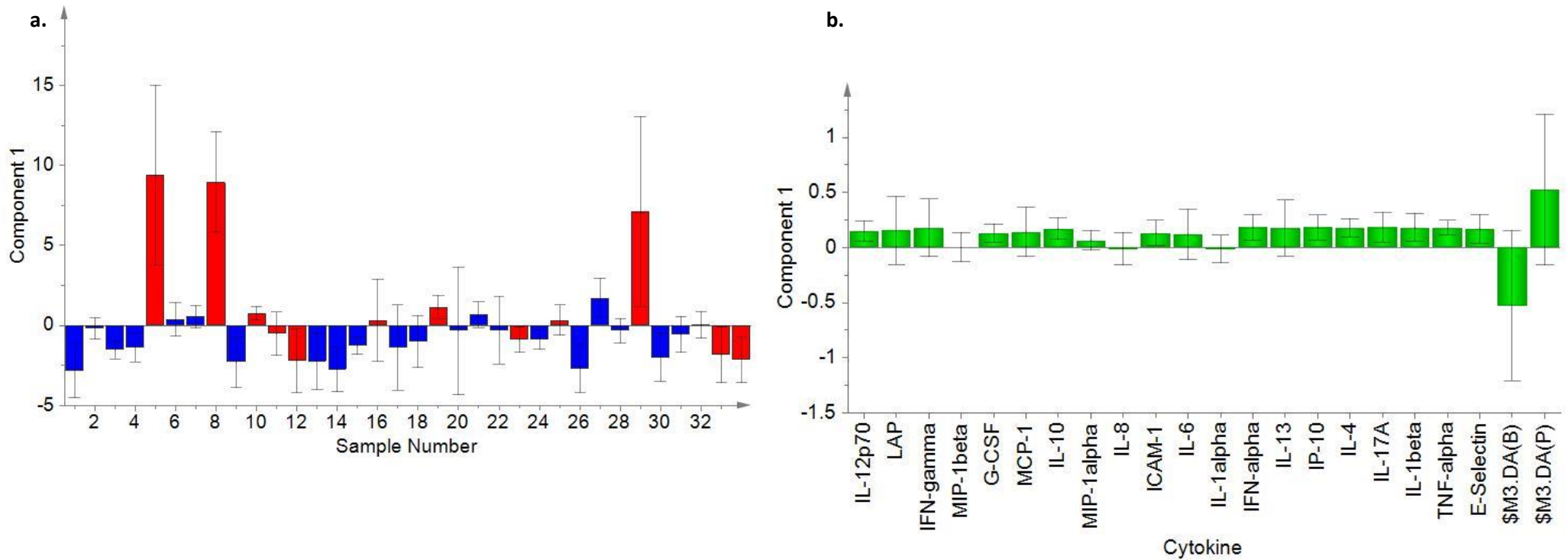


Figure 4.7. a. Single component OPLS-DA model (R^2Y 0.18 Q^2Y 0.11, $p=0.17$) based on cytokine analysis comparing samples taken at the first time point from patients admitted with pneumonia (red bars) to those admitted with brain injuries with no evidence of pneumonia when the first sample was taken (blue bars). Samples from brain injured patients tend to deflect downwards along component 1, y-axis, however, the samples from patients with pneumonia are distributed both upwards and downwards with three patients dominating the upward direction. b. Loadings plot for the OPLS-DA model showing that nearly all cytokines tend to dominate in the pneumonia patients whose samples deflect upwards along component 1 in the OPLS-DA model.



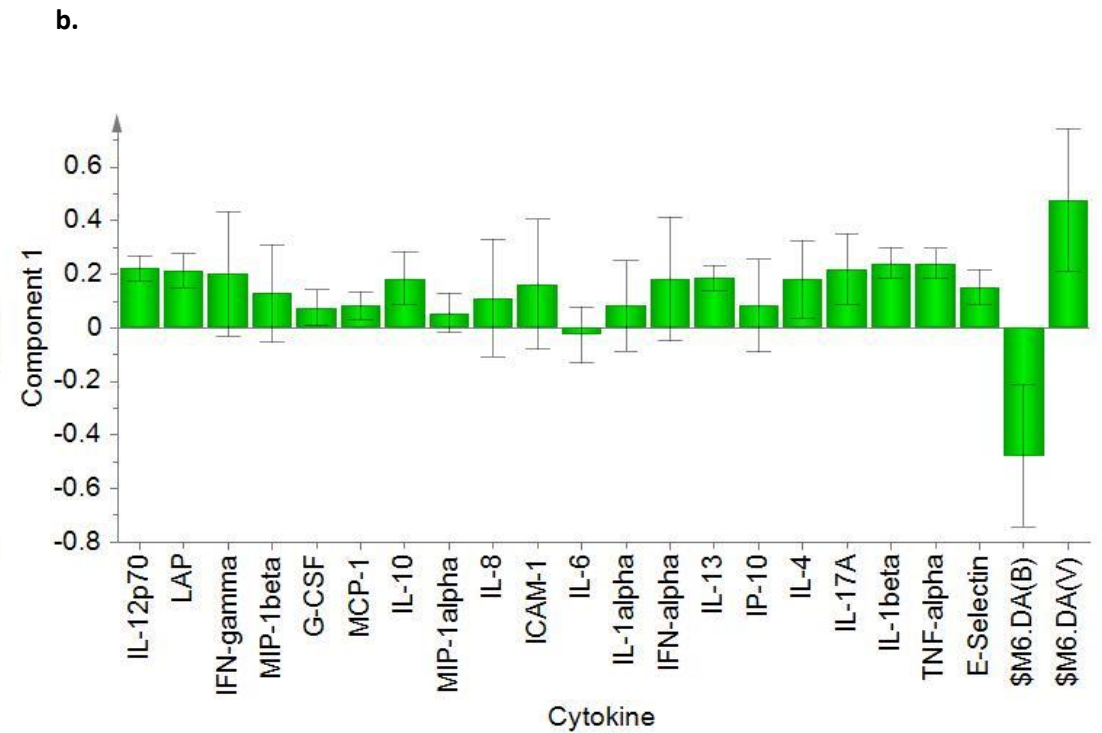
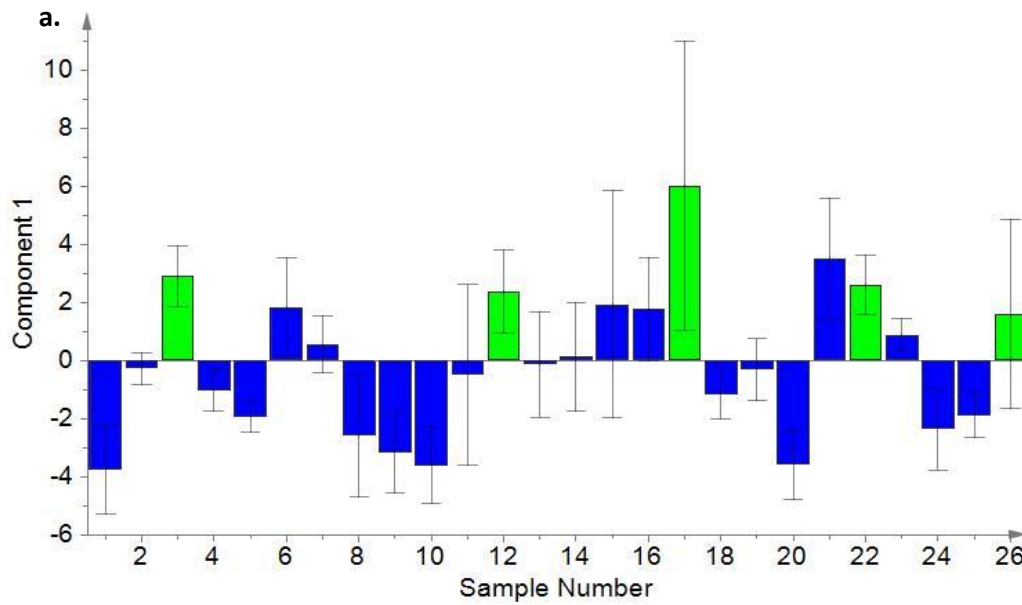
were more important, this was supported by the larger R^2X within the disease model (R^2X 0.43 vs 0.37).

4.5.3.3 Brain Injury vs VAP

Comparison of serum samples taken from the 21 patients with brain injuries without infection at the time of ventilation to the samples taken from the five brain injured patients who developed VAP based on CPIS scores showed no grouping on PCA (R^2X 0.492 Q^2X 0.17). However, a supervised model using OPLS-DA showed an improved predictive capacity (R^2Y 0.38 Q^2Y 0.16, $p=0.13$) compared to that made from eicosanoid measurements, figure 4.8. The loadings showed a tendency for all cytokines except IL-6 to increase in the VAP group, of these $TNF\alpha$, ICAM-1, IP-10, IL-13, iL-12p70, IL-17A, INF γ and IL-1beta caused the majority of the separation based on their VIP scores. The predictive capacity was only marginally improved (R^2Y 0.49 Q^2Y 0.22, $p=0.18$) when only brain injured patients who did not develop VAP at any point were used as controls with the same trend, including IL-6, of all cytokines increasing with VAP. However, when the samples taken from the time that VAP developed were compared to the first samples taken from the same patients, before VAP developed, the model lacked any predictive capacity (R^2Y 0.44 Q^2Y -0.53) and this remained the case even with a larger group made up from a combination of VAP diagnosed from CPIS scores and classification of borderline cases (R^2Y 0.21 Q^2Y -0.80).

The influence of batch on this model appeared greater than when brain injured patients were compared to those with pneumonia at admission. When an OPLS-DA model comparing batch was constructed from the subgroups of patients with brain injuries or VAP (R^2Y 0.19, Q^2Y 0.09, $p=0.39$) the predictive capacity was less than that for the model comparing disease classes. However, the amount of variation explained in the overall population was greater (R^2X 0.46 vs 0.31) again possibly relating to the small number of patients in the VAP group.

Figure 4.8. a. Single component OPLS-DA model (R^2Y 0.38, Q^2Y 0.16, $p=0.13$) based on cytokine analysis comparing samples taken at the first time point from patients admitted with brain injuries with no evidence of pneumonia at the time of sampling (blue bars) to the time point that VAP developed (green bars). VAP samples are all oriented upwards along component 1 and brain injury samples generally deflect downwards, however, a number of brain injury patients overlap the VAP group showing positive orientation. b. Loadings plot for this model showing that nearly all cytokines tend to dominate in patients whose samples show upwards orientation along component 1 in the OPLS-DA model.



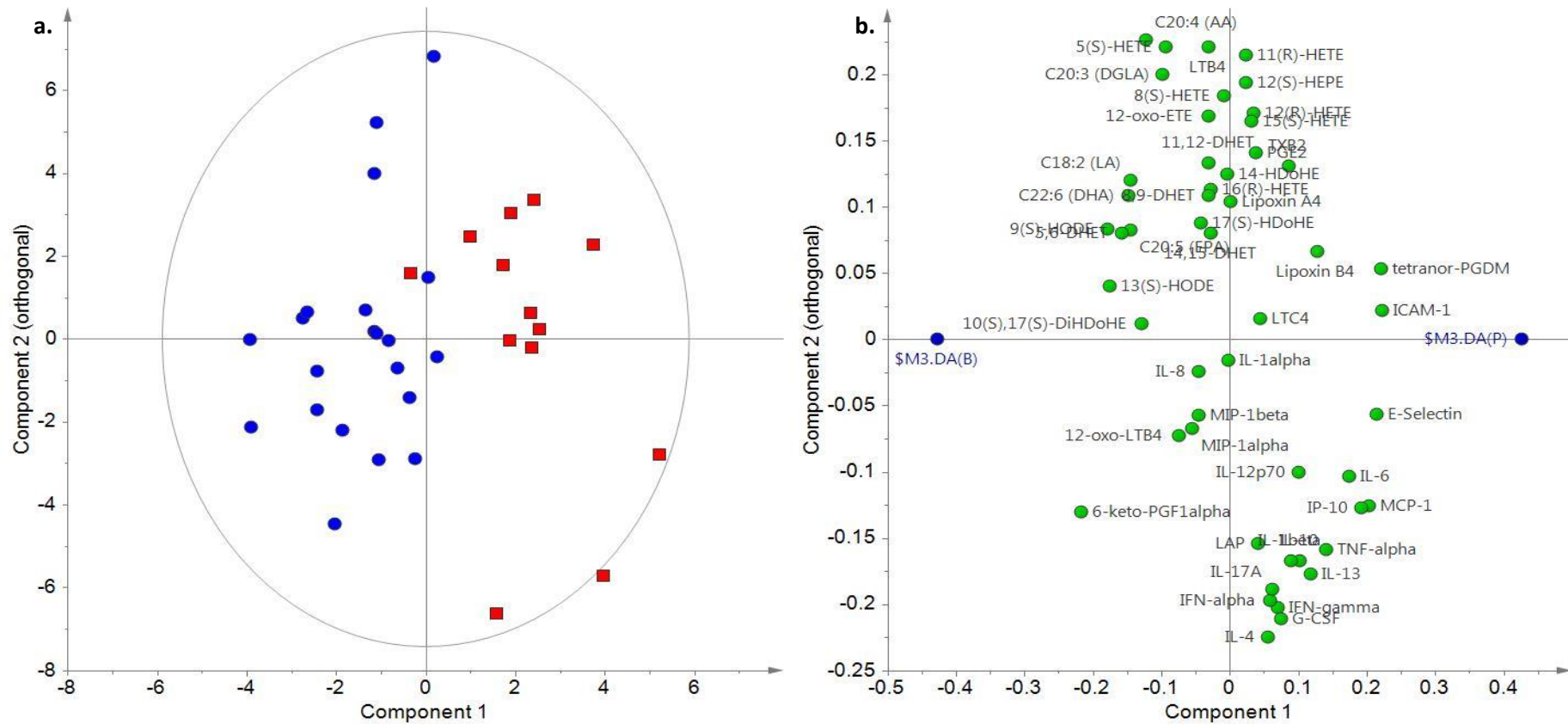
4.5.4 Combining Eicosanoids and Cytokines

4.5.4.1 Brain Injury vs Pneumonia

Combining the cytokine and eicosanoids together into one model produced a two component PCA which still failed to show any natural separation into pneumonia and non-pneumonia groups. Clustering continued to mirror the PCA model using only eicosanoid levels with one group demonstrating a predominance of fatty acids. Similarly three of the pneumonia patients naturally separated out from the others due to dominant levels of nearly all cytokines. Supervised analysis produced an OPLS-DA model (R^2Y 0.69, Q^2Y 0.35, $p=0.01$) with a slightly reduced predictive capacity compared to that from the eicosanoids alone. The loadings from this model, figure 4.9, demonstrated that most of the measured cytokines dominated in the pneumonia group with the exception of MIP-1 α , MIP-1 β , IL-8 and IL-1 α . The cytokines dominating the separation based on VIP scoring were ICAM-1, E-selectin, IP-10, MCP-1, IL-13, TNF α , INF γ and IL-6. Fatty acids dominated the brain injury group, as seen in the eicosanoid model, with 6-keto-PGF1 α , 5,6-DHET, DHA, EPA, 9(S)-HODE, 13(S)-HODE, 10(S),17(S)-DiHDoHE, AA, and 5(S)-HETE causing most separation. Tetranor-PGDM and lipoxin B4 were the eicosanoids differentiating the patients with pneumonia. Validation of the model using the classified borderline cases gave a sensitivity 0.6, specificity 0.67, positive predictive value 0.6 and negative predictive value 0.67, similar to both the eicosanoid and cytokine models. Building a model based only on the most important mediators produced a model with a slightly improved predictive capacity to that using all inflammatory molecules (R^2Y 0.49, Q^2Y 0.43, $p<0.001$), however, although the sensitivity 0.40, and negative predictive value 0.625 reduced the specificity 0.83 and positive predictive value 0.67 both increased.

As it was possible that some of the brain injured patients could be developing VAP earlier than was clinically apparent a further model was constructed comparing only those patients who never developed VAP with those with pneumonia on admission. This two component model (R^2Y 0.78, Q^2Y

Figure 4.9. a. OPLS-DA model with one orthogonal component (R^2Y 0.69 Q^2Y 0.35, $p=0.01$) before cross validation, comparing cytokines and eicosanoids at the first time point from patients admitted with pneumonia (red squares) to those admitted with brain injuries with no evidence of pneumonia at sampling (blue circles). Pneumonia samples cluster in a positive direction along the first component, x-axis, and brain injury samples in the negative direction. b. Loadings plot for the model shown in a, inflammatory molecules to the right of the plot dominate in the pneumonia group and those on the left in the brain injury group.



0.25, $p=0.19$), figure 4.10, had an improved sensitivity of 0.8, a specificity 0.67, positive predictive value 0.67 and negative predictive value of 0.8. Similarly to the model using all brain injured patients ICAM-1, IL-6, MCP-1, E-selectin, IP-10, IL-17A and IL-13 were the cytokines causing most of the separation. Fatty acids again dominated in the brain injury group, with 5,6-DHET, 6-keto-PGF1 α , DHA, 9(S)-HODE, EPA, 13(S)-HODE, 10(S),17(S)-DiHDoHE, 5(S)-HETE, AA, LA and LTB4, causing most separation. Lipoxin B4 and tetranor-PGDM again appeared in the pneumonia group.

4.5.4.2 Brain Injury vs VAP

Combining cytokine and eicosanoid data into one model improved the predictive capacity, after cross validation, when patients with VAP were compared to the first time point from brain injury patients before infection developed (R^2Y 0.76 Q^2Y 0.27, $p=0.14$), figure 4.11. In this model the separating molecules all dominated in the VAP group and were almost all cytokines, predominantly TNF α , ICAM-1, IP-10, IL-13, IL-12p70, IL-17A, INF γ , IL-1beta, IL-10, and IL-4. The eicosanoids causing separation also dominated in the VAP group and were LTC4, 14,15-DHET, LTB4, 8,9-DHET, tetranor-PGDM, 11,12-DHET and Lipoxin A4. LA and DHA both dominated in the brain injury group.

When samples taken at the time patients developed VAP were compared to those at the start of ventilation from brain injured patients who never developed VAP the OPLS-DA model improved (R^2Y 0.90 Q^2Y 0.38, $p=0.19$), figure 4.12. The mediators causing most of the separation in this model were IL-12p70, IL-17A, TNF α , IP-10, INF γ , ICAM-1, IL-13, IL-4, IL-10, IL-1beta and MCP-1, the eicosanoids causing separation, also dominating in the VAP group, were 12-oxo-LTB4, 14,15-DHET, Lipoxin A4, LTB4, tetranor-PGDM and LTC4. In this model DHA, LA, EPA and 14-HDoHe became important in identifying the first time point from brain injured patients who never developed VAP.

However, when the patients diagnosed with VAP based on CPIS were combined with those with borderline scores that were independently classified the model lost all predictive capacity on cross-

Figure 4.10. a. OPLS-DA model with one orthogonal component (R^2Y 0.78 Q^2Y 0.25, $p=0.19$) shown prior to cross validation, comparing cytokines and eicosanoids at the first time point from patients admitted with pneumonia (red squares) to those admitted with brain injuries who never developed VAP during their stay (blue circles). Pneumonia patients separate from brain injured patients along the first component, x axis. b. Loadings plot for the OPLS-DA model. Inflammatory molecules dominating in the pneumonia group are positioned on the right of the plot, predominantly cytokines, and those in the brain injury group are to the left, predominantly eicosanoids.

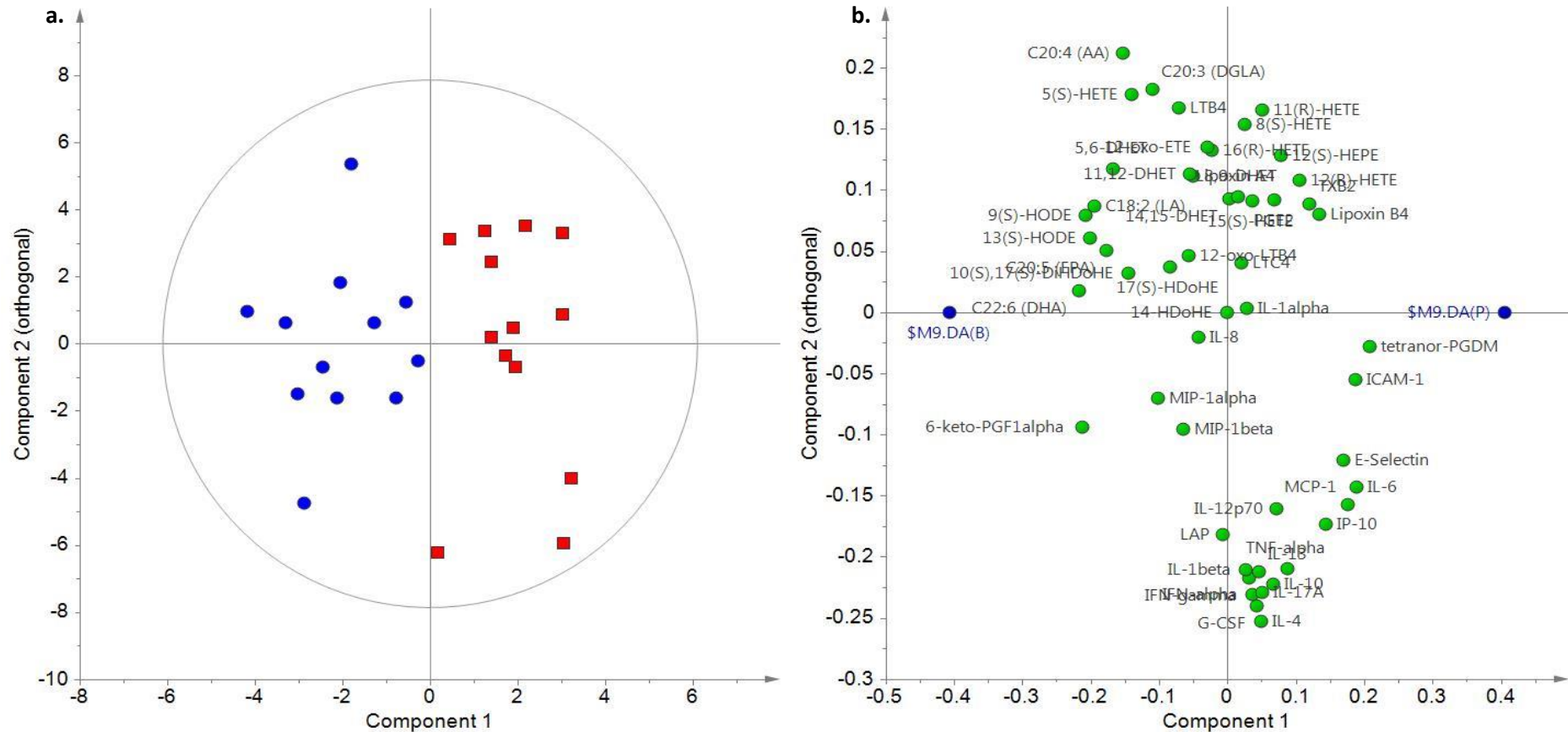


Figure 4.11. a. OPLS-DA model with one orthogonal component (R^2Y 0.76, Q^2Y 0.27, $p=0.14$), comparing samples taken at the first time point from patients admitted with brain injuries (blue circles) to samples taken from those brain injury patients who developed VAP at the time point that VAP developed (green triangles). VAP samples separate in the positive direction along the first component. b. Loadings plot for the OPLS-DA model. Inflammatory molecules important in the VAP group are positioned on the right of the plot whilst those important in the brain injured group are to the left.

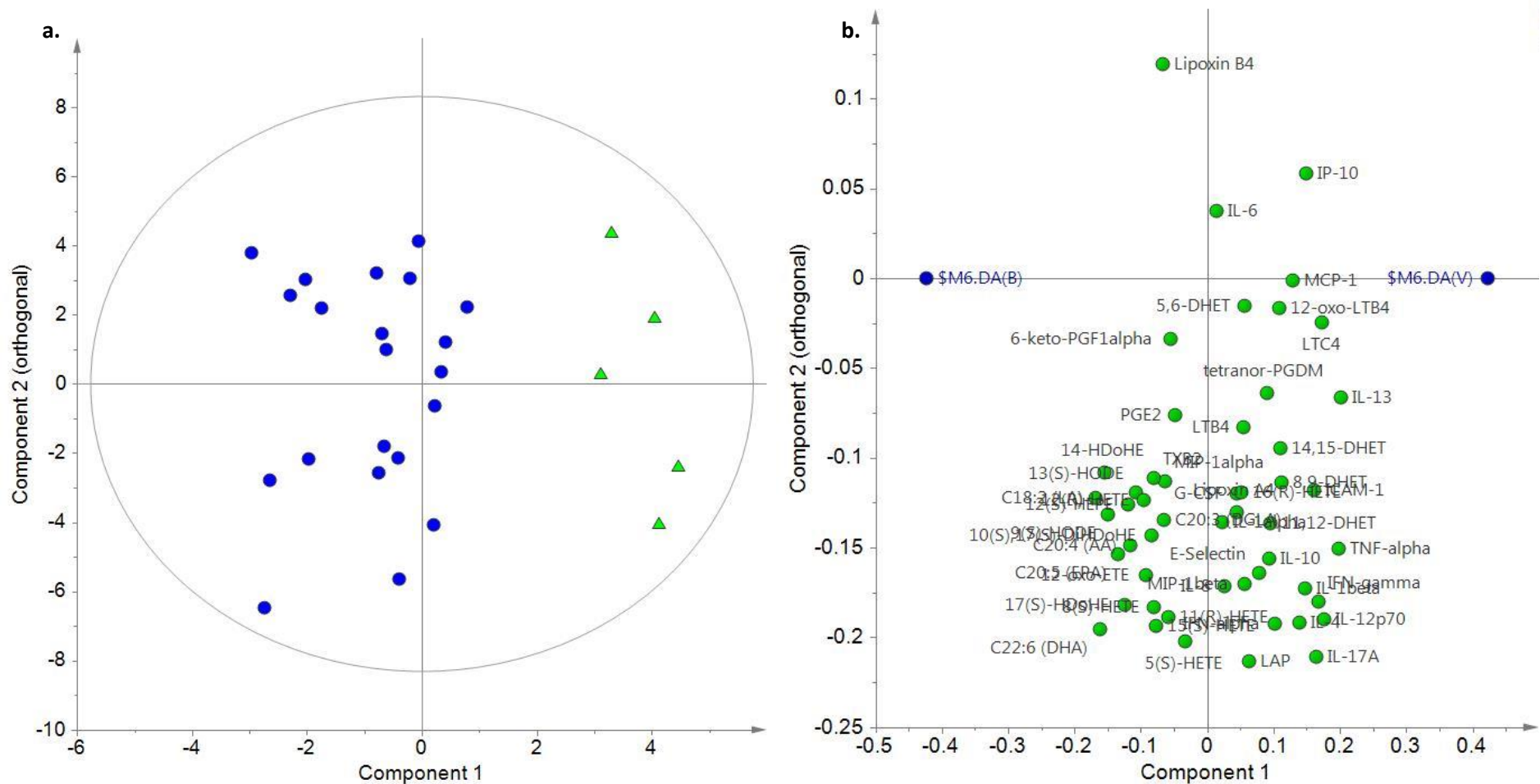
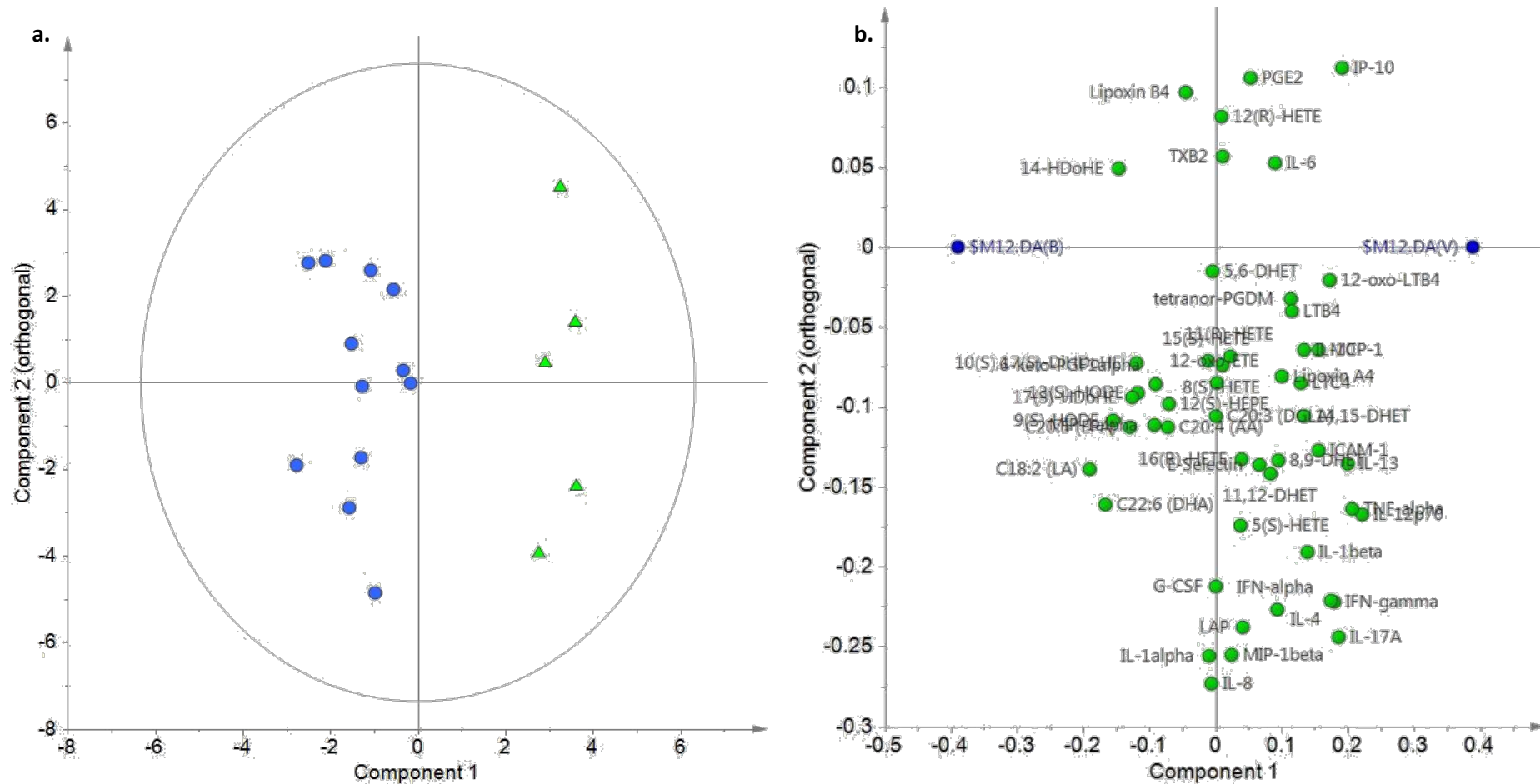


Figure 4.12. a. OPLS-DA model with one orthogonal component (R^2Y 0.90, Q^2Y 0.38, $p=0.19$), comparing samples taken at the first time point from patients admitted with brain injuries (blue circles) who never developed VAP to samples taken when VAP developed in those that did (green triangles). VAP samples separate in the positive direction along the first component. b. Loadings plot for the OPLS-DA model. Inflammatory molecules important in the VAP group are positioned on the right of the plot whilst those important in the brain injured group are to the left.



validation (R^2Y 0.51 Q^2Y -0.42). Also, even when cytokines and eicosanoids were combined, the models were still unable to differentiate samples from the time that VAP developed from those at the start of ventilation (R^2Y 0.60 Q^2Y -0.17) in the same patients.

4.5.4.3 Time Course

So far samples taken from the start of ventilation have been compared to samples taken at the time VAP developed. However, changes seen between these groups may not have been genuinely due to development of VAP and may have represented changes associated with a prolonged stay on intensive care. In the majority of cases VAP developed around time point three and four. In order to get a sense of the inflammatory changes over this time frame the samples from the first time point from brain injured patients who did not develop VAP were compared to samples taken at the fourth time point. OPLS-DA modelling (R^2Y 0.96, Q^2Y 0.66, $p=0.05$), figure 4.13, suggested that the dominance of fatty acids at the first time point shifts towards the metabolites of arachidonic acid, in the form of 5,6-DHET, 8,9-DHET and 14,15-DHET and 16(R)-HETE, 12(R)-HETE, 15(S)-HETE and 11(R)-HETE. Cytokines seemed generally to be at higher concentrations at the beginning of the ICU stay but over time the levels of IL-13, IL-4, IL-1 β , TNF α and IP-10 increased.

If samples from patients diagnosed with VAP based on CPIS scoring were compared to the fourth time point samples from brain injury patients who did not develop VAP a cross validated OPLS-DA model (R^2Y 0.98, Q^2Y 0.56, $p=0.31$), figure 4.14, could be made. The loadings from this model showed a greater dominance of cytokines in those who developed VAP than in those who did not develop infection. The cytokines causing separation of these group were IL-6, MCP-1, IL-12p70, IFN γ , IL-17A, IFN α , IL-10, ICAM-1, G-CSF, IL-1beta, IP-10 and TNF α within the VAP group. The eicosanoids 12-oxo-LTB4 and Lipoxin A4 were the only eicosanoids dominating in the VAP group. Fatty acid metabolites continued to dominate in the final time point of the non-VAP group with 5,6-DHET and 8,9-DHET being responsible for the separation. When only the metabolites causing the greatest

Figure 4.13. a. OPLS-DA model with one aligned and two orthogonal components (R^2Y 0.96 Q^2Y 0.66, $p=0.05$), comparing samples taken at the first time point from patients admitted with brain injuries (blue circles) who never developed VAP to the fourth time point sample (blue squares). Fourth time point samples are separated in a positive direction along the first component, x-axis, and first time point samples in a negative direction. b. Loadings plot for the OPLS-DA model. Inflammatory mediators that increase over time are on the right of the plot and those that decrease are on the left.

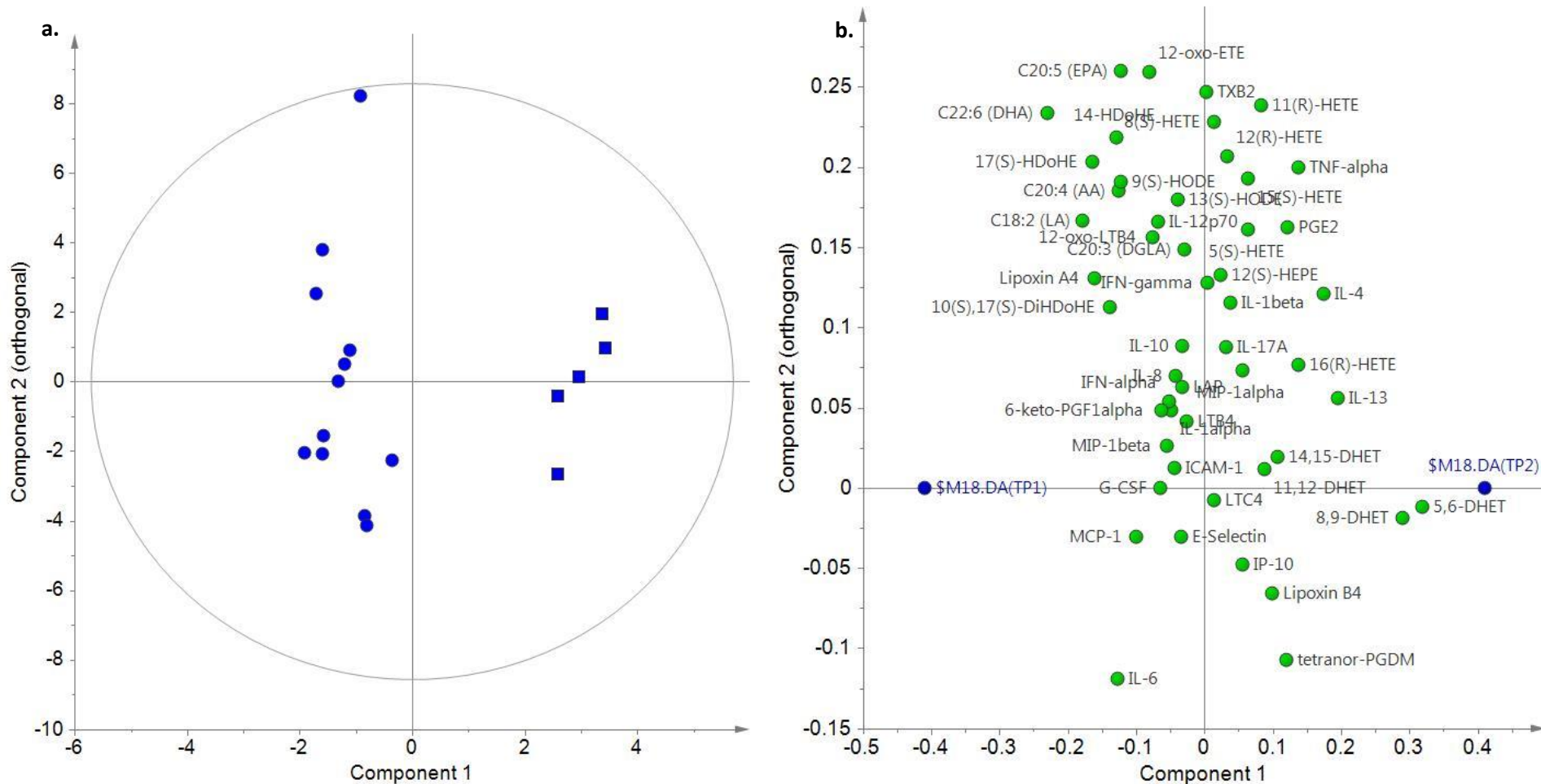
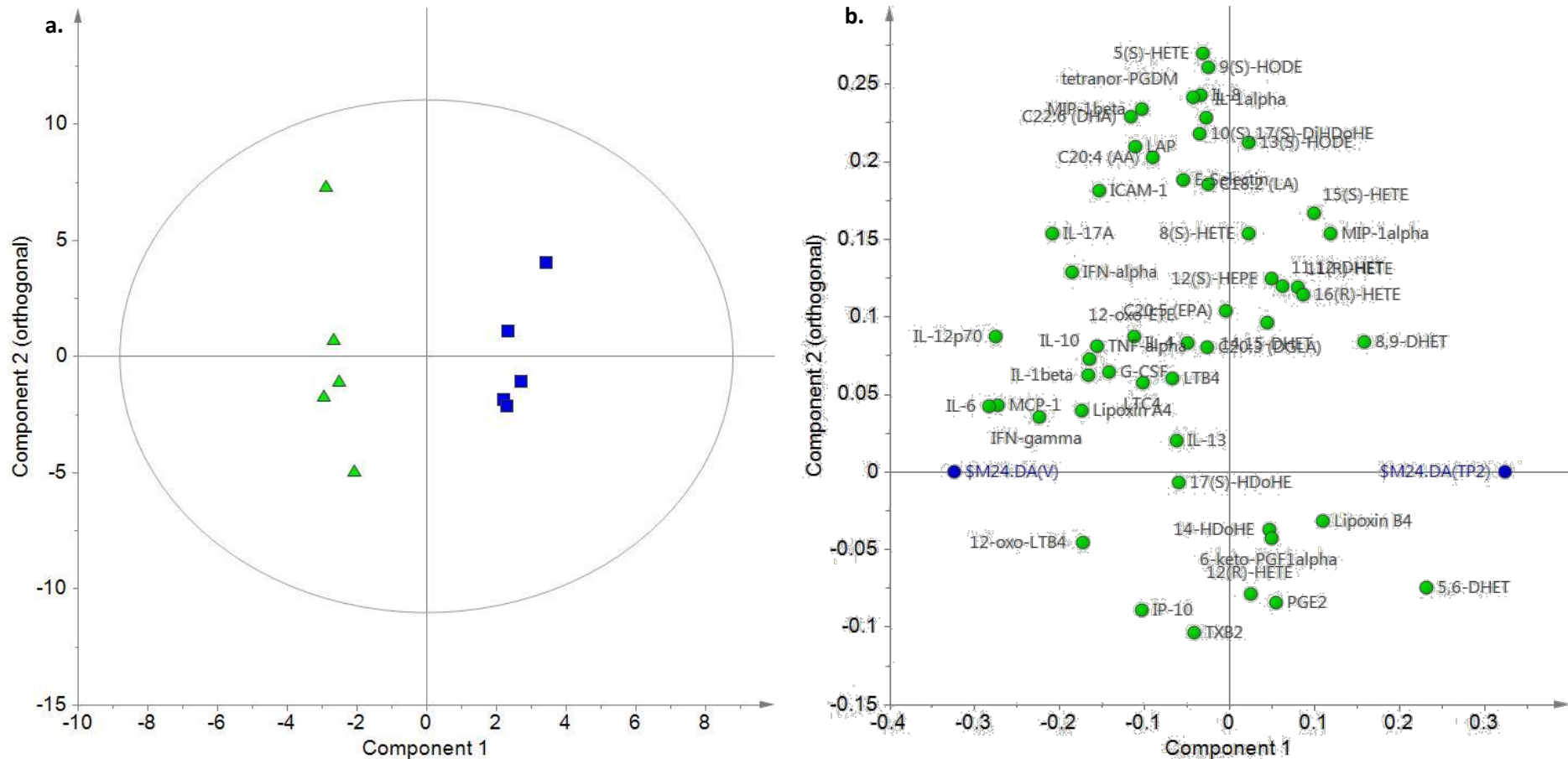
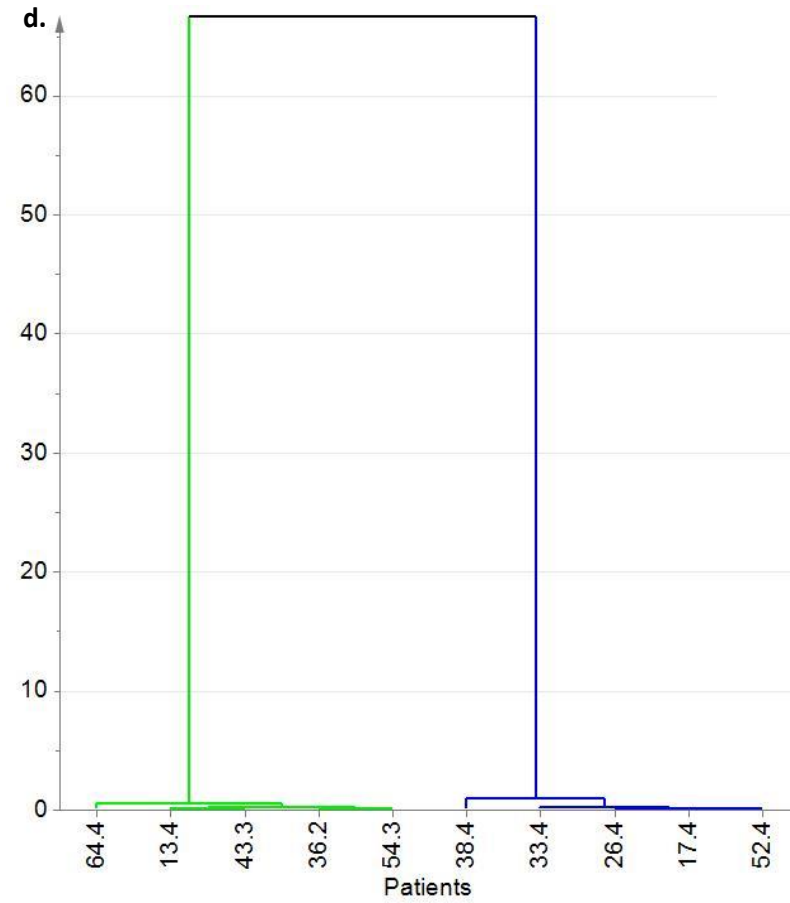
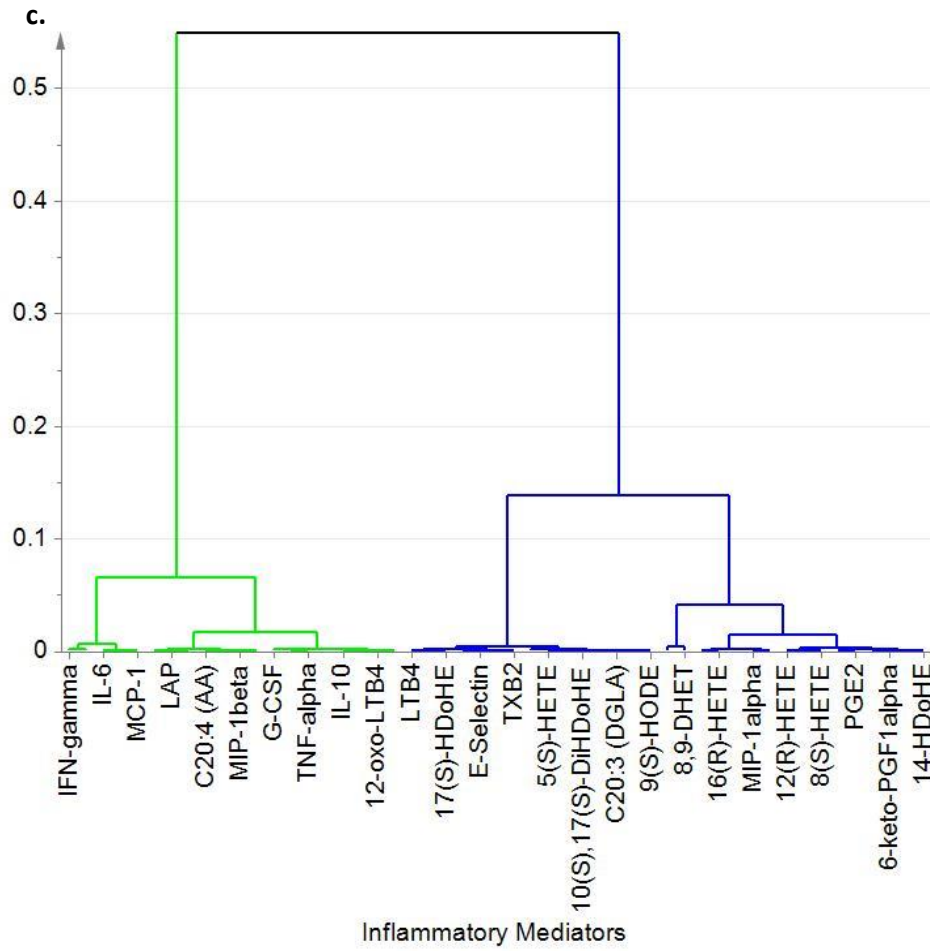


Figure 4.14. a. OPLS-DA model with one orthogonal component (R^2Y 0.98 Q^2Y 0.56, $p=0.31$), comparing samples taken at the fourth time point from patients with brain injuries (blue squares) who never developed VAP to samples taken from those patients with VAP (green triangles). Brain injured patients separate in a positive direction along the first component and VAP patients in a negative direction, x-axis b. Loadings plot for the OPLS-DA model. Inflammatory mediators that increase in VAP are on the left side of the plot. c and d. Hierarchical dendrograms illustrating, c, the cytokines and eicosanoids involved in separating the two groups and, d, the sub-clustering of patients in both groups (group 1 – VAP group 2 – time point 4 from BI patients not developing VAP).



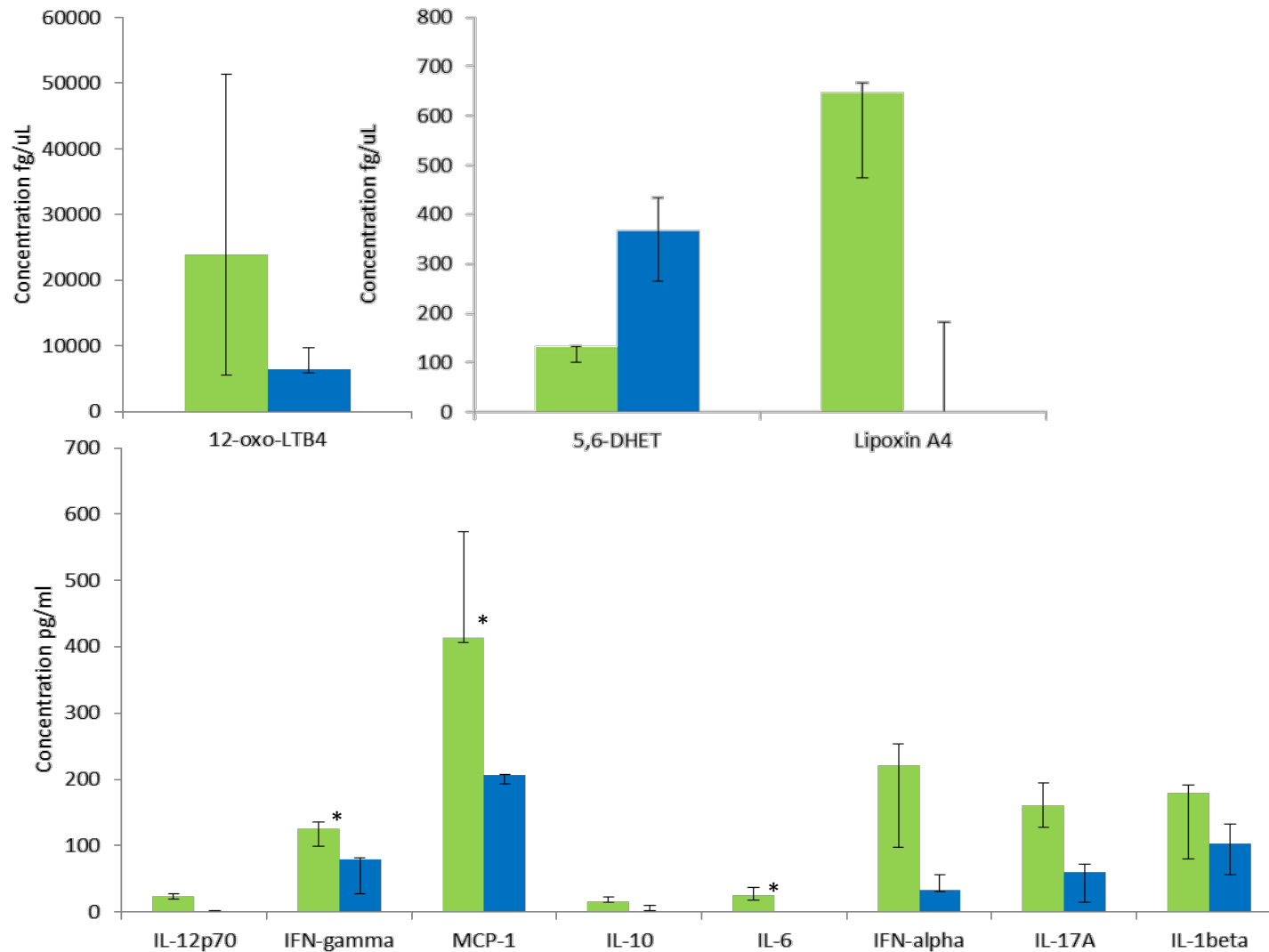


separation were used to construct the OPLS-DA model the predictive capacity improved (R^2Y 0.90, Q^2Y 0.78, $p < 0.01$). Univariate statistics were performed on those analytes, figure 4.15, that were associated with a VIP of >1.0 and a $p(\text{corr}) > 0.5$ in either direction in this model. The non-parametric Mann-Whitney U test was used to compare individual markers as none of these followed a normal distribution when Kolmogorov-Smirnov or Shapiro-Wilk tests of normality were applied. Before correction for multiple comparisons was applied, table 4.4, Lipoxin A4, IL-12p70, IFN γ , MCP-1 and IL-6 showed a tendency towards being elevated in those with VAP and 5,6-DHET showed a tendency to be increased in those brain injury patients not developing VAP at their final time point. IL-10, IFN α , IL-17A, IL-1 β and 12-oxo-LTB4 failed to reach statistical significance between the groups. After the Benjamini-Hochberg procedure was applied to control the false discovery rate only the differences observed for IFN γ ($p=0.04$), MCP-1 ($p=0.04$) and IL-6 ($p=0.04$) remained significant.

Table 4.4. Univariate comparison of discriminant mediators based on an OPLS-DA model comparing brain injury patients at the time point that VAP develops (VAP) to those who do not develop VAP at their final time point (BI TP4). Concentrations are given as median and interquartile range. P-values are from Mann-Whitney U test prior to correction for false discovery rate.

Mediator	VAP	BI TP4	p-value
Lipoxin A4 (fg/ μ L)	647.1 (473.6-667.6)	0 (0-183.2)	0.04
IL-12p70 (pg/ml)	23.49 (18.97-27.3)	0.74 (0-1.38)	0.02
IFN γ (pg/ml)	124.56 (99.76-135.92)	78.55 (26.60-81.96)	0.01
MCP-1 (pg/ml)	412.78 (405.61-573.24)	207.1 (192.90-207.14)	0.01
IL-6 (pg/ml)	24.48 (18.55-36.89)	0 (0-0)	0.01
5,6-DHET (fg/ μ L)	132.2 (101.9-132.8)	367.3 (266.0-434.2)	0.04
IL-10 (pg/ml),	15.49 (15.0-22.29)	1.67 (1.31-9.87)	0.14
IFN α (pg/ml)	220.25 (97.24-253.31)	32.63 (30.71-55.89)	0.06
IL-17A (pg/ml)	161.01 (127.88-194.05)	60.54 (14.53-72.59)	0.06
IL-1 β (pg/ml)	179.95 (80.26-192.03)	102.26 (56.58-132.70)	0.21
12-oxo-LTB4 (fg/ μ L)	23947.1 (5529.9-51405)	6467.6 (5912.2-9771)	0.40

Figure 4.15. Univariate comparison of the mediators associated with a $p(\text{corr})$ of >0.5 in either direction from the OPLS-DA model comparing the final time point from brain injured patients who did not develop VAP to the time point VAP developed in those that did. Green bars VAP time point, blue bars final time point from brain injured patients who did not develop VAP. Data displayed as median \pm inter-quartile range. VAP $n=5$ Brain Injury $n=5$. Comparisons marked * are significant at $p<0.05$ after application of the Benjamini-Hochberg procedure.



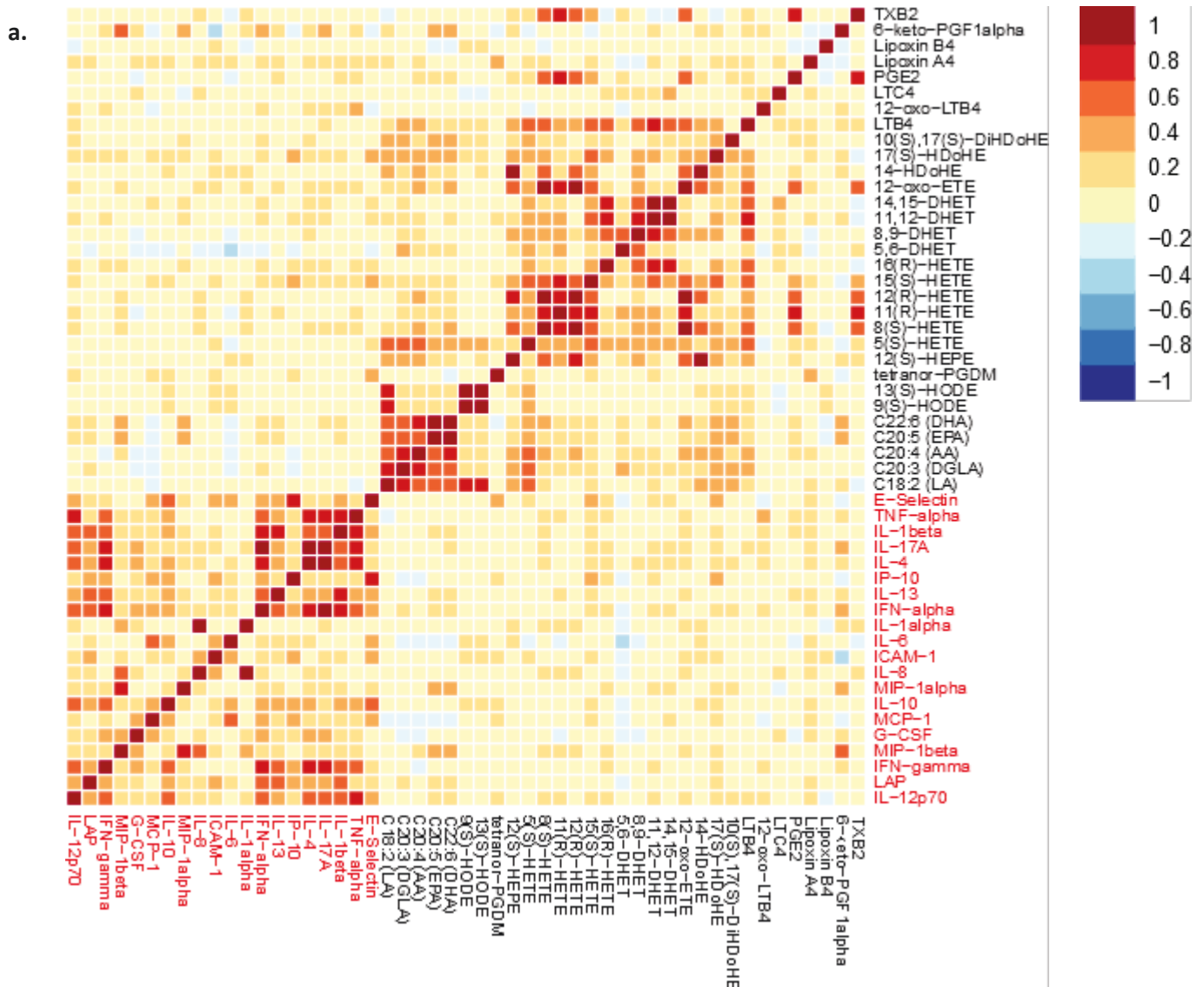
Even when both cytokines and eicosanoids were combined it was not possible to distinguish patients with brain injuries who went on to develop pneumonia from those who did not at the first sample time point, before pneumonia had become clinically apparent (R^2Y 0.35, Q^2Y -0.191).

4.5.4.4 Correlation

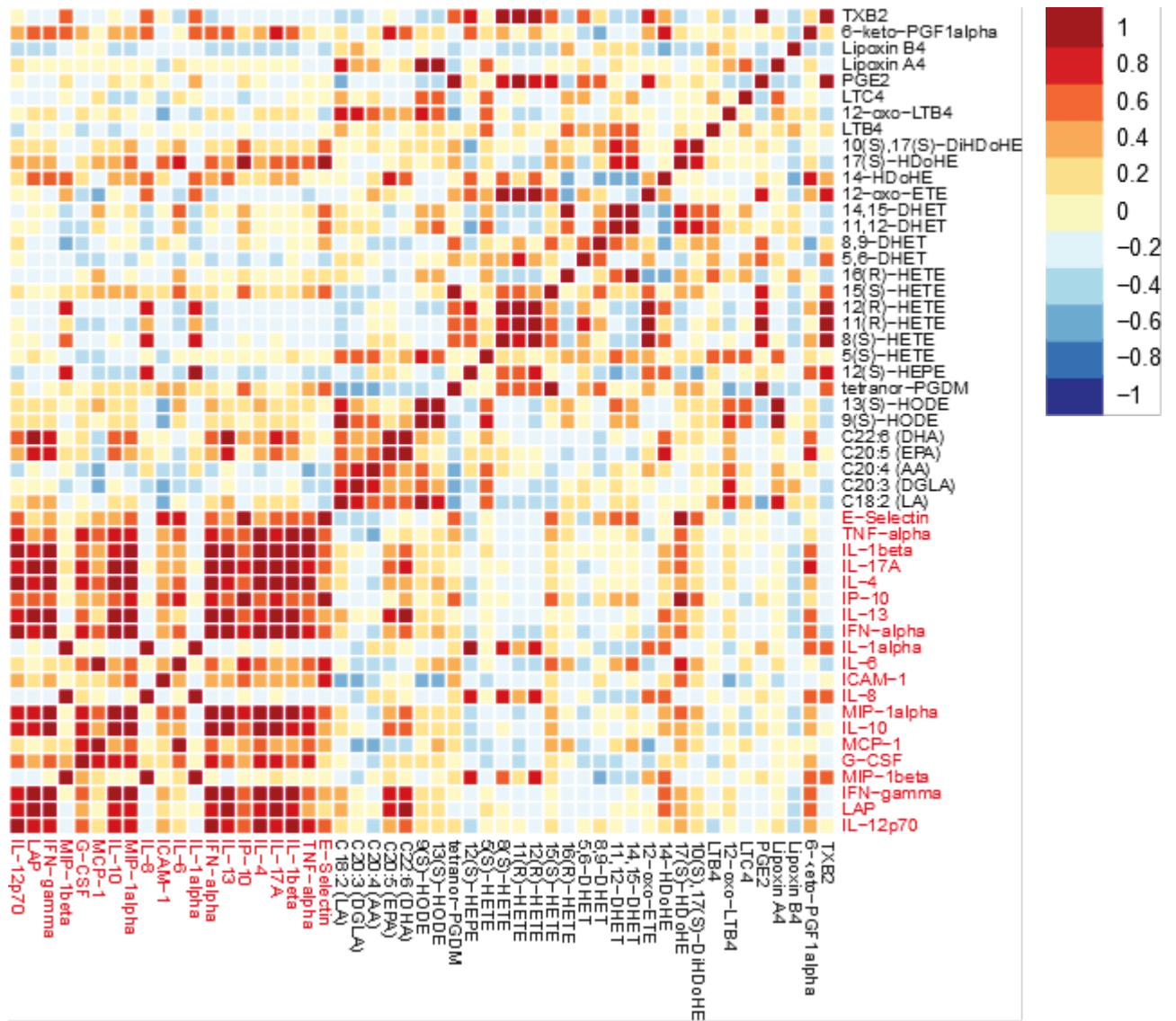
The correlation of all inflammatory mediators was checked against each other to produce correlation heatmaps, figure 4.16. When all samples were explored together there was clearly a trend for the cytokines to broadly correlate in a positive direction and the eicosanoids to do the same. Only low level correlation was seen between the two classes of inflammatory mediators. Within the eicosanoids the precursor fatty acids such as AA, EPA and LA seemed to correlate together and strong correlation was seen between several of their metabolites such as the HETE group of metabolites. When only samples taken at the first time point from patients with pneumonia were considered the strength of correlation between the cytokines generally increased with strong correlation between several of the interleukins with the exception of IL-8 and IL-1 α , which correlated with each other. Some correlation between cytokines and eicosanoids became apparent within this group. For example, 6-keto-PGF1 α , a break down product of prostacycline which mediates vasodilation, was seen to correlate with several, mainly pro-inflammatory, cytokines.

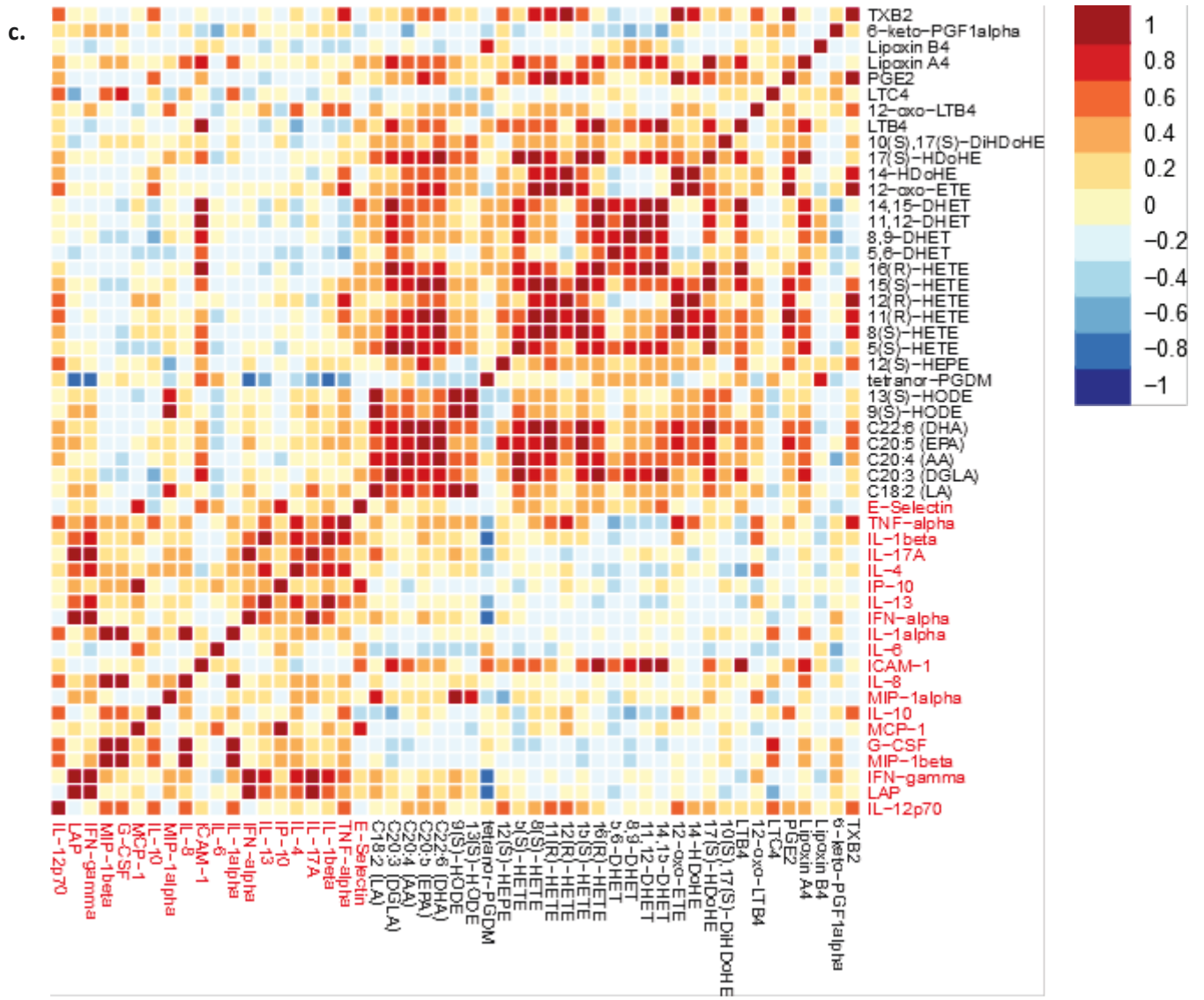
Alternatively when the first time point samples from the brain injured patients who never developed pneumonia, including two patients clearly without pneumonia at enrolment but with borderline CPIS scores during their ICU stay who were independently assessed and classified as not developing VAP, were examined, although correlation still existed between cytokines, the greatest correlation was seen between the eicosanoids. This correlation was seen predominantly between families of similar molecules, such as the fatty acid precursor molecules, the HETEs and the DHETs. Interestingly the cytokine which correlated with the most eicosanoids in this group was ICAM-1, which has previously been associated with subarachnoid haemorrhage.

Figure 4.16. Heat maps showing the correlation between all cytokines and eicosanoids a. all samples from all time points (n=167) b. samples from pneumonia patients at the start of ventilation (n=13) c. samples from brain injury patients who do not go on to develop VAP (n=12). Colours indicate the strength of the Pearson correlation co-efficient (R) and are given in the colour bar next to each plot, the closer to red the stronger the positive correlation. Cytokines are indicated in red ink and eicosanoids in black.



b.





4.6 Discussion

This chapter has explored the potential of a panel approach to eicosanoid, using a MS methodology, and cytokine, using a flow cytometry based method, measurement to assist the diagnosis of both pneumonia and VAP. Not only has the independent ability of each of these panels to differentiate patients with pneumonia from those with brain injuries been examined but also a combined approach using both panels together.

Neither the eicosanoid nor cytokine measurements appeared to suffer from a significant batch effect when PCA was used to look for natural separation within all samples. Differences between individual patients, especially for the cytokine experiments, seemed to dominate over either an effect due to batch or that related to samples taken from different time points during a patient's stay. In both cases, however, it was possible to produce multivariate models that showed some ability to separate samples based on batch and thus identify the analytes that may be most affected by batch effect.

Use of only eicosanoid measurements to differentiate pneumonia from brain injuries at the time of admission to ICU allowed a model to be constructed that had a moderate predictive capacity at cross-validation and both sensitivity and specificity of 60-70% when validated with a small independent group of patients. Interestingly the markers that caused most of the separation dominated in the brain injured group. These markers were predominantly fatty acids and their direct metabolites. Polyunsaturated fatty acids such as docosahexaenoic acid (DHA) and eicosapentaenoic acid (EPA) may inhibit platelet function (285) and increase risk of bleeding and thus subarachnoid haemorrhage (SAH), the predominant injury in this brain injury group. In some populations higher risk of haemorrhagic stroke has been seen in patients with high levels of these polyunsaturated fatty acids in their fat composition (286), however, this has not been seen in all populations (287). Although little is written about serum levels of free fatty acids in patients with brain injury, the brain

has a high composition of polyunsaturated fatty acids, especially DHA, and all free fatty acids have been seen to be elevated in the cerebrospinal fluid of patients with SAH (288) and the F4-neuroprostanes, the oxidative metabolites of DHA, have also been seen to increase in the CSF of both patients with SAH and traumatic brain injury (289). EPA may be involved in brain injury and may play an important role in the modulation of cerebral circulation (290-292). Similarly, in an experimental model hydroxyeicosatetraenoic acids have been found to be elevated in the CSF, haemorrhagic clot and basilar artery following SAH (293) and levels of 6-keto-PGF1 α have been seen to be elevated in the urine of patients following haemorrhagic stroke (294). As 6-keto-PGF1 α represents the metabolic product of prostacyclin a possible causal relationship may exist through alterations in the regulation of cerebral blood flow associated with brain injury.

Although the differences in eicosanoids potentially represented both risk factors for and the result of cerebral haemorrhage it is also possible that they represented different temporal courses of the two diseases in question. Brain injury usually occurs rapidly in patients who were often previously well, however, pneumonia takes several days to develop with a prodromal phase when patients may feel unwell and have altered or diminished dietary intake. Levels of polyunsaturated fatty acids, such as LA, have been seen to fall in states of reduced oral intake such as anorexia nervosa (295) and similar changes may be occurring seen in this context.

Within the pneumonia group lipoxin B4, a metabolic product of lipoxin A4, and tetranor-PGDM, the stable degradation product of prostaglandin D2, were the two eicosanoids that were greater than in the brain injured patients. The lipoxins have been associated with the resolution phase of inflammation and inhibit the actions of the leukotrienes, especially LTB4. Lipoxin A4 has been measured in the BAL fluid of patients with several pulmonary diseases including pneumonia (162) and PGD2 has been suggested to have an anti-inflammatory role in lung inflammation (296).

Interestingly it was not possible to use eicosanoid measurements to predict patients with brain injuries who went on to develop VAP either in comparison to all brain injured patients at time point one or to only those that were known not to develop infection at any time. This suggests that the lack of ability to identify these patients was not due to confounding factors from the patients who went on to develop VAP exhibiting important metabolic changes at the time of first sampling. As the eicosanoids identified in those patients with pneumonia at admission seemed to be predominantly anti-inflammatory it is possible that by looking at the serum samples that were taken when VAP seemed to be developing clinically it was too early in disease progression to see these markers in VAP patients. The number of patients developing VAP was small in comparison to both the brain injury and pneumonia groups and it is possible that with this sample size it was not possible to detect subtle changes in eicosanoid levels in this group.

Use of a cytokine panel to try to differentiate patients with pneumonia from those with brain injury performed less well than the model using eicosanoids alone. On the whole all cytokines tended towards an increase in the pneumonia group. Of the most predominant cytokines IP-10 and MCP-1 are involved in chemoattraction for monocytes and IP-10 is secreted in response to INF γ . ICAM-1 and E-selectin are involved in leucocyte cellular adhesion and TNF α is an acute phase reactant associated with several inflammatory conditions. Interestingly out of the most important cytokines in this model IL-10 is the only one that has a predominantly anti-inflammatory role.

In a mouse model of *E.Coli* pulmonary infection the importance of MCP-1 has been demonstrated and it is suggested that it may control production of other cytokines such as TNF α , IL-6 and eicosanoids such as LTB₄ (297). In humans systemic levels of TNF α , IL-6, IL-10 and IFN- γ were significantly higher in severe community acquired pneumonia than in non-severe pneumonia and healthy individuals (298, 299), however, TNF α has also been seen to be higher in ARDS than severe pneumonia (300). Some of these cytokine changes may act as predisposing factors to CAP

as opposed to direct responses to infection as high TNF α and IL-6 levels have been suggested to predispose to CAP (301). In another study using stimulated leukocytes from patients who had recovered from Gram negative pneumonia, stimulated leukocytes produce less IL12p70 and TNF α than healthy controls but more G-CSF, and similar IL-10 levels (302). In paediatric patients with influenza and secondary pneumonia both IL-10 and IL-5 were significantly greater in patients with pneumonia than in those without. Serum concentrations of INF γ , TNF α , IL-4, and IL-2 were significantly lower in pneumonia patients with neutrophilic leukocytosis than in those without (303). Elevated levels of IL-6, IL-8, MCP-1 and TNF α associated with pneumonia have been shown to be reduced when patients are given dexamethasone, with the degree of suppression being linked to the causative organism (304). In an animal model the concentration of serum TNF α correlated to that in BAL specimens after an interbronchial *E.Coli* challenge and the serum concentration also appeared to be dependent on the degree of bacterial challenge (305). The patients with pneumonia in this study not only had community acquired pneumonia but some who had brain injuries possibly had an aspiration pneumonia. In models of aspiration MCP-1 and TNF α have been found in BAL fluid and used to predict the type of aspiration syndrome (306). Increased levels of IL-1beta and IL-6 have also been associated with other forms of lung disease such as those working in phosphate mines (307) suggesting a more generalised role in pulmonary inflammation.

Slight variations in cytokine levels in previously reported studies and the current study may be due to a number of factors, firstly the exact cytokines that are up-regulated may vary between causative organisms and in this population there was a range of responsible microorganisms causing pneumonia, see chapter 2. Secondly cytokine levels change with the stage and natural history of disease. Although an attempt was made to enrol all patients within 48h of the start of mechanical ventilation it was impossible to account for the duration of disease prior to enrolment and the phase of pulmonary inflammation for each patient, and thus the exact cytokines that may predominate.

Cytokine measurements performed better than eicosanoid measurements when trying to differentiate brain injured patients at the time of developing VAP from the first sample taken from brain injured patients without infection. However, even with these measurements the predictive capacity of these models following cross validation was limited.

When both cytokine and eicosanoid measurements were combined into one model the ability to differentiate pneumonia from brain injured patients was marginally reduced after cross-validation than with eicosanoids alone. When validated using the independently classified patients the test statistics were similar to those from models based on eicosanoids and cytokines alone, sensitivity 0.6, specificity 0.67, positive predictive value 0.6 and negative predictive value 0.67. As there is no gold standard by which to diagnose pneumonia there was no single test or score to which this method could be compared. The use of clinical diagnostic criteria in a paediatric population to predict radiologically confirmed pneumonia had a sensitivity of 0.45, specificity of 0.66 and positive and negative predictive values of 0.25 and 0.82 respectively (12). In adults abnormal vital signs have a high degree of sensitivity (14) but lack specificity for pneumonia, however, it is also known that features such as respiratory rate may be sensitive but not specific (16) limiting their usefulness. Decision aids have been evaluated that use clinical features to determine the likelihood of a radiological diagnosis of pneumonia. In a single study clinicians judgement was found to have a sensitivity of 0.74, a specificity of 0.84, a positive predictive value of 0.27 and a negative predictive value of 0.97 in primary care (18) and in another clinical diagnosis had a sensitivity of 0.29, a specificity of 0.99, positive predictive value of 0.57 and a negative predictive value of 0.96 (19).

No biomarker has been found to be a gold standard test for pneumonia, the most studied are C-reactive protein (CRP) and procalcitonin (PCT). In studies of CRP with and without clinical features of pneumonia sensitivity varied from 0.36-1.0 and specificity from 0.52-0.96 depending on the cut off of used (22-24), however, if an infiltrate was present on the x-ray then these values changed to sensitivity 0.36-0.89 and specificity 0.17-0.91 (24). In another primary care study a CRP>20mg/l had

a sensitivity of 0.73, a specificity of 0.65, a positive predictive value of 0.24 and a negative predictive value of 0.94 to diagnose pneumonia in patients already suspected of having lower respiratory tract infections (25). PCT may have sensitivities of 0.17-0.90, specificities of 0.59-1.0, positive predictive values of 0.24-1.0 and negative predictive values of 0.89-0.94 depending on the cut off levels used in the absence of radiology, however, if an infiltrate was already present on the CXR then these values changed to sensitivity 0.43-0.90 and specificity 0.39-0.87. In comparison blood cultures only had a sensitivity of 0.11 (24, 25).

Many of these studies used radiological findings as confirmation of pneumonia, however, depending on the frequency of bacterial infection infiltrates on chest radiograph have been found to have a positive predictive value of only 0.46-0.85 in one study (26) and lack sensitivity, with around 21% of radiographs being negative initially, in another (27).

The model described above using cytokine and eicosanoid measurement performed at least similarly to some of the clinical models outlined above. However, it must be remembered that the group of patients in this study were much more unwell than those in the primary care studies so the performance of clinical variables may be very different in this group. Also many of these studies used radiological findings as an end point where as the diagnosis of pneumonia in this model took radiology and all laboratory results into account when patients were classified as pneumonia. Clearly evaluating any new test to make a diagnosis of pneumonia is potentially limited when no gold standard exists, the calculated test performance statistics are based on patient classifications that have their own limited sensitivities and specificities as such it would be impossible to know if a new test outperformed the criteria used as the basis of study classification.

The inflammatory molecules that were of most importance in this model were almost identical to those identified with either eicosanoids or cytokines alone with the exception that in this model IL-6 assumed a new degree of importance.

Due to concerns that the differences between VAP and brain injured patients sampled at the first time point may have represented the effect of a prolonged stay on ICU, rather than the development of infection, a further model was constructed comparing an equivalent time point from those brain injury patients not developing VAP. This allowed a model to be constructed with reasonable predictive capacity on cross validation. Again cytokines dominated in the VAP group. As well as cytokines seen in previous models G-CSF, IL-1beta, IL-12p70 and IL-17A become important along with the eicosanoids 12-oxo-LTB4 and lipoxin A4. 12-oxo-LTB4 is a metabolite of LTB4 which has been associated with pneumonia in a number of ways. It has been seen to increase IL-6 levels (159), has been linked to pulmonary complications following trauma (160) and has been associated with an increase with both *Klebsiella* (308) and *Pneumococcus* (309) infections. LTB4 has also been measured in the EBC of children with CAP (310), in the pleural effusions of patients with pneumonia (311) and in BAL fluid from an animal model of brain trauma which was associated with a non-significant rise in serum LTB4, IL-1 β and IL-6 (312). In patients with severe head injuries IL-6, IL-10, IL-1 α , TNF α , and IL-8 have been associated with poor prognosis (313, 314) whilst TNF α , IL-8 and IL-10 were associated with longer mechanical ventilation and the development of VAP (314). Similarly in trauma patients who develop VAP IL-6 and 8 may be associated with antibiotic non-responders (315). Interestingly previous studies failed to find that serum or plasma cytokines were able to identify VAP but within BALF several cytokines have been noted to increase including IL-1 α , IL-1 β , IL-8, G-CSF, MIP1 α and TNF α (316, 317).

Cytokine production may not only be a response to infection but may result from the act of mechanical ventilation its-self, for example increased tidal volumes may cause increase in plasma cytokines (318) and following lung injury in animal models TNF α , IL-6 and IL-1B have been seen to act in combination to cause airway IgA secretion (319).

A limited amount of work exists examining the correlations of cytokines and eicosanoids especially between such an extensive number of inflammatory mediators. Looking at the correlation between all of the inflammatory mediators measured showed some interesting results. The most striking difference was that when all patients at time point one were taken very little correlation was seen between cytokines and eicosanoids, whereas strong correlations existed between molecules from within the same families of mediators. However, when either patients with pneumonia or those with brain injury who did not develop pneumonia were taken alone new patterns of correlation became apparent. In pneumonia negative correlation was seen between lipoxin B4 and almost all the cytokines whereas this was less marked when the brain injured patients were considered and was not apparent when all patients were combined. Similarly lipoxin A4 shows only weak correlation with cytokines in pneumonia patients but strong positive correlations with IL-12p70, MIP1b, GCSF, IL-8, ICAM-1 and IL-1 α in brain injured patients. 10(S)17(S)DiHDoHE and 17(S)-HDoHE both demonstrated similar patterns of correlation in pneumonia patients with positive correlation being seen with all cytokines except MIP-1b, IL-8 and IL-1 α where negative correlation was seen. These patterns were not the same in the brain injured patients. These two eicosanoids are both anti-inflammatory in nature and oppose the actions of the cytokines they showed negative correlation with.

Within the pneumonia patients DHA and EPA had strong positive correlation with IL-12p70, LAP, INF γ , IL-13 and IL-17A whereas AA and DGLA had predominantly negative correlation with almost all cytokines. In the brain injury cohort this pattern was less clear-cut, in this group there were similar patterns with all fatty acid precursors with negative correlations with MIP-1b, GCSF, MP-1 and IL-6. EPA and DHA have previously been shown to inhibit IL-6 and IL-8 production from endotoxin stimulated endothelial cells (320) and in this data set, negative correlation was seen between both EPA and DHA and IL-6 across all three clinical groups which is consistent with the previously reported data (320). EPA and DHA have also been seen to reduce TNF α , IL-1 β and IL-8 levels although this was

less clearly seen in these data. Adhesion molecule expression, including ICAM-1, have been reduced by both EPA and DHA (320), however, the correlation data from all three groups in this current data set did not support these previous finding with low levels of positive correlation seen.

In pneumonia tetranor-PGDM had a positive correlation with all cytokines, consistent with its action as a mediator of inflammation and vasodilation, but in the brain injury group there were several strong negative correlations including LAP, IFN γ , MIP1 α , IFN α , IL-13, IP-10, IL-4, IL-17A, IL-1 β and E-selectin. PGD2 is a predominant prostaglandin in the brain and in this organ is synthesized via an alternative pathway to that in the systemic circulation. It is possible that a difference in the expression of this prostaglandin exists between patients with brain injuries and pneumonia explaining the variation in correlation in these two conditions. Similarly 6-keto-PGF1 α correlated with all cytokines except ICAM-1 in pneumonia but in the brain injured group negative correlation with ICAM-1, IL-6, MCP-1, MIP1a and E-selectin was seen. 6-keto-PGF1 α is the more stable metabolite of prostacycline, a potent vasodilator, so correlation with cytokines in the infected group makes biological sense. In the pneumonia patients IL-8 had a positive correlation with the family of HETE metabolites but negative correlation with the DHET family

In a group of patients with severe sepsis IL-1 β was seen to correlate with both TNF α and IL-6 (321). In this data set the strongest correlations between these markers were also seen in the infected, pneumonia, patients.

A previous study has correlated phospholipase A2 activity with concentrations of IL-6, IL-8, TNF α , 6-keto-PGF1 α , LTB4 and TXB2 in patients with burns (322). Although we did not measure phospholipase 2 activity we measured the concentration of arachidonic acid (AA), the direct result of activity of this enzyme. However, only in the BI group did we see positive correlation between TXB2 and LTB4 with AA. With the other inflammatory markers and in the other groups the relationships often showed either a negative correlation or only a weak positive correlation. This may represent

downstream enzyme activity in our cohort converting AA into other eicosanoids thereby reducing AA levels. Notably in severe sepsis (321) other investigators failed to find significant correlation between phospholipase A2 activity and inflammatory mediator levels.

During cardiopulmonary bypass several positive inflammatory mediator correlations have been documented; IL-6 with IL-8; TXB2 with LTC4 and PGE2; LTB4 with PGE2 and 6-keto-PGF1 α and PGE2 with 6-keto-PGF1 α (323). Some of these observations are preserved in this data set. Local correlation of IL-1 α and PGE2 has been seen in the blister fluid of capsaicin induced skin irritation (324) with similar finding in our pneumonia patients where inflammation was prominent. IL-8 and PGE2 have previously been positively correlated in astrocytomas (325), however, in our brain injured patients this correlation was in fact negative.

The complexity of the relationship between eicosanoids and cytokines can be seen in the following example. Negative correlation of PGE2 and TNF α from LPS stimulated human macrophages in the plasma of decompensated liver disease has been observed (326), however, the same mediators have been seen to be positively correlated in the plasma of children with febrile convulsions (327). In the cohort of patients described above in both the analysis of all patients and when only brain injured patients were considered TNF α and PGE2 showed positive correlation, however, when those patients with pneumonia at admission were isolated this degree of correlation was no longer apparent. This may represent the regulatory effect of PGE2 on TNF α during infection (305).

Despite some promising findings it is important to note the limitations of this study. Firstly the small number of patients, especially in the VAP group, limited the interpretation that could be made of the multivariate models and the possibility of over-fitting had to be borne in mind. The optimal way to test for this would have been with a validation set of data, however, the low numbers in the VAP group meant there were insufficient patients to allow a validation set. We were able to add the few reclassified, borderline, patients to the model to explore if a slightly larger data set made a

difference to the predictive capacity or the inflammatory mediators of importance compared to the original models based on the original patients based on CPIS classification, however this potentially lead to new problems. These patients were likely to be different to those diagnosed based on CPIS as by being borderline ran a higher risk of having been misclassified before being put into the model. Although extensive effort was made to recruit groups of patients that were similar in most respects, including time from admission, time and methods of sampling, the inherent heterogeneity of ICU patients meant that even within a relatively defined group, such as patients admitted with brain injuries, a great deal of variation was likely to exist between individual patients which limiting the ability of multivariate models to define specific differences within the population.

4.7 Conclusion

Both eicosanoid and cytokine profiling demonstrated an ability to differentiate patients with pneumonia from those admitted to ICU with brain injuries. Models based on cytokines highlighted inflammatory changes present in the serum of pneumonia patients, whereas models based on eicosanoid profiling had a tendency to highlight fatty acids and their metabolites present in the serum of patients with brain injuries. Neither type of profiling was particularly able to identify those brain injured patients who went on to develop VAP. However, by combining both profiling methods a more predictive model of VAP could be created. A combined approach using a combination of both cytokines and eicosanoids shows promise for aiding the diagnosis of pneumonia and specifically VAP.

5. EXHALED BREATH CONDENSATE

5.1 Summary

Exhaled breath condensate (EBC) has been investigated using a number of modalities in a range of diseases. Some previous work has been done in relatively stable diseases using both NMR spectroscopy and mass spectrometry (MS). However, very little work has been done addressing pneumonia or metabolic profiling of EBC from ventilated patients. This chapter explores profiling of EBC with both NMR spectroscopy and MS to distinguish patients admitted for ventilation with pneumonia from those with brain injuries and also to identify those patients who develop ventilator associated pneumonia (VAP). NMR spectroscopy was only able to identify a limited number of, mainly volatile, metabolites, whereas MS was able to detect a greater number of metabolites, however, this was limited by a significant batch effect. Untargeted MS analysis showed some ability to distinguish pneumonia from brain injury. However, the biggest metabolic changes seen appeared to be those that occurred over time with the duration of mechanical ventilation.

5.2 Background

Volatile organic compounds (VOCs) in breath give signatures that are familiar to us from several disease processes, from the ketones associated with diabetic complications to the compounds that produce the recognisable hepatic fetor. Formalised breath analysis is used widely in law enforcement and in some diagnostic clinical tests such as for *Helicobacter pylori*.

Technology exists to perform online metabolic profiling of exhaled breath using selected ion flow tube mass spectrometry (SIFT-MS) and gas chromatography mass spectrometry (GC-MS) (170-172). Work in healthy volunteers has allowed metabolites such as acetone, ammonia and methane to be quantified (173, 174) and the repeatability of the technique has been demonstrated (175). Levels of exhaled nitric oxide (NO) have shown potential for detecting airway inflammation in asthma and

chronic obstructive pulmonary disease (COPD) (176) and carbon monoxide levels increase in systemic sepsis (178).

Trace gas analysis has detected elevated NO levels in patients suffering from pneumonia (177) and techniques such as SIFT-MS have shown a potential ability to detect a range of micro-organisms by examining headspace gas of cultures (179-181) including from bronchoalveolar lavage fluid from patients with pneumonia (182). Specifically pseudomonas has been investigated from cultures from patients with cystic fibrosis (183, 184) and breath has been analysed in an attempt to determine colonisation status (185-187). It is thus suspected that analysis of exhaled breath may allow detection of specific organisms causing pneumonia by differentiating metabolic profiles.

Along-side the gaseous phase of breath it is possible to condense and collect the water vapour contained in breath, known as exhaled breath condensate (EBC). EBC is 99% evaporated water but also contains droplets of fluid from the airway linings allowing non-volatile compounds to be detected. Many substances have been detected in EBC including interleukins (188), leukotrienes (189) and soluble triggering receptor expressed on myeloid cells (sTREM-1)(89). One of the most extensively investigated substances is hydrogen peroxide which is elevated in many inflammatory conditions including ARDS (190), asthma (191) and may correlate with treatment response in patients with cystic fibrosis treated with antibiotics (192). Similarly EBC isoprostanes have been noted to be increased in COPD (193), asthma (194) and ARDS (195). EBC pH also appears to decrease with lung inflammation and has been seen to fall in bronchiectasis, COPD and lung injury (196, 197). Limited work has been done in the field of pneumonia but thiobarbituric acid and hydrogen peroxide can be seen to increase in CAP (198, 199).

Limited work has been carried out applying metabonomic techniques to breath. Small scale studies with EBC have used NMR analysis to distinguish asthmatics from controls (201-203), stable from unstable patients with cystic fibrosis (200) and to investigate smoking related diseases (204). Studies

have made attempts at metabolite assignment based on NMR spectra (99, 200, 204, 205) identifying 26 compounds between them, table 5.1.

Table 5.1. Metabolites identified by H^1 NMR analysis of EBC across all diseases studied

Metabolites
1-methylimidazole ^
2-Propanol (Isopropanol) †^
Acetate *†‡^
Acetoin ^
Acetone †
Alanine *‡
Choline *
Ethanol †‡^
Formate †‡^
Glutamate *†
Glutamine *†
Isobutyrate ^
Lactate *†‡
Leucine ‡
Lysine *
Methanol * †‡^
N-Butyrate ‡
Phosphorylcholine *
Phenylalanine ‡
Propionate *†‡^
Pyruvate *‡
Succinate *‡
Saturated Fatty Acids †
Taurine *
Trimethylamine *‡
Threonine *‡

*de Laurentiis *et al* (205) † Montuschi *et al* (200) ‡ Sofia *et al* (99) ^ de Laurentiis *et al* (204)

Concern has been raised regarding the risk of contamination of EBC with disinfectant when reusable collection devices are used and some conflicting work has been done to investigate this (328, 329). As yet there is no experience of collecting EBC from ventilated patients for the purpose of metabolite analysis. As with the gaseous phase of breath the optimal methods for sample collection, processing and analysis are not known.

Although it is known that changes in respiratory parameters, especially minute ventilation, alter the volume of EBC obtained for a given time period of collection (330) it is unknown what effect this has

on metabolite concentrations. In the literature using NMR to analyse EBC, samples have been both freeze dried and used unaltered prior to spectral acquisition. It is debatable as to which method is better, although freeze drying may allow concentration of metabolites leading to improved detection it is conceivable that volatile compounds may be lost with this approach.

With its greater sensitivity mass spectrometry (MS) has potential advantages over NMR spectroscopy for the analysis of EBC given the very low concentrations of metabolites within this biofluid. Very little work has been done utilising MS as a profiling tool (206, 207), more work has focused on specific markers or panels of markers. Examples of markers that have been explored using MS modalities include glucose (208), urea (209, 210), volatile organic compounds (211, 212), aldehydes (213-216), isoprostanes (195, 217-226), markers of oxidative stress (218), cystinyl leukotrienes (218, 227, 228), leukotrienes (189, 227, 229-233), eicosanoids (234-239), 12-HETE (240), lysophosphatidic acid (241), asymmetric dimethylarginine (ADMA) (242, 243), adenosine (209), phenylalanine (209), lysine (244), tyrosine (245), hydroxyproline (245), proline (245), purines (246-249), metallic elements(250), 3-nitrotyrosine (245, 251-254), and proteins (255). In order to measure this number of markers a number of chromatographic techniques have been coupled to MS to analyse EBC including Liquid Chromatography – Mass Spectrometry (206-208, 218), Liquid Chromatography Tandem Mass Spectrometry (217, 241, 255), Gas Chromatography - Mass Spectrometry (211) and Ultra Performance Liquid Chromatography Tandem Mass Spectrometry (227, 243).

As was the case with NMR analysis of EBC, the majority of work with MS has focussed on relatively stable diseases including healthy subjects (215, 238, 256), asthma (189, 206, 218, 227, 232, 234-236, 239, 242, 248), COPD (216, 247, 250, 255), pulmonary fibrosis (223, 224, 241), cystic fibrosis (208, 209), pulmonary hypertension (211), bronchopulmonary dysplasia (207), pneumoconiosis (229), silicosis (221), asbestosis (226), ARDS (195), Churg Strauss (240) and seasonal rhinitis (233). Almost

all of the studies so far have been performed in spontaneously ventilating patients with only two in those requiring mechanical ventilation (195, 210). No studies have been carried out utilising this approach in patients with pneumonia either with or without the need for mechanical ventilation. Analysis of EBC is an appealing tool for the diagnosis of pneumonia in ventilated patients as it provides a non-invasive method to directly sample from the site of pathology so may be able to provide early diagnostic markers and allow for repeated sampling.

In this chapter I outline an attempt to use a metabonomic profiling approach using $^1\text{H-NMR}$ and MS methods to analyse EBC collected from ventilated patients with and without pneumonia.

5.3 Aims

The overall aim of this study was to investigate the usefulness of metabonomic analysis of EBC in an attempt to improve the diagnosis of pneumonia in patients requiring ventilation, specifically those going on to develop VAP. The following questions were addressed:

- 1. Can $^1\text{H-NMR}$ and MS be used as methods for analysing EBC collected from ventilated patients?*
- 2. Can metabolic profiling of EBC have the potential to aid in the diagnosis of pneumonia in ventilated patients?*

5.4 Protocols

5.4.1 Patient Recruitment and Sample Collection

Patients were recruited and samples taken as described in chapter 2. Patients were defined as either having pneumonia or a brain injury as described earlier. All patients were followed up over time and those brain injured patients developing VAP were defined based on CPIS scoring. For a breakdown of

the CPIS score used see chapter 2. Patients with borderline scores were assessed and classified as VAP or no VAP by an independent assessor.

Where healthy volunteer EBC was required for method development, samples were taken from a single investigator, DA. In order to simulate collection of samples from a ventilated patient as far as possible samples were collected using the same equipment as described in chapter 2. The volunteer breathed through a non-invasive ventilation mask connected to a Servo-I ventilator set up to provide non-invasive ventilation. EBC samples were collected from the expiratory limb of the ventilator for 15 minutes as described previously, aliquotted into 500 μ l aliquots and immediately frozen at -80°C.

To explore the potential contribution of the collection equipment to the metabolic profiles obtained from samples of EBC, blanks were prepared with distilled and sterile water to simulate the EBC collection. Approximately 2ml of distilled water was placed into an RTube™ and left for 15 minutes, the water was then collected using the aluminium plunger and aliquotted into 500 μ l aliquots before being frozen at -80°C. When these blanks were processed similar samples of the distilled and sterile water, that had not been through and RTube™, were also run in an attempt to determine whether additional signals originated from the water or the RTube™.

5.4.2 ¹H-NMR Spectroscopy

5.4.2.1 ¹H-NMR Experiments

As EBC is >99% water initial assessment was of different methods of water suppression. Samples from both a healthy subject and a ventilated patient were prepared by the addition of 100 μ l of D₂O to 500 μ l of EBC. 550 μ l were then transferred to a 5mm NMR tube. Four different 1D NMR experiments using different pulse sequences were acquired for comparison on an 800MHz spectrometer, a standard one-dimensional experiment using the first increment of a Nuclear Overhauser Effect pulse sequence to achieve pre-saturation of the water resonance (110), water suppression using excitation

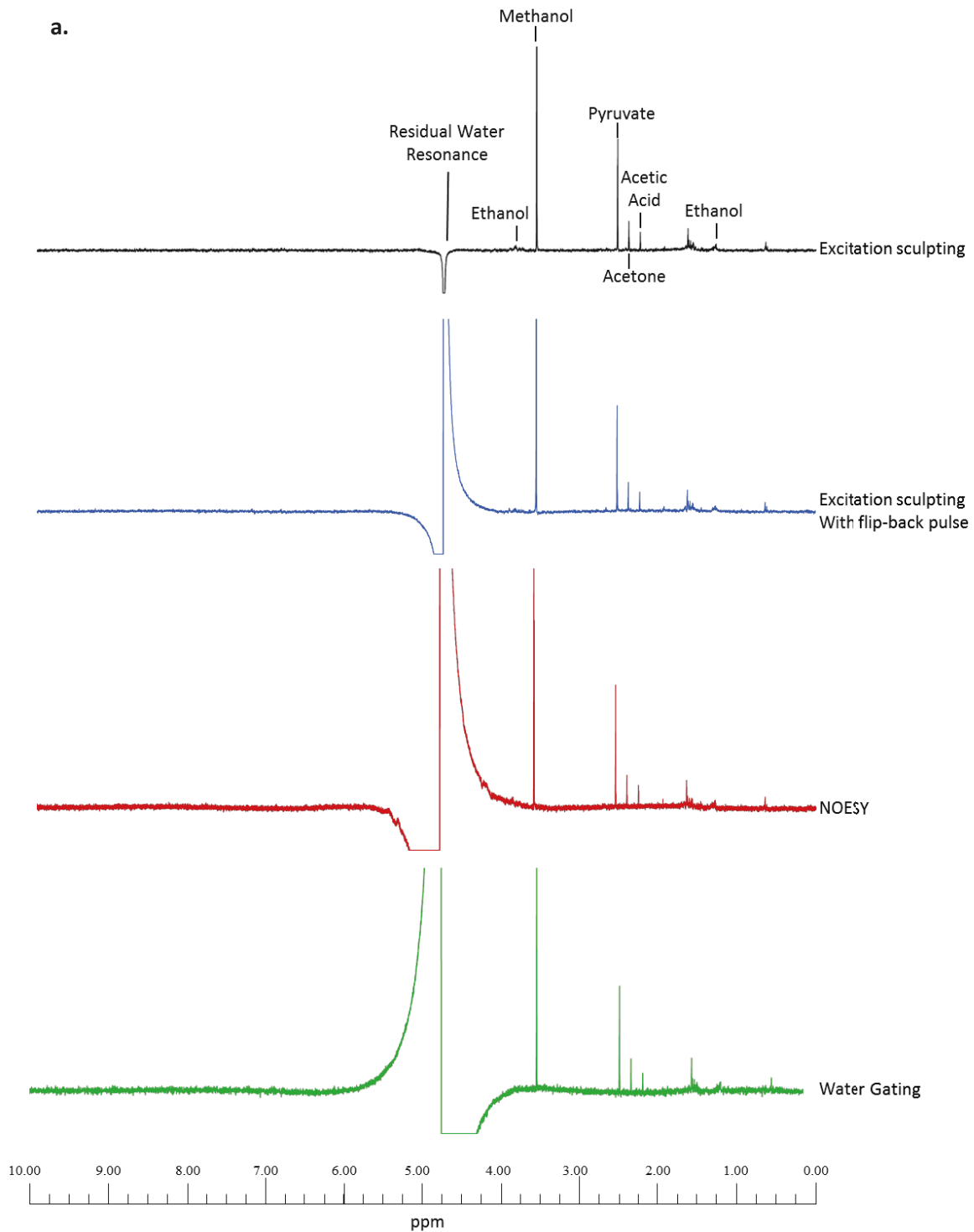
sculpting with gradients, water suppression using excitation sculpting with gradients with a flip back pulse and a water gated experiment using water suppression with a 3-9-19 pulse sequence with gradients. All experiments were run at a constant temperature of 300 K. 128 FIDs were accumulated for each experiment using a 20 ppm spectral width centred at δ 4.75. The relaxation delay was set at 2s and a water pre-saturation pulse was applied during this period to cancel the water signal and the receiver gain was kept constant.

For both the volunteer sample, figure 5.1, and that from the patient, figure 5.2, water suppression using excitation sculpting without the flip back pulse provided the optimal water suppression. However, few new metabolites became apparent with the different pulse sequences. Although more spectral peaks were apparent in the patient sample when compared to that from the volunteer, there remained relatively few metabolites apparent in these spectra.

5.4.2.2 Freeze Drying

In some of the previously published work EBC has been freeze dried and reconstituted in an attempt to improve the yield of metabolites at low concentrations. To explore this method the EBC samples were processed as follows. 500 μ l aliquots were left to dry in the freeze drier overnight. The samples were then reconstituted with either 500 μ l D₂O and 100 μ l 0.1mM TSP with 550 μ l being placed in a 5mm NMR tube or with 167 μ l D₂O and 33mcl 0.1mM TSP with 180 μ l being placed into a 3mm NMR tube. 1D NMR experiments using excitation sculpting for water suppression were then performed as described above.

Figure 5.1. a. Comparison of excitation sculpting, excitation sculpting with flip back pulse, presaturation (NOESY) and water gated experiments on EBC from a healthy control. Water suppression can be seen to be best with the excitation sculpting experiment with little difference in recovered metabolites. b. Magnified section from 1.0 to 2.5ppm from the first excitation sculpting experiment demonstrating the signal to noise ratio.



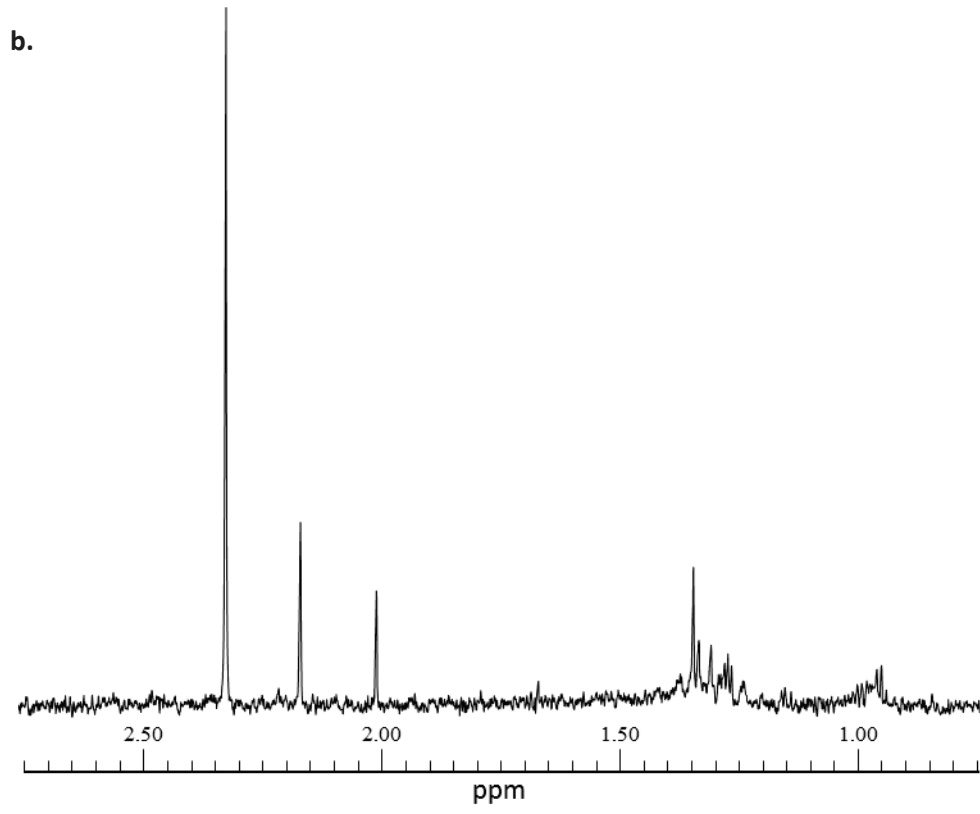
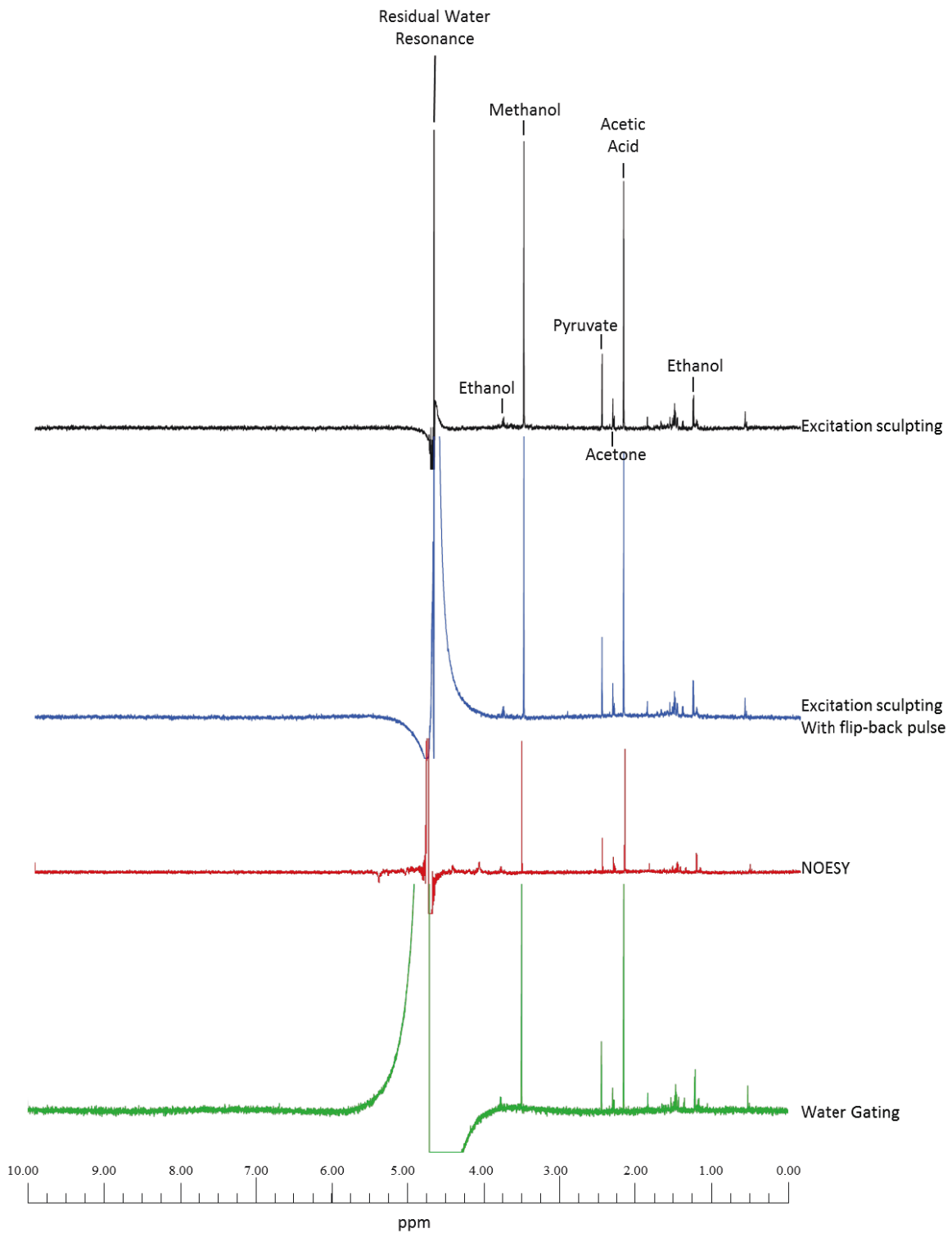


Figure 5.2. Comparison of excitation sculpting, excitation sculpting with flip back pulse, presaturation (NOESY) and water gated experiments on EBC from a ventilated patient. Water suppression can be seen to be best with the excitation sculpting experiment with little difference in recovered metabolites.

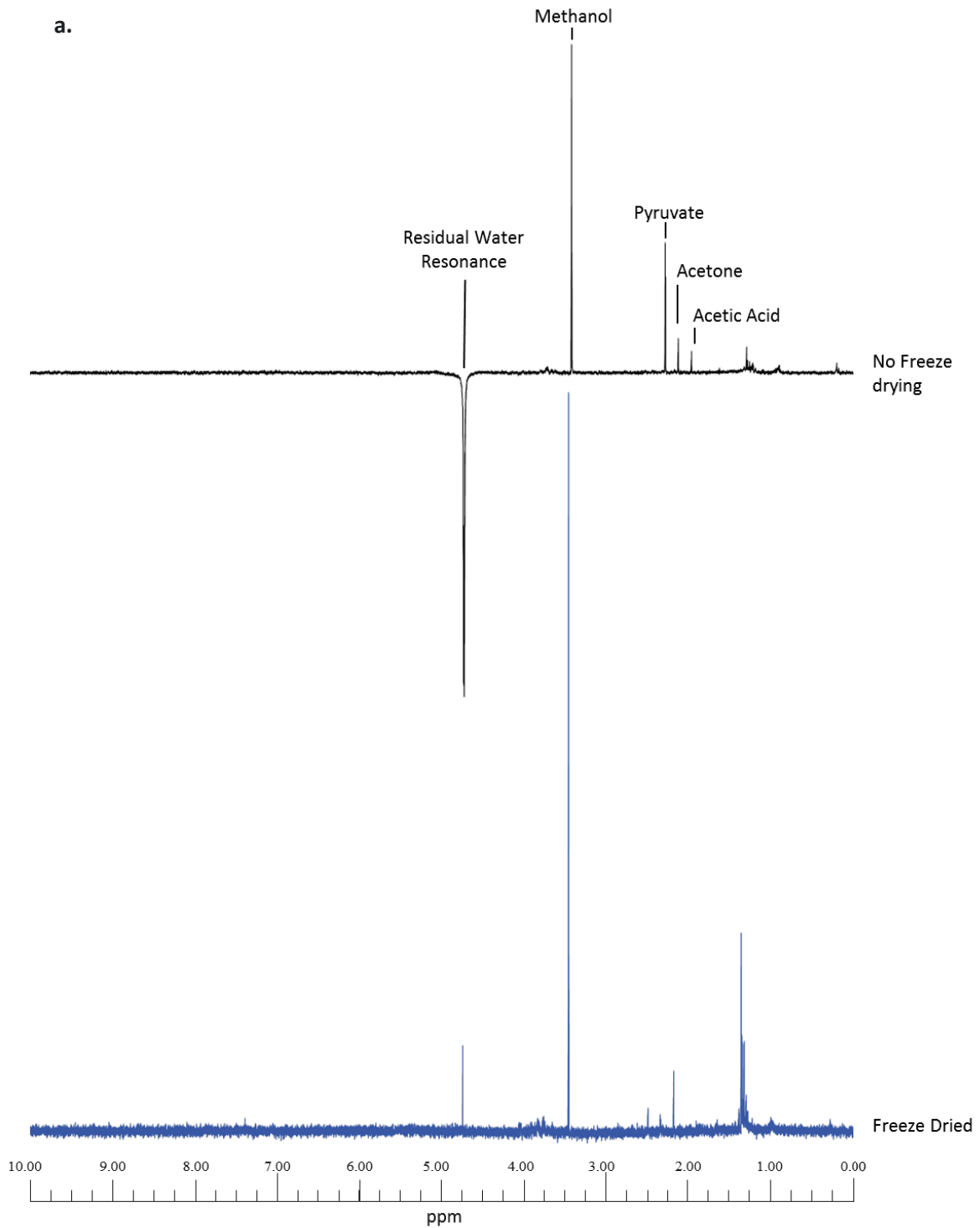


When samples obtained from a healthy volunteer were compared with and without freeze drying, figure 5.3, loss of several of the metabolites was seen, especially those which were volatile such as methanol, acetone and acetic acid. When the same experiments were performed on a sample obtained from a ventilated patient, figure 5.4, the results were less clear cut. Many signals appeared to be enhanced when samples were freeze dried, with little difference between samples reconstituted into 5mm and 3mm tubes.

5.4.2.3 Effect of Collection Equipment.

In order to assess the potential for the observed metabolites to originate, not from the samples, but from the D₂O, the TSP or the RTube™ collecting equipment several blanks were run of the added chemicals, figure 5.5, and of D₂O instilled into the RTube™, figure 5.6. The spectrum obtained from the TSP demonstrated many of the peaks also seen in the freeze dried patient sample, figure 5.5, suggesting that much of what was seen did not represent endogenous metabolites but additive peaks from the TSP, however, when the spectra from D₂O instilled into the RTube™ was compared to that from the TSP very few additional signals were seen suggesting that the RTube™ itself had minimal effect on the NMR spectra from EBC samples collected using this device.

Figure 5.3. a. Comparison of NMR experiments using excitation sculpting to suppress the water signal in identical samples acquired from a healthy volunteer. Comparison between spectra obtained with no freeze drying and freeze drying with reconstitution to 600 μ l and placed into a 5mm NMR tube. b. Magnified section from 1.0 to 2.5ppm from both spectra demonstrating the signal to noise ratio.



b.

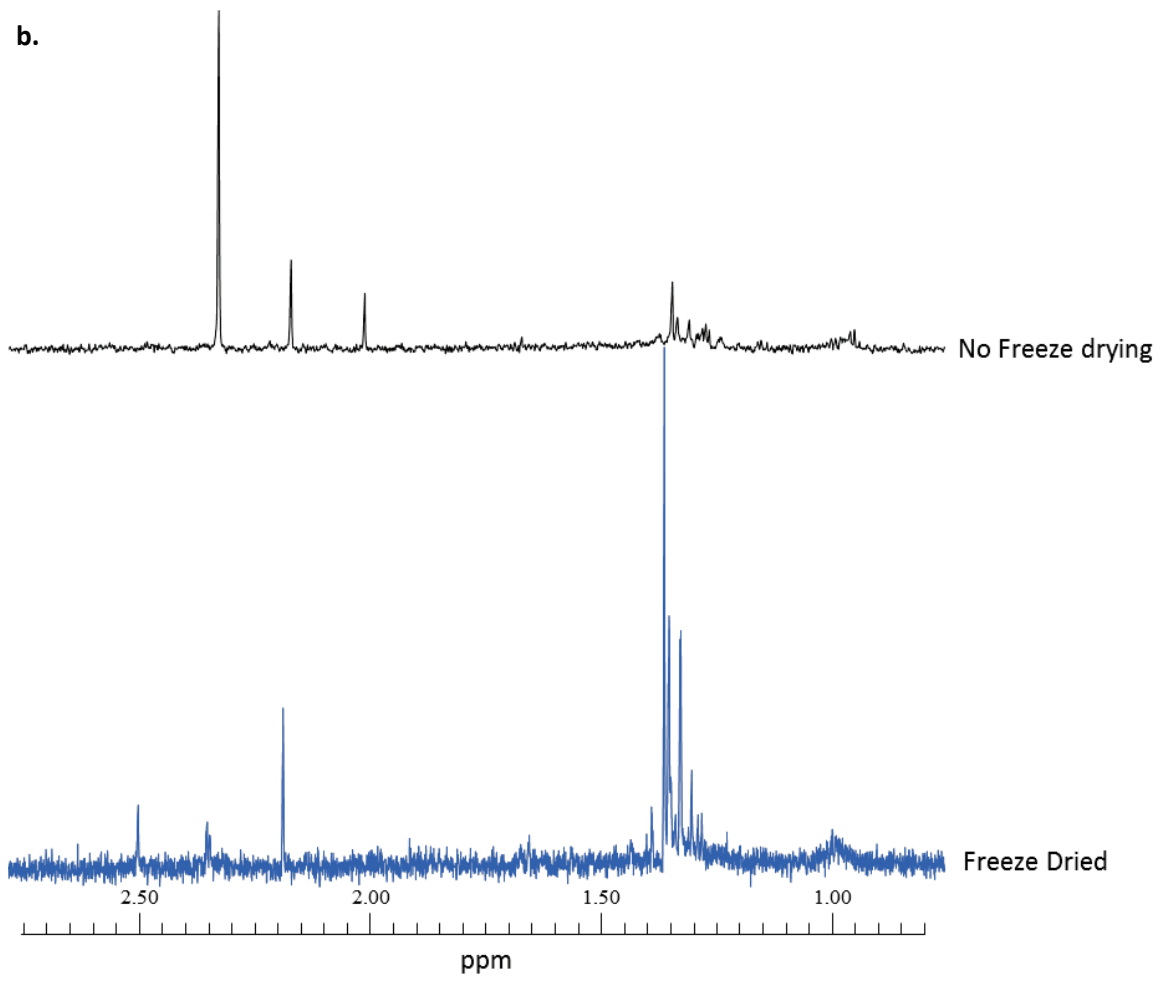


Figure 5.4. Comparison of NMR experiments using excitation sculpting to suppress the water signal in identical samples acquired from a ventilated patient after preparation with no freeze drying, freeze drying with reconstitution into a 5mm NMR tube and freeze drying with reconstitution into a 3mm NMR tube.

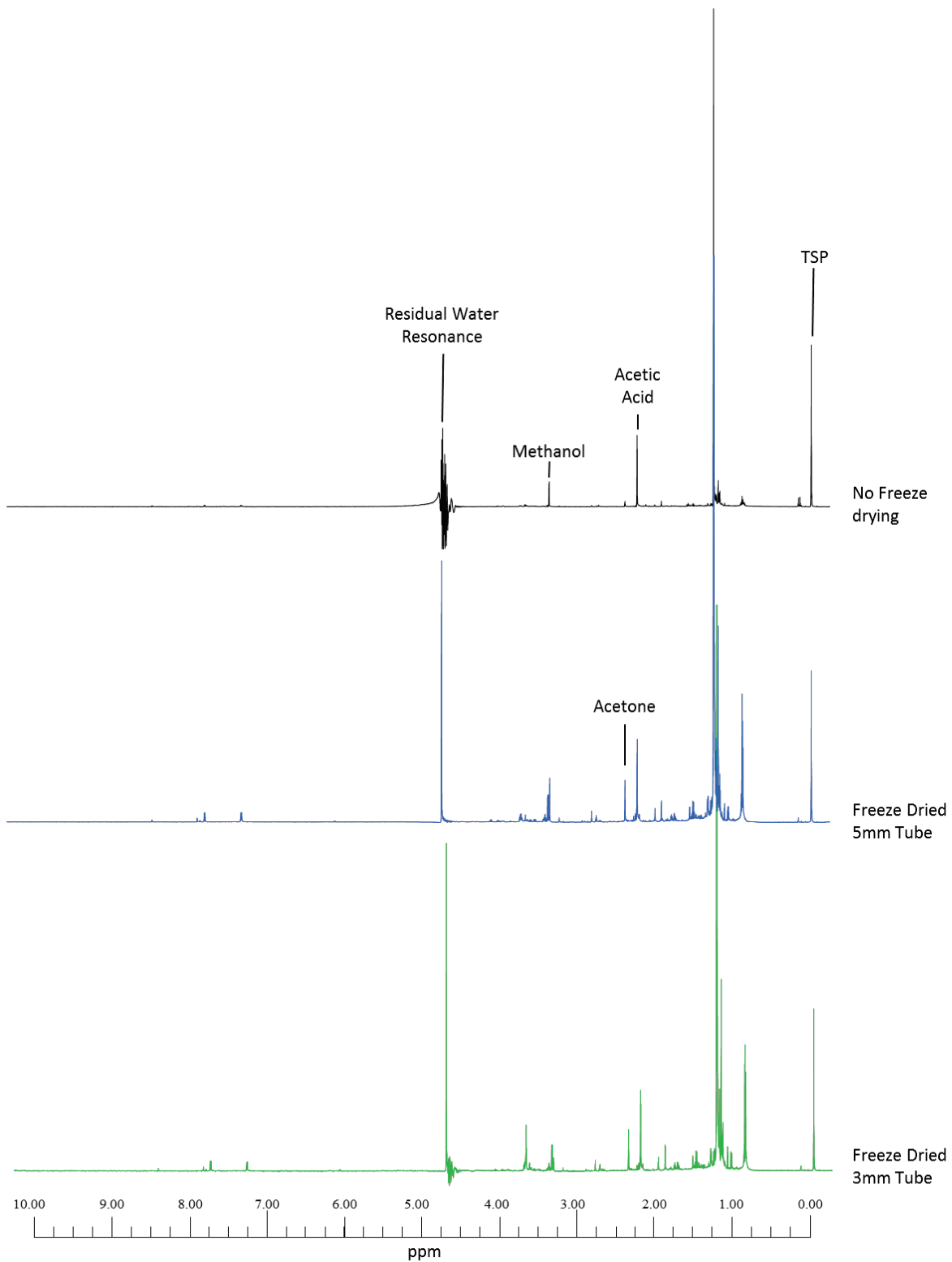


Figure 5.5. Comparison spectra of obtained from D_2O , TSP and a freeze dried patient sample reconstituted into a 5mm NMR tube. Many of the signals present in the patient sample can be seen to be present in the spectrum from the TSP and to a lesser extent the D_2O .

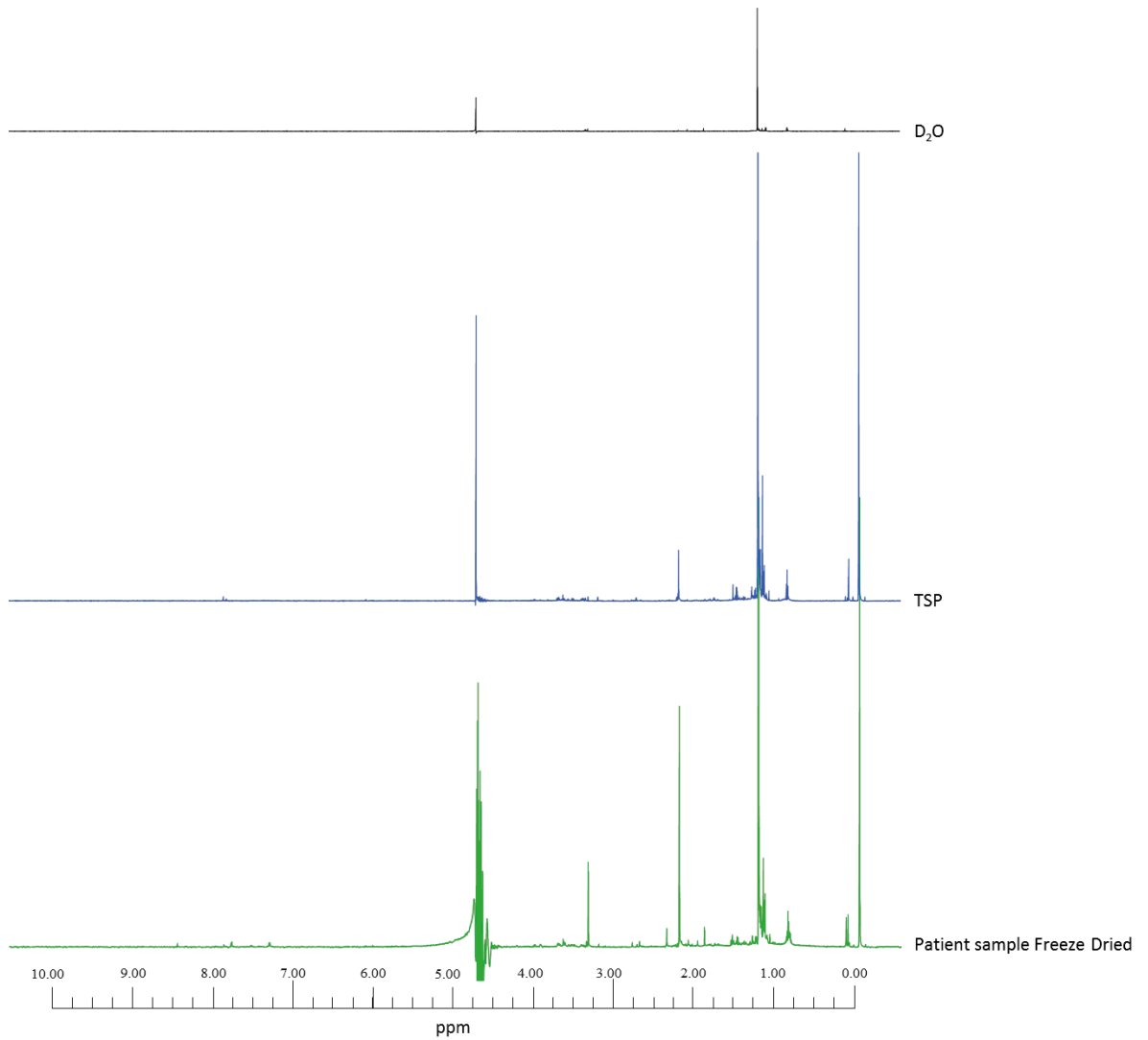
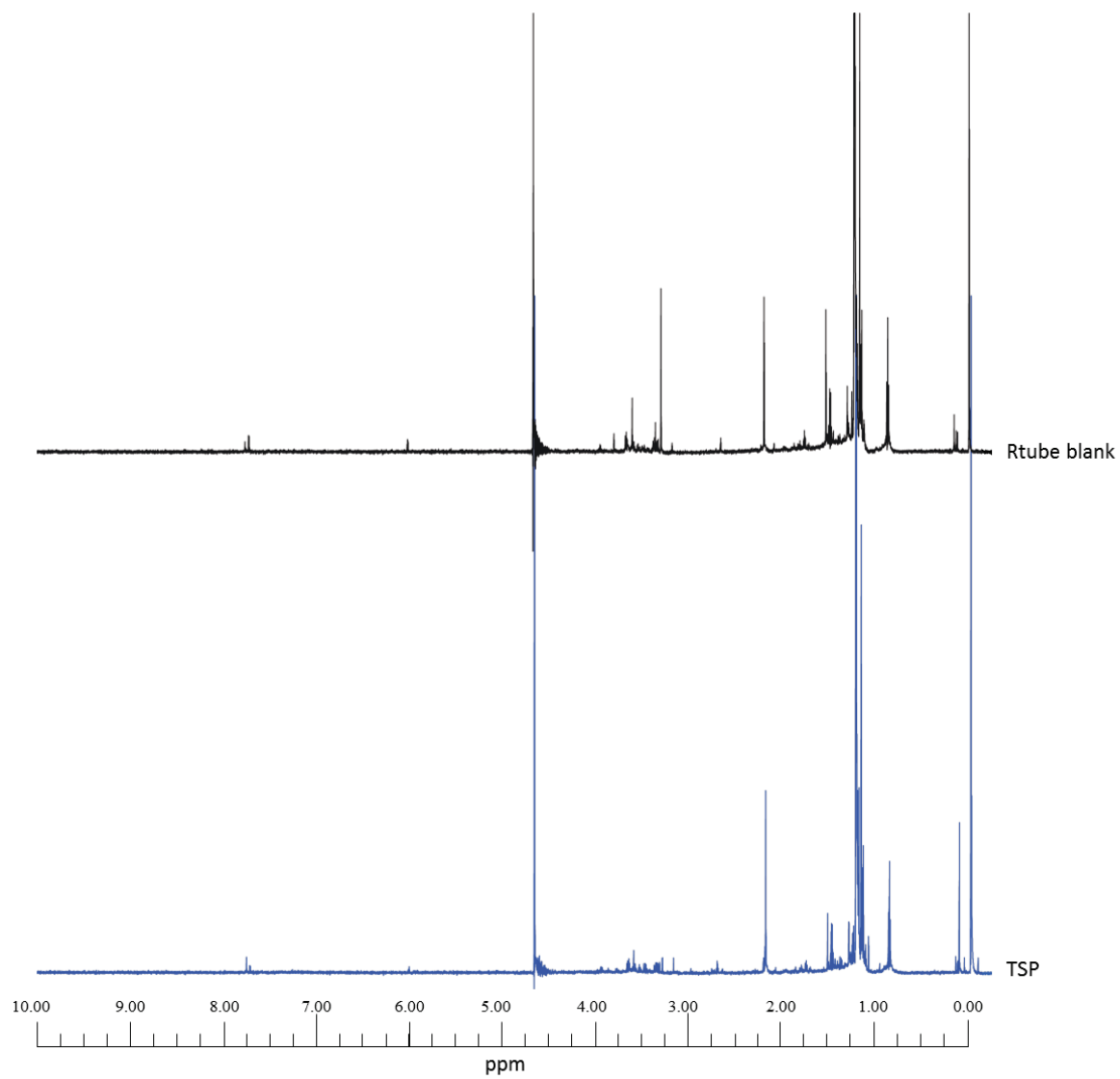


Figure 5.6. Comparison spectra of a blank prepared with D₂O placed into the RTube™ collection device and that from the TSP in D₂O to demonstrate the metabolites potentially originating from the RTube™.



5.4.2.4 Summary of ¹H-NMR

Only a small number of metabolites were recovered from the EBC using NMR without a freeze drying step. Although the use of freeze drying could potentially make metabolites apparent that could not otherwise be seen, some of the volatile metabolites were lost in this process and it was unclear how reproducible this step may be. Also as there was limited capacity for freeze drying samples would have had to be processed in batches making this process unsuitable for either large sample sets or a high throughput methodology and adding an additional, time consuming, step that would be unwanted in a clinical test. For these reasons, the risk of the additive batch effect with freeze drying and the limited number of metabolites recovered without this step it was decided to shift focus from NMR analysis of EBC to a method based on MS with the greater sensitivity offered by this method.

5.4.3 Mass Spectrometry

EBC samples were randomised and thawed at room temperature prior to preparation. Methanol was added to the samples as a solvent prior to MS analysis. In order to optimise the method a range of methanol to sample ratios were tested using a sample of healthy control EBC, the best signal acquisition was found to be obtained using a ratio of 1:5 sample to methanol. 40µl of EBC was placed into each well of a 96 well plate and then 200µl of methanol was added to each well. The plate was then heat sealed with foil prior to mixing in an ultrasonic bath for 5 minutes and then a plate shaker for a further 5 minutes. For each 96 well plate a number of blanks were run consisting of methanol only. Also blanks to examine the RTube™ collecting system were made with distilled water as described earlier, along with these blanks samples of the distilled water that had not been through the RTube™ were also run to ensure detected metabolites were not from the water itself.

A high-throughput screening method was used using an Exactive Instrument equipped with TriVersa NanoMate ion source (Advion, Ithaca, NY, USA). Chip-based infusion mode measurements were

performed using 5µm nominal internal diameter nozzle chips, and a sample volume of 5µL was injected. Total data acquisition time was 2 min, 1 min in negative ion mode and 1 min in positive ion mode with automatic polarity switching. EBC samples were run in three batches.

5.4.3.1 Data processing

Following data acquisition spectral data were imported into MatLab 2013 (MathWorks, Massachusetts, USA) using in-house scripts for all processing steps. Firstly peak picking using a threshold of 0.7 was performed to reduce the size of the data matrix and remove noise from the data. Probabilistic quotient normalisation was performed to counter for intensity multiplier effects such as concentration. Finally data were scaled to reduce the influence of a small number of intense peaks that dominate the variance of the un-scaled dataset. Log scaling was used with an offset of the median of all values greater than zero.

5.4.3.2 Statistical Analysis

Processed data were imported into the SIMCA 13.0 statistical package (Umetrics, Sweden) and multivariate statistics were used for analysis. Initial exploration with principal component analysis (PCA) was performed to look for natural clustering and to detect outliers before supervised multivariate analysis using orthogonal partial least squared discriminant analysis (OPLS-DA) was used to generate models to optimally separate predefined groups. OPLS-DA models were cross validated using seven fold cross-validation using a “leave-one-out” methodology. Important ions within the OPLS-DA models were identified by examining the ‘s-plots’ for the models. The ‘s-plots’ show the covariance plotted against the correlation with the model for each variable. Variables that are likely to be important have a high covariance, indicating a real biological effect on the model and not just one driven by analytical variation or noise, and a high correlation, suggesting greater reliability (112, 331). Such variables lie at the extreme tips of the ‘S’ formed in this plot.

An attempt was made to assign potential metabolites to the m/z ratios that appeared in multiple comparisons by comparing them with entries in both the Human Metabolome Database, Canada (332) and the Scripps Center for Metabolomics METLIN database, USA (333).

5.5 Results

5.5.1 Patients

Thirty four patients, that fulfilled the criteria defined in chapter 2, had samples of EBC taken and analysed with MS. Of these 13 had pneumonia on admission and 21 had brain injuries with no suggestion of pneumonia when the first samples were taken. Five brain injured patients went on to develop VAP based on CPIS scoring. Clinical features of these patients can be seen in table 5.2. As previously described in chapter 2, patients with borderline CPIS scores were reviewed by an independent clinical assessor and classified as non-infected, pneumonia or VAP based on clinical course. Based on this assessment a further six brain injured patients were classified as not having pneumonia on admission, five were defined as pneumonia and three as VAP. All initial comparisons were made with the original grouping of patients based on CPIS.

Patients were similar across the groups with respect to their demographic details. Features that identified the pneumonia and VAP groups from those with brain injuries included markers of infection such as CRP, use of antibiotics and the higher oxygen requirement as would be expected in patients with pulmonary infection.

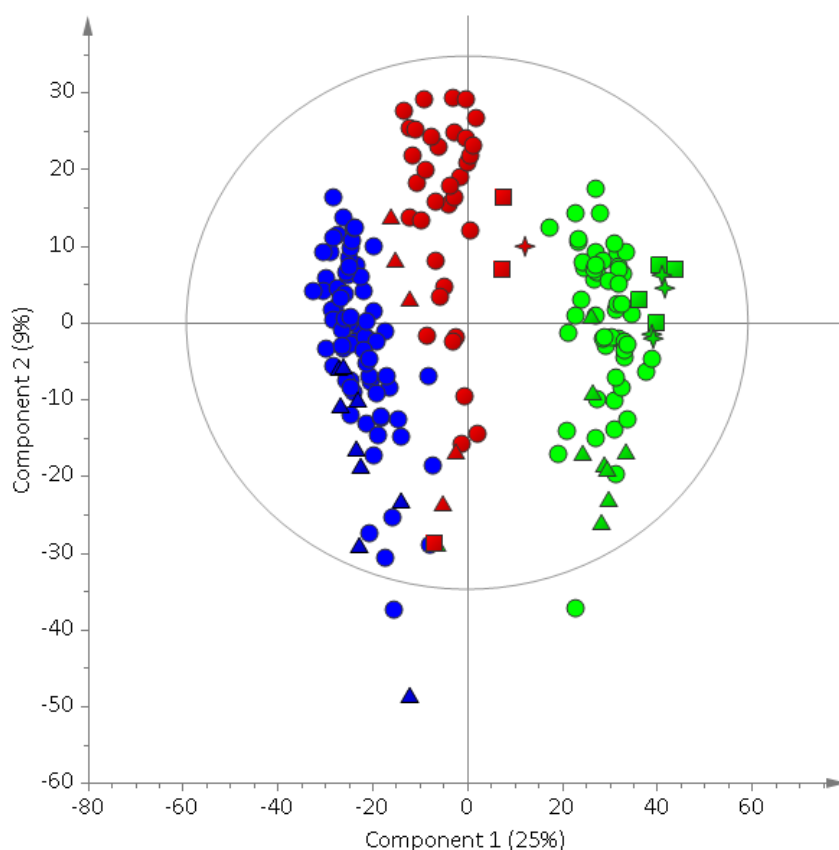
5.5.2 Evaluation of Batch Effect

The EBC was run on three separate occasions so a PCA was performed to look for natural separation of the samples by batch, figure 5.7. Clear separation could be seen between the three batches along the first component. The methanol blanks run at the same time as the samples were seen to cluster with the samples as were those blanks prepared from the RTubes™ and distilled water. Separation of

Table 5.2. Clinical features of included patients with EBC for MS analysis. Continuous variables are given as mean and standard deviation and categorical variables as number and percentage. P-values presented in bold text relate to parameters that were significant at the $p < 0.05$ level.

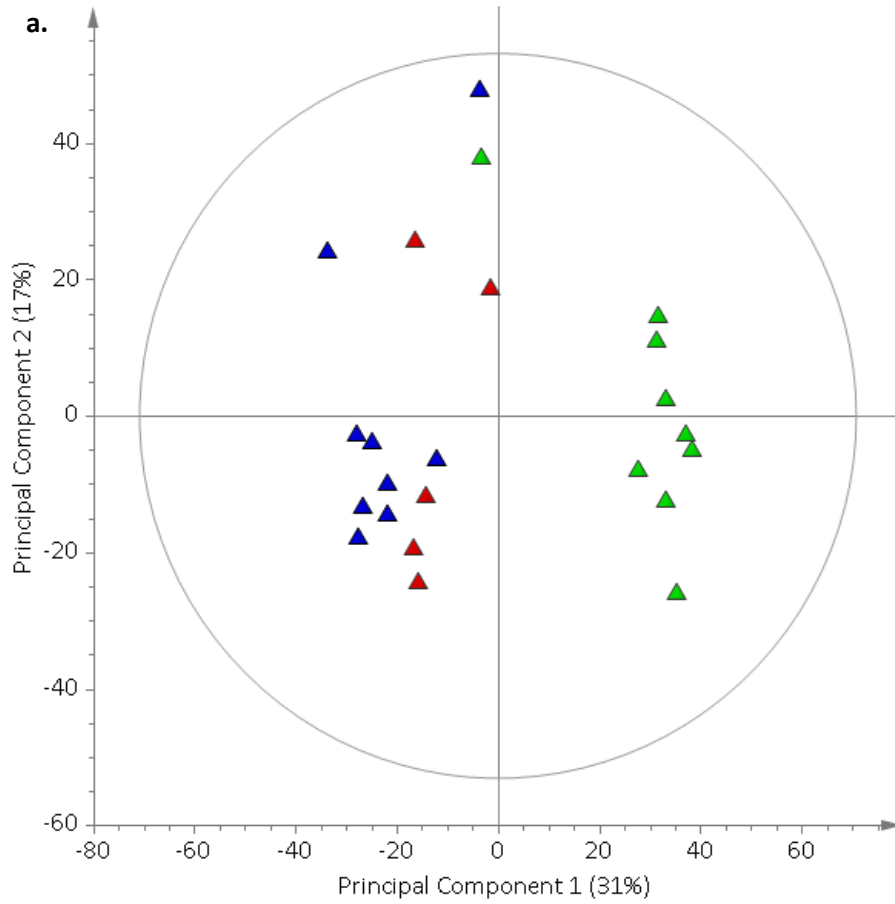
	Pneumonia (P)	Brain Injury (BI)	p-value (BI vs P)	VAP	p-value (BI vs VAP)
n	13	21	-	5	-
Age (Mean +/- SD)	55.4±17.7	52.3±14.9	0.60	50.8±17.2	0.87
Sex, Number of males (%)	9 (69)	12 (57)	0.72	3 (60)	1.00
Ethnicity, number White European (%)	11 (84)	15 (71)	0.44	4 (80)	1.00
Outcome, Number alive (%)	10 (77)	16 (76)	1.00	3 (60)	0.59
APACHE II Score (Mean +/- SD)	18.9±5.3	17.0±6.0	0.32	17.8±9.4	0.86
SOFA Score (Mean +/- SD)	9.9±2.8	8.9±2.6	0.28	8.6±3.1	0.87
CPIS (Mean +/- SD)	5.8±1.1	2.1±1.4	<0.001	7.0±1.6	<0.01
Lowest WCC ($10^9/L$) (Mean +/- SD)	14.3±5.4	10.0±3.8	0.02	10.5±3.2	0.76
Highest WCC ($10^9/L$) (Mean +/- SD)	14.9±5.2	11.2±3.9	0.04	10.5±3.2	0.70
Lowest CRP (mg/L) (Mean +/- SD)	174.8±109.8	49.4±54.2	<0.01	116.7±28.2	<0.01
Highest CRP (mg/L)(Mean +/- SD)	192.8±101.0	62.0±52.5	<0.001	116.7±28.2	<0.01
Lowest Temperature (°C) (Mean +/- SD)	36.0±0.6	36.0±0.7	0.96	36.0±1.6	0.95
High Temperature (°C) (Mean +/- SD)	37.5±0.9	37.6±0.7	0.93	38.0±1.3	0.45
Lowest FiO2 (Mean +/- SD)	0.43±0.15	0.40±0.22	0.57	0.36±0.07	0.51
Lowest PaO2:FiO2 (Mean +/- SD)	26.2±8.4	41.8±15.5	<0.001	18.6±8.5	<0.001
Lowest MAP (mmHg) (Mean +/- SD)	70.4±9.8	74.0±11.3	0.33	71.0±12.4	0.64
Use of noradrenaline, N (%)	9 (69)	13 (62)	0.72	1 (20)	0.15
Use of antibiotics N (%)	13 (100)	10 (48)	<0.01	5 (100)	0.05
Enteral nutrition, N (%)	11 (85)	15 (71)	0.44	5 (100)	0.30
Time to sampling from start of ventilation (h) (Mean +/- SD)	39.4±8.6	40.4±16.7	0.82	143.6±45.2	<0.01
Time of day of sample, Number taken in the morning (%)	10 (77)	13 (62)	0.47	5 (100)	0.28

Figure 5.7. PCA (R^2X 0.86, Q^2X 0.66) showing separation of batch 1, blue, batch 2, red, and batch 3, green. The blanks, triangles, RTube™ blanks, squares, and distilled water blanks, stars, cluster with the samples run at the same time point. Separation between the batches is seen along the first component, horizontal axis, indicating that the variation caused by batch is of much greater magnitude than biological or sample preparation variance.



the blanks by batch could also be seen when a PCA using only the blank samples was constructed, figure 5.8. The spectra obtained from the blanks can be seen in figure 5.8 with most of the difference being seen between batch 3 and both batch 1 and 2. As much of the separation between batches seemed to be accounted for by signals originating from the methanol, the average spectral signal from each set of blanks was calculated then subtracted from each of the sample spectra from the same run. After subtraction from the raw spectra normalisation and scaling was re-applied as detailed above. PCA of the resulting spectra, figure 5.9 showed a reduction in batch effect especially

Figure 5.8. a. PCA (R^2X 0.61, Q^2X 0.35) showing separation of blanks run with each batch. Batch 1, blue, batch 2, red, and batch 3, green. The greatest separation is seen between batch 3 and batches 1 and 2. b. MS spectra of blanks run with batch 1 and c. MS spectra of blanks run with batch 3.



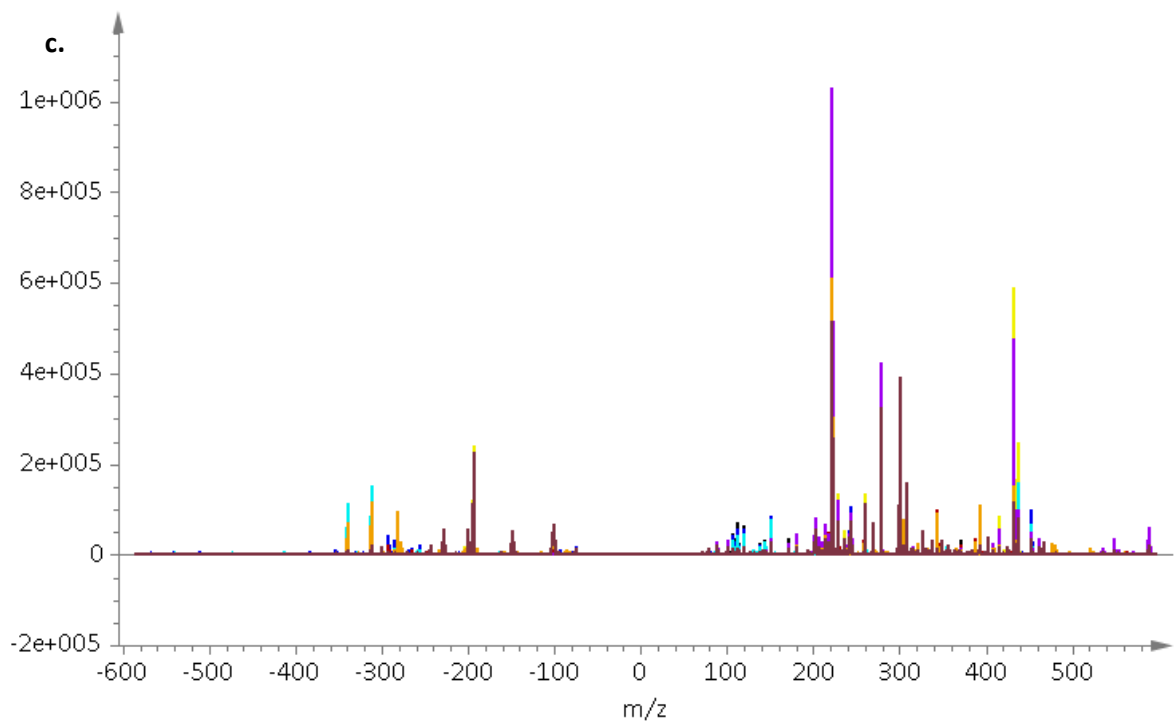
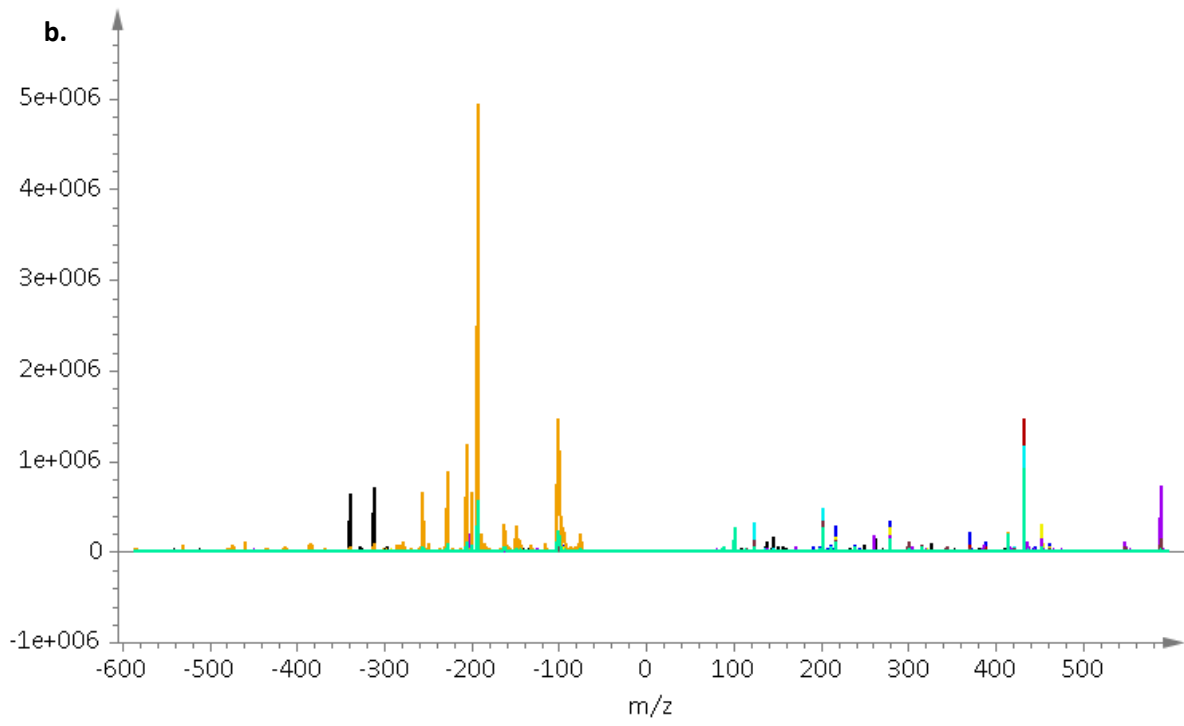
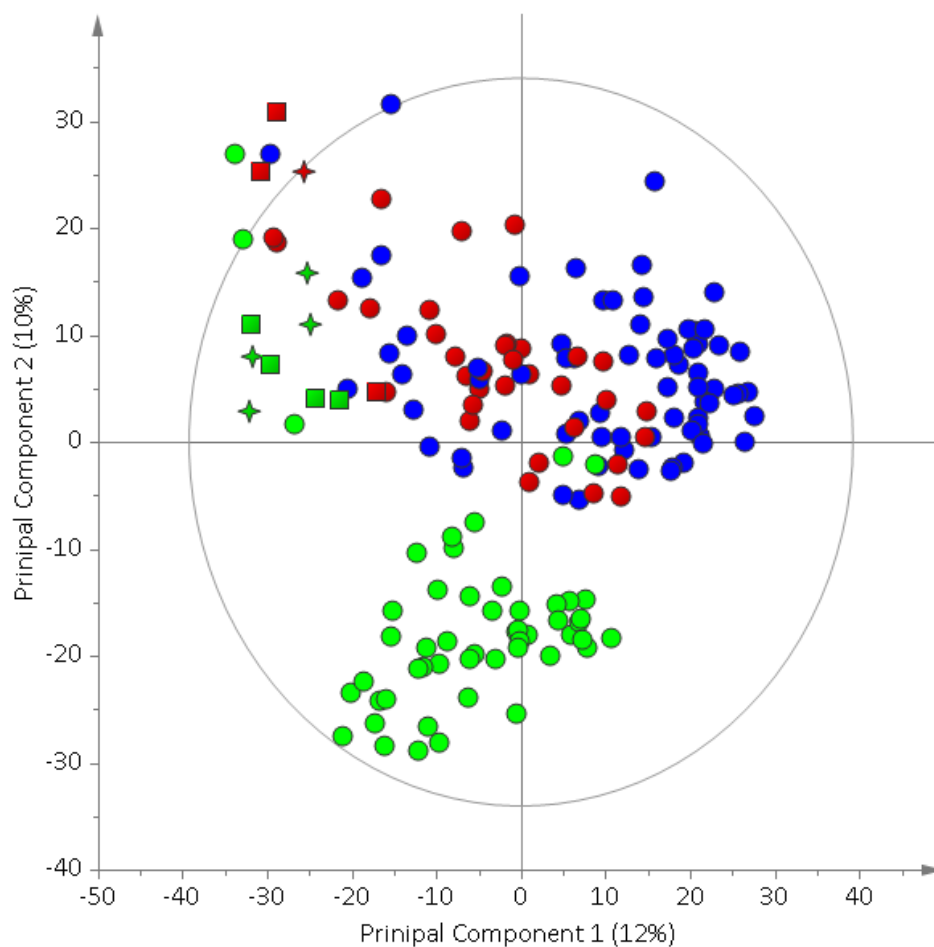


Figure 5.9. PCA (R^2X 0.77, Q^2X 0.48) showing separation of batch 1, blue, batch 2, red, and batch 3, green after subtraction of average signal from the blanks run simultaneously. The RTube™ blanks, squares, and distilled water blanks, stars, cluster with the samples run at the same time point. Less separation between the batches is seen than from the previous PCA although batch 3 still shows some separation along the second component, y- axis.



between the first and second batch, some separation of batch 3 was still observed along the second component.

5.5.3 Collection Equipment

After attempting to correct for the batch effect the blanks created to simulate sample collection in the RTube™ device could be seen to cluster together away from most of the samples on PCA analysis, figure 5.9. However, alongside the RTube™ blanks the blanks made up of only distilled water that had not been through an RTube™ could be seen to cluster in the same area. In fact it was impossible to construct an OPLS-DA model to separate the RTube™ blanks from the distilled water blanks. This implied that almost all of the signals coming from the RTube™ were due to the water that had been used to prepare them and not from the tubes themselves. As no water was used in any stage of sample preparation these signals could be discounted from interfering with the separation of samples based on clinical comparisons.

5.5.4 Brain Injury vs Pneumonia

When the 13 patients with pneumonia at admission were compared to the 21 with brain injuries and no evidence of pneumonia no natural separation on PCA could be seen (R^2X 0.33, Q^2X 0.12), figure 5.10. One outlier could be seen who seemed to have a generally greater intensity of metabolites, especially in negative mode. However, there were no technical issues either in the patient's care or sample collection that suggested they should be excluded from further analysis. An OPLS-DA model (R^2Y 0.90, Q^2Y 0.20, $p=0.64$), figure 5.11, could be constructed to separate the cases of pneumonia from those with brain injuries, however, the first orthogonal component is required to obtain a positive Q^2Y . When the set of patients who were classified by an independent assessor were used to validate this model, seven with pneumonia and six with brain injuries, this model had a sensitivity of 0.43, a specificity of 0.83, positive predictive value of 0.75 and a negative predictive

value of 0.56. The ions that were most significant in determining the difference between groups were determined by observing the s-plot for the model, figure 5.11 and table 5.3. If a group of brain injured patients were used who never went on to develop pneumonia during their stay as the control group it became impossible to construct an OPLS-DA model to separate brain injury from pneumonia.

Figure 5.10. PCA scores plot (R^2X 0.33, Q^2X 0.12) comparing samples taken at the first time point from patients admitted with pneumonia (red squares) to those admitted with brain injuries with no evidence of pneumonia at sampling (blue circles). No natural separation can be seen between groups on the first and second component with only a single outlier being identified.

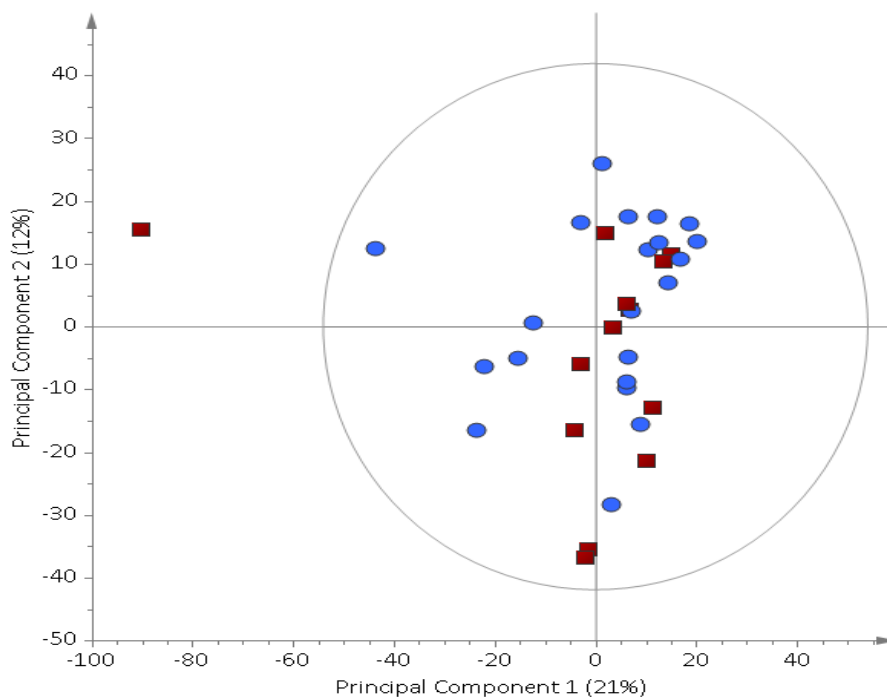


Figure 5.11. OPLS-DA model with three orthogonal components (R^2Y 0.90, Q^2Y 0.20, $p=0.64$) a. before and b. after cross validation, comparing samples taken at the first time point from patients admitted with pneumonia (red squares) to those admitted with brain injuries with no evidence of pneumonia at sampling (blue circles). c. demonstrates the s-plot for the model. This plot compares the covariance with the correlation co-efficient for each metabolite. Important metabolites appear at the extreme ends of the 'S' and are associated with the highest of both the correlation co-efficients and the covariance. Metabolites in the top right hand corner are associated with pneumonia and those in the bottom left are associated with brain injury. Important ions, labelled are those within the circles.

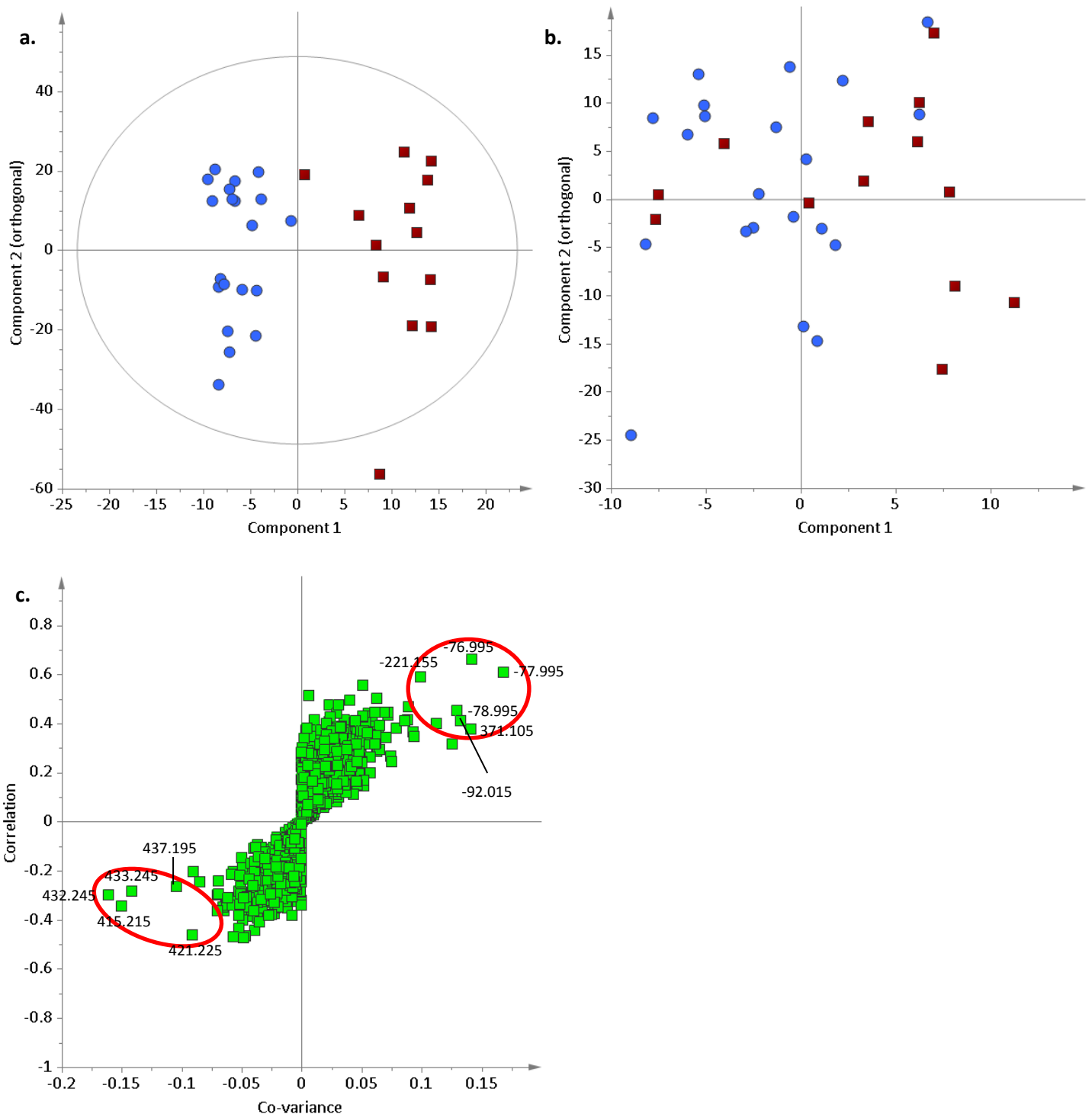


Table 5.3. *m/z* descriptors that were most important in separating patients with pneumonia from those with brain injuries at the start of ventilation, the arrows indicate in which of the two groups the *m/z* showed a predominance. Highlighted rows represent ions also identified in other comparisons.

<i>m/z</i>	Brain Injury	Pneumonia	Possible Assignments
-221.155		↑	
-92.015		↑	Cefuroxime
-78.995		↑	
-77.995		↑	
-76.995		↑	
371.105		↑	-
415.215	↑		Dexamethasone, Histidine, Lysine, Methionine
421.225	↑		
432.245	↑		Alanine, Arginine, Glutamine, Lysine, Tryptophan
433.245	↑		Lysophosphatidic acid
437.195	↑		

5.5.5 Brain Injury vs VAP

When the five patients who developed VAP based on CPIS were compared with those with BI with no infection at the start of ventilation PCA (R^2X 0.18, Q^2X 0.03) failed to separate the two groups. In fact it was not possible to build OPLS-DA models with either the original patients based on CPIS or with a combined group utilising patients classified with CPIS and those borderline patients classified by the independent assessor. However, if only those BI patients who never developed VAP were used from the original group an OPLS-DA model with weak classification ability could be constructed (R^2Y 0.58, Q^2Y 0.09, $p=0.54$) but this did not remain true of when the combined group was used. The ions that were important in this model can be seen in table 5.4.

Table 5.4. *m/z* descriptors that were most important in separating samples taken from patients as they developed VAP from those taken from patients with brain injuries, who never developed VAP, at the start of ventilation, the arrows indicate in which of the two groups the *m/z* showed a predominance. Highlighted rows represent ions also identified in other comparisons.

<i>m/z</i>	Brain Injury	VAP	Possible Assignments
135.054	↑		
358.205	↑		
371.105		↑	-
432.285	↑		
433.285	↑		

5.5.6 Time Course

To investigate whether with time there was a change in the metabolites present in EBC the samples taken from the first time point were compared to those taken at the fourth for those brain injured patients who did not develop VAP. OPLS-DA models were similar for both the original group based only on CPIS (R^2Y 0.93, Q^2Y 0.53, $p=0.05$)(TP1 $n=12$ and TP4 $n=5$), figure 5.12, and with a combined group (R^2Y 0.91, Q^2Y 0.59, $p<0.01$)(TP1 $n=16$ and TP4 $n=5$). When the samples were paired so that only those patients who had both a time point one and four sample were used the Q^2Y of the model was similar although the p -value fell to below significance due to the small number of subjects (R^2Y 0.96, Q^2Y 0.59, $p=0.26$)($n=5$ for each time point). The metabolites that were important in separating the time points can be seen in table 5.5 below.

When the time course of patients with pneumonia was examined an OPLS-DA model from the original group (R^2Y 0.52, Q^2Y 0.20, $p=0.89$) (TP1 $n=13$ and TP2 $n=5$) and the combined group could be made (R^2Y 0.49, Q^2Y 0.19, $p=0.08$) (TP1 $n=20$ and TP2 $n=7$). However, if only paired samples were used it was impossible to build a discriminant model. Table 5.6 shows the ions that were important in these models.

Figure 5.12. OPLS-DA model with one orthogonal component (R^2Y 0.93, Q^2Y 0.53, $p=0.05$) a. before and b. after cross validation, comparing samples taken at the first time point from patients admitted with brain injuries (blue circles) who never developed pneumonia to the fourth (blue squares). c. demonstrates the s-plot for the model. This plot compares the covariance with the correlation coefficient for each metabolite. Important metabolites appear at the extreme ends of the 'S' and are associated with the highest of both the correlation coefficients and the covariance. Metabolites in the top right hand corner are associated with pneumonia and those in the bottom left are associated with brain injury. Important ions, labelled are those within the circles.

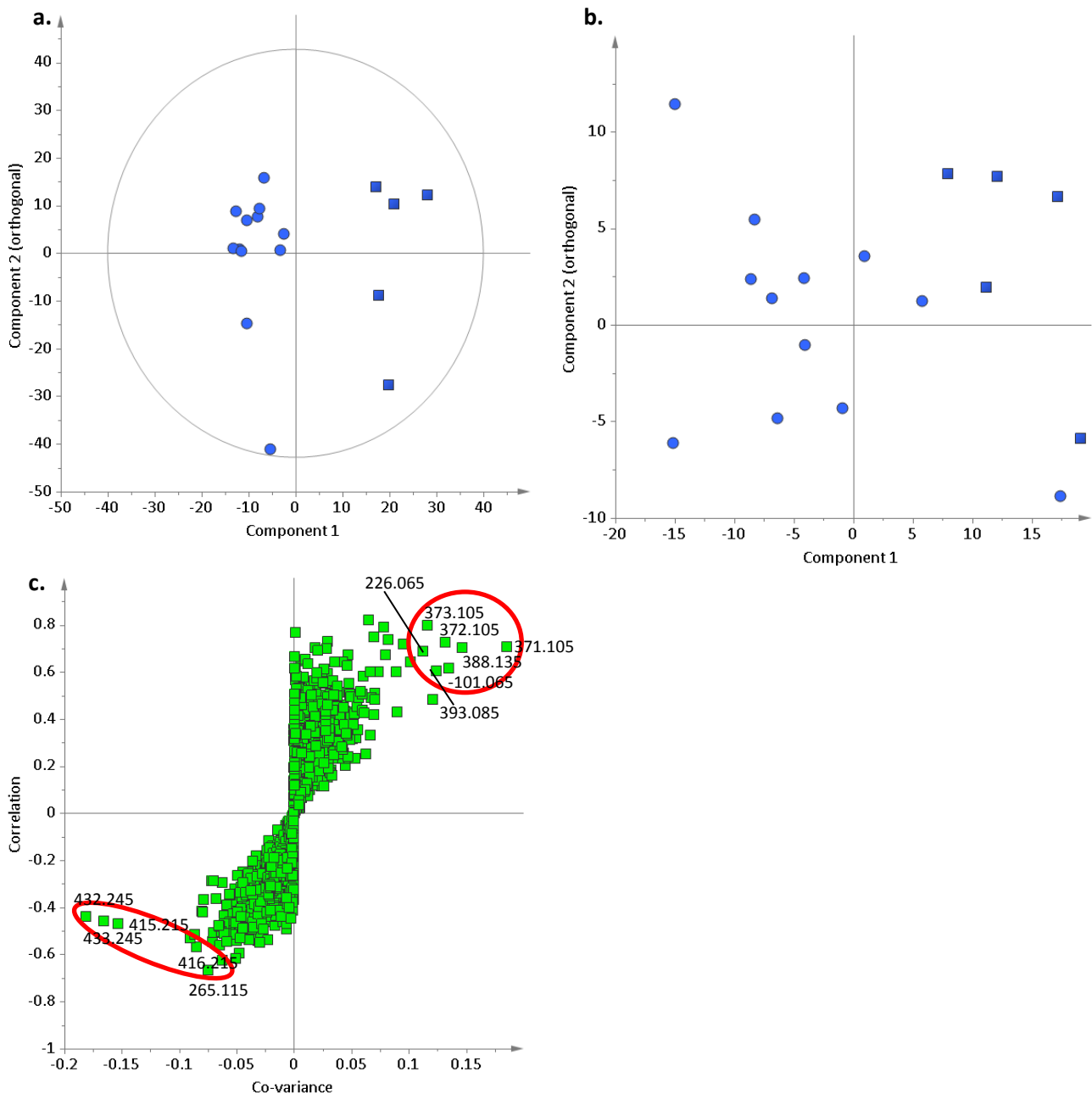


Table 5.5. *m/z* descriptors that were most important in separating samples taken from brain injured patients who never developed VAP comparing time point 1 (TP1) with time point 4 (TP4), the arrows indicate in which of the two groups the *m/z* showed a predominance. Results from the models based on both the original groups based on CPIS and the combined group including patients categorised by and independent assessor are shown Highlighted rows represent ions also identified in other comparisons.

<i>m/z</i>	Group based on CPIS		Combined group		Possible Assignments
	TP1	TP4	TP1	TP4	
-92.015			↑		Cefuroxime
-101.065		↑		↑	
226.065		↑			Alanine, Asparagine, Cysteine
265.115	↑		↑		
371.105		↑		↑	-
372.105		↑		↑	
373.105		↑		↑	
388.135		↑		↑	Cysteine, Glutamate, Glutamine, Histidine, Phenylalanine
393.085		↑		↑	-
395.085				↑	
415.215	↑		↑		Dexamethasone, Histidine, Lysine, Methionine
416.215	↑		↑		
432.245	↑		↑		Alanine, Arginine, Glutamine, Lysine, Tryptophan
432.265			↑		
433.245	↑		↑		Lysophosphatidic acid

Table 5.6. *m/z* descriptors that were most important in separating samples taken from patients with pneumonia at time point 1 (TP1) from time point 4 (TP4), the arrows indicate in which of the two groups the *m/z* showed a predominance. Results from the models based on both the original groups based on CPIS and the combined group including patients categorised by and independent assessor are shown. Highlighted rows represent ions also identified in other comparisons.

<i>m/z</i>	Group Based on CPIS		Combined Group		Possible Assignments
	TP1	TP4	TP1	TP4	
-302.225		↑			
-299.205		↑			
-199.175	↑				
82.045		↑			
89.065	↑				25-Hydroxycholesterol, Alanine, Aspartate, Cysteine, Glutamate, Histidine
111.555		↑		↑	
119.055		↑		↑	
135.045			↑		Noradrenaline, Prostaglandin G2, Arginine, Asparagine, Glutamine, Glycine, Isoleucine, Tyrosine
144.085		↑		↑	
207.165	↑		↑		
210.175			↑		
212.155	↑				-
214.095			↑		
279.165	↑		↑		
355.285		↑			
358.252	↑				
361.335		↑			
364.345		↑			
369.305		↑			

In order to establish if changes over time were different between those brain injured patients who did and did not go on to develop VAP the time point four samples were compared to those samples taken when VAP developed. Using the original group based on CPIS a discriminant OPLS-DA model could be built (R^2Y 0.93, Q^2Y 0.23, $p=0.82$) (BI $n=5$ and VAP $n=5$), figure 5.13. The predictive capacity improved when a combined group was used (R^2Y 0.93, Q^2Y 0.57, $p=0.11$) (BI $n=5$ and VAP $n=8$). The important metabolites in these models can be seen in table 5.7.

Figure 5.13. OPLS-DA model with one orthogonal component (R^2Y 0.93, Q^2Y 0.23, $p=0.82$) a. before and b. after cross validation, comparing samples taken from patients admitted with brain injuries (blue squares) at the fourth time point who never developed pneumonia to those with VAP (green triangles). c. demonstrates the s-plot for the model. This plot compares the covariance with the correlation coefficient for each metabolite. Important metabolites appear at the extreme ends of the 'S' and are associated with the highest of both the correlation coefficients and the covariance. Metabolites in the top right hand corner are associated with pneumonia and those in the bottom left are associated with brain injury. Important ions, labelled are those within the circles.

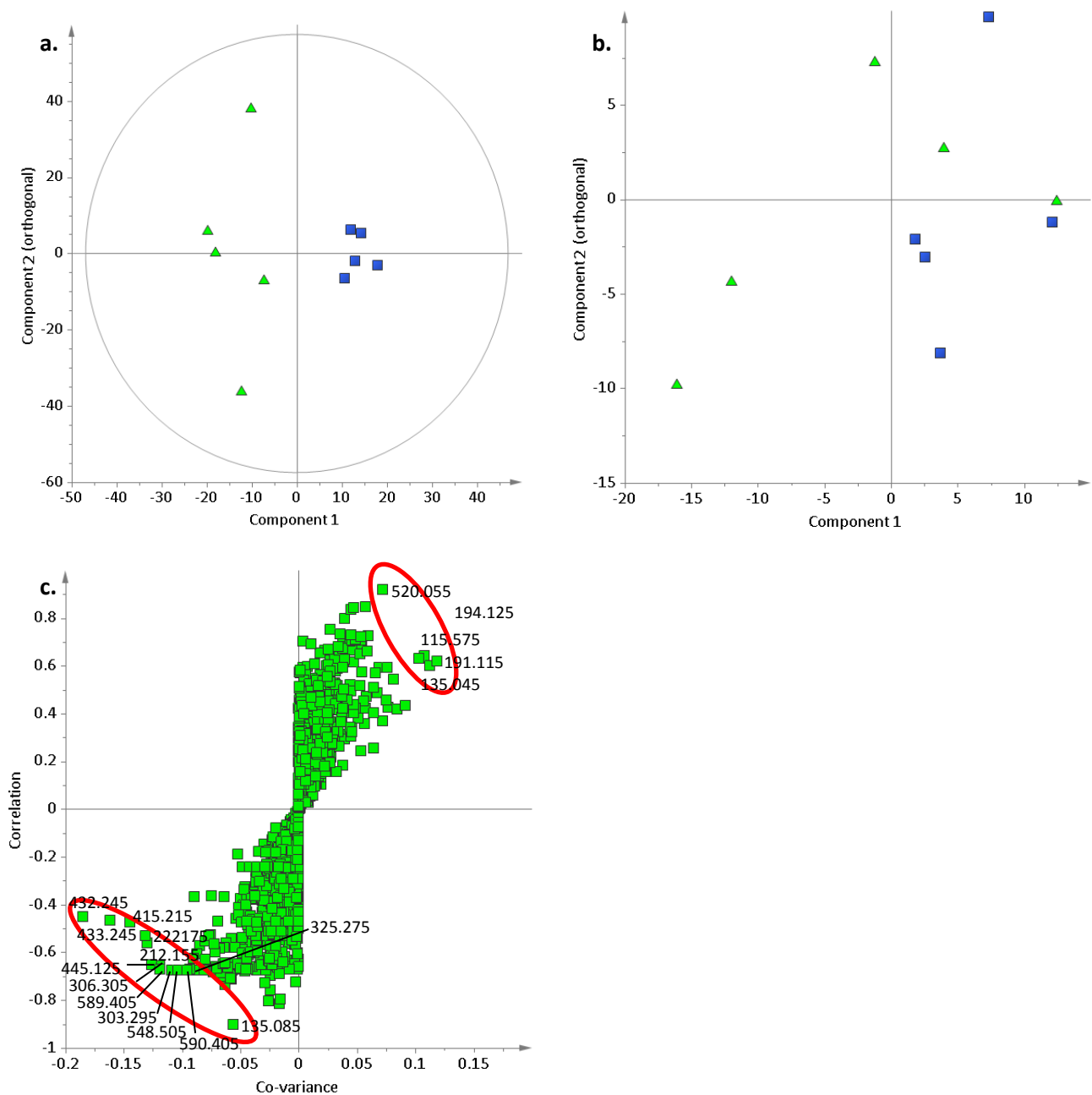


Table 5.7. *m/z* descriptors that were most important in separating samples taken from patients with VAP from time point 4 (TP4) samples taken from patients with brain injuries who never went on to develop VAP, the arrows indicate in which of the two groups the *m/z* showed a predominance. Results from the models based on both the original groups based on CPIS and the combined group including patients categorised by and independent assessor are shown. Highlighted rows represent ions also identified in other comparisons.

m/z	Group based on CPIS		Combined group		Possible Assignments
	VAP	TP4	VAP	TP4	
115.575		↑		↑	
135.045		↑			Noradrenaline, Prostaglandin G2, Arginine, Asparagine, Glutamine, Glycine, Isoleucine, Tyrosine
135.085	↑			↑	
191.115		↑			
194.125		↑			
212.155	↑		↑		-
222.175	↑				
226.065				↑	Alanine, Asparagine, Cysteine
226.565				↑	
303.295	↑				
306.305	↑				
325.275	↑				
371.105				↑	-
388.135				↑	Cysteine, Glutamate, Glutamine, Histidine, Phenylalanine
415.215	↑		↑		Dexamethasone, Histidine, Lysine, Methionine
432.245	↑		↑		Alanine, Arginine, Glutamine, Lysine, Tryptophan
433.245	↑		↑		Lysophosphatidic acid
445.125	↑				
520.055		↑			
548.505	↑				
589.405	↑				
590.405	↑				

When only those patients who developed VAP were examined it was impossible to build a model that would separate the first time point sample from the sample taken at the time that VAP developed.

Using the first time point samples from the brain injured patients it was possible to build a weakly predictive model to separate those patients who went on to develop VAP from those who did not from the group based on CPIS scoring (R^2Y 0.90, Q^2Y 0.20, $p=0.61$), however, when the combined group was used this failed to be the case. The metabolites that cause this separation can be seen in table 5.8 below.

Table 5.8. m/z that were most important in separating patients who did and did not go on to develop VAP using samples taken from patients with brain injuries at time point 1 (TP1), the arrows indicate in which of the two groups the m/z showed a predominance. Results from the models based on both the original groups based on CPIS and the combined group including patients categorised by and independent assessor are shown. Highlighted rows represent ions also identified in other comparisons.

m/z	VAP	No VAP	Possible Assignments
81.035	↑		
89.065		↑	25-Hydroxycholesterol, Alanine, Aspartate, Cysteine, Glutamate, Histidine
124.035		↑	
212.155		↑	-
246.175		↑	
277.185		↑	
393.085		↑	-
419.325	↑		
420.325	↑		
441.305	↑		
442.305	↑		
467.105	↑		
468.105	↑		

5.6 Discussion

In this chapter I have investigated the possibility of using a metabonomic approach to EBC to assist in the diagnosis of pneumonia in ventilated patients. The initial approach using $^1\text{H-NMR}$ spectroscopy found only a handful of metabolites in the samples that were run. An attempt to improve metabolite recovery by freeze drying the samples was made.

The majority of the identified metabolites within the EBC were volatile metabolites such as ethanol, methanol and acetone, such metabolites would be poor candidates for quantitation due to their volatility and instability. Similar metabolites have been identified before in the literature (99, 200, 204, 205), however, it is notable that the number of metabolites seen in this sample set is lower than that previously documented. There are a number of potential reasons for this, firstly this group of patients were clinically quite different from those studied previously, in none of the previous studies have patients who are critically ill been investigated. It is very possible that differences in disease processes account for some of the differences. In this study all samples were collected from intubated patients, where a tube lies in the patient's trachea, avoiding the potential for contamination of the EBC from metabolites originating in the oral cavity, from saliva, or from the digestive tract. For example trimethylamine, a noted cause of halitosis, originating from the gastrointestinal tract (334) has been found with NMR in samples of EBC collected from spontaneously breathing patients (200, 205). This raises the possibility that some of the metabolites within EBC that were identified with NMR that have previously been attributed to the respiratory tract may actually originate from other parts of the oropharynx. Finally, although no work has been done specifically examining the effect of different collection techniques on metabolic profiling, different equipment used to collect EBC has been seen to alter levels of other markers measured (335, 336). The majority of the NMR based metabonomic EBC studies to date have used the Ecoscreen collection device to collect samples (200, 201, 204, 205, 328, 329). This device has several reusable components and so needs cleaning between samples. There have previously been controversies regarding contamination of NMR spectra with metabolites originating from the disinfectant used to clean the reusable equipment (205, 328). The use of the disposable RTube™ in this study avoided the potential for such artefacts and may also account for the number of metabolites being observed appearing lower. The best method in which to handle the samples prior to NMR analysis is unclear. In the previous literature both methods involving drying (202) and using

samples with only the addition of deuterium have been used (200, 201, 204, 205, 328, 329). No studies exist comparing the two techniques. In this study an attempt was made to freeze dry samples to enhance metabolite recovery. However, during the freeze drying process volatile compounds could be easily lost and this method showed only a limited ability to improve the number of metabolites seen in the spectra. Due to the difficulty in standardising this technique and the possibility of both losing important volatile metabolites and adding in metabolites during the freeze drying process, this was judged to be an unappealing solution. Also the extra time needed to process the samples was unfeasible for large sample sets so this was not pursued further.

In an attempt to improve metabolite recovery from the EBC an approach using a direct injection MS methodology was used. This method initially demonstrated significant batch effects. The batch effect was reduced, although not entirely eliminated, when the peaks found in the methanol blanks were removed from the sample spectra.

When spectra obtained using MS were compared for patients at the start of ventilation who did and did not have pneumonia it was possible to build a model that had limited predictive value. As described earlier there is no gold standard by which to diagnose pneumonia. Use of vital signs, biomarkers and radiographs in differing combinations have all had varying performance characteristics in different patient groups (12-16, 18, 20, 22-24, 26, 27) and as such it is difficult to compare the current findings with what is known about currently available tests. However, a sensitivity of only 43% would make this test perform less well than many of those described in the literature.

EBC analysis did not perform well when VAP was compared to brain injured patients at the start of ventilation. However, although it was not possible to validate the models, EBC seemed to perform better after cross-validation when metabolic changes over time were considered for both brain injured patients and patients with pneumonia. In both cases a number of potential metabolites

could be seen to both increase and decrease over time. It is interesting to observe that the set of metabolites that changed over time for pneumonia and brain injured patients were different suggesting that what was being observed was not just an accumulation of metabolites from the plastic of the endotracheal tube and ventilator circuit. Differences in the changes in airway inflammation such as those caused by infection with pneumonia, patterns of airway micro-organism colonisation or airway stress from the differences in mechanics involved in the different approaches to ventilation in the two groups could all account for the differences seen over time.

Some of the best models seen could be made when EBC samples taken from similar time points were compared between brain injured patients with and without VAP suggesting important metabolic differences may develop as infection takes hold in the lower respiratory tract. However, it is notable that even at the first time point there was a suggestion that there may be some potential to distinguish patients before VAP became clinically apparent potentially representing metabolic predisposition to infection or the early development of infection itself.

Because of the nature of MS and the multiple ions that can be produced from the fragmentation of a given metabolite and the potential for two metabolites to produce fragmentation ions with similar mass/charge ratios metabolite identification is much more challenging with this modality than with NMR. An attempt was made to make some preliminary assignments of the ion fragments that appeared in multiple clinical models by comparison with published databases. Because of the overlap of m/z ratios firm assignment was not possible within the scope of this project. However, some interesting metabolites were potentially detected. Amino acid species seemed to be candidate metabolites for many of the detected ion fragments. Amino acids, especially adenosine (209), phenylalanine (209), lysine (244) and tyrosine (245), have been measured previously in EBC. Of note, alanine and glutamine were potentially identified in the breath of those patients with brain injuries, in keeping with the abundance of these amino acids seen in the serum of this group of patients, in chapter 3. Similarly phenylalanine may have been detected in samples taken from those with brain

injuries at time point four, again, in keeping with findings from serum. More detailed conclusions regarding the amino acids detected in EBC are difficult to make due to the great deal of overlap in the ion fragments of these species. Lysophosphatidic acid, a signalling molecule derived from phospholipids that has been implicated in increasing vascular permeability, promoting epithelial cell death and the development of fibrosis, was also potentially identified in the samples studied here and has also been previously reported in EBC of patients with pulmonary fibrosis (241). Although it may have been expected that lysophosphatidic acid was more abundant in those with pneumonia, due to its role in inflammation, it was generally found in the breath of those with brain injuries especially at the start of the ICU stay, the only case where this was not so was with VAP when it was more abundant than in those with brain injuries ventilated for a similar time. Other biological markers possibly detected included prostaglandin G2 at the start of ventilation in those with pneumonia and towards the end of ICU stay in those with brain injuries and 25-hydroxycholesterol in those with pneumonia, however, without further information these assignments are very tentative. Along with biological substances a number of drugs were potentially present. Breath analysis has been used before to detect the presence of drugs, for example to the anaesthetic agent propofol in the gaseous phase of breath (337). In this study cefuroxime, noradrenaline and dexamethasone were tentatively identified in the EBC. Dexamethasone was seen as a possible differentiating substance in those with brain injuries compared to those with pneumonia and was detected in the breath of those with brain injuries at the start of ventilation compared to the final time point. These findings make sense as dexamethasone was used in a number of the brain injured patients as an anti-inflammatory drug in certain diseases and as such was more likely to administered at the start of the ICU stay. Dexamethasone was also more likely to be associated with VAP than those brain injured patients who were ventilated for a similar amount of time, perhaps because of the immunosuppressive properties of steroids predisposing to infection. The antibiotic cefuroxime seemed to be more abundant in those with pneumonia compared to those with brain injuries, however, this seems unlikely as cephalosporins were more widely administered to those with brain injuries than to those with pneumonia suggesting that this is not a true assignment. This drug may have also been able to distinguish time point one from time point four samples from patients with brain injuries which makes much more sense as this antibiotic was more likely to be given around the time of admission to

intensive care than during a patient's stay. Noradrenaline is a vasopressor frequently given to patients on intensive care, and although no statistical significant differences existed in the use of this drug between the pneumonia, brain injured and VAP groups it was interesting that it may be associated with some capacity to help separate some of the groups with multivariate analysis. The fact that some drug metabolite may have been detected in these samples raises the concern that some of the predictive models were basing prediction not on genuine biological differences but treatment effect. In order to address this fully more detailed metabolite assignment would need to be performed.

This study represents the first attempt to investigate pneumonia using a metabonomic approach to the analysis of EBC and is one of only a few studies looking at ventilated patients with such techniques (195, 210). Almost all of the previous work has focused on relatively stable diseases in a clinic setting. Also although MS has been used to study EBC in a number of previous studies few have approached the problem with an entirely non-targeted, profiling, approach (206, 207) and this is the only one to use a direct-injection non-hyphenated technology.

The current study has a number of limitations. Firstly as no gold standard exists for the diagnosis of pneumonia any method used to define the clinical groups will lead to some misclassification so building a model with 100% accuracy is unlikely. Also this study used a limited number of patients, of all of those that were recruited only those with the clearest diagnosis of pneumonia were used in order to ensure the best clinical separation between comparison groups. This will limit the ability to build models to correctly classify patients. EBC itself poses a particular challenge with the metabolites it contains being present in very low concentrations thus requiring very sensitive equipment to detect them. This also leads to the problem that exogenous metabolites contained within solvents, collecting equipment and introduced by any laboratory equipment will also be more easily detected. Care had to be taken to minimise the potential for contamination in any of the assays. Despite extensive efforts to eliminate such confounders a great number of metabolites were still detected within the methanol used for MS analysis. Even after these were addressed batch

effect could still be observed between samples run at different times. Although when individual models were examined it was not apparent that the batch effect was having an influence on the models themselves this issue needs to be addressed when considering this approach as a clinical test. For this to be a useful approach in the clinical environment it would have to be reproducible day to day and location to location in order to provide accurate results that could influence clinical decision making. To further address the clinical importance of the MS based models further metabolite identification needs to be undertaken to address the biological importance of the ions identified as being discriminant in the models

5.7 Conclusion

Analysis of EBC using a metabonomic approach with either NMR spectroscopy or MS poses a number of challenges due to the low concentration of metabolites within this fluid. In this sample set NMR provided only a limited number of metabolites and freeze drying the sample prior to preparation failed to produce a feasible solution to the low metabolite count.

Analysis of EBC with a direct-injection MS methodology shows some possibility to assist with diagnosis of both pneumonia and VAP, however, this method has limitations with regard to its reproducibility and further work needs to be done in order to identify the metabolites that seem to differentiate the clinical groups in order to assess their clinical relevance.

6. MULTIVARIATE ANALYSIS OF CLINICAL DATA

6.1 Summary

Clinical data are typically analysed using simple statistics such as Student's t-test, ANOVA or Fishers exact test. There are relatively few examples of studies that have used multivariate techniques, usually associated with 'omics' data processing, to analyse routinely collected clinical data. In this chapter multivariate analysis was applied to a set of clinical data in an attempt to differentiate those patients with pneumonia and VAP from those with brain injuries. Several interesting differences were found between these groups that were not confined to typical clinical features that would have been expected to be different in those with and without pneumonia.

Within this chapter an attempt was made to combine clinical, inflammatory and metabolic data sets. Clinical data was important in all comparisons but the significance of inflammatory and metabolic data varied depending on the comparison being made. Overall there seemed to be an advantage to combining some or all data sets to improve discrimination of the models. Discrimination between clinical groups could be improved further by selecting the most important variables.

6.2 Background

For patients on the ICU there is an enormous amount of clinical data available from bedside clinical observations, for example blood pressure, heart rate and temperature, laboratory tests, such as haematological and clinical chemistry parameters, point of care tests, for example blood gas analysis and blood glucose measurement, to specific measurable parameters for particular interventions such as those associated with mechanical ventilation. Interpreting clinical data is clearly one of the skills of the physician. However, in some situations clinical judgement may be unable to detect some of the subtle changes in these parameters. In some conditions clinical features can overlap with

other medical conditions such as pulmonary oedema, ARDS and lobar collapse, this becomes especially problematic when the diagnosis, such as VAP, does not have a gold standard diagnostic test.

Clinical features have been found to have a variable ability to diagnose pneumonia (11, 14, 18, 19, 21) in the primary care setting and the addition of biomarkers such as CRP and PCT have a limited effect on improving diagnostic potential (22-25). Despite the greater amount of clinical information available on the ICU making the diagnosis of VAP is potentially more challenging than when pneumonia is the presenting diagnosis (72-74). This probably represents the greater complexity of ICU patients where several clinical conditions can exist simultaneously and the features of each can overlap. None of the features that are important in making the diagnosis of pneumonia are specific to this condition, a white cell count and temperature increase can be seen in any condition where there is a SIRS response; radiological changes of consolidation can be difficult to distinguish from lobar collapse or ARDS (73, 75) and similarly oxygen requirements can increase due to these other lung conditions.

The integration of clinical data on ICU has mainly been focused on outcome scores such as the Acute Physiology and Chronic Health Evaluation II score (APACHEII) (338) and the Simplified Acute Physiology Score II (SAPS II) (339) to predict the risk of death and organ dysfunction scores such as the Logistic Organ Dysfunction Score (LODS) (340), Multiple Organ Dysfunction Score (MODS) (341), and the Sequential Organ Failure Assessment (SOFA) (342). These scores are generally derived from logistic regression models of clinical variables and then validated in large ICU populations. However, on the whole these scores have little impact on an individual patient and are used predominantly in the context of clinical research to compare patient groups or as a marker of ICU performance (343). So far the only attempt to combine clinical data into a model to diagnose VAP has been the CPIS developed by Pugin *et al* based on six clinical parameters, temperature, white cell count, secretion

load, radiological changes, oxygen requirement and microbiology, which gives a score from 0-12 (83) with a score of greater than six correlating with high bacterial load on bronchoalveolar lavage. This score has been used to guide prescribing with a significant reduction in antibiotic prescribing without increase in mortality (84). However, CPIS doesn't work well in all clinical scenarios such as burn and trauma patients (86) and it is plausible that the addition of further parameters available on the ICU may be able to strengthen this score.

There have been a few attempts to use the multivariate statistical methods used previously in this study to analyse clinical data. For example, PLS has been used to predict survival in patients with multiple myeloma following treatment (344), to predict outcome in children following surgery for tuberous sclerosis (345) and using specific measurements of dental disease to predict outcome following dental intervention (346). No studies exist that attempt to apply these methods to either intensive care patients or to those with pneumonia.

Further, despite the number of studies that exist using 'omics' sciences there is little available attempting to combine 'omics' data with clinical features. A few studies exist that attempt to combine different 'omics' data sets. For example, an animal study looking at liver toxicity combined NMR, microarray and clinical chemistry data (347).

6.3 Aims

The overall aim of this study was to use multivariate techniques with clinical data to attempt to improve the diagnosis of pneumonia in patients requiring ventilation, specifically those going on to develop VAP. The following questions were addressed:

- 1. Can multivariate methods applied to routinely collected clinical data produced discriminant models to differentiate those with and without pneumonia?*

2. *Can combining clinical data with metabolic and inflammatory data more accurately differentiate pneumonia than any one set of data alone?*

6.4 Protocols

6.4.1 Patient Recruitment

Patients were recruited as described in chapter 2. Patients were defined as either having pneumonia or a brain injury as described earlier. All patients were followed up over time and those brain injured patients developing VAP were defined based on CPIS scoring, for a breakdown of the CPIS score used see chapter 2. Patients with borderline scores were assessed and classified as VAP or no VAP by an independent assessor.

6.4.2 Clinical Data

A comprehensive set of clinical data was recorded for each day of a patient's ICU stay. Data included all physiological variables, laboratory test results, radiology results, arterial blood gas results, microbiology results and administered drugs, fluid and feed. Data were collected at 8:00am every morning and covered the preceding 24h period. For all variables the minimum and maximum values were recorded for the 24h period. Where data were not recorded or had not been measured the relevant data point was left blank. Where patients were spontaneously breathing and receiving oxygen via nasal cannula or facemask the number of litres of oxygen was converted into an FiO_2 using the conversion in table 6.1 to allow comparison to patients receiving titrated oxygen therapy either through the ventilator or via a face mask such as a venturi or humidified system.

Table 6.1. Conversion table for litres of oxygen to FiO_2 .

Method	O ₂ Flow (l/min)	Estimated FiO ₂
Nasal Cannula	1	0.24
	2	0.28
	3	0.32
	4	0.36
	5	0.40
	6	0.44
Facemask	5	0.40
	6-7	0.50
	7-8	0.60

All clinical data were checked by hand to ensure that recorded values fell within physiological ranges. Numerical data were selected to build multivariate models to compare pneumonia to brain injured patients leaving a data set made of continuous variables that could be objectively measured. The complete list of variables acquired can be seen in table 6.2, giving 106 variables for multivariate analysis.

6.4.3 Metabolic and Inflammatory Data

The two most reliable data sets from the earlier analysis, the metabonomic and inflammasome data from serum samples, were chosen to combine with the clinical data in an attempt to build an all-encompassing model taking into account clinical, inflammatory and metabolic data. Because of the much larger data set that was the metabonomic data this data set was handled in two ways, first the entire spectral data was combined with the two other data sets and then a smaller data set using only the integrals of the identified peaks. The integrals were calculated using an in-house Matlab script and reduced this data set from thousands of data points to just over 200.

Table 6.2. Clinical variables used for multivariate analysis, for all values other than those which are averages over 24h (*) the minimum and maximum values for each variable for the 24h period prior to sampling were taken. Some variables (‡) were only available for certain ventilation modes.

Bedside Variables	Laboratory Variables
Ventilator Settings	Laboratory Parameters
Peak end expiratory pressure (PEEP) (cmH ₂ O)‡	White Blood Cell Count (x10 ⁹ /L)
FiO ₂	Haemoglobin (g/dl)
Respiratory rate set (breaths/min)‡	Haematocrit (%)
Respiratory rate measured (breaths/min)	Platelet Count (x10 ⁹ /L)
Set tidal volume (ml)‡	Prothrombin Time (s)
Expiratory tidal volume (ml)	Activated Partial Thromboplastin Time (s)
Pressure support (cmH ₂ O)‡	Fibrinogen (g/L)
Pressure control (cmH ₂ O)‡	Sodium (mmol/L)
Expiratory minute volume (L)	Potassium (mmol/L)
Peak airway pressure (cmH ₂ O)	Creatinine (µmol/L)
	Urea (mmol/L)
Physiological Parameters	Chloride (mmol/L)
Glasgow Coma Scale	Magnesium (mmol/L)
Heart rate (beats/min)	C-Reactive Protein (mg/l)
Systolic blood pressure (mmHg)	Alanine Transaminase (IU/L)
Diastolic blood pressure (mmHg)	Alkaline Phosphatase (IU/L)
Mean arterial pressure (mmHg)	Bilirubin (µmol/L)
Temperature (°C)	Albumin (g/L)
Oxygen saturations (SpO ₂) (%) with associated FiO ₂	Corrected Calcium (mmol/L)
Ratio of saturation (SpO ₂) to FiO ₂	Phosphate (mmol/L)
Hourly urine output (ml/h)	
Total urine output over 24 hours (ml)	Blood Gas Parameters
Average hourly urine output (ml)*	PaO ₂ with associated FiO ₂
Total fluid input over 24 hours (ml)	PaO ₂ :FiO ₂ ratio (kPa)
Average hourly fluid input (ml)*	PaCO ₂ (kPa)
Fluid balance over previous 24h (ml)	pH
Number of tracheal secretions over 24h	Bicarbonate (mmol/L)
Central Venous Pressure (CVP)(cmH ₂ O)	Base excess
	Lactate (mmol/L)
	Glucose (mmol/L)

6.4.4 Statistical Analysis

Prior to multivariate analysis all data were scaled to unit variance. Standardising the variance attempts to take into account the influence on multivariate models of variables with naturally higher values that tend to be associated with higher variance and allows smaller parameters to have similar weight within the model. This technique also allows parameters measured with different units to be combined without other manipulation. Multivariate statistics were used to analyse the data. Initial exploration with principal component analysis (PCA) was performed to look for natural clustering and to detect outliers before supervised multivariate analysis using orthogonal partial least squared discriminant analysis (OPLS-DA) was used to generate models to optimally separate predefined groups. OPLS-DA models were cross validated using seven fold cross-validation using a “leave-one-out” methodology. Important variables in each model were identified by examining the loadings associated with each model and the variable importance, VIP, scores. VIP is a parameter which summarizes the influence on Y, the defined groups, of each variable in the model. It is a sum over all model dimensions of the variable contributions. Variables important in the models were defined as those with VIP greater than 1.0 (112). All multivariate analysis was performed using the SIMCA 13.0 statistical package (Umetrics, Sweden). Where it was necessary to compare models constructed with clinical data combined with inflammatory and metabolic data with those using only metabolic or inflammatory data new models were constructed with the inflammatory or metabolic data utilizing only those patients who had both sets of data. This was done to ensure that the same patients were being compared to avoid bias based on the slightly differences in the patient groups who had both types of data. Univariate analysis was performed using the Student’s t-test with the Benjamini-Hochberg procedure to correct for false discovery rate from multiple comparisons.

6.5 Results

6.5.1 Patients

21 patients with brain injuries, 12 with pneumonia and 5 who developed VAP had all three of sets of data: clinical, inflammatory and serum metabonomic, to allow combined models to be built.

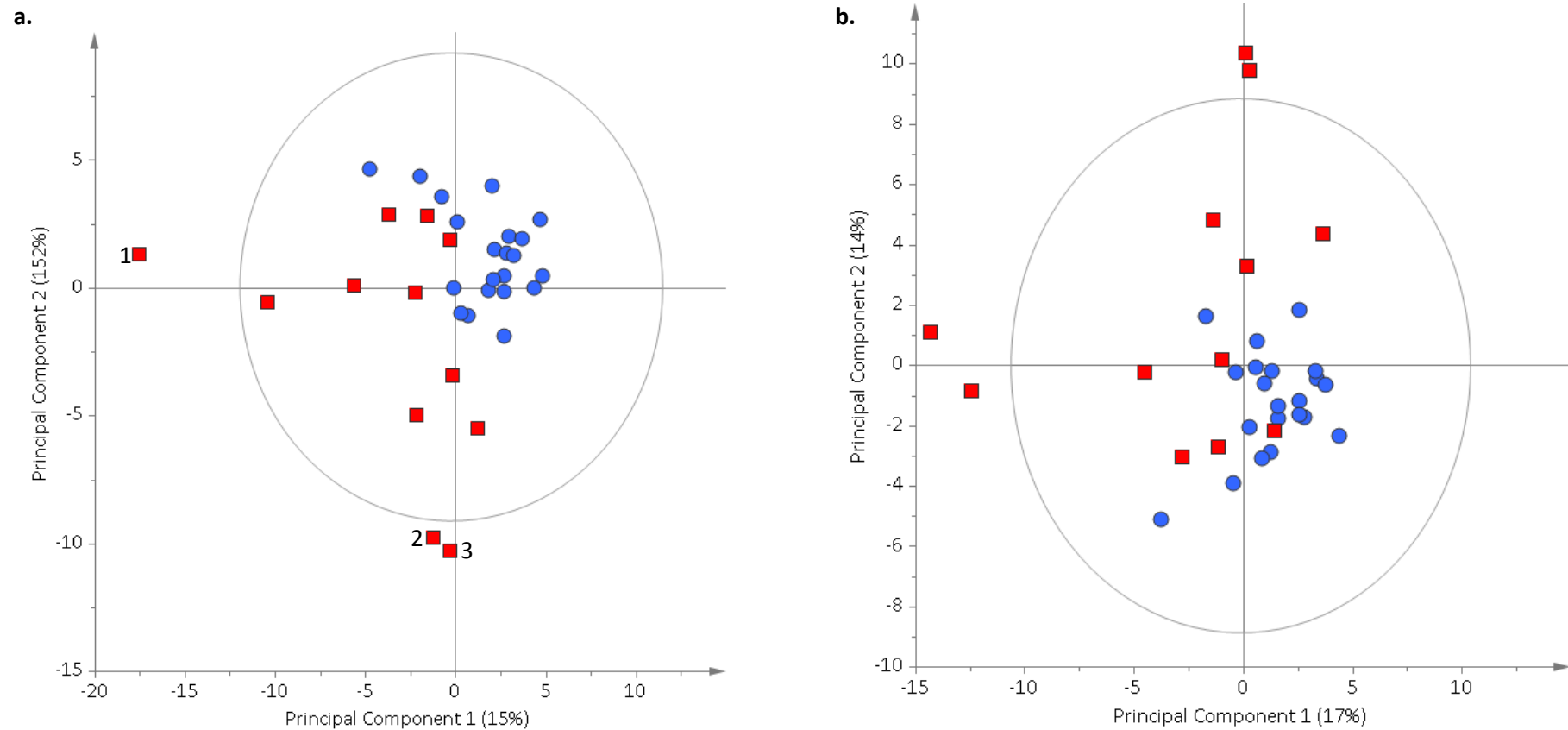
Overall from these patients 6.1% of the clinical data was missing, however, the majority of the 'missing data' originated from certain ventilator parameters that were only applicable when some ventilator modes were used, for example pressure support and set tidal volume. Excluding these parameters the rate of missing data was only 3.2%. Excluding ventilation parameters, rates of missing data varied from 0-60.5%. The parameter with the largest proportion of missing data was the central venous pressure which was missing in over 60% of cases. Selected models were examined with and without this parameter and little difference was found when it was included or excluded, therefore to simulate the clinical environment, where not all data is necessarily available, it was left in for initial comparisons. After CVP the next most common missing variable was ALT which was missing 9.3% of the time. 31 parameters had no missing data and a further 51 had only 2% missing data, representing data missing from only a single patient. Fourteen variables had 4% missing data representing only 2 missed data points.

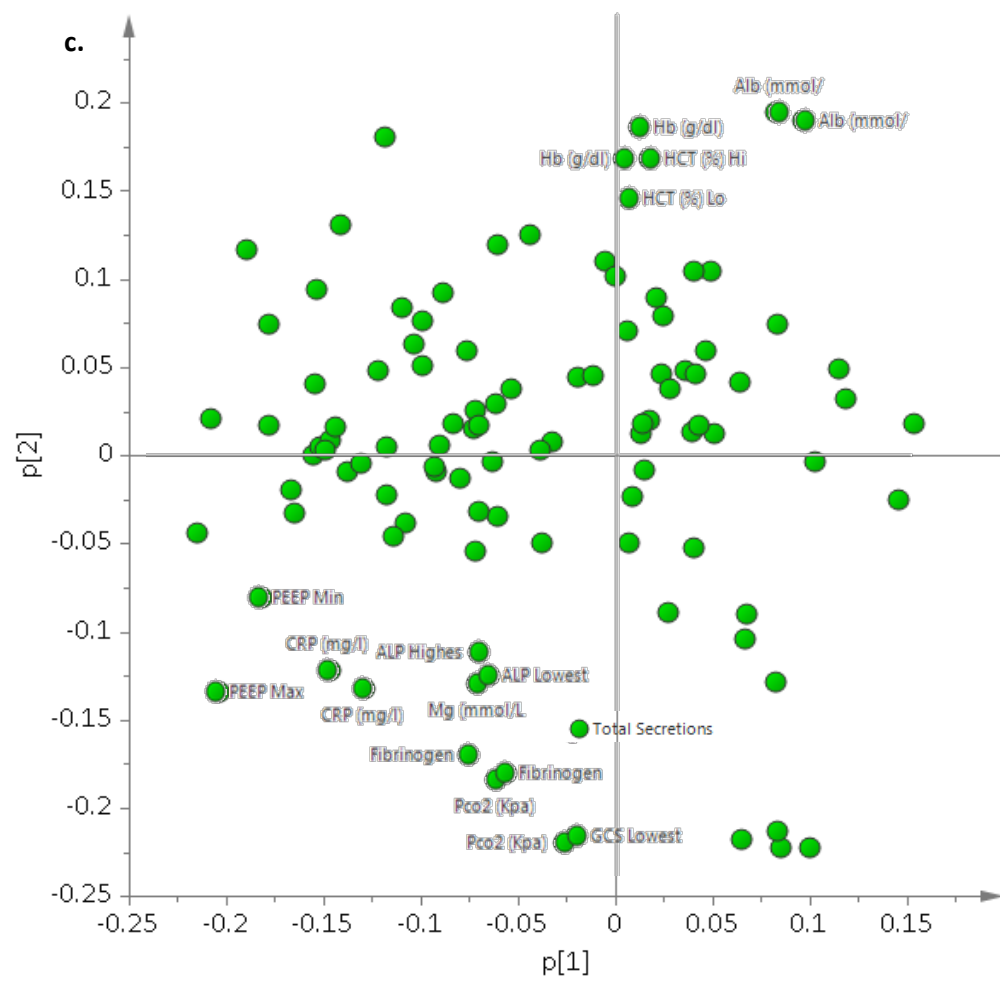
6.5.2 Clinical Data Models

6.5.2.1 Brain Injuries vs Pneumonia

Principal component analysis of the clinical variables demonstrated natural separation of the brain injured and pneumonia patients (R^2X 0.27, Q^2X 0.05), figure 6.1, but the predictive value for this model was only 5% implying that the data set was very heterogeneous. Three of the pneumonia patients were outliers, the first lying to the left of the plot was distinguished by having a marked

Figure 6.1 a. Three component PCA comparing samples taken from patients with brain injuries, blue circles, and patients with pneumonia, red squares, at the start of ventilation (R^2X 0.27, Q^2X 0.05) with all clinical parameters and b. excluding those used in the CPIS (R^2X 0.31, Q^2X 0.12). The ellipse represents Hotelling's T^2 at $p=0.05$. Some natural separation can be seen between the two groups in the first and second components, in figure 6.1a two of the pneumonia patients are outliers as demonstrated by lying outside the Hotelling's ellipse, numbered.





inflammatory response with a higher white cell count and CRP along with renal failure as suggested by high urea, also for this patient several respiratory parameters were not available as they had both of their lungs independently ventilated at the start of recruitment so a single set of parameters were impossible to obtain. The second two patients presenting as outliers at the bottom of the plot were characterised by the high carbon dioxide, bicarbonate and base excess values. This is not unexpected as these individual had compensated chronic respiratory failure secondary to previous brain injuries. All of these patients were retained for further analysis as ideally a good clinical model would be able provide discrimination across a range of patients with various associated comorbidities. The natural separation between the pneumonia and brain injured groups was not entirely surprising as the classification of pneumonia was based on an adaption of the CPIS score which is based on several of the clinical parameters here. When the model was rebuilt excluding temperature, secretion load, white cell count and markers of oxygenation there was still a suggestion of separation along the first two components (R^2X 0.31, Q^2X 0.12), figure 6.1b. When the loadings from the first PCA were examined, figure 6.1c, the features that caused the separation were not those from the CPIS but parameters such as haemoglobin, PEEP, CRP, fibrinogen and $PaCO_2$.

When a supervised model was constructed using OPLS-DA then good separation was achieved on cross validation (R^2Y 0.71, Q^2Y 0.53, $p < 0.001$), figure 6.2, and this predictive capacity was only slightly reduced when features from the CPIS were excluded (R^2Y 0.62, Q^2Y 0.43, $p < 0.001$). The clinical features that were most important in building this model can be seen in table 6.3.

Figure 6.2. OPLS-DA model based on clinical data with one component comparing patients admitted with brain injuries, blue bars, to those with pneumonia, red bars, at the start of ventilation (R^2Y 0.70, Q^2Y 0.53, $p < 0.001$) a. before and b. after cross validation. Before cross validation the groups can be seen to be separated with pneumonia samples separated in the positive direction along the first component. After cross validation this separation is less with some of the pneumonia patients crossing between groups.

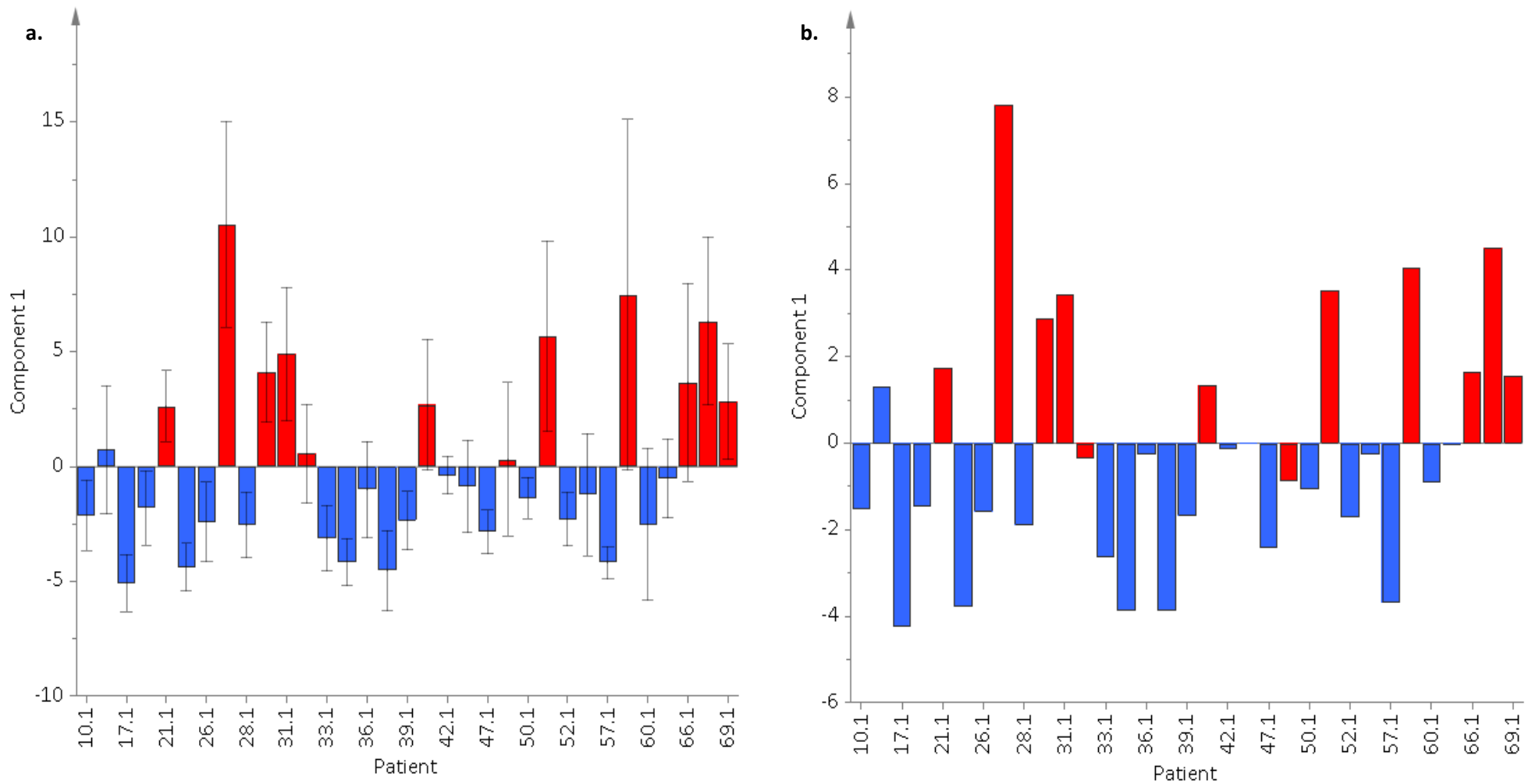


Table 6.3 Clinical features with VIP>1.0 for the OPLS-DA model (R^2Y 0.71, Q^2Y 0.53, $p<0.001$) comparing patients with pneumonia to those with brain injuries, including features making up the CPIS.

Variables Increased in Pneumonia			Variables Reduced in Pneumonia		
Variable	VIP	Direction of Change in Pneumonia	Variable	VIP	Direction of Change in Pneumonia
Highest PEEP	2.68	↑	Highest Albumin	2.08	↓
Highest CRP	2.10	↑	Lowest Albumin	2.04	↓
Lowest CRP	1.95	↑	Highest PaO ₂ :FiO ₂ ratio	1.75	↓
Lowest PEEP	1.82	↑	Lowest PaO ₂ :FiO ₂ ratio	1.70	↓
Highest Peak Airway Pressure	1.68	↑	Highest SpO ₂ :FiO ₂ Ratio	1.58	↓
Highest Respiratory Rate	1.62	↑	Highest pH	1.55	↓
Highest Fibrinogen	1.59	↑	Highest Haemoglobin	1.40	↓
Highest PaCO ₂	1.53	↑	Lowest pH	1.30	↓
Lowest Fibrinogen	1.53	↑	Lowest SpO ₂ :FiO ₂ Ratio	1.25	↓
Lowest White Cell Count	1.51	↑	Lowest PaO ₂	1.12	↓
Lowest Glasgow Coma Score	1.43	↑	Lowest Expiratory Tidal Volume	1.07	↓
Total Secretions	1.40	↑	Lowest Haemoglobin	1.06	↓
Highest White Cell Count	1.39	↑			
Lowest FiO ₂	1.38	↑			
FiO ₂ for highest SpO ₂	1.38	↑			
Highest Haematocrit	1.27	↑			
Lowest PaCO ₂	1.26	↑			
FiO ₂ to get the highest PaO ₂	1.20	↑			
Highest Heart Rate	1.20	↑			
Lowest Heart Rate	1.14	↑			
Lowest Peak Airway Pressure	1.11	↑			
Lowest ALP	1.10	↑			
Highest Prothrombin Time	1.09	↑			
Lowest Urea	1.08	↑			
Lowest APTT	1.07	↑			
Highest Expiratory Minute Volume	1.02	↑			

When only those variables with VIP >1.0 were used to construct the model, including features used in the CPIS then predictive capacity improved (R^2Y 0.72, Q^2Y 0.65, $p<0.001$) and when the nine independently classified patients were used as a small validation cohort then the model had a sensitivity of 0.75, specificity of 0.80, positive predictive value of 0.75 and negative predictive value of 0.80.

6.5.2.2 Brain Injury vs VAP

OPLS-DA models comparing the five patients who developed VAP to those admitted with brain injuries continued to have good predictive capacity both when all clinical data was used (R^2Y 0.69, Q^2Y 0.52, $p < 0.001$), figure 6.3, and when the features in the CPIS were excluded (R^2Y 0.71, Q^2Y 0.50, $p < 0.001$). Table 6.4 gives the most important parameters in this model. When the patients with VAP were compared to those brain injured patients who never developed VAP but who had data for an equivalent time point then the model remained good (R^2Y 0.83, Q^2Y 0.54, $p = 0.08$) with oxygenation and associated parameters having a much greater influence than in previous models, table 6.5. When the CPIS variables were removed the predictive capacity fell (R^2Y 0.75, Q^2Y 0.26, $p = 0.44$).

Table 6.4 Clinical features with $VIP > 1.0$ for the OPLS-DA model used (R^2Y 0.69, Q^2Y 0.52, $p < 0.001$) comparing patients with VAP to those with brain injuries, including features making up the CPIS.

Variables increased in VAP			Variables decreased in VAP		
Variable	VIP	Direction of Change in VAP	Variable	VIP	Direction of Change in VAP
Lowest ALP	2.32	↑	Highest SpO ₂ :FiO ₂ Ratio	1.66	↓
Highest ALP	2.28	↑	Lowest PaO ₂ :FiO ₂ ratio	1.65	↓
Lowest Fibrinogen	2.23	↑	Lowest SpO ₂	1.59	↓
Highest Expiratory Tidal Volume	2.23	↑	Highest Albumin	1.46	↓
Highest Fibrinogen	2.16	↑	Lowest Albumin	1.32	↓
FiO ₂ to give highest SpO ₂	1.78	↑	Highest PaO ₂ :FiO ₂ ratio	1.30	↓
Total Secretions	1.74	↑	Lowest PaO ₂	1.08	↓
Lowest ALT	1.74	↑	Lowest SpO ₂ :FiO ₂ Ratio	1.06	↓
Highest ALT	1.71	↑			
Highest Respiratory Rate	1.70	↑			
Lowest Expiratory Tidal Volume	1.67	↑			
Lowest Respiratory Rate	1.66	↑			
Lowest Urea	1.63	↑			
Highest Peak Airway pressure	1.56	↑			
Lowest CRP	1.51	↑			
Highest Expiratory Tidal Volume	1.51	↑			
Lowest FiO ₂	1.49	↑			
Highest PEEP	1.41	↑			
Highest Urea	1.39	↑			
Highest Systolic Blood Pressure	1.38	↑			
Highest CRP	1.32	↑			
Lowest PEEP	1.27	↑			
FiO ₂ to give lowest PaO ₂	1.09	↑			
Lowest Bilirubin	1.08	↑			

Figure 6.3. OPLS-DA model, with one component, based on clinical data comparing patients admitted with brain injuries, blue bars, to those who developed VAP, green bars, a) with all clinical variables (R^2Y 0.69, Q^2Y 0.52, $p < 0.001$) and b) without those used in the CPIS (R^2Y 0.71, Q^2Y 0.50, $p < 0.001$). Before cross validation the groups can be seen to be separated with pneumonia samples separated in the positive direction along the first component.

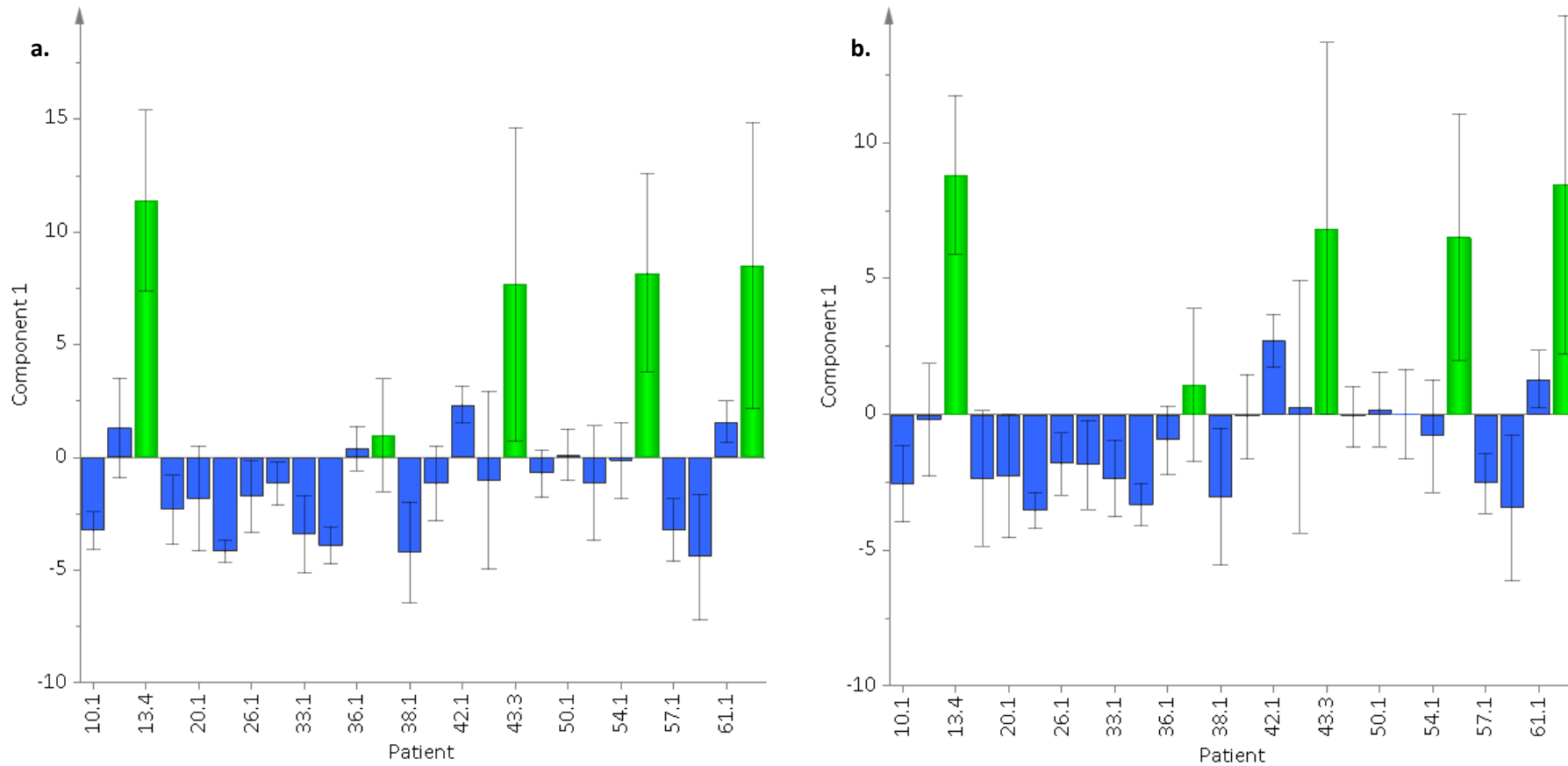


Table 6.5 Clinical features with VIP>1.0 for the OPLS-DA model (R^2Y 0.83, Q^2Y 0.54, $p=0.08$) comparing patients with VAP to those with brain injuries at an equivalent time point, including features making up the CPIS.

Variables Increased in VAP			Variables Decreased in VAP		
Variable	VIP	Direction of Change in VAP	Variable	VIP	Direction of Change in VAP
Lowest FiO ₂	1.81	↑	Lowest PaO ₂ :FiO ₂ ratio	1.99	↓
Highest FiO ₂	1.71	↑	Highest SpO ₂ :FiO ₂ ratio	1.93	↓
FiO ₂ to give highest SpO ₂	1.69	↑	Lowest SpO ₂ :FiO ₂ ratio	1.92	↓
FiO ₂ to give highest PaO ₂	1.65	↑	Highest PaO ₂ :FiO ₂ ratio	1.61	↓
Lowest CRP	1.61	↑	Lowest PaO ₂	1.58	↓
Highest CRP	1.61	↑	Lowest SpO ₂	1.58	↓
FiO ₂ to give lowest PaO ₂	1.61	↑	Lowest Platelet Count	1.48	↓
Lowest Creatinine	1.54	↑	Highest Platelet Count	1.48	↓
Highest Creatinine	1.54	↑	Lowest Urine Output	1.37	↓
Lowest Inspired Tidal Volume	1.51	↑	Lowest pH	1.27	↓
FiO ₂ to give lowest SpO ₂	1.37	↑	Total Urine Output in 24h	1.25	↓
Highest PaCO ₂	1.36	↑	Average Hourly Urine Output	1.25	↓
Highest Central Venous Pressure	1.36	↑	Lowest Diastolic Blood Pressure	1.18	↓
Highest PEEP	1.28	↑	Total Fluid Input in 24h	1.13	↓
Highest Systolic Blood Pressure	1.26	↑	Average Fluid Intake per Hour	1.12	↓
Highest Inspired Tidal Volume	1.24	↑	Lowest Mean Arterial Pressure	1.05	↓
Highest Peak Airway Pressure	1.24	↑			
Lowest Bilirubin	1.15	↑			
Highest Bilirubin	1.15	↑			
Lowest ALP	1.13	↑			
Highest ALP	1.13	↑			
Lowest Sodium	1.11	↑			
Highest Sodium	1.11	↑			
Highest Expiratory Minute Volume	1.05	↑			
Highest Pressure Support	1.00	↑			

6.5.3 Combining Clinical Variables with Metabonomic and Inflammasome Data

6.5.3.1 Brain Injury vs Pneumonia

6.5.3.1.1 Clinical and Metabonomic Data

Combining clinical data with full spectral serum data provided an OPLS-DA model with a reasonable Q^2Y (R^2Y 0.95, Q^2Y 0.42, $p=0.003$) although slightly lower than that using clinical data alone but identical to a model using only the spectral data for this patient set (R^2Y 0.95, Q^2Y 0.42, $p=0.003$). From this model the variables with the highest VIP were metabolites corresponding to lipids at 0.81-0.74ppm, lipids at 1.18-1.11ppm, alanine at 1.49-1.46ppm, lipids at 1.558-1.51, Glycoproteins at 2.04, lipids at 2.21-2.17, glutamine at 2.49-2.42ppm, an unidentified metabolite at 3.07, phospholipids at 3.20ppm, glycerol at 3.57ppm, phenylalanine at 7.45-7.41ppm and formate at 8.45ppm. Clinical variables of importance were maximum and minimum PEEP, highest and lowest CRP, highest and lowest albumin and highest $PaO_2:FiO_2$ ratio.

Due to concerns that the vastly overwhelming number of data points contributed by the metabolic data may dominate these models similar analysis was carried out using the integrals of all of the NMR peaks. When clinical data were combined with the integrals of the metabolic peaks via OPLS-DA a model could be created that was similar to that using the entire spectral data (R^2Y 0.86, Q^2Y 0.43, $p=0.003$) and was better than using only the integrals of the metabolic data alone (R^2Y 0.72, Q^2Y 0.29, $p=0.04$). Using this method the metabolites that were most important can be seen in table 6.6. They were similar to those that were seen when the entire spectrum was utilised, with formate, alanine, glycoprotein and phospholipids being some of the most important metabolites differentiating between patients with brain injury and pneumonia. Univariate comparison of these integrals found all but one of the unidentified metabolites to be significantly different between the two groups even after correction for false discovery rate, table 6.6. Many of the lipid species seen to

be important when brain injured patients were compared to those with pneumonia using only metabolic data, in chapter 3, appeared no longer to differentiate the groups when spectral integrals were used.

Table 6.6. Integrals of metabolites with the most influence on the OPLS-DA model comparing pneumonia with brain injuries. p-values represent comparisons between groups of individual integrals using the Student's t-test corrected for the false discovery rate using the Benjamini-Hochberg procedure.

Metabolite Integral	ppm Range		VIP	p-value	Direction of Change in Pneumonia
Phospholipids	3.196	3.188	2.89	0.02	↓
Glycoproteins	2.046	2.022	2.69	0.02	↑
Formate	8.455	8.450	2.58	0.03	↑
Unknown	3.074	3.059	2.40	0.03	↑
Unknown	2.057	2.052	2.34	0.02	↑
Unknown	2.063	2.057	2.32	0.03	↑
Unknown	3.016	3.01	2.29	0.02	↓
Glutamine	2.453	2.449	2.25	0.02	↓
Alanine	1.489	1.461	2.24	0.02	↓
Unknown	7.812	7.805	2.15	0.07	↑
Unknown	2.052	2.046	2.06	0.03	↑
Glutamine	2.470	2.460	2.02	0.03	↓

6.5.3.1.2 Clinical and Inflammatory Data

Combining clinical and inflammasome data provided an OPLS-DA model with a good predictive capacity (R^2Y 0.68 Q^2Y 0.49, $p < 0.001$) which was better than that using the inflammatory data alone, from these patients (R^2Y 0.45 Q^2Y 0.26, $p = 0.012$). The variables that were most important in this model can be seen in table 6.7, the most important variables in this model were predominantly clinical.

Table 6.7. Variables with VIP>1.0 in the OPLS-DA model (R^2Y 0.68, Q^2Y 0.49, $p<0.001$) combining inflammatory and clinical data comparing patients with pneumonia and brain injuries. Clinical variables are in black and inflammatory variables blue.

Variables Increased in Pneumonia			Variables Decreased in Pneumonia		
Variable	VIP	Direction of Change in Pneumonia	Variable	VIP	Direction of Change in Pneumonia
Highest PEEP	2.84	↑	Highest Albumin	2.20	↓
Highest CRP	2.22	↑	Lowest Albumin	2.16	↓
Lowest CRP	2.06	↑	Highest PaO ₂ :FiO ₂ ratio	1.86	↓
Lowest PEEP	1.97	↑	Lowest PaO ₂ :FiO ₂ ratio	1.80	↓
Highest Peak Airway pressure	1.76	↑	Highest SpO ₂ :FiO ₂ ratio	1.68	↓
Highest Respiratory Rate	1.72	↑	Highest pH	1.64	↓
Highest Fibrinogen	1.69	↑	6-keto-PGF1 α	1.58	↓
Highest PaCO ₂	1.62	↑	Highest Haemoglobin	1.48	↓
Lowest Fibrinogen	1.61	↑	5,6-DHET	1.41	↓
Lowest White Cell Count	1.60	↑	Lowest pH	1.37	↓
Lipoxin B4	1.52	↑	Highest Haematocrit	1.34	↓
Lowest Glasgow Coma Score	1.52	↑	Lowest SpO ₂ :FiO ₂ ratio	1.33	↓
Total Secretions	1.48	↑	C22:6 (DHA)	1.32	↓
Highest White Cell Count	1.47	↑	Lowest PaO ₂	1.18	↓
Lowest FiO ₂	1.46	↑	Lowest Expiratory Tidal Volume	1.13	↓
FiO ₂ to get the highest SpO ₂	1.46	↑	Lowest Haemoglobin	1.12	↓
E-Selectin	1.38	↑	C20:5 (EPA)	1.07	↓
MCP-1	1.38	↑	10(S),17(S)-DiHDoHE	1.04	↓
ICAM-1	1.35	↑	9(S)-HODE	1.00	↓
IP-10	1.34	↑			
Lowest PaCO ₂	1.34	↑			
FiO ₂ to get the highest PaO ₂	1.28	↑			
Highest Heart Rate	1.27	↑			
Tetranor-PGDM	1.26	↑			
TNF α	1.26	↑			
Lowest Heart Rate	1.21	↑			
IL-13	1.19	↑			
Lowest ALP	1.17	↑			
Lowest Peak Airway Pressure	1.16	↑			
Highest Prothrombin Time	1.15	↑			
Lowest Urea	1.15	↑			
Lowest APTT	1.13	↑			
Highest Expiratory Minute Volume	1.07	↑			
Lowest Creatinine	1.05	↑			
Highest APTT	1.05	↑			
Highest Urea	1.05	↑			
Lowest Magnesium	1.04	↑			
Highest ALP	1.04	↑			

6.5.3.1.3 Clinical, Metabonomic and Inflammatory Data

Combining the clinical variables, metabolic spectral data and the inflammatory data yielded an OPLS-DA model (R^2Y 0.95, Q^2Y 0.42, $p=0.003$) ,figure 6.4, which had a Q^2Y similar to that from the metabolic data alone but not as good as that seen when only the clinical data were used. However, when the model was constructed using only variables that had a VIP greater than 1.0 the model improved, figure 6.5, (R^2Y 0.95, Q^2Y 0.73, $p<0.001$) but when variables with a VIP greater than 2.0 were used no further improvement in Q^2Y was gained (R^2Y 0.91, Q^2Y 0.71, $p<0.001$).

When the integrals of the metabolite peaks were used instead of the full spectral data the model was similar to that using the whole spectral data (R^2Y 0.69, Q^2Y 0.38, $p<0.001$) and when only features with VIP greater than 1.0 (R^2Y 0.70, Q^2Y 0.60, $p<0.001$) or greater than 2.0 (R^2Y 0.66, Q^2Y 0.63, $p<0.001$) were used the models were no better than using the full spectra.

Although the best model was found when clinical and metabolic spectral data were combined, without the addition of inflammatory data, and features with a VIP greater than 2.0 were selected (R^2Y 0.91, Q^2Y 0.75, $p<0.001$) many of the areas of spectral data included appeared to be associated with baseline noise. Much of this was removed by using a VIP cut off of 2.5 (R^2Y 0.77, Q^2Y 0.66, $p<0.001$), without the loss of metabolic information, which was similar to the models produced when only the clinical and metabolic integral data were used, with a VIP cut off of 2.0 (R^2Y 0.70, Q^2Y 0.68, $p<0.001$). This model was made up of 15 variables: Minimum and maximum PEEP, highest respiratory rate, highest peak pressure, minimum and maximum CRP, minimum and maximum albumin, glycoproteins, formate, minimum and maximum $PaO_2:FiO_2$ ratio and three unidentified metabolites. When the independently classified patients were used to validate the model it had a sensitivity of 0.50, specificity of 1.0, positive predictive value of 1.0 and negative predictive value of 0.71. As there was a great deal of, seemingly, duplicate information within this model, for example with the inclusion of both minimum and maximum PEEP, the model was reconstructed using only

Figure 6.4. OPLS-DA model based on clinical, metabolic and inflammatory data with one component and one orthogonal component comparing patients admitted with brain injuries, blue circles, to those with pneumonia, red squares, at the start of ventilation (R^2Y 0.95, Q^2Y 0.42, $p=0.003$) a. before and b. after cross validation. Before cross validation the groups can be seen to be separated with pneumonia samples separated in the positive direction along the first component. After cross validation this separation is less with several samples crossing between groups.

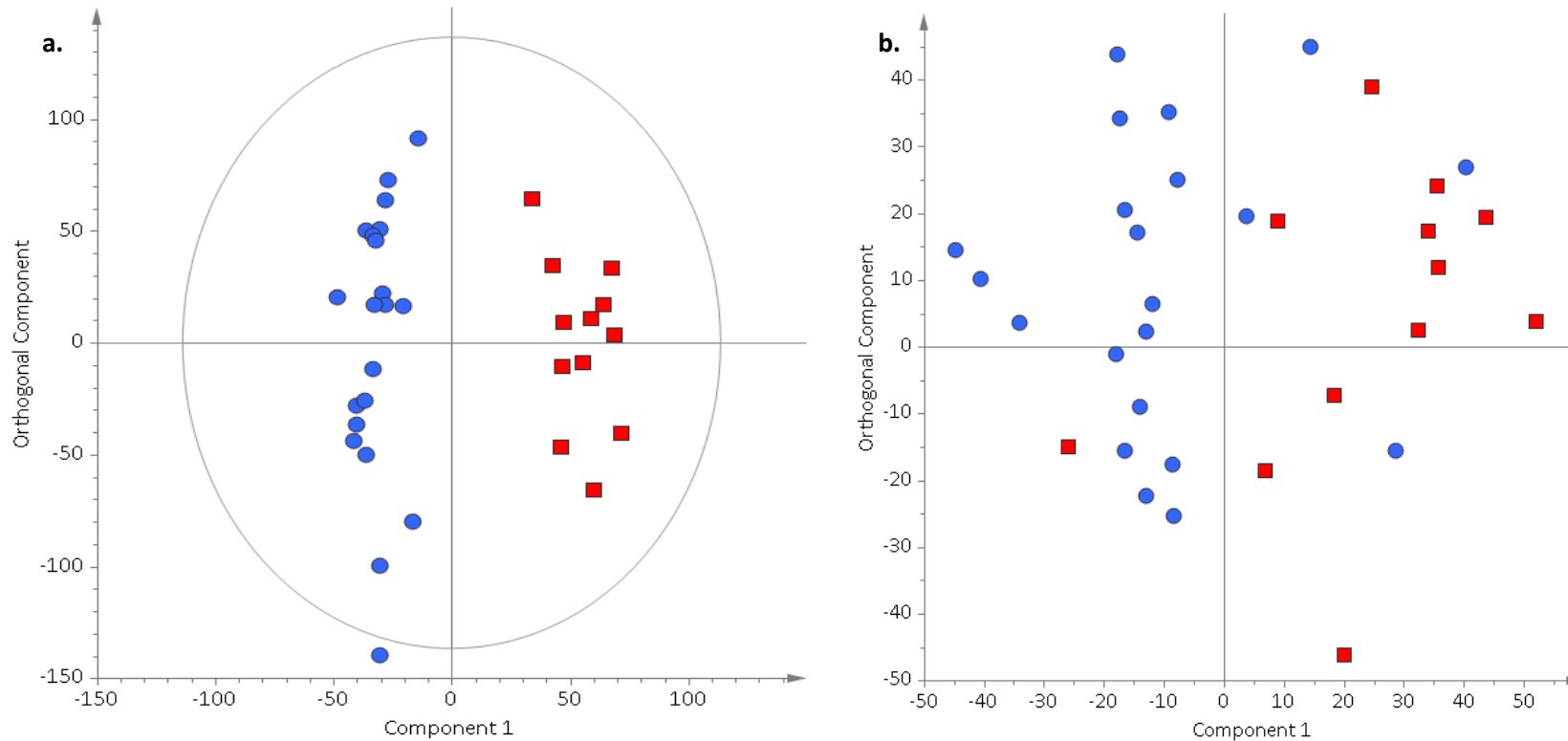
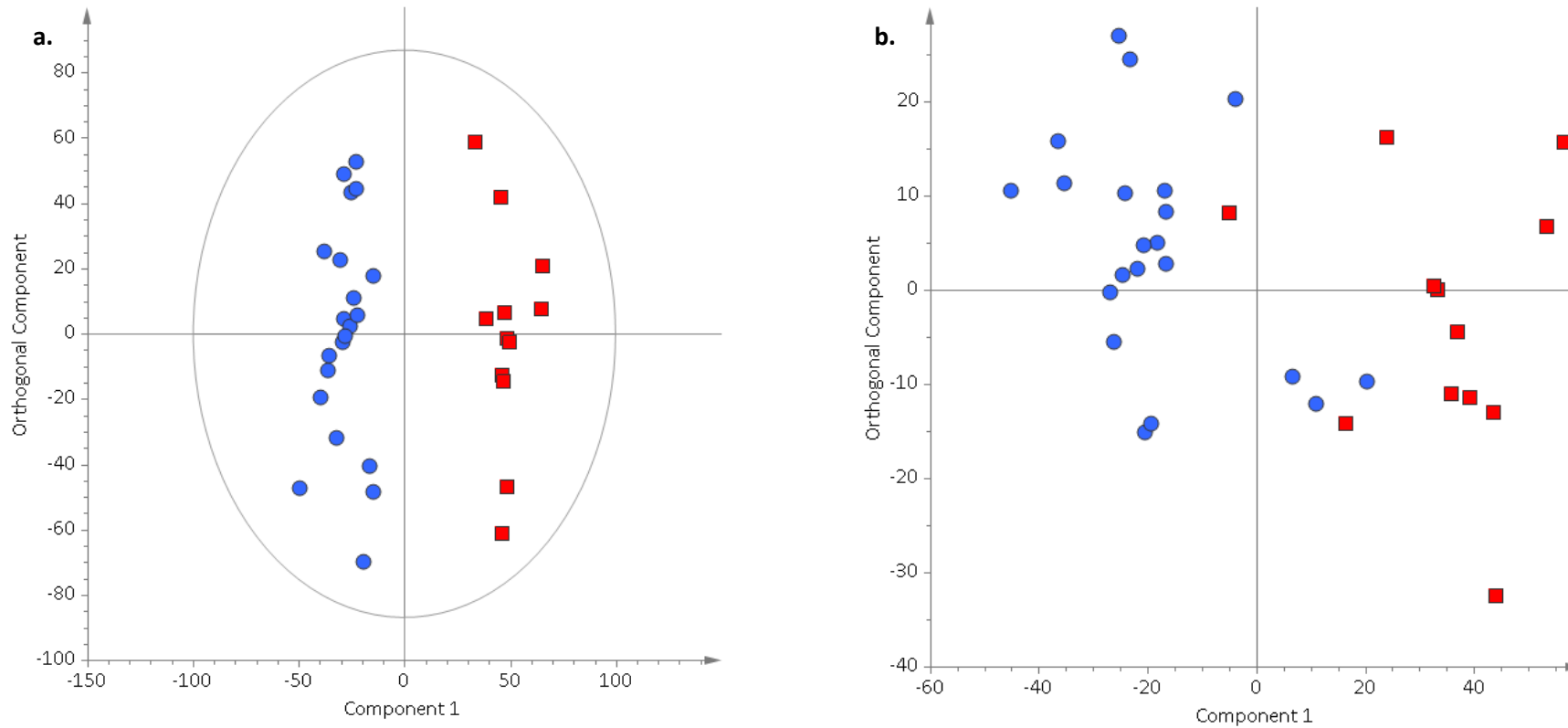


Figure 6.5. OPLS-DA model based on clinical, metabolic and inflammatory data using only variables with a $VIP > 1.0$ with one component and one orthogonal component comparing patients admitted with brain injuries, blue circles, to those with pneumonia, red squares, at the start of ventilation (R^2Y 0.95, Q^2Y 0.73, $p < 0.001$) a. before and b. after cross validation. Before cross validation the groups can be seen to be separated with pneumonia cases separated in the positive direction along the first component. After cross validation this separation remains good with only a few patients crossing between groups.



the variable from each pair with the highest VIP. In this case there was no change to the model parameters (R^2Y 0.70, Q^2Y 0.68, $p < 0.001$).

6.5.3.2 *Brain Injury vs VAP*

6.5.3.2.1 Clinical and Metabonomic Data

When the brain injured patients who developed VAP were compared to the brain injured patients without infection at the start of ventilation using OPLS-DA, combining metabolic and clinical data was only just able to produce a model with discriminant capacity (R^2Y 0.94, Q^2Y 0.16, $p = 0.45$) which was almost identical to that using only the metabolic data (R^2Y 0.94, Q^2Y 0.15, $p = 0.46$) for this patient group.

When metabolite integrals were used instead of the entire spectrum the OPLS-DA model was more predictive (R^2Y 0.77, Q^2Y 0.37, $p = 0.04$) and functioned better than that based only on metabolic data (R^2Y 0.64, Q^2Y 0.15, $p = 0.47$) for this set of patients. However, this model was not as good as that using clinical data alone (R^2Y 0.69, Q^2Y 0.52, $p < 0.001$). Metabolites that were important in this model can be seen in table 6.8. The most important variables were those from the clinical data but the metabolites causing the largest effect on the model were phenylalanine, glycoproteins, and phospholipids as previously seen, along with a number of metabolites that have not previously been identified in this work.

Table 6.8. features important, VIP>1.0, in an OPLS-DA model (R^2Y 0.77, Q^2Y 0.37, $p=0.04$) comparing patients admitted with brain injuries to those developing VAP using a combination of clinical data and the integrals of the metabolic spectral data. Clinical variables are in black and metabolic variables in red.

Variables increased in VAP			Variables decreased in VAP		
Variable	VIP	Direction of change in VAP	Variable	VIP	Direction of change in VAP
Highest Expiratory Minute Volume	2.91	↑	Highest SpO ₂ :FiO ₂ ratio	2.16	↓
Lowest ALP	2.85	↑	Lowest PaO ₂ :FiO ₂ ratio	2.15	↓
Highest ALP	2.80	↑	Lowest SpO ₂	2.07	↓
Lowest Fibrinogen	2.72	↑	Highest Expiratory Tidal Volume	1.97	↓
Highest Fibrinogen	2.62	↑	Highest Albumin	1.86	↓
Phenylalanine (7.446-7.404)	2.34	↑	Highest PaO ₂ :FiO ₂ ratio	1.70	↓
FiO ₂ to give highest SpO ₂	2.32	↑	Lowest Albumin	1.68	↓
Total Secretions	2.27	↑	Unknown (3.196-3.188)	1.51	↓
Highest Respiratory Rate	2.20	↑	Lactate (4.120-4.084)	1.46	↓
Lowest Expiratory Minute Volume	2.18	↑	Lowest PaO ₂	1.41	↓
Lowest Respiratory Rate	2.14	↑	Unknown (3.016-3.01)	1.41	↓
Unknown (2.063-2.057)	2.12	↑	Alanine (1.489-1.461)	1.38	↓
Lowest ALT	2.04	↑	Lowest SpO ₂ :FiO ₂ ratio	1.38	↓
Highest Peak Airway Pressure	2.04	↑	Citrate (2.521-2.511)	1.30	↓
Highest ALT	2.00	↑	Phospholipids (3.225-3.213)	1.30	↓
Lowest Urea	1.99	↑	Unknown (2.370-2.363)	1.27	↓
Lowest FiO ₂	1.94	↑	Glutamine (2.470-2.460)	1.26	↓
Unknown (2.078-2.063)	1.92	↑	Citrate (2.547-2.537)	1.24	↓
Unknown (2.052-2.046)	1.91	↑	Phospholipids (3.213-3.196)	1.24	↓
Lowest CRP	1.88	↑	Highest PaO ₂	1.23	↓
Highest PEEP	1.84	↑	Unknown (2.899-2.894)	1.22	↓
Glycoproteins (2.046-2.022)	1.80	↑	Average Fluid Intake per Hour	1.18	↓
Highest Systolic Blood Pressure	1.80	↑	Unknown (2.970-2.960)	1.16	↓
Phenylalanine (7.340-7.313)	1.75	↑	Unknown (3.443-3.438)	1.15	↓
Unknown (1.052-1.045)	1.73	↑	Glutamine (2.460-2.453)	1.12	↓
Highest Urea	1.69	↑	Unknown (2.912-2.907)	1.10	↓
Lowest PEEP	1.65	↑	Glutamine (2.449-2.444)	1.09	↓
Unknown (2.057-2.052)	1.64	↑	Lowest Expiratory Tidal Volume	1.07	↓
Tyrosine (7.201-7.176)	1.63	↑	Glutamine (2.453-2.449)	1.06	↓
Highest CRP	1.62	↑	Fluid Balance	1.05	↓
Unknown (7.497-7.471)	1.60	↑			
Unknown (8.127-8.12)	1.60	↑			

Unknown (5.474-5.457)	1.60	↑
Unknown (8.078-8.071)	1.60	↑
Unknown (7.857-7.850)	1.60	↑
Tyrosine (6.907-6.882)	1.58	↑
Unknown (1.037-1.032)	1.54	↑
Unknown (1.18-1.174)	1.47	↑
Unknown (1.168-1.163)	1.46	↑
Unknown (7.670-7.664)	1.44	↑
Unknown (1.025-1.019)	1.43	↑
FiO ₂ to give lowest PaO ₂	1.42	↑
Unknown (2.356-2.342)	1.40	↑
Unknown (1.062-1.057)	1.38	↑
Lowest Bilirubin	1.36	↑
Unknown (5.101-5.080)	1.34	↑
Unknown (7.79-7.756)	1.31	↑
Unknown (1.074-1.068)	1.31	↑
Highest Inspired Tidal Volume	1.30	↑
Lowest Magnesium	1.29	↑
Unknown (1.174-1.168)	1.25	↑
Unknown (1.458-1.443)	1.23	↑
FiO ₂ to give lowest SpO ₂	1.21	↑
Unknown (1.113-1.107)	1.21	↑
Unknown (5.454-5.445)	1.20	↑
Highest Mean Arterial Pressure	1.19	↑
Unknown (4.901-4.894)	1.18	↑
Highest Central Venous Pressure	1.16	↑
Formate (8.488-8.484)	1.10	↑
Highest FiO ₂	1.08	↑
Lowest Potassium	1.06	↑
Highest Diastolic Blood Pressure	1.05	↑
Highest Base Excess	1.04	↑
Unknown (5.501-5.495)	1.04	↑
Unknown (2.342-2.331)	1.03	↑
Highest Pressure Support	1.01	↑

6.5.3.2.2 Clinical and Inflammatory Data

Combining clinical and inflammatory data into a single OPLS-DA model (R^2Y 0.74, Q^2Y 0.50, $p < 0.001$)

performed better than those detailed above with metabolic data and better than the inflammatory

data used alone (R^2Y 0.76, Q^2Y 0.27, $p=0.14$) for this patient group. The features contributing most to this combined model can be seen in table 6.9. The model was similar, although not quite as good, as that using only the clinical data (R^2Y 0.69, Q^2Y 0.52, $p<0.001$).

6.5.3.2.3 Clinical, Metabonomic and Inflammatory Data

Combining all three data types into a single OPLS-DA model performed only as well as the metabolic data alone (R^2Y 0.94, Q^2Y 0.16, $p=0.44$). If integrals of the metabolites were used instead of the whole spectra the model was better (R^2Y 0.82, Q^2Y 0.4, $p=0.03$) and could be improved further by taking either those features with a VIP greater than 1.0 (R^2Y 0.70, Q^2Y 0.56, $p<0.001$) or with VIP greater than 2.0 (R^2Y 0.72, Q^2Y 0.68, $p<0.001$), figure 6.6. The features that made up the last of these models can be seen in table 6.10.

This model could only be improved upon by using the full metabolic spectra when only metabolites with VIP greater than 2.0 were used (R^2Y 0.94, Q^2Y 0.73, $p<0.001$), figure 6.7. This model had the same features as that in table 6.10 with the addition of maximum and minimum PEEP, Highest $PaO_2:FiO_2$, IP-10, IL-17A, IL-13, IL-12p70, ICAM-1, highest systolic blood pressure, minimum FiO_2 and maximum expiratory tidal volume. However, within the metabolic component of this model were areas of the spectrum that corresponded to the baseline and not specific metabolic features. This was not improved by taking $VIP>2.5$.

Table 6.9. Variables with VIP>1.0 in the OPLS-DA model (R^2Y 0.74, Q^2Y 0.50, $p<0.001$) combining inflammatory and clinical data comparing patients with VAP and brain injuries before infection developed. Clinical variables are in black and inflammatory variables blue.

Variables Increased in VAP			Variables Decreased in VAP		
Variable	VIP	Direction of Change in VAP	Variable	VIP	Direction of Change in VAP
Lowest ALP	2.50	↑	Highest SpO ₂ :FiO ₂ ratio	1.83	↓
Highest ALP	2.46	↑	Lowest PaO ₂ :FiO ₂ ratio	1.82	↓
Highest Expiratory Minute Volume	2.45	↑	Lowest SpO ₂	1.75	↓
Lowest Fibrinogen	2.37	↑	Highest Albumin	1.55	↓
Highest Fibrinogen	2.29	↑	Highest PaO ₂ :FiO ₂ ratio	1.43	↓
FiO ₂ to give highest SpO ₂	1.96	↑	Lowest Albumin	1.42	↓
Total Secretions	1.92	↑	Lowest PaO ₂	1.19	↓
TNF α	1.91	↑	Lowest SpO ₂ :FiO ₂ ratio	1.17	↓
Highest Respiratory Rate	1.87	↑	Highest PaO ₂	1.03	↓
Lowest Expiratory Minute Volume	1.84	↑			
Lowest ALT	1.82	↑			
Lowest Respiratory Rate	1.82	↑			
Highest ALT	1.79	↑			
Lowest Urea	1.73	↑			
Highest Peak Airway Pressure	1.73	↑			
Highest Expiratory Tidal Volume	1.66	↑			
Lowest FiO ₂	1.64	↑			
Lowest CRP	1.61	↑			
Highest PEEP	1.55	↑			
ICAM-1	1.53	↑			
IP-10	1.52	↑			
Highest Systolic Blood Pressure	1.52	↑			
IL-13	1.48	↑			
IL-12p70	1.47	↑			
Highest Urea	1.47	↑			
IL-17A	1.47	↑			
Highest CRP	1.40	↑			
Lowest PEEP	1.39	↑			
IFN γ	1.25	↑			
FiO ₂ to give lowest PaO ₂	1.20	↑			
LTC4	1.16	↑			
Lowest Bilirubin	1.14	↑			
Highest Inspired Tidal Volume	1.12	↑			
Lowest Magnesium	1.08	↑			
IL-1 β	1.05	↑			
FiO ₂ to give lowest SpO ₂	1.02	↑			
Highest Central Venous Pressure	1.02	↑			
Highest Mean Arterial Pressure	1.01	↑			

Figure 6.6. OPLS-DA model with one component comparing patients admitted with brain injuries, blue bars, to those with VAP, green bars, based on clinical data, inflammatory data and integrals of metabolic spectral features using only variables with a $VIP > 2.0$. (R^2Y 0.72, Q^2Y 0.68, $p < 0.001$) a. before and b. after cross validation. VAP cases can be seen to separate in a positive direction along the first component, there is little change after cross validation.

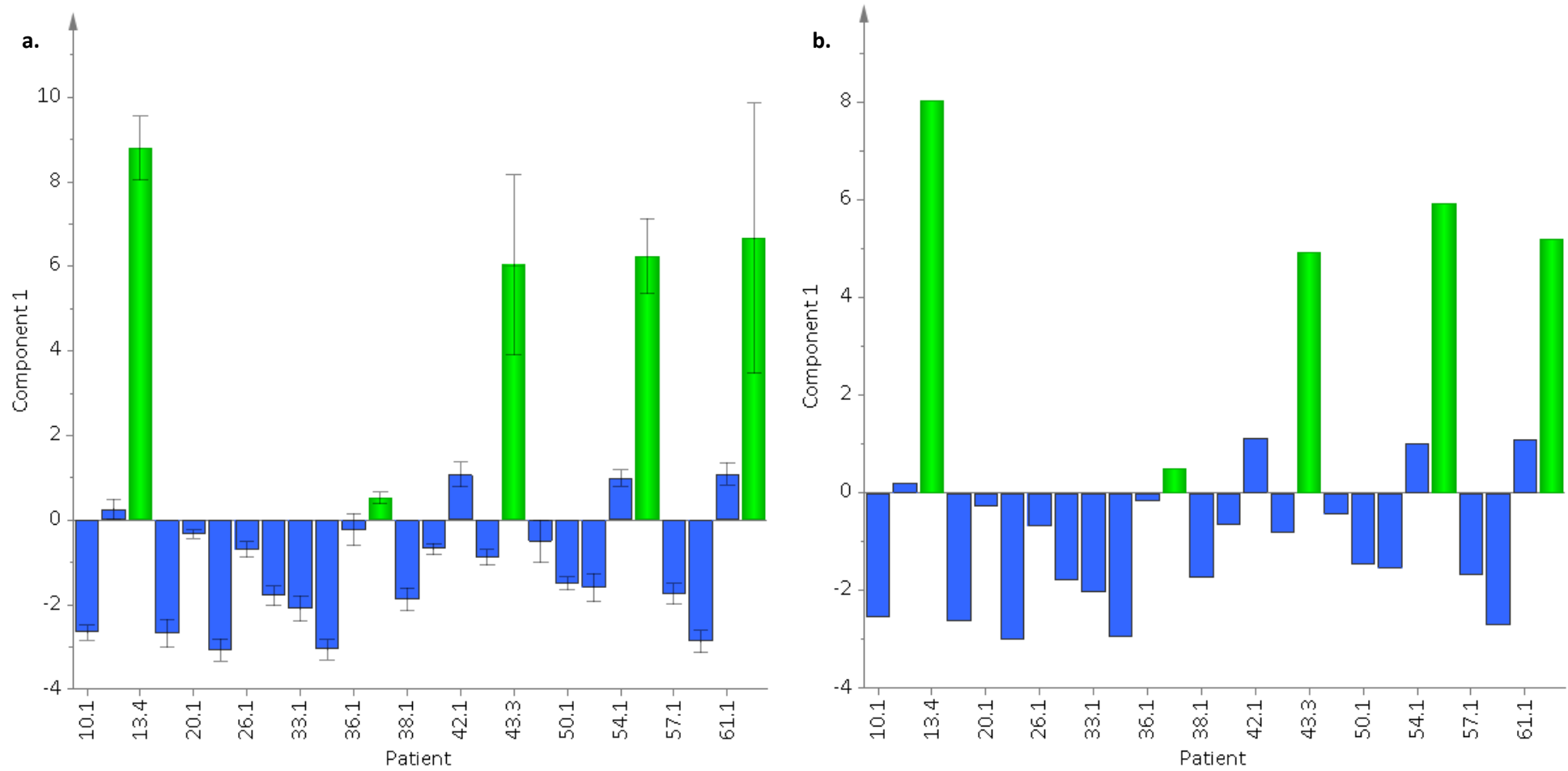


Figure 6.7. OPLS-DA model with one component and one orthogonal component comparing patients admitted with brain injuries, blue circles, to those with VAP, green triangles, based on clinical data, inflammatory data and full metabolic spectral features using only variables with a $VIP > 2.0$. (R^2Y 0.94, Q^2Y 0.73, $p < 0.001$) a. before and b. after cross validation. VAP cases can be seen to separate along the first component and after cross validation this separation remains good.

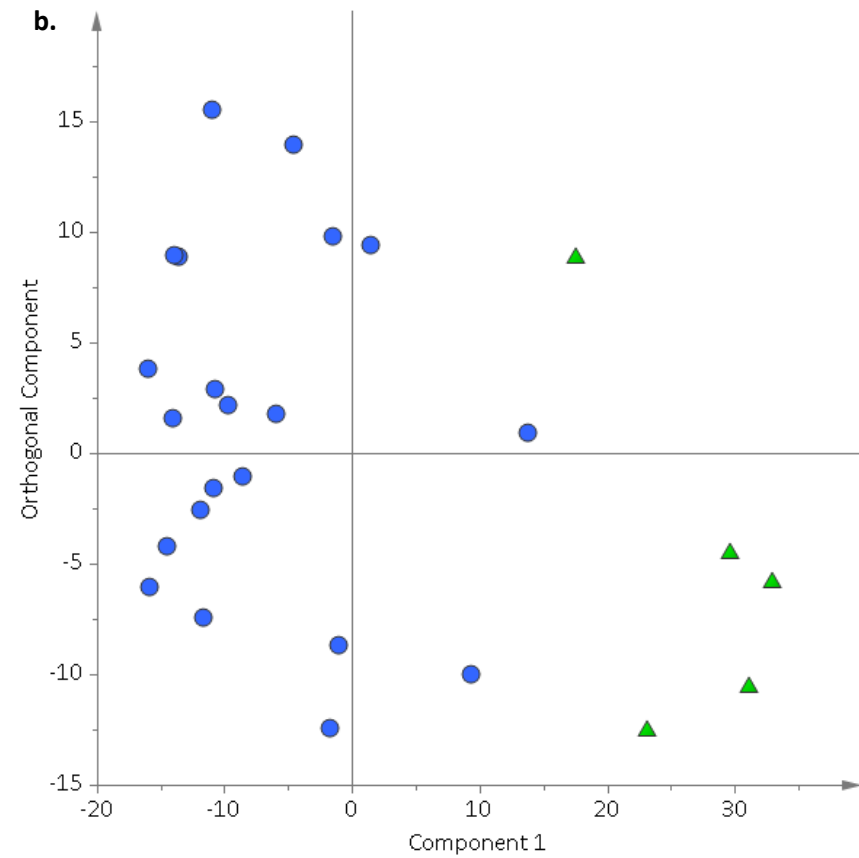
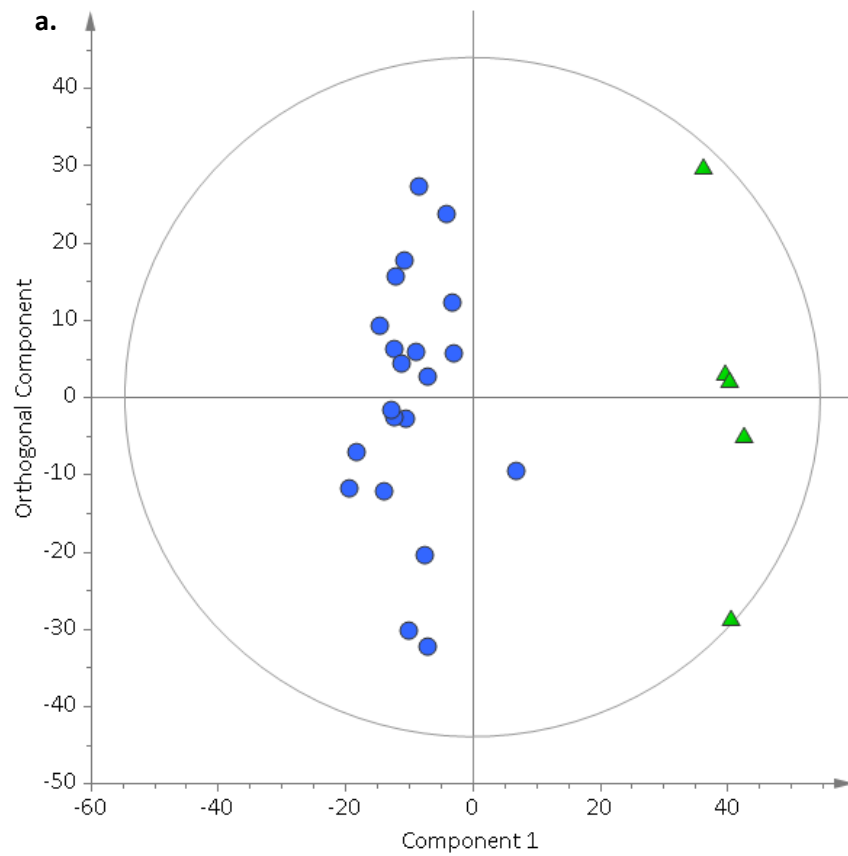


Table 6.10. Features comprising an OPLS-DA model (R^2Y 0.72, Q^2Y 0.68, $p < 0.001$) comparing patients with brain injuries to those with VAP using only features with $VIP > 2.0$, combining clinical, inflammatory and integrals of metabolic data. Clinical variables are in black, metabolic variables in red and inflammatory variables blue.

Variable
Lowest ALP
Highest ALP
Lowest Fibrinogen
Highest Expiratory Minute Volume
Highest Fibrinogen
Phenylalanine (7.446-7.404)
FiO ₂ to give highest SpO ₂
Lowest ALT
Total Secretions
TNF α
Highest ALT
Highest Respiratory Rate
Lowest Expiratory Minute Volume
Highest SpO ₂ :FiO ₂ ratio
Lowest Respiratory Rate
Lowest PaO ₂ :FiO ₂ ratio
Unknown (2.063-2.057)
Lowest SpO ₂
Highest Peak Airway Pressure

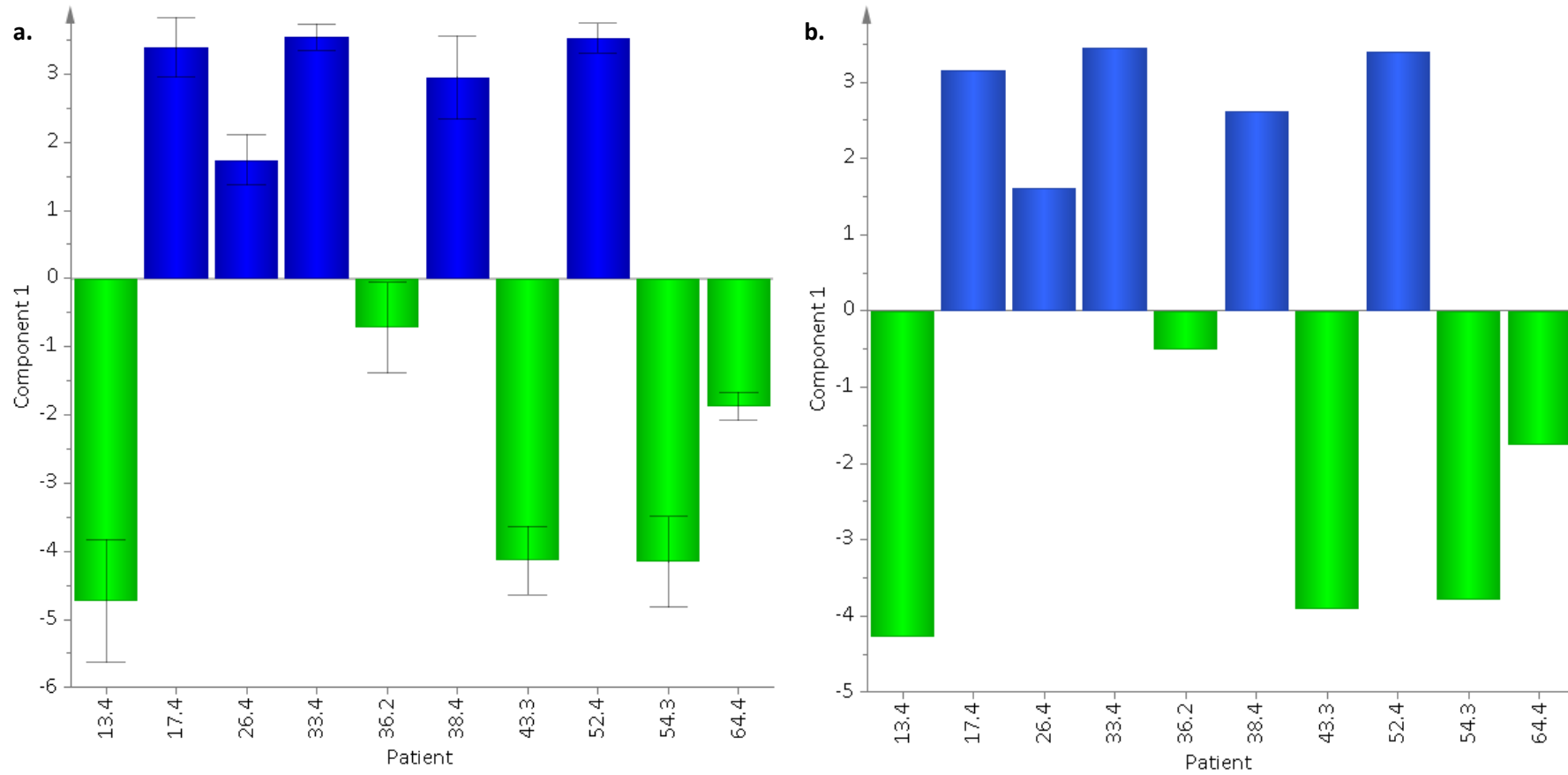
When the patients with VAP were compared to those with brain injuries who did not develop infection, but spent a similar time on ICU, combining clinical with metabolic data and combining all data types failed to produce OPLS-DA models with any predictive capacity with negative Q^2 in all cases. Combining clinical and Inflammatory data (R^2Y 0.88, Q^2Y 0.55, $p=0.07$) produced a model that was similar to that with clinical data alone, however, using only the inflammatory data for this group of patients produced a more predictive model (R^2Y 0.98, Q^2Y 0.56, $p=0.31$). Combining clinical data and metabolite integrals (R^2Y 0.86, Q^2Y 0.18, $p=0.9$) and using all data with metabolite integrals (R^2Y 0.69 Q^2Y 0.16, $p=0.59$) generated predictive models, although, not as good as those with only inflammatory data. The most predictive model was made when all data were combined using metabolite integrals selecting those features with $VIP > 2.0$, figure 6.8, (R^2Y 0.87, Q^2Y 0.84, $p=0.001$). The features that were important in this model can be seen in table 6.11. Many of the variables used

in this model represented oxygenation so the model was reconstructed only using the one with the highest VIP, the lowest PaO₂:FiO₂ ratio, the other markers of oxygenation and the duplicate CRP value with the lowest VIP were omitted. When this was performed the model (R²Y 0.92, Q²Y 0.86, p=0.001) performed similarly.

Table 6.11. Features used in an OPLS-DA model (R²Y 0.87, Q²Y 0.84, p=0.001) comparing patients with VAP to those with brain injuries without infection at a similar time point to that when VAP developed. Using a combination of clinical, inflammatory and metabolite integral data but only selecting features with VIP>2.0. Clinical variables are in black, metabolic variables in red and inflammatory variables blue.

Variable
Lowest PaO ₂ :FiO ₂ ratio
IL-6
Highest SpO ₂ :FiO ₂ ratio
Lowest SpO ₂ :FiO ₂ ratio
MCP-1
IL-12p70
Lowest FiO ₂
Highest FiO ₂
5,6-DHET
FiO ₂ to give highest SpO ₂
IFN γ
FiO ₂ to give highest PaO ₂
Highest PaO ₂ :FiO ₂ ratio
Lowest CRP
Highest CRP
FiO ₂ to give lowest PaO ₂
Unknown (6.938-6.911)

Figure 6.8. OPLS-DA model with one component comparing patients admitted with brain injuries without infection at time point 4, blue bars, to those with VAP, green bars, based on clinical data, inflammatory data and metabolic integrals using only variables with a $VIP > 2.0$ (R^2Y 0.87, Q^2Y 0.84, $p=0.001$). a. before and b. after cross validation. VAP cases can be seen to separate along the first component and after cross validation this separation remains good.



6.6 Discussion

This chapter focused on the application of multivariate analysis in the form of PCA and OPLS-DA to clinical data and the combination of clinical data with metabonomic and inflammatory data. Few attempts have been made previously to use these techniques with clinical data sets (344-346) and no studies exist using either data sets from patients on ICU or from those with pneumonia.

The use of multivariate techniques with clinical data produced both PCA and OPLS-DA models that were able to separate patients with brain injuries from those with either pneumonia or VAP. This was not entirely unexpected as some of the clinical data, oxygenation, secretions, temperature and white blood cell count were part of the CPIS that was used to define both VAP and pneumonia. However, even when these and closely related features were removed from the models they retained a great deal of their predictive capacity. The clinical variables that were important in the comparison of patients admitted with pneumonia or VAP to those with brain injuries were not the same. Comparing pneumonia to brain injury the features that were most important was the amount of PEEP which was highest in the pneumonia group and was likely to represent the difficulty with oxygenation that occurs with pneumonia. CRP was also higher in the pneumonia group as may be expected as CRP has previously been used as an aid to the diagnosis of this condition (22-25). Patients with pneumonia had higher airway pressures, respiratory rate, PaCO₂, and minute ventilation and lower pH and lowest expiratory tidal volume than those with brain injuries suggesting a greater difficulty with ventilation and CO₂ clearance in this group (348-350). All variables that reflected oxygen requirement for example, PaO₂:FiO₂ ratio, SpO₂:FiO₂ ratio and lowest PaO₂ demonstrated the greater degree of hypoxaemia in those with pneumonia as expected from both the natural history of the condition and the CPIS. Similarly white cell count and volume of secretions were predictably higher in those with pneumonia as expected as both are components of the CPIS. Of note temperature did not appear in the multivariate model comparing brain injury with

pneumonia, perhaps reflecting the disregulated temperature control that often occurs in brain injury. Of the other variables to appear important albumin levels were higher in those with brain injuries. Low albumin has previously been associated with poorer outcomes and worse severity with pneumonia (351-354) and may reflect the longer duration of disease, poorer nutritional status in patients with pneumonia or the effect on albumin of having a pro-inflammatory state such as infection, other pro-inflammatory conditions such as a surgical insult are known to lower albumin. Similarly haemoglobin levels were lower in those with pneumonia, although haematocrit was higher in this group, and may represent a combination of anaemia associated with a more prolonged disease and a degree of dehydration occurring in pneumonia. Anaemia (355, 356) with an increased red cell distribution width (357) has been associated with a complicated hospital course in those with pneumonia so it is not surprising that anaemic patients with pneumonia find themselves on ICU. Although there is no work looking at anaemia as a risk factor for pneumonia in adults it has been recognised as such in children in certain populations (358, 359) with anaemia being associated with two to five times the risk of pneumonia, potentially as a result of underlying iron deficiency in the majority of cases.

Fibrinogen levels were also found to be higher in those with pneumonia which likely reflects the way in which it acts as an acute phase reactant, activates pro-inflammatory processes (360, 361) by activating cytokines such as $\text{TNF}\alpha$ and $\text{IL-1}\beta$ and possibly has a role in promoting certain bacterial survival (362). However, other clotting features, prothrombin time and activated partial thromboplastin time, were found to be elevated in those with pneumonia suggesting that there may be either a predisposition to coagulopathy (363) in this group or that in the brain injury group there was more aggressive correction of coagulopathy due to the risk of bleeding. Tachycardia in those with pneumonia was a useful marker in building a model to separate pneumonia from brain injury and pneumonia patients had a higher level of consciousness than the brain injury cohort as may be expected either from the underlying pathology in the brain injury group rendering the patients

unconscious or because of the use of sedative drugs to ensure deep sedation, as a neuroprotective measure, in this group. Alkaline phosphatase and urea levels both had VIP scores of just over 1. Urea has previously been recognised as a marker of severity in pneumonia (364-366) and is likely to represent relative dehydration in this group of patients. The higher ALP in pneumonia patients is interesting as although it has not been specifically described in pneumonia, elevated ALP can be associated with sepsis (367-369) through sepsis induced cholestasis.

When brain injured patients were compared to those with VAP the pattern of clinical variables that were important in separating the two groups were quite different from those separating pneumonia from brain injuries. Although features representing the degree of hypoxaemia were important in the model, including the level of set PEEP, suggesting a greater degree of hypoxaemia in the VAP group, as would be expected, they were not the most important variables. The levels of ALP in the VAP patients were higher than in those admitted with brain injuries. The reason for this may be either because of sepsis related cholestasis (367-369) or that the VAP group had a greater time to be exposed to drugs increasing the chances of drug induced cholestasis and liver dysfunction, either of these explanations may also account for the appearance of bilirubin as a distinguishing variable in this model. Fibrinogen was again important in this model acting as an acute phase reactant (360, 361). Variables relating to higher tidal volumes, respiratory rates and minute ventilation were greater in the VAP group suggesting greater difficulty in CO₂ control. Secretion burden was greater in the VAP group, again as would be expected from the CPIS. Other than hypoxaemia and secretion burden the other features of the CPIS, temperature and white cell count, did not appear in the multivariate model implying that within this group these are not important features to differentiate VAP. Similar results have been reported previously in a group of brain injured patients (370).

Other features that formed the most important variables to differentiate VAP from brain injuries included albumin levels that were lower in those with VAP, probably representing the greater duration of ICU stay of these patients and their heightened catabolism. Similar to the ALP levels

alanine transaminase levels were also greater in the VAP group but were not as important in the model. High CRP was also a variable that played a part in identifying those with VAP, although not to such a degree as for pneumonia. CRP has previously been seen to have use in identifying VAP (92, 371) and to track its response to antibiotics and predict survival (372-374) although this has not always been the case and the importance of CRP has been controversial (370, 375). Urea was again seen to be higher in the VAP than brain injury group.

When VAP was compared with brain injury patients without infection who had spent a similar time on intensive care parameters associated with oxygenation dominated the model. However, the next most important variables were CRP as discussed above. In this model creatinine and sodium became important, with higher levels being present in those with VAP, implying a trend towards relatively higher rates of renal failure within those who developed VAP, this was also supported by the fact that urine output was lower in those with VAP. Within this model hourly fluid input and total fluid input over 24h were lower in those with VAP than in those with brain injuries which may have accounted for the other renal parameter trends. However, when the data were inspected the absolute sodium and creatinine levels were all within the normal range suggesting only a relative impairment in renal function, not one generally recognised as renal failure, but these may represent subtle changes occurring in those developing infection that may not be apparent to a bedside clinician. Again features suggesting greater difficulty with ventilation, including tidal volume, arterial PaCO₂, minute ventilation and peak airway pressure were higher in those with VAP implying a greater difficulty in achieving neuroprotective CO₂ targets in patients with VAP. Platelet count was higher in those who did not develop VAP but on closer inspection of the raw data this difference could be seen to reflect variations within the normal range for all participants except one of the patients without VAP whose result lay above the upper level of normal. This may reflect slight reduction of platelet count in the context of sepsis or the elevated platelet count in a single patient may reflect ongoing systemic inflammation as a response to intracerebral blood. The influence of

blood pressure measurements on the differentiation of VAP from those without infection was a little contradictory. The lowest recorded mean arterial and diastolic blood pressures were greater in those without VAP, which may represent the lack of sepsis in this group. However, highest recorded systolic pressures were higher in those with VAP. As with the model comparing VAP to patients with brain injuries at admission to ICU, ALP and bilirubin are higher in those with VAP than those without, although these features were not as important in constructing this model as in the other models. This added support to the idea that these results may represent cholestasis in the context of infection as opposed to results relating to duration of ICU stay, such as exposure to drugs. Results from the comparisons of those with VAP to other groups have to be interpreted with care as the small number of patients in this group meant that small changes in the variables of one patient potentially had a great impact on the models and variables' apparent importance. Also of note is that fact that in some of the models, especially when brain injured patients were compared to those with VAP, the number of patients in each group were unbalanced which may have had an impact on the statistical analysis.

Combining clinical data with data from the inflammasome was more straight forward than combining clinical data with metabonomic data. This was because the inflammatory data consisted of individually measured variables that could be considered as parameters similar to those laboratory variables contained within the clinical data set. However, combining clinical data with spectral metabolic data was more of a challenge. The metabonomic data set was made up of a continuum of variables with each metabolite being comprised of a collection of many data points. As little work has been done combining these two types of data before there was little precedent by which to proceed. In order to try to account for the potential problem that the sheer number of variables contained within the metabolic data may have saturated the data set, models were made using both the metabolic spectral data and a simpler data set using integrals of all the peaks in the spectral data. On the whole, similar metabolites were seen to be important with both methods.

However, the importance of lipids was under represented when integral data was used. This probably reflected the fact that several lipid species occupy similar spectral regions. Subtleties in the spectral waveform pattern could be elucidated, when the entire spectral data set was used, that represent changes in these different species. When only integrals were used these subtleties were lost and the lipids seemed to be unimportant. For example, a typical lipid peak may contain around 350 data points from the spectral data set whereas a metabolite such as formate only around 20, leading to lipids being over represented in the spectral data. Similarly when the integrals were used some metabolites that had previously not seemed important and thus not identified appeared prominent in the models, which may have reflected slight differences in alignment of the different spectra with some spectra having part of the metabolite missed in the integral region. Finally, when VIP scores of 1.0 or 2.0 were used as a threshold for important variables in combined models this method failed to be of value for the spectral data as several areas of baseline variation were detected as important, although baseline variation was not apparent when the spectra were examined manually this differences may suggest differences in the protein content of the two sample sets. This issue was solved by using a higher threshold of 2.5 for models with these data sets. Previously when metabolic data were used this problem was not identified as the spectral data, when analysed alone, could be displayed on the OPLS-DA regression co-efficient plots where the colour of the peaks represented the significance of the variable and in these cases baseline variation never appeared to be a problem. When the data sets were combined these figures could no longer be used as not all the data was spectral in nature.

Combining clinical data with either the metabolic or inflammatory data to compare pneumonia with brain injury at admission produced models that were better than models based on either of these 'omics' data sets alone although not quite as good as when only clinical data were used. This may be because the initial diagnosis of pneumonia was based firstly on clinicians' opinion and then refined using the CPIS. It may have been expected that the most predictive variables would be those that

the physician had access to when making their judgement. Importantly, however, even when variables that were related to the CPIS score were omitted from the models only a little predictive capacity was lost, similarly when the most important variables were examined for these models those from the CPIS were not the most important and some did not feature in these models at all.

When combining clinical and metabolic data both data types appeared important in the models to differentiate pneumonia from brain injuries, when the whole spectra were used important metabolites appeared similar to those identified in chapter 3 with lipid species, alanine, glycoproteins, phospholipids, phenylalanine and formate appearing important. Of these formate, glycoproteins, phospholipids and alanine were significantly different, after correction for the false discovery rate, when the metabolite integrals were compared using univariate methods. The clinical features were those described when clinical variables alone were used. When the inflammatory data set was combined with clinical variables, the clinical data dominated the models. The only inflammatory molecules that appeared important in the model were lipoxin B4, E-selectin, MCP-1, ICAM-1, IP-10, tetranor-PGDM and TNF- α , IL-13, which were higher in those with pneumonia and 6-keto-PGF1 α , 5,6-DHET, DHA, EPA, 10(S),17(S)-DiHDoHE and 9(S)-HODE in those with brain injuries. These were almost identical to the most important inflammatory mediators seen in chapter 4, with the exception of 13(S)HODE, which was previously seen to be useful in separating patients with pneumonia from those with brain injuries. In the model combining clinical and inflammatory data this substance only just missed out on being important with a VIP of 0.98. There was a slight difference in the order in which some of these inflammatory mediators appeared in the models between those made here and those constructed in chapter 4. This may reflect slight differences in the total number of patients included in the two chapters, as here only patients who had all three sets of clinical, metabolic and inflammatory data were used.

Combining all three data types failed to improve the model to a degree that outperformed using clinical data alone. The best model based on the Q^2Y from cross validation was that made using a combination of metabolic and clinical data using either the entire spectral data or the integrals of the peaks using only features with a $VIP > 2.0$. It is of note that inflammatory data were not involved in the best model. This may have been because many of these inflammatory mediators are known to have a transient role in the inflammatory processes in infection. The variable amount of time between patients with pneumonia becoming unwell and being admitted to ICU may have meant that this group of patients were captured at different stages in their inflammatory cascades, lessening the apparent importance of these markers. The factors that made up the best model made clinical sense. The important clinical variables were PEEP and $PaO_2:FiO_2$ ratio reflecting the increased difficulty in oxygenating patients with pneumonia, CRP as has been used previously as an aid to pneumonia diagnosis (22-25) indicating the inflammatory processes ongoing in this group and albumin which may be a marker of either the more prolonged duration of illness in patients with pneumonia prior to critical care admission, poorer nutritional status or an ongoing inflammatory process and maybe a marker of severity of disease (351-354). The metabolites that formed part of this model were lipid species which may reflect either a response to infection (269, 270) or risk factor for brain injury (276, 278) as described earlier. Alanine was again seen to be reduced in those with pneumonia as previously described (145, 281), potentially reflecting either alterations in nutritional status or release of amino-acids from muscle. Formate was once again seen to be higher in those with pneumonia than in those without as described in chapter 3 as were acetylated glycoproteins that may represent acute phase reactants, such as immunoglobulins, often raised in infection and inflammation (376). On validation with the independently classified patients this model performed well with sensitivity of 50%, specificity of 100%, positive predictive value of 100% and negative predictive value of 71%. This is similar, if not better than reports of the performance of

clinical variables (12, 13, 16-19), CRP and PCT (22-24) or radiographs (26, 27) to aid in the diagnosis of primary pneumonia.

When data sets were combined to compare VAP to brain injured patients combining clinical and metabolic data failed to perform as well as clinical data alone. However, a combination of clinical and inflammatory variables performed better than when clinical and metabolic data were combined and similarly to when only clinical data were used. This model contained a number of inflammatory mediators along with a similar pattern of clinical variables as described earlier. All of the most discriminant inflammatory mediators occurred in the VAP group and these included TNF α , ICAM-1, IP-10, IL-13, IL-12p70, IL-17A, INF γ , LTC4 and IL-1beta, as described in chapter 4, most of which are pro-inflammatory. The best model to distinguish patients with VAP from those with brain injuries at the start of ventilation was made when combining all three data types and taking variables with a VIP greater than 2.0. In this model clinical features appeared most important and were made up of ALP suggesting cholestasis, fibrinogen as an acute phase reactant, markers of oxygenation and ventilation and the burden of secretions as previously identified in the CPIS, metabolic data formed only a small component of this model with the only positively identified metabolites being part of phenylalanine, possibly representing changes in its metabolism in sepsis to activate the immune system or because of increased oxidative stress (282-284), phospholipids, acetyl groups of glycoproteins and some lipid species. Several inflammatory mediators formed part of this model with TNF α , a well-known mediator of inflammation, being the most important as has been noted before in pneumonia (163, 299). Other inflammatory mediators were predominantly cytokines including the chemotractant IP-10 and adhesion molecule ICAM-1 along with the interleukins IL-13, IL-12p70 and IL-17A, all of which have pro-inflammatory actions. IL-13 has been associated with airways inflammation. Interestingly several of these inflammatory mediators work synergistically supporting the fact that they are found to be important together. The fact that inflammatory mediators were much more important in this model than in the model comparing patients with

pneumonia at admission is interesting. This may be because the subtlety of the changes in the inflammasome are lost in the pneumonia cohort who present at different stages of their disease where as we were able to track the VAP patients, allowing sampling at more similar times during the disease process possibly meaning that their cytokine swings were more in alignment.

When patients with VAP were compared to brain injured patients without infection who had spent a similar amount of time on the intensive care unit several of the models were unable to differentiate the two groups which may reflect the small number of patients in each group. The best model was made using a combination of clinical, inflammatory and metabolic data where integrals of the metabolic spectra were used and only those variables with a VIP greater than 2.0 were selectively used. In this model metabolic data played only a very limited part with only a single, previously unidentified metabolite being important. The majority of variables in this model were clinical, mainly representing the worse oxygenation in those developing VAP, and higher CRP levels. A combination of cytokines and eicosanoids formed part of this model. IL-6, MCP-1, IL-12p70 and IFN γ were all higher in those with VAP compared to those without whilst 5,6-DHET was higher in those without. IL-6 is an important pro-inflammatory mediator in sepsis and has been seen to be higher in VAP (377) and pneumonia (298, 299) as has IFN γ (298).

The use of multivariate methods with clinical and combinations of clinical and 'omics' data showed promise in building models comparing patients with brain injuries to those with either pneumonia at admission or VAP. Combining clinical and 'omics' data may also have other advantages beyond improving diagnostics by helping to improve understanding of underlying mechanisms of disease and the interaction of metabonomics, inflammatory state and easily measured clinical parameters. However, there are several limitations to this study. Firstly there was some missing data within the clinical data set, which was not a problem with either the metabolic or inflammatory data sets. However, on the whole the rate of missing parameters was low. Where rates were higher it was usually because certain parameters were only applicable in some situations such as with some

modes of ventilation. Missing clinical data is unfortunately not uncommon in the clinical environment. It was decided to include all variables within the models, even those with a significant proportion of missing data. However, this may become problematic when the number of patients is very small. For example when the VAP group was examined there was one patient with VAP who did not have a set of laboratory tests sent during the 24h period of interest, it is possible that this missing data has a significant impact on the model when there are only five such patients in the group.

Another concern with clinical data is that it was recorded manually at the bedside and is therefore open to error or potential subjective assessment. All the bedside clinical data were recorded by hand on an hourly basis by the nurses caring for the patients. This meant that for each hour a single value for each parameter was taken to represent the clinical situation during that time. Inaccuracy could have occurred either if a non-representative value was chosen or if there was a transcription error. Further error may have then occurred where this data was transcribed onto the study data sheets where the minimum and maximum values for each variable were taken for each 24h period. To attempt to detect errors all the clinical data were inspected to find non-physiological values that would imply transcription error, very few of these were found suggesting a good rate of transcription accuracy.

Patients were selected for inclusion based on either clinical opinion or CPIS all of which are based on clinical data. It was therefore not entirely surprising that clinical data performs well in differentiating the groups. However, in the absence of a gold standard test to diagnose either pneumonia or VAP clinical features are all that were available by which to allocate groups. The fact that components of the CPIS were frequently either not present or not the most important variables in these models supports the validity of looking at the clinical data in this fashion. Similarly the fact that predictive models could be built even when CPIS components were omitted implies that other discriminant features exist in the data set than were initially used to define the groups.

Unlike either the metabolic or inflammatory data, clinical data has the added problem that many of the measured variables that make up the models also serve as targets or triggers for intervention that may not be the same for each group in question. Differentiating variables may then in fact represent confounding based on treatment targets and not genuine clinical differences. An example of this may be both blood pressure and arterial carbon dioxide tensions. Although vasopressors and inotropes would be routinely started to ensure adequate perfusion pressures in both brain injured and pneumonia patients, blood pressure targets may be higher in those with brain injuries where cerebral perfusion pressure needs to be maintained. Similarly, in patients with brain injuries tight carbon dioxide control is desirable to prevent exacerbation of cerebral injury this may lead to more aggressive ventilation strategies than may be used in those with pneumonia. It is conceivable that in both of these situations blood pressure, carbon dioxide or ventilation parameters may appear as differentiating factors in a model when in fact they are confounders brought about by the different clinical requirements of the two groups under investigation. In this data set, however, it seemed unlikely that confounding was a significant issue. Firstly, when the comparison of pneumonia and brain injuries was examined most of the variables that were important either make clinical sense, such as the predominance of features suggesting impaired oxygenation, or are laboratory tests that are not specifically manipulated such as albumin and CRP levels. Secondly, when the patients with VAP were used in comparisons they were compared to other patients with brain injuries where similar clinical targets would have been employed. Some features, however, were present in these models that could imply confounding. Firstly PEEP was an important feature when those with pneumonia were examined. This may be a result of the treating doctor being aware of radiological changes thus influencing their decision for a higher PEEP setting in an attempt to re-expand consolidated or collapsed lung and may not then be an independent predictor of pneumonia. Also higher carbon dioxide levels were seen in those with pneumonia which may represent a more relaxed carbon dioxide target as part of a long protective ventilation strategy in this group.

This data set was limited to only those clinical variables that were routinely recorded in the unit where these patients were recruited. It may be possible to build more predictive models by incorporating other clinical variables. For example, pro-calcitonin has been used as a diagnostic aid in both pneumonia (24, 25) and VAP (91, 93) and it is conceivable that an improved model could be made with its incorporation. In the models described here clinical data were confined to measureable, numerical variables. This meant that other potentially important variables such as secretion colour, radiograph appearances and microbiology data were omitted. The models may well be improved if these data could be incorporated.

Finally these models were made using a slightly smaller group of patients than had been used when either the metabolic or inflammatory data were examined alone as only those patients with all three sets of data were selected. However, it appears that the slightly reduced number of patients had little impact on the models as the features that were important using the inflammatory and metabolic data were relatively consistent between the models.

6.7 Conclusions

Using multivariate techniques, usually applied to 'omics' data sets, with clinical data showed promise in separating those with both pneumonia and those with VAP from those with brain injuries. The features found were not only those used to group the patients in the first place but other variables that may not have otherwise been thought of as discriminant. Combining clinical data with both metabolic and inflammatory data may have a greater ability to differentiate pneumonia and VAP from brain injured patients than using any one data set alone. This seems especially true when only the most important variables are used to construct the models.

7. FINAL CONCLUSIONS

Pneumonia is a common cause for admission to the critical care unit and development of VAP is the most common nosocomial infection occurring whilst patients are ventilated. Clinical features and laboratory tests lack sensitivity and specificity for this diagnosis and chest radiographs can be abnormal for a number of reasons other than infection. Although microbiological confirmation of infection is often sought, these results can take several days to return from the laboratory and are not able to distinguish infection from colonisation of the respiratory tract. Often patients with severe pneumonia are too unwell to undergo more invasive sampling techniques, such as bronchoscopy, which themselves are not without risks. The inability to make an accurate diagnosis of pneumonia and specifically VAP leads to both the under and over prescription of antibiotics both of which are associated with an increase in morbidity and mortality. New tests are required to improve the diagnosis of pneumonia in critically unwell patients and allow more targeted antibiotic therapy. This programme of study was an attempt to assess the potential of various profiling techniques applied to serum, urine and exhaled breath condensate to aid in the diagnosis of pneumonia in a prospectively recruited group of critically unwell patients.

Metabonomics, the study of global metabolic changes in the context of disease states, has been used in a number of clinical conditions with a range of biofluids, however, little work has been done previously focusing on either pneumonia or the critically ill. Application of $^1\text{H-NMR}$ spectroscopy to the serum of patients with pneumonia allowed them to be successfully distinguished from a similar cohort of ventilated patients admitted with brain injuries. The metabolites allowing these patients to be identified fell into four main classes: lipids, glycoproteins, amino acids and formate. Amino acid changes followed previously described patterns with alanine and glutamine being reduced (145, 148, 281) in those with infection and phenylalanine being increased (145, 148, 281). Explanations for such amino acid changes may be many. They may reflect changes in oxidative metabolism, nutritional

state, release from skeletal muscle or direct immune activation. The finding that formate was more abundant in those with pneumonia has not previously been described.

Glycoproteins are a non-specific class of molecule that include members of a range of mediator classes from hormones to antibodies and major histocompatibility complex molecules so their increase in those with pneumonia may have represented immune activation. However, to understand these changes more fully and understand the exact glycoproteins involved in class differentiation further targeted analysis would have to be performed. Lipid changes have been previously recognised in both infection (149, 265, 267, 269, 270) and brain injury (274-278) so it was unsurprising that there was a change in the balance of these species between the two groups in this study. However, NMR is unable to differentiate individual lipid species so further lipid identification was not possible.

In order to explore the role of both immune activation and one class of lipids, experiments were conducted to measure fatty acids and their metabolites, the eicosanoids, as well as a panel of cytokine and soluble adhesion molecules giving a panel of over fifty inflammatory mediators. Results from comparing inflammatory profiles showed that the use of a panel of eicosanoids was able to differentiate pneumonia from brain injury with a similar predictive capacity to that using an untargeted metabolomic approach. Cytokines alone performed less well but when cytokines and eicosanoids were combined predictive capacity was better. The overall pattern of inflammatory changes seen showed that the fatty acids and their metabolites were more abundant in those patients with brain injuries than pneumonia whereas the converse was true for cytokine species. Specifically arachidonic acid, eicosapentanoic acid, 6-keto-PGF1 α , 5,6-DHET, docosahexaenoic acid, 9(S)-HODE, 13(S)-HODE, 10(S),17(S)-DiHDoHE, and 5(S)-HETE were the most important species in those with brain injuries and ICAM-1, E-selectin, IP-10, MCP-1, IL-13, TNF α , INF γ and IL-6 in those with pneumonia. The greater levels of eicosanoids in those with brain injuries may have arisen as a

predisposition to brain injury in these patients (285, 286) or may have been a direct result from the injury (290-294) via mechanisms modulating cerebral circulation. It was perhaps not a surprise that cytokines were abundant in those with infection. The most important cytokines were those involved in chemoattraction and those recognised to play an active role in inflammation confirming the inflammatory nature of this group.

Unfortunately the application of metabonomic methods to both urine and exhaled breath condensate performed less well than serum. Metabolite presence in urine was much more heterogeneous from patient to patient than those in serum with a greater degree of peak misalignment. This made metabolite identification much more challenging. The patients in intensive care were subject to treatment with a large number of therapeutic drugs, with over 200 being documented across all recruits, many of which would be excreted either unchanged or as metabolites in the urine. This was compounded by the fact that drug metabolism would be altered depending on patient factors, such as enzyme activity, concomitant use of other drugs that may interact or alter metabolisms and potentially different disease states. This made detecting drugs within the urine difficult and raised the concern that many of the models that could differentiate clinical groups were in fact finding treatment differences and not genuine metabolic differences.

Exhaled breath condensate was an attractive biofluid to study as it originates directly from the site of infection, however, it posed its own challenges with the metabolites it contained being at very low concentrations. This meant that NMR had insufficient sensitivity to detect a large enough number of metabolites to allow statistical comparison. When a more sensitive MS based methodology was applied to these samples it was overly sensitive to both the effects of batch and impurities within the solvents used and thus the data required adjustment to attempt to limit these effects. Although models could be made that had some ability to differentiate pneumonia from brain injury they performed less well than those using metabolic and inflammatory profiling of serum.

When only those brain injured patients who did not go on to develop VAP were used as controls it became impossible to build a predictive model raising concerns over the validity of the original models. In order for EBC to be clinically useful much more work will need to be done, that was outside the scope of this project, to establish the best collection and analytical methods for this type of sample in this patient group. Technological advances, such as those being used to develop intelligent surgical instruments (378) that can analyse vapour in real time, may prove beneficial in improving the analysis of EBC. Once these technical issues are resolved this biofluid may still have potential to give useful diagnostic information for the critically ill, however, from the data presented here its use remains uncertain.

As clinical tests are rarely used in isolation and are usually combined with clinical data and clinical opinion the same multivariate techniques were applied to a large set of clinical data. As may be expected, for a diagnosis which is based predominantly on clinical features, the clinical data performed well when comparing pneumonia to brain injuries, even when components of the CPIS were removed. Many of the discriminating features were expected, including ventilation parameters such as PEEP, peak airway pressures and respiratory rate along with general markers of infection, such as CRP, and markers of nutritional state including albumin. When clinical data were combined with both metabolic and inflammatory data the best model (R^2 0.70, Q^2 0.68, $p < 0.001$) could be made by taking the fifteen most important features including minimum and maximum PEEP, minimum and maximum CRP, minimum and maximum albumin, glycoproteins, formate, minimum and maximum $PaO_2:FiO_2$ ratio, maximum Peak airway pressure, maximum respiratory rate and two unidentified metabolites. Of note this model only contained clinical and metabolic data, addition of inflammasome data were not able to improve classification.

Across all profiling methodologies prediction of brain injured patients developing VAP from other brain injured patients was more difficult than differentiating patients with pneumonia on admission.

There were a number of reasons to explain this. Firstly those admitted with pneumonia were likely to have been unwell for longer in the community prior to hospital admission having implications for their nutritional and inflammatory state. Also the number of patients developing VAP was small compared to both those with brain injuries and those admitted with pneumonia, making any changes potentially more difficult to detect. Finally it may be expected that the clinical difference between a patient with only pneumonia compared to one with only a brain injury may be much greater than that between one with both a brain injury and VAP and a brain injury alone and this may have been reflected in the limited differences in the inflammatory and metabolic profiles.

Serum metabolic data had only a weak ability to differentiate patients with VAP from those without and the metabolites that showed the most discriminant potential were similar to those when a primary diagnosis of pneumonia was considered with lipids, glycoproteins and phenylalanine showing a small amount of discriminant potential. When the inflammatory data were considered, eicosanoids showed no ability to differentiate VAP and cytokines only a weak ability. However, when these modalities were combined the predictive capacity improved, although still with a non-significant p-value, perhaps a reflection on the small number of patients involved. In this comparison important inflammatory mediators were again most abundant in the VAP patients, this time being a combination of the cytokines and soluble adhesion molecules. The differences between those with VAP and brain injuries were more pronounced, although again with a non-significant p-value, when samples were compared from similar time points. Most mediators were more abundant in those with VAP and included IL-6, MCP-1, IL-12p70, IFN γ , IL-17A, IFN α , IL-10, ICAM-1, G-CSF, IL-1beta, IP-10, TNF α , 12-oxo-LTB4 and lipoxin A4 demonstrating the inflammatory nature of pneumonia.

Clinical variables once again performed well to differentiate those with VAP from those with brain injuries, however, in this comparison some unsuspected clinical features including alkaline phosphatase, perhaps relating to cholestasis relating to sepsis (367-369), and fibrinogen, acting as an

acute phase reactant (360, 361), levels were important in those with VAP. The best models could be made to either distinguish VAP from brain injured patients at the start of ventilation (R^2 0.72, Q^2 0.68, $p < 0.001$) or VAP from brain injured patients who had spent a similar amount of time on intensive care (R^2 0.97, Q^2 0.89, $p = 0.014$) by combining clinical, metabolic and inflammatory data into a single model and selecting only the most important variables.

Sequential sampling of all of the enrolled patients allowed some interesting findings regarding the metabolic and inflammatory changes over time. Patients with brain injuries were seen to have a reduction in glucose and mannitol with an increase in phenylalanine and glycoproteins over the course of their ICU stay combined with a shift in the dominance of fatty acids at the first time point towards the metabolites of arachidonic acid, in the form of 5,6-DHET, 8,9-DHET and 14,15-DHET and 16(R)-HETE, 12(R)-HETE, 15(S)-HETE and 11(R)-HETE. Cytokine levels seemed generally to be at higher concentrations at the beginning of the ICU stay and fall over time with the exception of IL-13, IL-4, IL-1 β , TNF α and IP-10 levels which increased.

This study was limited by the relatively small numbers of patients included, especially when VAP was being considered. However, it would have been difficult in the time available to recruit many more patients from a single centre. Another limitation was the lack of a gold standard test by which to make a diagnosis of pneumonia or VAP. In attempt to address this we used a diagnosis based on CPIS scoring to allow a homogenous patient group with a limited amount of diagnostic bias from clinical opinion. Unfortunately two features of the CPIS were not routinely measured in our institution leading to some scores that were borderline. Patients with such scores were assessed by an independent assessor who was blinded to all other analysis and, where possible, these were used as a small validation group or to explore disease models in more detail. The use of bronchoalveolar lavage as a diagnostic tool was considered for this study, however, the fact that it is invasive, not routine practice in the critical care unit where the study was performed and not feasible to repeat

on a daily basis made CPIS scoring a more attractive daily screen for infection. The lack of a gold standard test meant that some of the patients identified as cases and controls may have been misclassified in the original groups prior to sample analysis adding bias to the multivariate models. Thus it was possible that the multivariate models could have had a better classification accuracy than the data used to define the groups. This study has only been able to separate those with pneumonia or VAP from controls with brain injuries, we have not been able to make any attempts to differentiate pneumonia from other types of infection or patients with acute lung injury, both frequent clinical problems.

Future work based on this study would involve replicating these findings in a larger cohort of patients, including a larger validation set and another patient group with infection of a non-pulmonary origin to establish if these techniques have the ability to distinguish pneumonia from other causes of sepsis. Further analytical work would include more detailed exploration of the serum metabolome with the use of MS methods to detect metabolites not seen with NMR and the application of lipidomic and proteomic methods to further identify the lipids and acetylated glycoproteins that appear important in identifying pneumonia patients. In order for these techniques to become useful clinical tests some adaption may need to be made to the modalities used for sample processing as, for example, NMR is not routinely available in the clinical setting. Once a robust panel of biomarkers is established it may be necessary to find other, more accessible, analytical platforms by which to measure them.

In summary this study has added to the field by demonstrating the potential of serum metabolic and inflammatory profiles to aid the diagnosis of pneumonia and VAP in intensive care patients especially when combined with clinical data.

8. REFERENCES

1. Niederman MS, McCombs JS, Unger AN, Kumar A, Popovian R. The cost of treating community-acquired pneumonia. *Clinical therapeutics*. 1998;20(4):820-37. Epub 1998/09/16.
2. Deaths Registered in England and Wales (Series DR), 2012: Office for National Statistics; 2013.
3. Strehlow MC, Emond SD, Shapiro NI, Pelletier AJ, Camargo CA, Jr. National study of emergency department visits for sepsis, 1992 to 2001. *Annals of emergency medicine*. 2006;48(3):326-31, 31 e1-3. Epub 2006/08/29.
4. Pneumonia: Diagnosis and Management of Community and Hospital Acquired Pneumonia in Adults: National Institute of Health and Care Excellence; 2014.
5. Mandell LA, Wunderink RG, Anzueto A, Bartlett JG, Campbell GD, Dean NC, et al. Infectious Diseases Society of America/American Thoracic Society consensus guidelines on the management of community-acquired pneumonia in adults. *Clinical infectious diseases : an official publication of the Infectious Diseases Society of America*. 2007;44 Suppl 2:S27-72. Epub 2007/02/06.
6. Simonetti AF, Viasus D, Garcia-Vidal C, Carratala J. Management of community-acquired pneumonia in older adults. *Therapeutic advances in infectious disease*. 2014;2(1):3-16. Epub 2014/08/29.
7. DiBardino DM, Wunderink RG. Aspiration pneumonia: A review of modern trends. *Journal of critical care*. 2015;30(1):40-8. Epub 2014/08/19.
8. Guest JF, Morris A. Community-acquired pneumonia: the annual cost to the National Health Service in the UK. *The European respiratory journal*. 1997;10(7):1530-4. Epub 1997/07/01.
9. Rodrigo C, McKeever TM, Woodhead M, Welham S, Lim WS. Admission via the emergency department in relation to mortality of adults hospitalised with community-acquired pneumonia: an analysis of the British Thoracic Society national community-acquired pneumonia audit. *Emergency medicine journal : EMJ*. 2015;32(1):55-9. Epub 2014/08/01.
10. Spoorenberg SM, Bos WJ, Heijligenberg R, Voorn PG, Grutters JC, Rijkers GT, et al. Microbial aetiology, outcomes, and costs of hospitalisation for community-acquired pneumonia; an observational analysis. *BMC infectious diseases*. 2014;14:335. Epub 2014/06/19.
11. Niederman MS, Mandell LA, Anzueto A, Bass JB, Broughton WA, Campbell GD, et al. Guidelines for the management of adults with community-acquired pneumonia. Diagnosis, assessment of severity, antimicrobial therapy, and prevention. *American journal of respiratory and critical care medicine*. 2001;163(7):1730-54. Epub 2001/06/13.
12. Rothrock SG, Green SM, Fanelli JM, Cruzen E, Costanzo KA, Pagane J. Do published guidelines predict pneumonia in children presenting to an urban ED? *Pediatric emergency care*. 2001;17(4):240-3. Epub 2001/08/09.

13. Lynch T, Platt R, Gouin S, Larson C, Patenaude Y. Can we predict which children with clinically suspected pneumonia will have the presence of focal infiltrates on chest radiographs? *Pediatrics*. 2004;113(3 Pt 1):e186-9. Epub 2004/03/03.
14. Gennis P, Gallagher J, Falvo C, Baker S, Than W. Clinical criteria for the detection of pneumonia in adults: guidelines for ordering chest roentgenograms in the emergency department. *The Journal of emergency medicine*. 1989;7(3):263-8. Epub 1989/05/01.
15. Metlay JP, Schulz R, Li YH, Singer DE, Marrie TJ, Coley CM, et al. Influence of age on symptoms at presentation in patients with community-acquired pneumonia. *Archives of internal medicine*. 1997;157(13):1453-9. Epub 1997/07/14.
16. McFadden JP, Price RC, Eastwood HD, Briggs RS. Raised respiratory rate in elderly patients: a valuable physical sign. *Br Med J (Clin Res Ed)*. 1982;284(6316):626-7. Epub 1982/02/27.
17. Emerman CL, Dawson N, Speroff T, Siciliano C, Effron D, Rashad F, et al. Comparison of physician judgment and decision aids for ordering chest radiographs for pneumonia in outpatients. *Annals of emergency medicine*. 1991;20(11):1215-9. Epub 1991/11/01.
18. Lieberman D, Shvartzman P, Korsonsky I. Diagnosis of ambulatory community-acquired pneumonia. Comparison of clinical assessment versus chest X-ray. *Scandinavian journal of primary health care*. 2003;21(1):57-60. Epub 2003/04/30.
19. van Vugt SF, Verheij TJ, de Jong PA, Butler CC, Hood K, Coenen S, et al. Diagnosing pneumonia in patients with acute cough: clinical judgment compared to chest radiography. *The European respiratory journal*. 2013;42(4):1076-82. Epub 2013/01/26.
20. Mehr DR, Binder EF, Kruse RL, Zweig SC, Madsen RW, D'Agostino RB. Clinical findings associated with radiographic pneumonia in nursing home residents. *The Journal of family practice*. 2001;50(11):931-7. Epub 2001/11/17.
21. Chandra A, Nicks B, Maniago E, Nouh A, Limkakeng A. A multicenter analysis of the ED diagnosis of pneumonia. *The American journal of emergency medicine*. 2010;28(8):862-5. Epub 2010/10/05.
22. Flanders SA, Stein J, Shochat G, Sellers K, Holland M, Maselli J, et al. Performance of a bedside C-reactive protein test in the diagnosis of community-acquired pneumonia in adults with acute cough. *The American journal of medicine*. 2004;116(8):529-35. Epub 2004/04/06.
23. Hopstaken RM, Muris JW, Knottnerus JA, Kester AD, Rinkens PE, Dinant GJ. Contributions of symptoms, signs, erythrocyte sedimentation rate, and C-reactive protein to a diagnosis of pneumonia in acute lower respiratory tract infection. *The British journal of general practice : the journal of the Royal College of General Practitioners*. 2003;53(490):358-64. Epub 2003/07/02.
24. Muller B, Harbarth S, Stolz D, Bingisser R, Mueller C, Leuppi J, et al. Diagnostic and prognostic accuracy of clinical and laboratory parameters in community-acquired pneumonia. *BMC infectious diseases*. 2007;7:10. Epub 2007/03/06.
25. Holm A, Pedersen SS, Nexoe J, Obel N, Nielsen LP, Koldkjaer O, et al. Procalcitonin versus C-reactive protein for predicting pneumonia in adults with lower respiratory tract infection in primary

care. *The British journal of general practice : the journal of the Royal College of General Practitioners*. 2007;57(540):555-60. Epub 2007/08/31.

26. Graffelman AW, Willemsen FE, Zonderland HM, Neven AK, Kroes AC, van den Broek PJ. Limited value of chest radiography in predicting aetiology of lower respiratory tract infection in general practice. *The British journal of general practice : the journal of the Royal College of General Practitioners*. 2008;58(547):93-7. Epub 2008/03/01.

27. Hagaman JT, Rouan GW, Shipley RT, Panos RJ. Admission chest radiograph lacks sensitivity in the diagnosis of community-acquired pneumonia. *The American journal of the medical sciences*. 2009;337(4):236-40. Epub 2009/04/15.

28. Guidelines for the management of adults with hospital-acquired, ventilator-associated, and healthcare-associated pneumonia. *Am J Respir Crit Care Med*. 2005;171(4):388-416. Epub 2005/02/09.

29. Chastre J, Fagon JY. Ventilator-associated pneumonia. *American journal of respiratory and critical care medicine*. 2002;165(7):867-903. Epub 2002/04/06.

30. Rello J, Sonora R, Jubert P, Artigas A, Rue M, Valles J. Pneumonia in intubated patients: role of respiratory airway care. *American journal of respiratory and critical care medicine*. 1996;154(1):111-5. Epub 1996/07/01.

31. Hospital-acquired pneumonia in adults: diagnosis, assessment of severity, initial antimicrobial therapy, and preventive strategies. A consensus statement, American Thoracic Society, November 1995. *American journal of respiratory and critical care medicine*. 1996;153(5):1711-25. Epub 1996/05/01.

32. Adair CG, Gorman SP, Feron BM, Byers LM, Jones DS, Goldsmith CE, et al. Implications of endotracheal tube biofilm for ventilator-associated pneumonia. *Intensive care medicine*. 1999;25(10):1072-6. Epub 1999/11/07.

33. Langer M, Mosconi P, Cigada M, Mandelli M. Long-term respiratory support and risk of pneumonia in critically ill patients. Intensive Care Unit Group of Infection Control. *The American review of respiratory disease*. 1989;140(2):302-5. Epub 1989/08/01.

34. Celis R, Torres A, Gatell JM, Almela M, Rodriguez-Roisin R, Agusti-Vidal A. Nosocomial pneumonia. A multivariate analysis of risk and prognosis. *Chest*. 1988;93(2):318-24. Epub 1988/02/01.

35. Langer M, Cigada M, Mandelli M, Mosconi P, Tognoni G. Early onset pneumonia: a multicenter study in intensive care units. *Intensive Care Med*. 1987;13(5):342-6. Epub 1987/01/01.

36. Fagon JY, Chastre J, Domart Y, Trouillet JL, Pierre J, Darne C, et al. Nosocomial pneumonia in patients receiving continuous mechanical ventilation. Prospective analysis of 52 episodes with use of a protected specimen brush and quantitative culture techniques. *The American review of respiratory disease*. 1989;139(4):877-84. Epub 1989/04/01.

37. Torres A, Aznar R, Gatell JM, Jimenez P, Gonzalez J, Ferrer A, et al. Incidence, risk, and prognosis factors of nosocomial pneumonia in mechanically ventilated patients. *The American review of respiratory disease*. 1990;142(3):523-8. Epub 1990/09/01.

38. Baker AM, Meredith JW, Haponik EF. Pneumonia in intubated trauma patients. Microbiology and outcomes. *American journal of respiratory and critical care medicine*. 1996;153(1):343-9. Epub 1996/01/01.
39. Long MN, Wickstrom G, Grimes A, Benton CF, Belcher B, Stamm AM. Prospective, randomized study of ventilator-associated pneumonia in patients with one versus three ventilator circuit changes per week. *Infection control and hospital epidemiology : the official journal of the Society of Hospital Epidemiologists of America*. 1996;17(1):14-9. Epub 1996/01/01.
40. Sirvent JM, Torres A, El-Ebiary M, Castro P, de Batlle J, Bonet A. Protective effect of intravenously administered cefuroxime against nosocomial pneumonia in patients with structural coma. *American journal of respiratory and critical care medicine*. 1997;155(5):1729-34. Epub 1997/05/01.
41. Cook DJ, Walter SD, Cook RJ, Griffith LE, Guyatt GH, Leasa D, et al. Incidence of and risk factors for ventilator-associated pneumonia in critically ill patients. *Annals of internal medicine*. 1998;129(6):433-40. Epub 1998/09/12.
42. Leal-Noval SR, Marquez-Vacaro JA, Garcia-Curiel A, Camacho-Larana P, Rincon-Ferrari MD, Ordonez-Fernandez A, et al. Nosocomial pneumonia in patients undergoing heart surgery. *Critical care medicine*. 2000;28(4):935-40. Epub 2000/05/16.
43. Rello J, Ollendorf DA, Oster G, Vera-Llonch M, Bellm L, Redman R, et al. Epidemiology and outcomes of ventilator-associated pneumonia in a large US database. *Chest*. 2002;122(6):2115-21. Epub 2002/12/12.
44. Bouza E, Perez A, Munoz P, Jesus Perez M, Rincon C, Sanchez C, et al. Ventilator-associated pneumonia after heart surgery: a prospective analysis and the value of surveillance. *Critical care medicine*. 2003;31(7):1964-70. Epub 2003/07/09.
45. Rosenthal VD, Guzman S, Orellano PW. Nosocomial infections in medical-surgical intensive care units in Argentina: attributable mortality and length of stay. *American journal of infection control*. 2003;31(5):291-5. Epub 2003/07/31.
46. Lizan-Garcia M, Peyro R, Cortina M, Crespo MD, Tobias A. Nosocomial infection surveillance in a surgical intensive care unit in Spain, 1996-2000: a time-trend analysis. *Infection control and hospital epidemiology : the official journal of the Society of Hospital Epidemiologists of America*. 2006;27(1):54-9. Epub 2006/01/19.
47. Joseph NM, Sistla S, Dutta TK, Badhe AS, Parija SC. Ventilator-associated pneumonia in a tertiary care hospital in India: incidence and risk factors. *J Infect Dev Ctries*. 2009;3(10):771-7. Epub 2009/12/17.
48. Chastre J, Trouillet JL, Vuagnat A, Joly-Guillou ML, Clavier H, Dombret MC, et al. Nosocomial pneumonia in patients with acute respiratory distress syndrome. *Am J Respir Crit Care Med*. 1998;157(4 Pt 1):1165-72. Epub 1998/05/01.
49. Delclaux C, Roupie E, Blot F, Brochard L, Lemaire F, Brun-Buisson C. Lower respiratory tract colonization and infection during severe acute respiratory distress syndrome: incidence and diagnosis. *Am J Respir Crit Care Med*. 1997;156(4 Pt 1):1092-8. Epub 1997/11/14.

50. Markowicz P, Wolff M, Djedaini K, Cohen Y, Chastre J, Delclaux C, et al. Multicenter prospective study of ventilator-associated pneumonia during acute respiratory distress syndrome. Incidence, prognosis, and risk factors. ARDS Study Group. *Am J Respir Crit Care Med.* 2000;161(6):1942-8. Epub 2000/06/14.
51. Cunnion KM, Weber DJ, Broadhead WE, Hanson LC, Pieper CF, Rutala WA. Risk factors for nosocomial pneumonia: comparing adult critical-care populations. *American journal of respiratory and critical care medicine.* 1996;153(1):158-62. Epub 1996/01/01.
52. Rello J, Diaz E, Roque M, Valles J. Risk factors for developing pneumonia within 48 hours of intubation. *American journal of respiratory and critical care medicine.* 1999;159(6):1742-6. Epub 1999/06/03.
53. Chevret S, Hemmer M, Carlet J, Langer M. Incidence and risk factors of pneumonia acquired in intensive care units. Results from a multicenter prospective study on 996 patients. European Cooperative Group on Nosocomial Pneumonia. *Intensive care medicine.* 1993;19(5):256-64. Epub 1993/01/01.
54. Kollef MH, Von Harz B, Prentice D, Shapiro SD, Silver P, St John R, et al. Patient transport from intensive care increases the risk of developing ventilator-associated pneumonia. *Chest.* 1997;112(3):765-73. Epub 1997/10/07.
55. Rello J, Ausina V, Ricart M, Puzo C, Quintana E, Net A, et al. Risk factors for infection by *Pseudomonas aeruginosa* in patients with ventilator-associated pneumonia. *Intensive care medicine.* 1994;20(3):193-8. Epub 1994/01/01.
56. Erbay RH, Yalcin AN, Zencir M, Serin S, Atalay H. Costs and risk factors for ventilator-associated pneumonia in a Turkish university hospital's intensive care unit: a case-control study. *BMC pulmonary medicine.* 2004;4:3. Epub 2004/04/28.
57. Kollef MH, Wragge T, Pasque C. Determinants of mortality and multiorgan dysfunction in cardiac surgery patients requiring prolonged mechanical ventilation. *Chest.* 1995;107(5):1395-401. Epub 1995/05/01.
58. Donowitz LG, Page MC, Mileur BL, Guenther SH. Alteration of normal gastric flora in critical care patients receiving antacid and cimetidine therapy. *Infection control : IC.* 1986;7(1):23-6. Epub 1986/01/01.
59. Messori A, Trippoli S, Vaiani M, Gorini M, Corrado A. Bleeding and pneumonia in intensive care patients given ranitidine and sucralfate for prevention of stress ulcer: meta-analysis of randomised controlled trials. *BMJ.* 2000;321(7269):1103-6. Epub 2000/11/04.
60. Drakulovic MB, Torres A, Bauer TT, Nicolas JM, Nogue S, Ferrer M. Supine body position as a risk factor for nosocomial pneumonia in mechanically ventilated patients: a randomised trial. *Lancet.* 1999;354(9193):1851-8. Epub 1999/12/10.
61. Torres A, Gatell JM, Aznar E, el-Ebiary M, Puig de la Bellacasa J, Gonzalez J, et al. Re-intubation increases the risk of nosocomial pneumonia in patients needing mechanical ventilation. *American journal of respiratory and critical care medicine.* 1995;152(1):137-41. Epub 1995/07/01.

62. Terragni PP, Antonelli M, Fumagalli R, Faggiano C, Berardino M, Pallavicini FB, et al. Early vs late tracheotomy for prevention of pneumonia in mechanically ventilated adult ICU patients: a randomized controlled trial. *JAMA : the journal of the American Medical Association*. 2010;303(15):1483-9. Epub 2010/04/22.
63. Gomes Silva BN, Andriolo RB, Saconato H, Atallah AN, Valente O. Early versus late tracheostomy for critically ill patients. *Cochrane Database Syst Rev*. 2012;3:CD007271. Epub 2012/03/16.
64. Rello J, Ausina V, Ricart M, Castella J, Prats G. Impact of previous antimicrobial therapy on the etiology and outcome of ventilator-associated pneumonia. *Chest*. 1993;104(4):1230-5. Epub 1993/10/01.
65. Spencer RC. Predominant pathogens found in the European Prevalence of Infection in Intensive Care Study. *European journal of clinical microbiology & infectious diseases : official publication of the European Society of Clinical Microbiology*. 1996;15(4):281-5. Epub 1996/04/01.
66. Rello J, Ricart M, Ausina V, Net A, Prats G. Pneumonia due to *Haemophilus influenzae* among mechanically ventilated patients. Incidence, outcome, and risk factors. *Chest*. 1992;102(5):1562-5. Epub 1992/11/01.
67. Vanhems P, Lepape A, Savey A, Jambou P, Fabry J. Nosocomial pulmonary infection by antimicrobial-resistant bacteria of patients hospitalized in intensive care units: risk factors and survival. *The Journal of hospital infection*. 2000;45(2):98-106. Epub 2000/06/22.
68. Rello J, Torres A, Ricart M, Valles J, Gonzalez J, Artigas A, et al. Ventilator-associated pneumonia by *Staphylococcus aureus*. Comparison of methicillin-resistant and methicillin-sensitive episodes. *American journal of respiratory and critical care medicine*. 1994;150(6 Pt 1):1545-9. Epub 1994/12/01.
69. Baraibar J, Correa H, Mariscal D, Gallego M, Valles J, Rello J. Risk factors for infection by *Acinetobacter baumannii* in intubated patients with nosocomial pneumonia. *Chest*. 1997;112(4):1050-4. Epub 1997/10/23.
70. Pinner RW, Haley RW, Blumenstein BA, Schaberg DR, Von Allmen SD, McGowan JE, Jr. High cost nosocomial infections. *Infection control : IC*. 1982;3(2):143-9. Epub 1982/03/01.
71. Beyt BE, Jr., Troxler S, Cavaness J. Prospective payment and infection control. *Infection control : IC*. 1985;6(4):161-4. Epub 1985/04/01.
72. Fagon JY, Chastre J, Hance AJ, Domart Y, Trouillet JL, Gibert C. Evaluation of clinical judgment in the identification and treatment of nosocomial pneumonia in ventilated patients. *Chest*. 1993;103(2):547-53. Epub 1993/02/01.
73. Fabregas N, Ewig S, Torres A, El-Ebiary M, Ramirez J, de La Bellacasa JP, et al. Clinical diagnosis of ventilator associated pneumonia revisited: comparative validation using immediate post-mortem lung biopsies. *Thorax*. 1999;54(10):867-73. Epub 1999/09/24.
74. Andrews CP, Coalson JJ, Smith JD, Johanson WG, Jr. Diagnosis of nosocomial bacterial pneumonia in acute, diffuse lung injury. *Chest*. 1981;80(3):254-8. Epub 1981/09/01.

75. Wunderink RG, Woldenberg LS, Zeiss J, Day CM, Ciemins J, Lacher DA. The radiologic diagnosis of autopsy-proven ventilator-associated pneumonia. *Chest*. 1992;101(2):458-63. Epub 1992/02/01.
76. Marquette CH, Copin MC, Wallet F, Nevriere R, Saulnier F, Mathieu D, et al. Diagnostic tests for pneumonia in ventilated patients: prospective evaluation of diagnostic accuracy using histology as a diagnostic gold standard. *American journal of respiratory and critical care medicine*. 1995;151(6):1878-88. Epub 1995/06/01.
77. Jourdain B, Novara A, Joly-Guillou ML, Dombret MC, Calvat S, Trouillet JL, et al. Role of quantitative cultures of endotracheal aspirates in the diagnosis of nosocomial pneumonia. *American journal of respiratory and critical care medicine*. 1995;152(1):241-6. Epub 1995/07/01.
78. el-Ebiary M, Torres A, Gonzalez J, de la Bellacasa JP, Garcia C, Jimenez de Anta MT, et al. Quantitative cultures of endotracheal aspirates for the diagnosis of ventilator-associated pneumonia. *The American review of respiratory disease*. 1993;148(6 Pt 1):1552-7. Epub 1993/12/01.
79. Sanchez-Nieto JM, Torres A, Garcia-Cordoba F, El-Ebiary M, Carrillo A, Ruiz J, et al. Impact of invasive and noninvasive quantitative culture sampling on outcome of ventilator-associated pneumonia: a pilot study. *American journal of respiratory and critical care medicine*. 1998;157(2):371-6. Epub 1998/02/26.
80. Heyland DK, Cook DJ, Marshall J, Heule M, Guslits B, Lang J, et al. The clinical utility of invasive diagnostic techniques in the setting of ventilator-associated pneumonia. *Canadian Critical Care Trials Group. Chest*. 1999;115(4):1076-84. Epub 1999/04/20.
81. Shorr AF, Sherner JH, Jackson WL, Kollef MH. Invasive approaches to the diagnosis of ventilator-associated pneumonia: a meta-analysis. *Critical care medicine*. 2005;33(1):46-53. Epub 2005/01/13.
82. Baselski VS, el-Torky M, Coalson JJ, Griffin JP. The standardization of criteria for processing and interpreting laboratory specimens in patients with suspected ventilator-associated pneumonia. *Chest*. 1992;102(5 Suppl 1):571S-9S. Epub 1992/11/01.
83. Pugin J, Auckenthaler R, Mili N, Janssens JP, Lew PD, Suter PM. Diagnosis of ventilator-associated pneumonia by bacteriologic analysis of bronchoscopic and nonbronchoscopic "blind" bronchoalveolar lavage fluid. *The American review of respiratory disease*. 1991;143(5 Pt 1):1121-9. Epub 1991/05/01.
84. Singh N, Rogers P, Atwood CW, Wagener MM, Yu VL. Short-course empiric antibiotic therapy for patients with pulmonary infiltrates in the intensive care unit. A proposed solution for indiscriminate antibiotic prescription. *American journal of respiratory and critical care medicine*. 2000;162(2 Pt 1):505-11. Epub 2000/08/10.
85. Fartoukh M, Maitre B, Honore S, Cerf C, Zahar JR, Brun-Buisson C. Diagnosing pneumonia during mechanical ventilation: the clinical pulmonary infection score revisited. *American journal of respiratory and critical care medicine*. 2003;168(2):173-9. Epub 2003/05/10.
86. Zilberberg MD, Shorr AF. Ventilator-associated pneumonia: the clinical pulmonary infection score as a surrogate for diagnostics and outcome. *Clinical infectious diseases : an official publication of the Infectious Diseases Society of America*. 2010;51 Suppl 1:S131-5. Epub 2010/07/06.

87. Anand NJ, Zuick S, Klesney-Tait J, Kollef MH. Diagnostic implications of soluble triggering receptor expressed on myeloid cells-1 in BAL fluid of patients with pulmonary infiltrates in the ICU. *Chest*. 2009;135(3):641-7. Epub 2008/10/14.
88. Oudhuis GJ, Beuving J, Bergmans D, Stobberingh EE, ten Velde G, Linssen CF, et al. Soluble Triggering Receptor Expressed on Myeloid cells-1 in bronchoalveolar lavage fluid is not predictive for ventilator-associated pneumonia. *Intensive care medicine*. 2009;35(7):1265-70. Epub 2009/04/04.
89. Horonenko G, Hoyt JC, Robbins RA, Singarajah CU, Umar A, Pattengill J, et al. Soluble triggering receptor expressed on myeloid cell-1 is increased in patients with ventilator-associated pneumonia: a preliminary report. *Chest*. 2007;132(1):58-63. Epub 2007/05/17.
90. Ramirez P, Garcia MA, Ferrer M, Aznar J, Valencia M, Sahuquillo JM, et al. Sequential measurements of procalcitonin levels in diagnosing ventilator-associated pneumonia. *The European respiratory journal : official journal of the European Society for Clinical Respiratory Physiology*. 2008;31(2):356-62. Epub 2007/10/26.
91. Oppert M, Reinicke A, Muller C, Barckow D, Frei U, Eckardt KU. Elevations in procalcitonin but not C-reactive protein are associated with pneumonia after cardiopulmonary resuscitation. *Resuscitation*. 2002;53(2):167-70. Epub 2002/05/16.
92. Pova P, Coelho L, Almeida E, Fernandes A, Mealha R, Moreira P, et al. C-reactive protein as a marker of infection in critically ill patients. *Clinical microbiology and infection : the official publication of the European Society of Clinical Microbiology and Infectious Diseases*. 2005;11(2):101-8. Epub 2005/02/01.
93. Schuetz P, Christ-Crain M, Thomann R, Falconnier C, Wolbers M, Widmer I, et al. Effect of procalcitonin-based guidelines vs standard guidelines on antibiotic use in lower respiratory tract infections: the ProHOSP randomized controlled trial. *JAMA : the journal of the American Medical Association*. 2009;302(10):1059-66. Epub 2009/09/10.
94. Kibe S, Adams K, Barlow G. Diagnostic and prognostic biomarkers of sepsis in critical care. *The Journal of antimicrobial chemotherapy*. 2011;66 Suppl 2:ii33-40. Epub 2011/03/16.
95. Holmes E, Wilson ID, Nicholson JK. Metabolic phenotyping in health and disease. *Cell*. 2008;134(5):714-7. Epub 2008/09/09.
96. Nicholson JK, Connelly J, Lindon JC, Holmes E. Metabonomics: a platform for studying drug toxicity and gene function. *Nat Rev Drug Discov*. 2002;1(2):153-61. Epub 2002/07/18.
97. Nicholson JK, Lindon JC. Systems biology - Metabonomics. *Nature*. 2008;455(7216):1054-6.
98. Beckonert O, Keun HC, Ebbels TM, Bundy J, Holmes E, Lindon JC, et al. Metabolic profiling, metabolomic and metabonomic procedures for NMR spectroscopy of urine, plasma, serum and tissue extracts. *Nat Protoc*. 2007;2(11):2692-703. Epub 2007/11/17.
99. Sofia M, Mascalco M, de Laurentiis G, Paris D, Melck D, Motta A. Exploring airway diseases by NMR-based metabonomics: a review of application to exhaled breath condensate. *J Biomed Biotechnol*. 2011;2011:403260. Epub 2011/03/26.

100. Cohen MJ, Serkova NJ, Wiener-Kronish J, Pittet JF, Niemann CU. ¹H-NMR-based metabolic signatures of clinical outcomes in trauma patients--beyond lactate and base deficit. *The Journal of trauma*. 2010;69(1):31-40. Epub 2010/07/14.
101. Mao H, Wang H, Wang B, Liu X, Gao H, Xu M, et al. Systemic metabolic changes of traumatic critically ill patients revealed by an NMR-based metabolomic approach. *Journal of proteome research*. 2009;8(12):5423-30. Epub 2009/10/20.
102. Sato E, Kohno M, Yamamoto M, Fujisawa T, Fujiwara K, Tanaka N. Metabolomic analysis of human plasma from haemodialysis patients. *Eur J Clin Invest*. 2011;41(3):241-55. Epub 2010/10/20.
103. Beger RD, Holland RD, Sun J, Schnackenberg LK, Moore PC, Dent CL, et al. Metabonomics of acute kidney injury in children after cardiac surgery. *Pediatr Nephrol*. 2008;23(6):977-84. Epub 2008/03/06.
104. Al-Ismaili Z, Palijan A, Zappitelli M. Biomarkers of acute kidney injury in children: discovery, evaluation, and clinical application. *Pediatr Nephrol*. 2011;26(1):29-40. Epub 2010/07/14.
105. Dunne VG, Bhattachayya S, Besser M, Rae C, Griffin JL. Metabolites from cerebrospinal fluid in aneurysmal subarachnoid haemorrhage correlate with vasospasm and clinical outcome: a pattern-recognition ¹H NMR study. *Nmr Biomed*. 2005;18(1):24-33. Epub 2004/09/30.
106. Stringer KA, Serkova NJ, Karnovsky A, Guire K, Paine R, 3rd, Standiford TJ. Metabolic consequences of sepsis-induced acute lung injury revealed by plasma (1)H-nuclear magnetic resonance quantitative metabolomics and computational analysis. *American journal of physiology Lung cellular and molecular physiology*. 2011;300(1):L4-L11. Epub 2010/10/05.
107. Hornak J. The Basics of NMR. Available from: <https://www.cis.rit.edu/htbooks/nmr/>.
108. Reusch W. Guide to NMR Spectroscopy. Available from: <http://www2.chemistry.msu.edu/faculty/reusch/VirtTxtJml/Spectrpy/nmr/nmr1.htm>.
109. Dumas ME, Maibaum EC, Teague C, Ueshima H, Zhou B, Lindon JC, et al. Assessment of analytical reproducibility of ¹H NMR spectroscopy based metabolomics for large-scale epidemiological research: the INTERMAP Study. *Analytical chemistry*. 2006;78(7):2199-208. Epub 2006/04/04.
110. Beckonert O, Keun HC, Ebbels TM, Bundy J, Holmes E, Lindon JC, et al. Metabolic profiling, metabolomic and metabolomic procedures for NMR spectroscopy of urine, plasma, serum and tissue extracts. *Nature protocols*. 2007;2(11):2692-703. Epub 2007/11/17.
111. Lenz EM, Wilson ID. Analytical strategies in metabolomics. *Journal of proteome research*. 2007;6(2):443-58. Epub 2007/02/03.
112. SIMCA-13 Manual Sweden: Umetrics; 2013.
113. Muller C, Dietz I, Tziotis D, Moritz F, Rupp J, Schmitt-Kopplin P. Molecular cartography in acute *Chlamydia pneumoniae* infections--a non-targeted metabolomics approach. *Analytical and bioanalytical chemistry*. 2013;405(15):5119-31. Epub 2013/01/29.

114. Gupta A, Dwivedi M, Gowda GA, Mahdi AA, Jain A, Ayyagari A, et al. ¹H NMR spectroscopy in the diagnosis of *Klebsiella pneumoniae*-induced urinary tract infection. *NMR in biomedicine*. 2006;19(8):1055-61. Epub 2006/08/24.
115. Antti H, Fahlgren A, Nasstrom E, Kouremenos K, Sundén-Cullberg J, Guo Y, et al. Metabolic profiling for detection of *Staphylococcus aureus* infection and antibiotic resistance. *PloS one*. 2013;8(2):e56971. Epub 2013/03/02.
116. Gupta A, Dwivedi M, Nagana Gowda GA, Ayyagari A, Mahdi AA, Bhandari M, et al. (¹H) NMR spectroscopy in the diagnosis of *Pseudomonas aeruginosa*-induced urinary tract infection. *NMR in biomedicine*. 2005;18(5):293-9. Epub 2005/03/11.
117. Bourne R, Himmelreich U, Sharma A, Mountford C, Sorrell T. Identification of *Enterococcus*, *Streptococcus*, and *Staphylococcus* by multivariate analysis of proton magnetic resonance spectroscopic data from plate cultures. *Journal of clinical microbiology*. 2001;39(8):2916-23. Epub 2001/07/28.
118. Himmelreich U, Somorjai RL, Dolenko B, Daniel HM, Sorrell TC. A rapid screening test to distinguish between *Candida albicans* and *Candida dubliniensis* using NMR spectroscopy. *FEMS microbiology letters*. 2005;251(2):327-32. Epub 2005/09/17.
119. Himmelreich U, Somorjai RL, Dolenko B, Lee OC, Daniel HM, Murray R, et al. Rapid identification of *Candida* species by using nuclear magnetic resonance spectroscopy and a statistical classification strategy. *Applied and environmental microbiology*. 2003;69(8):4566-74. Epub 2003/08/07.
120. Delpassand ES, Chari MV, Stager CE, Morrisett JD, Ford JJ, Romazi M. Rapid identification of common human pathogens by high-resolution proton magnetic resonance spectroscopy. *Journal of clinical microbiology*. 1995;33(5):1258-62. Epub 1995/05/01.
121. Hoerr V, Zbytniuk L, Leger C, Tam PP, Kubes P, Vogel HJ. Gram-negative and Gram-positive bacterial infections give rise to a different metabolic response in a mouse model. *Journal of proteome research*. 2012;11(6):3231-45. Epub 2012/04/10.
122. Fahrner R, Beyoglu D, Beldi G, Idle JR. Metabolomic markers for intestinal ischemia in a mouse model. *The Journal of surgical research*. 2012;178(2):879-87. Epub 2012/09/06.
123. Chen L, Fan J, Li Y, Shi X, Ju D, Yan Q, et al. Modified Jiu Wei Qiang Huo decoction improves dysfunctional metabolomics in influenza A pneumonia-infected mice. *Biomedical chromatography : BMC*. 2014;28(4):468-74. Epub 2013/10/18.
124. Shin JH, Yang JY, Jeon BY, Yoon YJ, Cho SN, Kang YH, et al. (¹H) NMR-based metabolomic profiling in mice infected with *Mycobacterium tuberculosis*. *Journal of proteome research*. 2011;10(5):2238-47. Epub 2011/04/02.
125. Antunes LC, Arena ET, Menendez A, Han J, Ferreira RB, Buckner MM, et al. Impact of salmonella infection on host hormone metabolism revealed by metabolomics. *Infection and immunity*. 2011;79(4):1759-69. Epub 2011/02/16.

126. Ghosh S, Sengupta A, Sharma S, Sonawat HM. Metabolic perturbations of kidney and spleen in murine cerebral malaria: (1)H NMR-based metabolomic study. *PloS one*. 2013;8(9):e73113. Epub 2013/09/17.
127. Xu PB, Lin ZY, Meng HB, Yan SK, Yang Y, Liu XR, et al. A metabonomic approach to early prognostic evaluation of experimental sepsis. *The Journal of infection*. 2008;56(6):474-81. Epub 2008/05/13.
128. Izquierdo-Garcia JL, Nin N, Ruiz-Cabello J, Rojas Y, de Paula M, Lopez-Cuenca S, et al. A metabolomic approach for diagnosis of experimental sepsis. *Intensive care medicine*. 2011. Epub 2011/10/07.
129. Lin ZY, Xu PB, Yan SK, Meng HB, Yang GJ, Dai WX, et al. A metabonomic approach to early prognostic evaluation of experimental sepsis by (1)H NMR and pattern recognition. *NMR in biomedicine*. 2009;22(6):601-8. Epub 2009/03/27.
130. Liu XR, Zheng XF, Ji SZ, Lv YH, Zheng DY, Xia ZF, et al. Metabolomic analysis of thermally injured and/or septic rats. *Burns : journal of the International Society for Burn Injuries*. 2010;36(7):992-8. Epub 2010/06/12.
131. Li Y, Liu H, Wu X, Li D, Huang J. An NMR metabolomics investigation of perturbations after treatment with Chinese herbal medicine formula in an experimental model of sepsis. *Omics : a journal of integrative biology*. 2013;17(5):252-8. Epub 2013/04/19.
132. Li Y, Hou M, Wang JG, Wang T, Wan J, Jiao BH, et al. Changes of lymph metabolites in a rat model of sepsis induced by cecal ligation and puncture. *The journal of trauma and acute care surgery*. 2012;73(6):1545-52. Epub 2012/11/14.
133. Steelman SM, Johnson P, Jackson A, Schulze J, Chowdhary BP. Serum metabolomics identifies citrulline as a predictor of adverse outcomes in an equine model of gut-derived sepsis. *Physiological genomics*. 2014;46(10):339-47. Epub 2014/03/13.
134. Langley RJ, Tipper JL, Bruse S, Baron RM, Tsalik EL, Huntley J, et al. Integrative "omic" analysis of experimental bacteremia identifies a metabolic signature that distinguishes human sepsis from systemic inflammatory response syndromes. *American journal of respiratory and critical care medicine*. 2014;190(4):445-55. Epub 2014/07/24.
135. Kamisoglu K, Sleight KE, Calvano SE, Coyle SM, Corbett SA, Androulakis IP. Temporal metabolic profiling of plasma during endotoxemia in humans. *Shock*. 2013;40(6):519-26. Epub 2013/10/04.
136. Lam CW, Law CY, To KK, Cheung SK, Lee KC, Sze KH, et al. NMR-based metabolomic urinalysis: a rapid screening test for urinary tract infection. *Clinica chimica acta; international journal of clinical chemistry*. 2014;436:217-23. Epub 2014/06/10.
137. Lam CW, Law CY, Sze KH, To KK. Quantitative metabolomics of urine for rapid etiological diagnosis of urinary tract infection: evaluation of a microbial-mammalian co-metabolite as a diagnostic biomarker. *Clinica chimica acta; international journal of clinical chemistry*. 2015;438:24-8. Epub 2014/08/12.

138. Gupta A, Dwivedi M, Mahdi AA, Khetrpal CL, Bhandari M. Broad identification of bacterial type in urinary tract infection using (1)h NMR spectroscopy. *Journal of proteome research*. 2012;11(3):1844-54. Epub 2012/02/02.
139. Gupta A, Dwivedi M, Mahdi AA, Gowda GA, Khetrpal CL, Bhandari M. 1H-nuclear magnetic resonance spectroscopy for identifying and quantifying common uropathogens: a metabolic approach to the urinary tract infection. *BJU international*. 2009;104(2):236-44. Epub 2009/02/26.
140. Nevedomskaya E, Pacchiarotta T, Artemov A, Meissner A, van Nieuwkoop C, van Dissel JT, et al. (1)H NMR-based metabolic profiling of urinary tract infection: combining multiple statistical models and clinical data. *Metabolomics : Official journal of the Metabolomic Society*. 2012;8(6):1227-35. Epub 2012/11/09.
141. Al-Mubarak R, Vander Heiden J, Broeckling CD, Balagon M, Brennan PJ, Vissa VD. Serum metabolomics reveals higher levels of polyunsaturated fatty acids in lepromatous leprosy: potential markers for susceptibility and pathogenesis. *PLoS neglected tropical diseases*. 2011;5(9):e1303. Epub 2011/09/13.
142. Coen M, O'Sullivan M, Bubb WA, Kuchel PW, Sorrell T. Proton nuclear magnetic resonance-based metabolomics for rapid diagnosis of meningitis and ventriculitis. *Clinical infectious diseases : an official publication of the Infectious Diseases Society of America*. 2005;41(11):1582-90. Epub 2005/11/04.
143. Su L, Huang Y, Zhu Y, Xia L, Wang R, Xiao K, et al. Discrimination of sepsis stage metabolic profiles with an LC/MS-MS-based metabolomics approach. *BMJ open respiratory research*. 2014;1(1):e000056. Epub 2015/01/02.
144. Langley RJ, Tsalik EL, van Velkinburgh JC, Glickman SW, Rice BJ, Wang C, et al. An integrated clinico-metabolomic model improves prediction of death in sepsis. *Science translational medicine*. 2013;5(195):195ra95. Epub 2013/07/26.
145. Mickiewicz B, Duggan GE, Winston BW, Doig C, Kubes P, Vogel HJ. Metabolic profiling of serum samples by 1H nuclear magnetic resonance spectroscopy as a potential diagnostic approach for septic shock. *Critical care medicine*. 2014;42(5):1140-9. Epub 2013/12/26.
146. Schmerler D, Neugebauer S, Ludewig K, Bremer-Streck S, Brunkhorst FM, Kiehntopf M. Targeted metabolomics for discrimination of systemic inflammatory disorders in critically ill patients. *Journal of lipid research*. 2012;53(7):1369-75. Epub 2012/05/15.
147. Fanos V, Caboni P, Corsello G, Stronati M, Gazzolo D, Noto A, et al. Urinary (1)H-NMR and GC-MS metabolomics predicts early and late onset neonatal sepsis. *Early human development*. 2014;90 Suppl 1:S78-83. Epub 2014/04/09.
148. Mickiewicz B, Vogel HJ, Wong HR, Winston BW. Metabolomics as a novel approach for early diagnosis of pediatric septic shock and its mortality. *American journal of respiratory and critical care medicine*. 2013;187(9):967-76. Epub 2013/03/09.
149. Dong F, Wang B, Zhang L, Tang H, Li J, Wang Y. Metabolic response to *Klebsiella pneumoniae* infection in an experimental rat model. *PloS one*. 2012;7(11):e51060. Epub 2012/12/12.

150. Slupsky CM, Cheyesh A, Chao DV, Fu H, Rankin KN, Marrie TJ, et al. Streptococcus pneumoniae and Staphylococcus aureus pneumonia induce distinct metabolic responses. *Journal of proteome research*. 2009;8(6):3029-36. Epub 2009/04/17.
151. Dang NA, Janssen HG, Kolk AH. Rapid diagnosis of TB using GC-MS and chemometrics. *Bioanalysis*. 2013;5(24):3079-97. Epub 2013/12/11.
152. Frediani JK, Jones DP, Tukvadze N, Uppal K, Sanikidze E, Kipiani M, et al. Plasma metabolomics in human pulmonary tuberculosis disease: a pilot study. *PloS one*. 2014;9(10):e108854. Epub 2014/10/21.
153. Laiakis EC, Morris GA, Fornace AJ, Howie SR. Metabolomic analysis in severe childhood pneumonia in the Gambia, West Africa: findings from a pilot study. *PloS one*. 2010;5(9). Epub 2010/09/17.
154. Slupsky CM, Rankin KN, Fu H, Chang D, Rowe BH, Charles PG, et al. Pneumococcal pneumonia: potential for diagnosis through a urinary metabolic profile. *Journal of proteome research*. 2009;8(12):5550-8. Epub 2009/10/13.
155. Seymour CW, Yende S, Scott MJ, Pribis J, Mohny RP, Bell LN, et al. Metabolomics in pneumonia and sepsis: an analysis of the GenIMS cohort study. *Intensive care medicine*. 2013;39(8):1423-34. Epub 2013/05/16.
156. Evans CR, Karnovsky A, Kovach MA, Standiford TJ, Burant CF, Stringer KA. Untargeted LC-MS metabolomics of bronchoalveolar lavage fluid differentiates acute respiratory distress syndrome from health. *Journal of proteome research*. 2014;13(2):640-9. Epub 2013/12/03.
157. Blaise BJ, Gouel-Cheron A, Floccard B, Monneret G, Allaouchiche B. Metabolic phenotyping of traumatized patients reveals a susceptibility to sepsis. *Analytical chemistry*. 2013;85(22):10850-5. Epub 2013/11/10.
158. Rogers AJ, McGeachie M, Baron RM, Gazourian L, Haspel JA, Nakahira K, et al. Metabolomic derangements are associated with mortality in critically ill adult patients. *PloS one*. 2014;9(1):e87538. Epub 2014/02/06.
159. Rola-Pleszczynski M, Stankova J. Leukotriene B4 enhances interleukin-6 (IL-6) production and IL-6 messenger RNA accumulation in human monocytes in vitro: transcriptional and posttranscriptional mechanisms. *Blood*. 1992;80(4):1004-11. Epub 1992/08/15.
160. Auner B, Geiger EV, Henrich D, Lehnert M, Marzi I, Relja B. Circulating leukotriene B4 identifies respiratory complications after trauma. *Mediators of inflammation*. 2012;2012:536156. Epub 2012/04/25.
161. Szymanski KV, Toennies M, Becher A, Fatykhova D, N'Guessan PD, Gutbier B, et al. Streptococcus pneumoniae-induced regulation of cyclooxygenase-2 in human lung tissue. *The European respiratory journal*. 2012;40(6):1458-67. Epub 2012/03/24.
162. Lee TH, Crea AE, Gant V, Spur BW, Marron BE, Nicolaou KC, et al. Identification of lipoxin A4 and its relationship to the sulfidopeptide leukotrienes C4, D4, and E4 in the bronchoalveolar lavage fluids obtained from patients with selected pulmonary diseases. *The American review of respiratory disease*. 1990;141(6):1453-8. Epub 1990/06/01.

163. Kellum JA, Kong L, Fink MP, Weissfeld LA, Yealy DM, Pinsky MR, et al. Understanding the inflammatory cytokine response in pneumonia and sepsis: results of the Genetic and Inflammatory Markers of Sepsis (GenIMS) Study. *Archives of internal medicine*. 2007;167(15):1655-63. Epub 2007/08/19.
164. van Vught LA, Endeman H, Meijvis SC, Zwinderman AH, Scicluna BP, Biesma DH, et al. The effect of age on the systemic inflammatory response in patients with community-acquired pneumonia. *Clinical microbiology and infection : the official publication of the European Society of Clinical Microbiology and Infectious Diseases*. 2014. Epub 2014/06/17.
165. Muszynski JA, Nofziger R, Greathouse K, Steele L, Hanson-Huber L, Nateri J, et al. Early adaptive immune suppression in children with septic shock: a prospective observational study. *Crit Care*. 2014;18(4):R145. Epub 2014/07/10.
166. Ye Q, Xu XJ, Shao WX, Pan YX, Chen XJ. *Mycoplasma pneumoniae* Infection in Children Is a Risk Factor for Developing Allergic Diseases. *TheScientificWorldJournal*. 2014;2014:986527. Epub 2014/07/01.
167. Buhling F, Tholert G, Kaiser D, Hoffmann B, Reinhold D, Ansorge S, et al. Increased release of transforming growth factor (TGF)-beta1, TGF-beta2, and chemoattractant mediators in pneumonia. *Journal of interferon & cytokine research : the official journal of the International Society for Interferon and Cytokine Research*. 1999;19(3):271-8. Epub 1999/04/23.
168. Wang X, Jiang J, Cao Z, Yang B, Zhang J, Cheng X. Diagnostic performance of multiplex cytokine and chemokine assay for tuberculosis. *Tuberculosis (Edinb)*. 2012;92(6):513-20. Epub 2012/07/25.
169. Calfee CS, Delucchi K, Parsons PE, Thompson BT, Ware LB, Matthay MA. Subphenotypes in acute respiratory distress syndrome: latent class analysis of data from two randomised controlled trials. *The Lancet Respiratory medicine*. 2014;2(8):611-20. Epub 2014/05/24.
170. Smith D, Spanel P. The challenge of breath analysis for clinical diagnosis and therapeutic monitoring. *Analyst*. 2007;132(5):390-6. Epub 2007/05/02.
171. Smith D, Spanel P. Selected ion flow tube mass spectrometry (SIFT-MS) for on-line trace gas analysis. *Mass Spectrom Rev*. 2005;24(5):661-700. Epub 2004/10/21.
172. Spanel P, Smith D. Progress in SIFT-MS: breath analysis and other applications. *Mass Spectrom Rev*. 2011;30(2):236-67. Epub 2010/07/22.
173. Turner C, Spanel P, Smith D. A longitudinal study of ammonia, acetone and propanol in the exhaled breath of 30 subjects using selected ion flow tube mass spectrometry, SIFT-MS. *Physiol Meas*. 2006;27(4):321-37. Epub 2006/03/16.
174. Dryahina K, Smith D, Spanel P. Quantification of methane in humid air and exhaled breath using selected ion flow tube mass spectrometry. *Rapid Commun Mass Spectrom*. 2010;24(9):1296-304. Epub 2010/04/15.
175. Boshier PR, Marczin N, Hanna GB. Repeatability of the measurement of exhaled volatile metabolites using selected ion flow tube mass spectrometry. *J Am Soc Mass Spectrom*. 2010;21(6):1070-4. Epub 2010/03/26.

176. Kharitonov SA, Barnes PJ. Exhaled biomarkers. *Chest*. 2006;130(5):1541-6. Epub 2006/11/14.
177. Adrie C, Monchi M, Dinh-Xuan AT, Dall'Ava-Santucci J, Dhainaut JF, Pinsky MR. Exhaled and nasal nitric oxide as a marker of pneumonia in ventilated patients. *American journal of respiratory and critical care medicine*. 2001;163(5):1143-9. Epub 2001/04/24.
178. Zegdi R, Perrin D, Burdin M, Boiteau R, Tenaillon A. Increased endogenous carbon monoxide production in severe sepsis. *Intensive care medicine*. 2002;28(6):793-6. Epub 2002/07/11.
179. Allardyce RA, Langford VS, Hill AL, Murdoch DR. Detection of volatile metabolites produced by bacterial growth in blood culture media by selected ion flow tube mass spectrometry (SIFT-MS). *J Microbiol Methods*. 2006;65(2):361-5. Epub 2005/10/27.
180. Scotter JM, Allardyce RA, Langford VS, Hill A, Murdoch DR. The rapid evaluation of bacterial growth in blood cultures by selected ion flow tube-mass spectrometry (SIFT-MS) and comparison with the BacT/ALERT automated blood culture system. *J Microbiol Methods*. 2006;65(3):628-31. Epub 2005/11/08.
181. Thorn RM, Reynolds DM, Greenman J. Multivariate analysis of bacterial volatile compound profiles for discrimination between selected species and strains in vitro. *J Microbiol Methods*. 2011;84(2):258-64. Epub 2010/12/21.
182. Julak J, Stranska E, Rosova V, Geppert H, Spanel P, Smith D. Bronchoalveolar lavage examined by solid phase microextraction, gas chromatography--mass spectrometry and selected ion flow tube mass spectrometry. *J Microbiol Methods*. 2006;65(1):76-86. Epub 2005/07/29.
183. Gilchrist FJ, Alcock A, Belcher J, Brady M, Jones A, Smith D, et al. Variation in hydrogen cyanide production between different strains of *Pseudomonas aeruginosa*. *The European respiratory journal : official journal of the European Society for Clinical Respiratory Physiology*. 2011;38(2):409-14. Epub 2011/01/29.
184. Carroll W, Lenney W, Wang T, Spanel P, Alcock A, Smith D. Detection of volatile compounds emitted by *Pseudomonas aeruginosa* using selected ion flow tube mass spectrometry. *Pediatr Pulmonol*. 2005;39(5):452-6. Epub 2005/03/15.
185. Robroeks CM, van Berkel JJ, Dallinga JW, Jobsis Q, Zimmermann LJ, Hendriks HJ, et al. Metabolomics of volatile organic compounds in cystic fibrosis patients and controls. *Pediatric Research*. 2010;68(1):75-80. Epub 2010/03/31.
186. Enderby B, Smith D, Carroll W, Lenney W. Hydrogen cyanide as a biomarker for *Pseudomonas aeruginosa* in the breath of children with cystic fibrosis. *Pediatr Pulmonol*. 2009;44(2):142-7. Epub 2009/01/17.
187. Shestivska V, Nemec A, Drevinek P, Sovova K, Dryahina K, Spanel P. Quantification of methyl thiocyanate in the headspace of *Pseudomonas aeruginosa* cultures and in the breath of cystic fibrosis patients by selected ion flow tube mass spectrometry. *Rapid Commun Mass Spectrom*. 2011;25(17):2459-67. Epub 2011/08/06.
188. Garey KW, Neuhauser MM, Robbins RA, Danziger LH, Rubinstein I. Markers of inflammation in exhaled breath condensate of young healthy smokers. *Chest*. 2004;125(1):22-6. Epub 2004/01/14.

189. Cap P, Chladek J, Pehal F, Maly M, Petru V, Barnes PJ, et al. Gas chromatography/mass spectrometry analysis of exhaled leukotrienes in asthmatic patients. *Thorax*. 2004;59(6):465-70. Epub 2004/06/01.
190. Kietzmann D, Kahl R, Muller M, Burchardi H, Kettler D. Hydrogen peroxide in expired breath condensate of patients with acute respiratory failure and with ARDS. *Intensive care medicine*. 1993;19(2):78-81. Epub 1993/01/01.
191. Jobsis Q, Raatgeep HC, Hermans PW, de Jongste JC. Hydrogen peroxide in exhaled air is increased in stable asthmatic children. *The European respiratory journal : official journal of the European Society for Clinical Respiratory Physiology*. 1997;10(3):519-21. Epub 1997/03/01.
192. Jobsis Q, Raatgeep HC, Schellekens SL, Kroesbergen A, Hop WC, de Jongste JC. Hydrogen peroxide and nitric oxide in exhaled air of children with cystic fibrosis during antibiotic treatment. *The European respiratory journal : official journal of the European Society for Clinical Respiratory Physiology*. 2000;16(1):95-100. Epub 2000/08/10.
193. Kostikas K, Papatheodorou G, Psathakis K, Panagou P, Loukides S. Oxidative stress in expired breath condensate of patients with COPD. *Chest*. 2003;124(4):1373-80. Epub 2003/10/14.
194. Montuschi P, Corradi M, Ciabattoni G, Nightingale J, Kharitonov SA, Barnes PJ. Increased 8-isoprostane, a marker of oxidative stress, in exhaled condensate of asthma patients. *American journal of respiratory and critical care medicine*. 1999;160(1):216-20. Epub 1999/07/03.
195. Carpenter CT, Price PV, Christman BW. Exhaled breath condensate isoprostanes are elevated in patients with acute lung injury or ARDS. *Chest*. 1998;114(6):1653-9. Epub 1999/01/01.
196. Kostikas K, Papatheodorou G, Ganas K, Psathakis K, Panagou P, Loukides S. pH in expired breath condensate of patients with inflammatory airway diseases. *American journal of respiratory and critical care medicine*. 2002;165(10):1364-70. Epub 2002/05/23.
197. Moloney ED, Mumby SE, Gajdocsi R, Cranshaw JH, Kharitonov SA, Quinlan GJ, et al. Exhaled breath condensate detects markers of pulmonary inflammation after cardiothoracic surgery. *American journal of respiratory and critical care medicine*. 2004;169(1):64-9. Epub 2003/10/11.
198. Stolarek RA, Kasielski M, Rysz J, Bialasiewicz P, Nowak D. Differential effect of cigarette smoking on hydrogen peroxide and thiobarbituric acid reactive substances exhaled in patients with community acquired pneumonia. *Monaldi archives for chest disease = Archivio Monaldi per le malattie del torace / Fondazione clinica del lavoro, IRCCS [and] Istituto di clinica fisiologica e malattie apparato respiratorio, Universita di Napoli, Secondo ateneo*. 2006;65(1):19-25. Epub 2006/05/17.
199. Majewska E, Kasielski M, Luczynski R, Bartosz G, Bialasiewicz P, Nowak D. Elevated exhalation of hydrogen peroxide and thiobarbituric acid reactive substances in patients with community acquired pneumonia. *Respir Med*. 2004;98(7):669-76. Epub 2004/07/15.
200. Montuschi P, Paris D, Melck D, Lucidi V, Ciabattoni G, Raia V, et al. NMR spectroscopy metabolomic profiling of exhaled breath condensate in patients with stable and unstable cystic fibrosis. *Thorax*. 2012;67(3):222-8. Epub 2011/11/23.

201. Ibrahim B, Marsden P, Smith JA, Custovic A, Nilsson M, Fowler SJ. Breath metabolomic profiling by nuclear magnetic resonance spectroscopy in asthma. *Allergy*. 2013;68(8):1050-6. Epub 2013/07/31.
202. Carraro S, Rezzi S, Reniero F, Heberger K, Giordano G, Zanconato S, et al. Metabolomics applied to exhaled breath condensate in childhood asthma. *American journal of respiratory and critical care medicine*. 2007;175(10):986-90. Epub 2007/02/17.
203. Sinha A, Krishnan V, Sethi T, Roy S, Ghosh B, Lodha R, et al. Metabolomic signatures in nuclear magnetic resonance spectra of exhaled breath condensate identify asthma. *The European respiratory journal : official journal of the European Society for Clinical Respiratory Physiology*. 2012;39(2):500-2. Epub 2012/02/03.
204. de Laurentiis G, Paris D, Melck D, Montuschi P, Maniscalco M, Bianco A, et al. Separating smoking-related diseases using NMR-based metabolomics of exhaled breath condensate. *J Proteome Res*. 2013;12(3):1502-11. Epub 2013/01/31.
205. de Laurentiis G, Paris D, Melck D, Maniscalco M, Marsico S, Corso G, et al. Metabonomic analysis of exhaled breath condensate in adults by nuclear magnetic resonance spectroscopy. *The European respiratory journal : official journal of the European Society for Clinical Respiratory Physiology*. 2008;32(5):1175-83. Epub 2008/07/26.
206. Carraro S, Giordano G, Reniero F, Carpi D, Stocchero M, Sterk PJ, et al. Asthma severity in childhood and metabolomic profiling of breath condensate. *Allergy*. 2013;68(1):110-7. Epub 2012/11/20.
207. Carraro S, Giordano G, Pirillo P, Maretta M, Reniero F, Cogo PE, et al. Airway Metabolic Anomalies in Adolescents with Bronchopulmonary Dysplasia: New Insights from the Metabolomic Approach. *The Journal of pediatrics*. 2014. Epub 2014/10/09.
208. Monge ME, Perez JJ, Dwivedi P, Zhou M, McCarty NA, Stecenko AA, et al. Ion mobility and liquid chromatography/mass spectrometry strategies for exhaled breath condensate glucose quantitation in cystic fibrosis studies. *Rapid Commun Mass Spectrom*. 2013;27(20):2263-71. Epub 2013/09/11.
209. Esther CR, Jr., Olsen BM, Lin FC, Fine J, Boucher RC. Exhaled breath condensate adenosine tracks lung function changes in cystic fibrosis. *Am J Physiol Lung Cell Mol Physiol*. 2013;304(7):L504-9. Epub 2013/01/29.
210. Quan Z, Purser C, Baker RC, Dwyer T, Bhagat R, Sheng Y, et al. Determination of derivatized urea in exhaled breath condensate by LC-MS. *Journal of chromatographic science*. 2010;48(2):140-4. Epub 2010/01/30.
211. Mansoor JK, Schelegle ES, Davis CE, Walby WF, Zhao W, Aksenov AA, et al. Analysis of volatile compounds in exhaled breath condensate in patients with severe pulmonary arterial hypertension. *PLoS One*. 2014;9(4):e95331. Epub 2014/04/22.
212. Hubbard HF, Sobus JR, Pleil JD, Madden MC, Tabucchi S. Application of novel method to measure endogenous VOCs in exhaled breath condensate before and after exposure to diesel exhaust. *Journal of chromatography B, Analytical technologies in the biomedical and life sciences*. 2009;877(29):3652-8. Epub 2009/10/03.

213. Manini P, Andreoli R, Sforza S, Dall'Asta C, Galaverna G, Mutti A, et al. Evaluation of Alternate Isotope-Coded Derivatization Assay (AIDA) in the LC-MS/MS analysis of aldehydes in exhaled breath condensate. *Journal of chromatography B, Analytical technologies in the biomedical and life sciences*. 2010;878(27):2616-22. Epub 2010/03/09.
214. Corradi M, Pignatti P, Manini P, Andreoli R, Goldoni M, Poppa M, et al. Comparison between exhaled and sputum oxidative stress biomarkers in chronic airway inflammation. *The European respiratory journal : official journal of the European Society for Clinical Respiratory Physiology*. 2004;24(6):1011-7. Epub 2004/12/02.
215. Andreoli R, Manini P, Corradi M, Mutti A, Niessen WM. Determination of patterns of biologically relevant aldehydes in exhaled breath condensate of healthy subjects by liquid chromatography/atmospheric chemical ionization tandem mass spectrometry. *Rapid Commun Mass Spectrom*. 2003;17(7):637-45. Epub 2003/03/28.
216. Corradi M, Rubinstein I, Andreoli R, Manini P, Caglieri A, Poli D, et al. Aldehydes in exhaled breath condensate of patients with chronic obstructive pulmonary disease. *American journal of respiratory and critical care medicine*. 2003;167(10):1380-6. Epub 2003/01/11.
217. Rosa MJ, Yan B, Chillrud SN, Acosta LM, Divjan A, Jacobson JS, et al. Domestic airborne black carbon levels and 8-isoprostane in exhaled breath condensate among children in New York City. *Environmental research*. 2014;135C:105-10. Epub 2014/09/30.
218. Pelclova D, Fenclova Z, Vlckova S, Klusackova P, Lebedova J, Syslova K, et al. Occupational asthma follow-up--which markers are elevated in exhaled breath condensate and plasma? *International journal of occupational medicine and environmental health*. 2014;27(2):206-15. Epub 2014/03/20.
219. Janicka M, Kubica P, Kot-Wasik A, Kot J, Namiesnik J. Sensitive determination of isoprostanes in exhaled breath condensate samples with use of liquid chromatography-tandem mass spectrometry. *Journal of chromatography B, Analytical technologies in the biomedical and life sciences*. 2012;893-894:144-9. Epub 2012/03/27.
220. Carraro S, Cogo PE, Isak I, Simonato M, Corradi M, Carnielli VP, et al. EIA and GC/MS analysis of 8-isoprostane in EBC of children with problematic asthma. *The European respiratory journal : official journal of the European Society for Clinical Respiratory Physiology*. 2010;35(6):1364-9. Epub 2009/11/10.
221. Pelclova D, Fenclova Z, Kacer P, Navratil T, Kuzma M, Lebedova JK, et al. 8-isoprostane and leukotrienes in exhaled breath condensate in Czech subjects with silicosis. *Industrial health*. 2007;45(6):766-74. Epub 2008/01/24.
222. Syslova K, Kacer P, Kuzma M, Klusackova P, Fenclova Z, Lebedova J, et al. Determination of 8-iso-prostaglandin F(2alpha) in exhaled breath condensate using combination of immunoseparation and LC-ESI-MS/MS. *Journal of chromatography B, Analytical technologies in the biomedical and life sciences*. 2008;867(1):8-14. Epub 2008/04/01.
223. Pelclova D, Fenclova Z, Syslova K, Vlckova S, Lebedova J, Pecha O, et al. Oxidative stress markers in exhaled breath condensate in lung fibroses are not significantly affected by systemic diseases. *Industrial health*. 2011;49(6):746-54. Epub 2011/10/25.

224. Syslova K, Kacer P, Kuzma M, Najmanova V, Fenclova Z, Vlckova S, et al. Rapid and easy method for monitoring oxidative stress markers in body fluids of patients with asbestos or silica-induced lung diseases. *Journal of chromatography B, Analytical technologies in the biomedical and life sciences*. 2009;877(24):2477-86. Epub 2009/07/04.
225. Wang CJ, Yang NH, Liou SH, Lee HL. Fast quantification of the exhaled breath condensate of oxidative stress 8-iso-prostaglandin F₂alpha using on-line solid-phase extraction coupled with liquid chromatography/electrospray ionization mass spectrometry. *Talanta*. 2010;82(4):1434-8. Epub 2010/08/31.
226. Pelclova D, Fenclova Z, Kacer P, Kuzma M, Navratil T, Lebedova J. Increased 8-isoprostane, a marker of oxidative stress in exhaled breath condensate in subjects with asbestos exposure. *Industrial health*. 2008;46(5):484-9. Epub 2008/10/09.
227. Syslova K, Bohmova A, Demirbag E, Simkova K, Kuzma M, Pelclova D, et al. Immunomagnetic molecular probe with UHPLC-MS/MS: a promising way for reliable bronchial asthma diagnostics based on quantification of cysteinyl leukotrienes. *Journal of pharmaceutical and biomedical analysis*. 2013;81-82:108-17. Epub 2013/05/07.
228. Syslova K, Kacer P, Vilhanova B, Kuzma M, Lipovova P, Fenclova Z, et al. Determination of cysteinyl leukotrienes in exhaled breath condensate: method combining immunoseparation with LC-ESI-MS/MS. *Journal of chromatography B, Analytical technologies in the biomedical and life sciences*. 2011;879(23):2220-8. Epub 2011/07/05.
229. Pelclova D, Fenclova Z, Vlckova S, Lebedova J, Syslova K, Pecha O, et al. Leukotrienes B₄, C₄, D₄ and E₄ in the exhaled breath condensate (EBC), blood and urine in patients with pneumoconiosis. *Industrial health*. 2012;50(4):299-306. Epub 2012/07/13.
230. Cap P, Maly M, Pehal F, Pelikan Z. Exhaled leukotrienes and bronchial responsiveness to methacholine in patients with seasonal allergic rhinitis. *Annals of allergy, asthma & immunology : official publication of the American College of Allergy, Asthma, & Immunology*. 2009;102(2):103-9. Epub 2009/02/24.
231. Montuschi P, Martello S, Felli M, Mondino C, Chiarotti M. Ion trap liquid chromatography/tandem mass spectrometry analysis of leukotriene B₄ in exhaled breath condensate. *Rapid Commun Mass Spectrom*. 2004;18(22):2723-9. Epub 2004/10/23.
232. Montuschi P, Martello S, Felli M, Mondino C, Barnes PJ, Chiarotti M. Liquid chromatography/mass spectrometry analysis of exhaled leukotriene B₄ in asthmatic children. *Respiratory research*. 2005;6:119. Epub 2005/10/21.
233. Cap P, Pehal F, Chladek J, Maly M. Analysis of exhaled leukotrienes in nonasthmatic adult patients with seasonal allergic rhinitis. *Allergy*. 2005;60(2):171-6. Epub 2005/01/14.
234. Sanak M, Gielicz A, Bochenek G, Kaszuba M, Nizankowska-Mogilnicka E, Szczeklik A. Targeted eicosanoid lipidomics of exhaled breath condensate provide a distinct pattern in the aspirin-intolerant asthma phenotype. *The Journal of allergy and clinical immunology*. 2011;127(5):1141-7 e2. Epub 2011/02/15.
235. Nording ML, Yang J, Hegedus CM, Bhushan A, Kenyon NJ, Davis CE, et al. Endogenous Levels of Five Fatty Acid Metabolites in Exhaled Breath Condensate to Monitor Asthma by High-

Performance Liquid Chromatography: Electrospray Tandem Mass Spectrometry. *IEEE sensors journal*. 2010;10(1):123-30. Epub 2010/11/26.

236. Glowacka E, Jedynak-Wasowicz U, Sanak M, Lis G. Exhaled eicosanoid profiles in children with atopic asthma and healthy controls. *Pediatr Pulmonol*. 2013;48(4):324-35. Epub 2012/07/12.

237. Gonzalez-Reche LM, Musiol AK, Muller-Lux A, Kraus T, Goen T. Method optimization and validation for the simultaneous determination of arachidonic acid metabolites in exhaled breath condensate by liquid chromatography-electrospray ionization tandem mass spectrometry. *J Occup Med Toxicol*. 2006;1:5. Epub 2006/05/26.

238. Sanak M, Gielicz A, Nagraba K, Kaszuba M, Kumik J, Szczeklik A. Targeted eicosanoids lipidomics of exhaled breath condensate in healthy subjects. *Journal of chromatography B, Analytical technologies in the biomedical and life sciences*. 2010;878(21):1796-800. Epub 2010/07/16.

239. Kielbasa B, Moeller A, Sanak M, Hamacher J, Hutterli M, Cmiel A, et al. Eicosanoids in exhaled breath condensates in the assessment of childhood asthma. *Pediatric allergy and immunology : official publication of the European Society of Pediatric Allergy and Immunology*. 2008;19(7):660-9. Epub 2008/07/23.

240. Szczeklik W, Sanak M, Mastalerz L, Sokolowska BM, Gielicz A, Soja J, et al. 12-hydroxy-eicosatetraenoic acid (12-HETE): a biomarker of Churg-Strauss syndrome. *Clinical and experimental allergy : journal of the British Society for Allergy and Clinical Immunology*. 2012;42(4):513-22. Epub 2012/03/16.

241. Montesi SB, Mathai SK, Brenner LN, Gorshkova IA, Berdyshev EV, Tager AM, et al. Docosatetraenoyl LPA is elevated in exhaled breath condensate in idiopathic pulmonary fibrosis. *BMC pulmonary medicine*. 2014;14:5. Epub 2014/01/29.

242. Carraro S, Giordano G, Piacentini G, Kantar A, Moser S, Cesca L, et al. Asymmetric dimethylarginine in exhaled breath condensate and serum of children with asthma. *Chest*. 2013;144(2):405-10. Epub 2013/02/16.

243. Di Gangi IM, Pirillo P, Carraro S, Gucciardi A, Naturale M, Baraldi E, et al. Online trapping and enrichment ultra performance liquid chromatography-tandem mass spectrometry method for sensitive measurement of "arginine-asymmetric dimethylarginine cycle" biomarkers in human exhaled breath condensate. *Analytica chimica acta*. 2012;754:67-74. Epub 2012/11/13.

244. Schettgen T, Tings A, Brodowsky C, Muller-Lux A, Musiol A, Kraus T. Simultaneous determination of the advanced glycation end product N (epsilon)-carboxymethyllysine and its precursor, lysine, in exhaled breath condensate using isotope-dilution-hydrophilic-interaction liquid chromatography coupled to tandem mass spectrometry. *Analytical and bioanalytical chemistry*. 2007;387(8):2783-91. Epub 2007/02/24.

245. Conventz A, Musiol A, Brodowsky C, Muller-Lux A, Dewes P, Kraus T, et al. Simultaneous determination of 3-nitrotyrosine, tyrosine, hydroxyproline and proline in exhaled breath condensate by hydrophilic interaction liquid chromatography/electrospray ionization tandem mass spectrometry. *Journal of chromatography B, Analytical technologies in the biomedical and life sciences*. 2007;860(1):78-85. Epub 2007/11/21.

246. Patel K, Davis SD, Johnson R, Esther CR, Jr. Exhaled breath condensate purines correlate with lung function in infants and preschoolers. *Pediatr Pulmonol*. 2013;48(2):182-7. Epub 2012/05/23.
247. Esther CR, Jr., Lazaar AL, Bordonali E, Qaqish B, Boucher RC. Elevated airway purines in COPD. *Chest*. 2011;140(4):954-60. Epub 2011/04/02.
248. Esther CR, Jr., Boysen G, Olsen BM, Collins LB, Ghio AJ, Swenberg JW, et al. Mass spectrometric analysis of biomarkers and dilution markers in exhaled breath condensate reveals elevated purines in asthma and cystic fibrosis. *Am J Physiol Lung Cell Mol Physiol*. 2009;296(6):L987-93. Epub 2009/03/24.
249. Esther CR, Jr., Jasin HM, Collins LB, Swenberg JA, Boysen G. A mass spectrometric method to simultaneously measure a biomarker and dilution marker in exhaled breath condensate. *Rapid Commun Mass Spectrom*. 2008;22(5):701-5. Epub 2008/02/08.
250. Corradi M, Acampa O, Goldoni M, Andreoli R, Milton D, Sama SR, et al. Metallic elements in exhaled breath condensate and serum of patients with exacerbation of chronic obstructive pulmonary disease. *Metallomics : integrated biometal science*. 2009;1(4):339-45. Epub 2009/07/07.
251. Celio S, Troxler H, Durka SS, Chladek J, Wildhaber JH, Sennhauser FH, et al. Free 3-nitrotyrosine in exhaled breath condensates of children fails as a marker for oxidative stress in stable cystic fibrosis and asthma. *Nitric oxide : biology and chemistry / official journal of the Nitric Oxide Society*. 2006;15(3):226-32. Epub 2006/08/26.
252. Baraldi E, Giordano G, Pasquale MF, Carraro S, Mardegan A, Bonetto G, et al. 3-Nitrotyrosine, a marker of nitrosative stress, is increased in breath condensate of allergic asthmatic children. *Allergy*. 2006;61(1):90-6. Epub 2005/12/21.
253. Goen T, Muller-Lux A, Dewes P, Musiol A, Kraus T. Sensitive and accurate analyses of free 3-nitrotyrosine in exhaled breath condensate by LC-MS/MS. *Journal of chromatography B, Analytical technologies in the biomedical and life sciences*. 2005;826(1-2):261-6. Epub 2005/09/07.
254. Larstad M, Soderling AS, Caidahl K, Olin AC. Selective quantification of free 3-nitrotyrosine in exhaled breath condensate in asthma using gas chromatography/tandem mass spectrometry. *Nitric oxide : biology and chemistry / official journal of the Nitric Oxide Society*. 2005;13(2):134-44. Epub 2005/07/12.
255. Fumagalli M, Ferrari F, Luisetti M, Stolk J, Hiemstra PS, Capuano D, et al. Profiling the proteome of exhaled breath condensate in healthy smokers and COPD patients by LC-MS/MS. *International journal of molecular sciences*. 2012;13(11):13894-910. Epub 2012/12/04.
256. Krug S, Kastenmuller G, Stuckler F, Rist MJ, Skurk T, Sailer M, et al. The dynamic range of the human metabolome revealed by challenges. *FASEB journal : official publication of the Federation of American Societies for Experimental Biology*. 2012;26(6):2607-19. Epub 2012/03/20.
257. Teahan O, Gamble S, Holmes E, Waxman J, Nicholson JK, Bevan C, et al. Impact of analytical bias in metabolomic studies of human blood serum and plasma. *Analytical chemistry*. 2006;78(13):4307-18. Epub 2006/07/01.

258. Lu C, Jiang Z, Fan X, Liao G, Li S, He C, et al. A metabonomic approach to the effect evaluation of treatment in patients infected with influenza A (H1N1). *Talanta*. 2012;100:51-6. Epub 2012/11/13.
259. Dieterle F, Ross A, Schlotterbeck G, Senn H. Probabilistic quotient normalization as robust method to account for dilution of complex biological mixtures. Application in ¹H NMR metabonomics. *Analytical chemistry*. 2006;78(13):4281-90. Epub 2006/07/01.
260. Le Moyec L, Racine S, Le Toumelin P, Adnet F, Larue V, Cohen Y, et al. Aminoglycoside and glycopeptide renal toxicity in intensive care patients studied by proton magnetic resonance spectroscopy of urine. *Critical care medicine*. 2002;30(6):1242-5. Epub 2002/06/20.
261. Godet C, Hira M, Adoun M, Eugene M, Robert R. Rapid diagnosis of alcoholic ketoacidosis by proton NMR. *Intensive care medicine*. 2001;27(4):785-6. Epub 2001/06/12.
262. Amathieu R, Triba MN, Nahon P, Bouchemal N, Kamoun W, Haouache H, et al. Serum ¹H-NMR metabolomic fingerprints of acute-on-chronic liver failure in intensive care unit patients with alcoholic cirrhosis. *PloS one*. 2014;9(2):e89230. Epub 2014/03/04.
263. Desmoulin F, Galinier M, Trouillet C, Berry M, Delmas C, Turkieh A, et al. Metabonomics analysis of plasma reveals the lactate to cholesterol ratio as an independent prognostic factor of short-term mortality in acute heart failure. *PloS one*. 2013;8(4):e60737. Epub 2013/04/11.
264. Park Y, Jones DP, Ziegler TR, Lee K, Kotha K, Yu T, et al. Metabolic effects of albumin therapy in acute lung injury measured by proton nuclear magnetic resonance spectroscopy of plasma: a pilot study. *Critical care medicine*. 2011;39(10):2308-13. Epub 2011/06/28.
265. Tiirola T, Erkkila L, Laitinen K, Leinonen M, Saikku P, Bloigu A, et al. Effect of acute Chlamydia pneumoniae infection on lipoprotein metabolism in NIH/S mice. *Scandinavian journal of clinical and laboratory investigation*. 2002;62(6):477-84. Epub 2002/12/10.
266. Langley RJ, Tsalik EL, Velkinburgh JC, Glickman SW, Rice BJ, Wang C, et al. An integrated clinico-metabolomic model improves prediction of death in sepsis. *Science translational medicine*. 2013;5(195):195ra95. Epub 2013/07/26.
267. de la Llera Moya M, McGillicuddy FC, Hinkle CC, Byrne M, Joshi MR, Nguyen V, et al. Inflammation modulates human HDL composition and function in vivo. *Atherosclerosis*. 2012;222(2):390-4. Epub 2012/03/30.
268. Izquierdo-Garcia JL, Naz S, Nin N, Rojas Y, Erazo M, Martinez-Caro L, et al. A Metabolomic Approach to the Pathogenesis of Ventilator-induced Lung Injury. *Anesthesiology*. 2014;120(3):694-702. Epub 2013/11/21.
269. Gruber M, Christ-Crain M, Stolz D, Keller U, Muller C, Bingisser R, et al. Prognostic impact of plasma lipids in patients with lower respiratory tract infections - an observational study. *Swiss medical weekly*. 2009;139(11-12):166-72. Epub 2009/03/31.
270. Deniz O, Tozkoparan E, Yaman H, Cakir E, Gumus S, Ozcan O, et al. Serum HDL-C levels, log (TG/HDL-C) values and serum total cholesterol/HDL-C ratios significantly correlate with radiological extent of disease in patients with community-acquired pneumonia. *Clinical biochemistry*. 2006;39(3):287-92. Epub 2006/02/21.

271. Rodriguez Reguero JJ, Iglesias Cubero G, Vazquez M, Folgueras I, Braga S, Bustillo E, et al. Variation in plasma lipid and lipoprotein concentrations in community-acquired pneumonia a six-month prospective study. *European journal of clinical chemistry and clinical biochemistry : journal of the Forum of European Clinical Chemistry Societies*. 1996;34(3):245-9. Epub 1996/03/01.
272. Tsai MH, Lin TY, Hsieh SY, Chiu CY, Chiu CH, Huang YC. Comparative proteomic studies of plasma from children with pneumococcal pneumonia. *Scandinavian journal of infectious diseases*. 2009;41(6-7):416-24. Epub 2009/04/28.
273. Laurila AL, Bloigu A, Nayha S, Hassi J, Leinonen M, Saikku P. Chlamydia pneumoniae antibodies associated with altered serum lipid profile. *International journal of circumpolar health*. 1998;57 Suppl 1:329-32. Epub 1999/03/27.
274. Walcott BP, Patel AP, Stapleton CJ, Trivedi RA, Young AM, Ogilvy CS. Multiplexed protein profiling after aneurysmal subarachnoid hemorrhage: Characterization of differential expression patterns in cerebral vasospasm. *Journal of clinical neuroscience : official journal of the Neurosurgical Society of Australasia*. 2014;21(12):2135-9. Epub 2014/08/02.
275. Phillips J, Roberts G, Bolger C, el Baghdady A, Bouchier-Hayes D, Farrell M, et al. Lipoprotein (a): a potential biological marker for unruptured intracranial aneurysms. *Neurosurgery*. 1997;40(5):1112-5; discussion 5-7. Epub 1997/05/01.
276. Han K, Jia N, Yang L, Min LQ. Correlation between ischemia-modified albumin and lipid levels in patients with acute cerebrovascular disease. *Molecular medicine reports*. 2012;6(3):621-4. Epub 2012/06/28.
277. Sandvei MS, Lindekleiv H, Romundstad PR, Muller TB, Vatten LJ, Ingebrigtsen T, et al. Risk factors for aneurysmal subarachnoid hemorrhage - BMI and serum lipids: 11-year follow-up of the HUNT and the Tromso Study in Norway. *Acta neurologica Scandinavica*. 2012;125(6):382-8. Epub 2011/07/29.
278. Tokuda Y, Stein GH. Serum lipids as protective factors for subarachnoid hemorrhage. *Journal of clinical neuroscience : official journal of the Neurosurgical Society of Australasia*. 2005;12(5):538-41. Epub 2005/06/25.
279. Raaymakers TW. Aneurysms in relatives of patients with subarachnoid hemorrhage: frequency and risk factors. MARS Study Group. *Magnetic Resonance Angiography in Relatives of patients with Subarachnoid hemorrhage*. *Neurology*. 1999;53(5):982-8. Epub 1999/09/25.
280. Samra JS, Summers LK, Frayn KN. Sepsis and fat metabolism. *The British journal of surgery*. 1996;83(9):1186-96. Epub 1996/09/01.
281. Vente JP, von Meyenfeldt MF, van Eijk HM, van Berlo CL, Gouma DJ, van der Linden CJ, et al. Plasma-amino acid profiles in sepsis and stress. *Annals of surgery*. 1989;209(1):57-62. Epub 1989/01/01.
282. Neurauter G, Grahmann AV, Klieber M, Zeimet A, Ledochowski M, Sperner-Unterweger B, et al. Serum phenylalanine concentrations in patients with ovarian carcinoma correlate with concentrations of immune activation markers and of isoprostane-8. *Cancer letters*. 2008;272(1):141-7. Epub 2008/08/15.

283. Ploder M, Neurauter G, Spittler A, Schroecksnadel K, Roth E, Fuchs D. Serum phenylalanine in patients post trauma and with sepsis correlate to neopterin concentrations. *Amino acids*. 2008;35(2):303-7. Epub 2007/12/29.
284. Wannemacher RW, Jr., Klainer AS, Dinterman RE, Beisel WR. The significance and mechanism of an increased serum phenylalanine-tyrosine ratio during infection. *The American journal of clinical nutrition*. 1976;29(9):997-1006. Epub 1976/09/01.
285. Dyerberg J, Bang HO. Haemostatic function and platelet polyunsaturated fatty acids in Eskimos. *Lancet*. 1979;2(8140):433-5. Epub 1979/09/01.
286. Pedersen HS, Mulvad G, Seidelin KN, Malcom GT, Boudreau DA. N-3 fatty acids as a risk factor for haemorrhagic stroke. *Lancet*. 1999;353(9155):812-3. Epub 1999/08/25.
287. Park Y, Park S, Yi H, Kim HY, Kang SJ, Kim J, et al. Low level of n-3 polyunsaturated fatty acids in erythrocytes is a risk factor for both acute ischemic and hemorrhagic stroke in Koreans. *Nutr Res*. 2009;29(12):825-30. Epub 2009/12/08.
288. Pilitsis JG, Coplin WM, O'Regan MH, Wellwood JM, Diaz FG, Fairfax MR, et al. Free fatty acids in human cerebrospinal fluid following subarachnoid hemorrhage and their potential role in vasospasm: a preliminary observation. *Journal of neurosurgery*. 2002;97(2):272-9. Epub 2002/08/21.
289. Corcoran TB, Mas E, Barden AE, Durand T, Galano JM, Roberts LJ, et al. Are isofurans and neuroprostanes increased after subarachnoid hemorrhage and traumatic brain injury? *Antioxidants & redox signaling*. 2011;15(10):2663-7. Epub 2011/06/28.
290. Yoneda H, Shirao S, Nakagawara J, Ogasawara K, Tominaga T, Suzuki M. A prospective, multicenter, randomized study of the efficacy of eicosapentaenoic acid for cerebral vasospasm: the EVAS study. *World neurosurgery*. 2014;81(2):309-15. Epub 2012/10/04.
291. Shirao S, Fujisawa H, Kudo A, Kurokawa T, Yoneda H, Kunitsugu I, et al. Inhibitory effects of eicosapentaenoic acid on chronic cerebral vasospasm after subarachnoid hemorrhage: possible involvement of a sphingosylphosphorylcholine-rho-kinase pathway. *Cerebrovasc Dis*. 2008;26(1):30-7. Epub 2008/05/31.
292. Yoneda H, Shirao S, Kurokawa T, Fujisawa H, Kato S, Suzuki M. Does eicosapentaenoic acid (EPA) inhibit cerebral vasospasm in patients after aneurysmal subarachnoid hemorrhage? *Acta neurologica Scandinavica*. 2008;118(1):54-9. Epub 2008/02/12.
293. Watanabe T, Asano T, Shimizu T, Seyama Y, Takakura K. Participation of lipoxygenase products from arachidonic acid in the pathogenesis of cerebral vasospasm. *Journal of neurochemistry*. 1988;50(4):1145-50. Epub 1988/04/01.
294. Saloheimo P, Juvela S, Riutta A, Pyhtinen J, Hillbom M. Thromboxane and prostacyclin biosynthesis in patients with acute spontaneous intracerebral hemorrhage. *Thrombosis research*. 2005;115(5):367-73. Epub 2005/03/01.
295. Zak A, Vecka M, Tvřizicka E, Hruby M, Novak F, Papezova H, et al. Composition of plasma fatty acids and non-cholesterol sterols in anorexia nervosa. *Physiological research / Academia Scientiarum Bohemoslovaca*. 2005;54(4):443-51. Epub 2004/12/14.

296. Murata T, Aritake K, Tsubosaka Y, Maruyama T, Nakagawa T, Hori M, et al. Anti-inflammatory role of PGD2 in acute lung inflammation and therapeutic application of its signal enhancement. *Proceedings of the National Academy of Sciences of the United States of America*. 2013;110(13):5205-10. Epub 2013/03/13.
297. Balamayooran G, Batra S, Balamayooran T, Cai S, Jeyaseelan S. Monocyte chemoattractant protein 1 regulates pulmonary host defense via neutrophil recruitment during *Escherichia coli* infection. *Infection and immunity*. 2011;79(7):2567-77. Epub 2011/04/27.
298. Paats MS, Bergen IM, Hanselaar WE, Groeninx van Zoelen EC, Hoogsteden HC, Hendriks RW, et al. Local and systemic cytokine profiles in nonsevere and severe community-acquired pneumonia. *The European respiratory journal*. 2013;41(6):1378-85. Epub 2012/12/22.
299. Monton C, Torres A, El-Ebiary M, Filella X, Xaubet A, de la Bellacasa JP. Cytokine expression in severe pneumonia: a bronchoalveolar lavage study. *Critical care medicine*. 1999;27(9):1745-53. Epub 1999/10/03.
300. Bauer TT, Monton C, Torres A, Cabello H, Fillela X, Maldonado A, et al. Comparison of systemic cytokine levels in patients with acute respiratory distress syndrome, severe pneumonia, and controls. *Thorax*. 2000;55(1):46-52. Epub 1999/12/23.
301. Yende S, Tuomanen EI, Wunderink R, Kanaya A, Newman AB, Harris T, et al. Preinfection systemic inflammatory markers and risk of hospitalization due to pneumonia. *American journal of respiratory and critical care medicine*. 2005;172(11):1440-6. Epub 2005/09/17.
302. Matsumoto T, Hayamizu K, Marubayashi S, Shimizu K, Hamamoto A, Yamaguchi T, et al. Relationship between the cAMP levels in leukocytes and the cytokine balance in patients surviving gram negative bacterial pneumonia. *Journal of clinical biochemistry and nutrition*. 2011;48(2):134-41. Epub 2011/03/05.
303. Matsumoto Y, Kawamura Y, Nakai H, Sugata K, Yoshikawa A, Ihira M, et al. Cytokine and chemokine responses in pediatric patients with severe pneumonia associated with pandemic A/H1N1/2009 influenza virus. *Microbiology and immunology*. 2012;56(9):651-5. Epub 2012/06/28.
304. Remmelts HH, Meijvis SC, Biesma DH, van Velzen-Blad H, Voorn GP, Grutters JC, et al. Dexamethasone downregulates the systemic cytokine response in patients with community-acquired pneumonia. *Clinical and vaccine immunology : CVI*. 2012;19(9):1532-8. Epub 2012/08/03.
305. Fukushima R, Alexander JW, Gianotti L, Ogle CK. Isolated pulmonary infection acts as a source of systemic tumor necrosis factor. *Critical care medicine*. 1994;22(1):114-20. Epub 1994/01/01.
306. Jaoude PA, Knight PR, Ohtake P, El-Solh AA. Biomarkers in the diagnosis of aspiration syndromes. *Expert review of molecular diagnostics*. 2010;10(3):309-19. Epub 2010/04/08.
307. Khelifi M, Zarrouk A, Nury T, Hamed H, Saguem S, Salah RB, et al. Cytokine and eicosanoid profiles of phosphate mine workers. *The Journal of toxicological sciences*. 2014;39(3):465-74. Epub 2014/05/23.

308. Batra S, Cai S, Balamayooran G, Jeyaseelan S. Intrapulmonary administration of leukotriene B(4) augments neutrophil accumulation and responses in the lung to Klebsiella infection in CXCL1 knockout mice. *J Immunol.* 2012;188(7):3458-68. Epub 2012/03/02.
309. Mancuso P, Lewis C, Serezani CH, Goel D, Peters-Golden M. Intrapulmonary administration of leukotriene B4 enhances pulmonary host defense against pneumococcal pneumonia. *Infection and immunity.* 2010;78(5):2264-71. Epub 2010/03/17.
310. Carraro S, Andreola B, Alinovi R, Corradi M, Freo L, Da Dalt L, et al. Exhaled leukotriene B4 in children with community acquired pneumonia. *Pediatric pulmonology.* 2008;43(10):982-6. Epub 2008/09/11.
311. Pace E, Profita M, Melis M, Bonanno A, Paterno A, Mody CH, et al. LTB4 is present in exudative pleural effusions and contributes actively to neutrophil recruitment in the inflamed pleural space. *Clinical and experimental immunology.* 2004;135(3):519-27. Epub 2004/03/11.
312. Kalsotra A, Zhao J, Anakk S, Dash PK, Strobel HW. Brain trauma leads to enhanced lung inflammation and injury: evidence for role of P4504Fs in resolution. *Journal of cerebral blood flow and metabolism : official journal of the International Society of Cerebral Blood Flow and Metabolism.* 2007;27(5):963-74. Epub 2006/09/21.
313. Woiciechowsky C, Schoning B, Cobanov J, Lanksch WR, Volk HD, Docke WD. Early IL-6 plasma concentrations correlate with severity of brain injury and pneumonia in brain-injured patients. *The Journal of trauma.* 2002;52(2):339-45. Epub 2002/02/09.
314. LaPar DJ, Rosenberger LH, Walters DM, Hedrick TL, Swenson BR, Young JS, et al. Severe traumatic head injury affects systemic cytokine expression. *Journal of the American College of Surgeons.* 2012;214(4):478-86; discussion 86-8. Epub 2012/02/22.
315. Cavalcanti M, Ferrer M, Ferrer R, Morforte R, Garnacho A, Torres A. Risk and prognostic factors of ventilator-associated pneumonia in trauma patients. *Critical care medicine.* 2006;34(4):1067-72. Epub 2006/02/18.
316. Conway Morris A, Kefala K, Wilkinson TS, Moncayo-Nieto OL, Dhaliwal K, Farrell L, et al. Diagnostic importance of pulmonary interleukin-1beta and interleukin-8 in ventilator-associated pneumonia. *Thorax.* 2010;65(3):201-7. Epub 2009/10/15.
317. Millo JL, Schultz MJ, Williams C, Weverling GJ, Ringrose T, Mackinlay CI, et al. Compartmentalisation of cytokines and cytokine inhibitors in ventilator-associated pneumonia. *Intensive care medicine.* 2004;30(1):68-74. Epub 2003/11/25.
318. Frank JA, Parsons PE, Matthay MA. Pathogenetic significance of biological markers of ventilator-associated lung injury in experimental and clinical studies. *Chest.* 2006;130(6):1906-14. Epub 2006/12/15.
319. Jonker MA, Sano Y, Hermsen JL, Lan J, Kudsk KA. Proinflammatory cytokine surge after injury stimulates an airway immunoglobulin a increase. *The Journal of trauma.* 2010;69(4):843-8. Epub 2010/02/23.
320. Calder PC. Marine omega-3 fatty acids and inflammatory processes: Effects, mechanisms and clinical relevance. *Biochimica et biophysica acta.* 2014. Epub 2014/08/26.

321. Guidet B, Piot O, Masliah J, Barakett V, Maury E, Bereziat G, et al. Secretory non-pancreatic phospholipase A2 in severe sepsis: relation to endotoxin, cytokines and thromboxane B2. *Infection*. 1996;24(2):103-8. Epub 1996/03/01.
322. Nakae H, Endo S, Inada K, Yamashita H, Yamada Y, Takakuwa T, et al. Plasma concentrations of type II phospholipase A2, cytokines and eicosanoids in patients with burns. *Burns : journal of the International Society for Burn Injuries*. 1995;21(6):422-6. Epub 1995/09/01.
323. Denizot Y, Feiss P, Nathan N. Are lipid mediators implicated in the production of pro- and anti-inflammatory cytokines during cardiopulmonary bypass graft with extracorporeal circulation? *Cytokine*. 1999;11(4):301-4. Epub 1999/05/18.
324. Reilly DM, Green MR. Eicosanoid and cytokine levels in acute skin irritation in response to tape stripping and capsaicin. *Acta dermato-venereologica*. 1999;79(3):187-90. Epub 1999/06/29.
325. Venza M, Visalli M, Alafaci C, Caffo M, Caruso G, Salpietro FM, et al. Interleukin-8 overexpression in astrocytomas is induced by prostaglandin E2 and is associated with the transcription factors CCAAT/enhancer-binding protein-beta and CCAAT/enhancer-binding homologous protein. *Neurosurgery*. 2011;69(3):713-21; discussion 21. Epub 2011/04/08.
326. O'Brien AJ, Fullerton JN, Massey KA, Auld G, Sewell G, James S, et al. Immunosuppression in acutely decompensated cirrhosis is mediated by prostaglandin E2. *Nature medicine*. 2014;20(5):518-23. Epub 2014/04/15.
327. Tutuncuoglu S, Kutukculer N, Kepe L, Coker C, Berdeli A, Tekgul H. Proinflammatory cytokines, prostaglandins and zinc in febrile convulsions. *Pediatrics international : official journal of the Japan Pediatric Society*. 2001;43(3):235-9. Epub 2001/07/24.
328. Izquierdo-Garcia JL, Peces-Barba G, Heili S, Diaz R, Want E, Ruiz-Cabello J. Is NMR-based metabolomic analysis of exhaled breath condensate accurate? *The European respiratory journal : official journal of the European Society for Clinical Respiratory Physiology*. 2011;37(2):468-70. Epub 2011/02/02.
329. Motta A, Paris D, Melck D, de Laurentiis G, Maniscalco M, Sofia M, et al. Nuclear magnetic resonance-based metabolomics of exhaled breath condensate: methodological aspects. *The European respiratory journal : official journal of the European Society for Clinical Respiratory Physiology*. 2012;39(2):498-500. Epub 2012/02/03.
330. Debley JS, Ohanian AS, Spiekerman CF, Aitken ML, Hallstrand TS. Effects of bronchoconstriction, minute ventilation, and deep inspiration on the composition of exhaled breath condensate. *Chest*. 2011;139(1):16-22. Epub 2010/04/13.
331. Wiklund S, Johansson E, Sjostrom L, Mellerowicz EJ, Edlund U, Shockcor JP, et al. Visualization of GC/TOF-MS-based metabolomics data for identification of biochemically interesting compounds using OPLS class models. *Analytical chemistry*. 2008;80(1):115-22. Epub 2007/11/22.
332. Human Metabolome Database. Available from: <http://www.hmdb.ca/>.
333. Scripps Center for Metabolomics METLIN database. Available from: <https://metlin.scripps.edu/index.php>.

334. Mackay RJ, McEntyre CJ, Henderson C, Lever M, George PM. Trimethylaminuria: causes and diagnosis of a socially distressing condition. *The Clinical biochemist Reviews / Australian Association of Clinical Biochemists*. 2011;32(1):33-43. Epub 2011/04/01.
335. Soyer OU, Dizdar EA, Keskin O, Lilly C, Kalayci O. Comparison of two methods for exhaled breath condensate collection. *Allergy*. 2006;61(8):1016-8. Epub 2006/07/27.
336. Huttmann EM, Greulich T, Hattesoehl A, Schmid S, Noeske S, Herr C, et al. Comparison of two devices and two breathing patterns for exhaled breath condensate sampling. *PLoS One*. 2011;6(11):e27467. Epub 2011/11/17.
337. Boshier PR, Cushnir JR, Mistry V, Knaggs A, Spanel P, Smith D, et al. On-line, real time monitoring of exhaled trace gases by SIFT-MS in the perioperative setting: a feasibility study. *The Analyst*. 2011;136(16):3233-7. Epub 2011/07/01.
338. Knaus WA, Draper EA, Wagner DP, Zimmerman JE. APACHE II: a severity of disease classification system. *Critical care medicine*. 1985;13(10):818-29. Epub 1985/10/01.
339. Le Gall JR, Lemeshow S, Saulnier F. A new Simplified Acute Physiology Score (SAPS II) based on a European/North American multicenter study. *JAMA : the journal of the American Medical Association*. 1993;270(24):2957-63. Epub 1993/12/22.
340. Le Gall JR, Klar J, Lemeshow S, Saulnier F, Alberti C, Artigas A, et al. The Logistic Organ Dysfunction system. A new way to assess organ dysfunction in the intensive care unit. ICU Scoring Group. *JAMA : the journal of the American Medical Association*. 1996;276(10):802-10. Epub 1996/09/11.
341. Marshall JC, Cook DJ, Christou NV, Bernard GR, Sprung CL, Sibbald WJ. Multiple organ dysfunction score: a reliable descriptor of a complex clinical outcome. *Critical care medicine*. 1995;23(10):1638-52. Epub 1995/10/01.
342. Vincent JL, Moreno R, Takala J, Willatts S, De Mendonca A, Bruining H, et al. The SOFA (Sepsis-related Organ Failure Assessment) score to describe organ dysfunction/failure. On behalf of the Working Group on Sepsis-Related Problems of the European Society of Intensive Care Medicine. *Intensive care medicine*. 1996;22(7):707-10. Epub 1996/07/01.
343. Vincent JL, Moreno R. Clinical review: scoring systems in the critically ill. *Crit Care*. 2010;14(2):207. Epub 2010/04/16.
344. Viala M, Bhakar AL, de la Loge C, van de Velde H, Esseltine D, Chang M, et al. Patient-reported outcomes helped predict survival in multiple myeloma using partial least squares analysis. *Journal of clinical epidemiology*. 2007;60(7):670-9. Epub 2007/06/19.
345. Ibrahim GM, Morgan BR, Fallah A. A partial least squares analysis of seizure outcomes following resective surgery for tuberous sclerosis complex in children with intractable epilepsy. *Child's nervous system : ChNS : official journal of the International Society for Pediatric Neurosurgery*. 2015;31(2):181-4. Epub 2014/12/03.
346. Tu YK, Gilthorpe MS, F DA, Woolston A, Clerehugh V. Partial least squares path modelling for relations between baseline factors and treatment outcomes in periodontal regeneration. *Journal of clinical periodontology*. 2009;36(11):984-95. Epub 2009/10/09.

347. Spicker JS, Brunak S, Frederiksen KS, Toft H. Integration of clinical chemistry, expression, and metabolite data leads to better toxicological class separation. *Toxicological sciences : an official journal of the Society of Toxicology*. 2008;102(2):444-54. Epub 2008/01/08.
348. Sin DD, Man SF, Marrie TJ. Arterial carbon dioxide tension on admission as a marker of in-hospital mortality in community-acquired pneumonia. *The American journal of medicine*. 2005;118(2):145-50. Epub 2005/02/08.
349. Naito T, Suda T, Yasuda K, Yamada T, Todate A, Tsuchiya T, et al. A validation and potential modification of the pneumonia severity index in elderly patients with community-acquired pneumonia. *Journal of the American Geriatrics Society*. 2006;54(8):1212-9. Epub 2006/08/18.
350. Al-Muhairi SS, Zoubeidi TA, Ellis ME, Safa WF, Joseph J. Risk factors predicting outcome in patients with pneumonia in Al-Ain, United Arab Emirates. *Saudi medical journal*. 2006;27(7):1044-8. Epub 2006/07/11.
351. Tseng CC, Fang WF, Leung SY, Chen HC, Chang YC, Wang CC, et al. Impact of serum biomarkers and clinical factors on intensive care unit mortality and 6-month outcome in relatively healthy patients with severe pneumonia and acute respiratory distress syndrome. *Disease markers*. 2014;2014:804654. Epub 2014/04/12.
352. Minakuchi H, Wakino S, Hayashi K, Inamoto H, Itoh H. Serum creatinine and albumin decline predict the contraction of nosocomial aspiration pneumonia in patients undergoing hemodialysis. *Therapeutic apheresis and dialysis : official peer-reviewed journal of the International Society for Apheresis, the Japanese Society for Apheresis, the Japanese Society for Dialysis Therapy*. 2014;18(4):326-33. Epub 2013/11/13.
353. Sahin F, Yildiz P. Distinctive biochemical changes in pulmonary tuberculosis and pneumonia. *Archives of medical science : AMS*. 2013;9(4):656-61. Epub 2013/09/21.
354. Viasus D, Garcia-Vidal C, Simonetti A, Manresa F, Dorca J, Gudiol F, et al. Prognostic value of serum albumin levels in hospitalized adults with community-acquired pneumonia. *The Journal of infection*. 2013;66(5):415-23. Epub 2013/01/05.
355. Doshi SM, Rueda AM, Corrales-Medina VF, Musher DM. Anemia and community-acquired pneumococcal pneumonia. *Infection*. 2011;39(4):379-83. Epub 2011/05/11.
356. Reade MC, Weissfeld L, Angus DC, Kellum JA, Milbrandt EB. The prevalence of anemia and its association with 90-day mortality in hospitalized community-acquired pneumonia. *BMC pulmonary medicine*. 2010;10:15. Epub 2010/03/18.
357. Braun E, Kheir J, Mashiach T, Naffaa M, Azzam ZS. Is elevated red cell distribution width a prognostic predictor in adult patients with community acquired pneumonia? *BMC infectious diseases*. 2014;14:129. Epub 2014/03/07.
358. Hussain SQ, Ashraf M, Wani JG, Ahmed J. Low Hemoglobin Level a Risk Factor for Acute Lower Respiratory Tract Infections (ALRTI) in Children. *Journal of clinical and diagnostic research : JCDR*. 2014;8(4):PC01-3. Epub 2014/06/25.

359. Mourad S, Rajab M, Alameddine A, Fares M, Ziade F, Merhi BA. Hemoglobin level as a risk factor for lower respiratory tract infections in Lebanese children. *North American journal of medical sciences*. 2010;2(10):461-6. Epub 2010/10/01.
360. Davalos D, Akassoglou K. Fibrinogen as a key regulator of inflammation in disease. *Seminars in immunopathology*. 2012;34(1):43-62. Epub 2011/11/01.
361. Jennewein C, Tran N, Paulus P, Ellinghaus P, Eble JA, Zacharowski K. Novel aspects of fibrin(ogen) fragments during inflammation. *Mol Med*. 2011;17(5-6):568-73. Epub 2011/01/07.
362. Adams RA, Passino M, Sachs BD, Nuriel T, Akassoglou K. Fibrin mechanisms and functions in nervous system pathology. *Molecular interventions*. 2004;4(3):163-76. Epub 2004/06/24.
363. Milbrandt EB, Reade MC, Lee M, Shook SL, Angus DC, Kong L, et al. Prevalence and significance of coagulation abnormalities in community-acquired pneumonia. *Mol Med*. 2009;15(11-12):438-45. Epub 2009/09/16.
364. Lim WS, van der Eerden MM, Laing R, Boersma WG, Karalus N, Town GI, et al. Defining community acquired pneumonia severity on presentation to hospital: an international derivation and validation study. *Thorax*. 2003;58(5):377-82. Epub 2003/05/03.
365. Fine MJ, Auble TE, Yealy DM, Hanusa BH, Weissfeld LA, Singer DE, et al. A prediction rule to identify low-risk patients with community-acquired pneumonia. *The New England journal of medicine*. 1997;336(4):243-50. Epub 1997/01/23.
366. Neill AM, Martin IR, Weir R, Anderson R, Cheresky A, Epton MJ, et al. Community acquired pneumonia: aetiology and usefulness of severity criteria on admission. *Thorax*. 1996;51(10):1010-6. Epub 1996/10/01.
367. Wiwanitkit V. High serum alkaline phosphatase levels, a study in 181 Thai adult hospitalized patients. *BMC family practice*. 2001;2:2. Epub 2001/09/08.
368. Maldonado O, Demasi R, Maldonado Y, Taylor M, Troncale F, Vender R. Extremely high levels of alkaline phosphatase in hospitalized patients. *Journal of clinical gastroenterology*. 1998;27(4):342-5. Epub 1998/12/17.
369. Kanai S, Honda T, Uehara T, Matsumoto T. Liver function tests in patients with bacteremia. *Journal of clinical laboratory analysis*. 2008;22(1):66-9. Epub 2008/01/18.
370. Pelosi P, Barassi A, Severgnini P, Gomiero B, Finazzi S, Merlini G, et al. Prognostic role of clinical and laboratory criteria to identify early ventilator-associated pneumonia in brain injury. *Chest*. 2008;134(1):101-8. Epub 2008/04/12.
371. Su LX, Meng K, Zhang X, Wang HJ, Yan P, Jia YH, et al. Diagnosing ventilator-associated pneumonia in critically ill patients with sepsis. *American journal of critical care : an official publication, American Association of Critical-Care Nurses*. 2012;21(6):e110-9. Epub 2012/11/03.
372. Povoas P, Coelho L, Almeida E, Fernandes A, Mealha R, Moreira P, et al. C-reactive protein as a marker of ventilator-associated pneumonia resolution: a pilot study. *The European respiratory journal*. 2005;25(5):804-12. Epub 2005/05/03.

373. Seligman R, Meisner M, Lisboa TC, Hertz FT, Filippin TB, Fachel JM, et al. Decreases in procalcitonin and C-reactive protein are strong predictors of survival in ventilator-associated pneumonia. *Crit Care*. 2006;10(5):R125. Epub 2006/09/08.
374. Lisboa T, Seligman R, Diaz E, Rodriguez A, Teixeira PJ, Rello J. C-reactive protein correlates with bacterial load and appropriate antibiotic therapy in suspected ventilator-associated pneumonia. *Critical care medicine*. 2008;36(1):166-71. Epub 2007/11/17.
375. Hillas G, Vassilakopoulos T, Plantza P, Rasidakis A, Bakakos P. C-reactive protein and procalcitonin as predictors of survival and septic shock in ventilator-associated pneumonia. *The European respiratory journal*. 2010;35(4):805-11. Epub 2009/09/01.
376. Bell JD, Brown JC, Nicholson JK, Sadler PJ. Assignment of resonances for 'acute-phase' glycoproteins in high resolution proton NMR spectra of human blood plasma. *FEBS letters*. 1987;215(2):311-5. Epub 1987/05/11.
377. Swanson JM, Mueller EW, Croce MA, Wood GC, Boucher BA, Magnotti LJ, et al. Changes in pulmonary cytokines during antibiotic therapy for ventilator-associated pneumonia. *Surgical infections*. 2010;11(2):161-7. Epub 2009/09/30.
378. Balog J, Sasi-Szabo L, Kinross J, Lewis MR, Muirhead LJ, Veselkov K, et al. Intraoperative tissue identification using rapid evaporative ionization mass spectrometry. *Science translational medicine*. 2013;5(194):194ra93. Epub 2013/07/19.

9. APPENDICES

Appendix I – Ethics and Research and Development Department Approval Letters


National Research Ethics Service

North London REC 3
 Level 7 Maternity, Room 019
 Northwick Park Hospital
 Watford Road
 Harrow
 HA1 3UJ

Telephone: 020 8869 3928
 Facsimile: 020 8869 5222

28 January 2011

Dr Anthony Gordon
 Department of Critical Care
 Charing Cross Hospital
 Fulham Palace Road,
 London
 W6 8RF

Dear Dr Gordon

Study title: Mechanisms of monocyte priming and tolerance in vitro and in vivo involving tumour necrosis factor alpha converting enzyme.
REC reference number: 10/H0709/77
SSA reference number: 10/H0706/96

The REC gave a favourable ethical opinion to this study on 14th January 2011

Notification(s) have been received from local assessor(s), following site-specific assessment. On behalf of the Committee, I am pleased to confirm the extension of the favourable opinion to the new site(s) and investigator(s) listed below:

Research Site	Principal Investigator / Local Collaborator
Imperial College London, Chelsea and Westminster Campus	Prof Masao Takata

The favourable opinion is subject to management permission or approval being obtained from the host organisation prior to the start of the study at the site concerned.

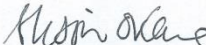
Statement of compliance

The Committee is constituted in accordance with the Governance Arrangements for Research Ethics Committees (July 2001) and complies fully with the Standard Operating Procedures for Research Ethics Committees in the UK.

10/H0709/77

Please quote this number on all correspondence

Yours sincerely,


Mrs. Alison O'Kane
Committee Co-ordinator

Email: alison.okane@nwlh.nhs.uk

Copy to: Becky Ward, Imperial College London/Healthcare NHS Trust

NRES Committee London - Harrow

Level 7 Maternity, Room 019
 Northwick Park Hospital
 Watford Road
 Harrow
 HA1 3UJ

Tel: 020 8869 3928
 Fax: 020 8869 5222

26 September 2011

Dr Anthony Gordon
 Clinical Senior Lecturer
 & Consultant, Critical Care Medicine
 Imperial College London
 Department of Critical Care
 Charing Cross Hospital
 Fulham Palace Road,
 London
 W6 8RF

Dear Dr Gordon

Study title: Mechanisms of monocyte priming and tolerance in vitro and in vivo involving tumour necrosis factor alpha converting enzyme.
REC reference: 10/H0709/77
Amendment number:
Amendment date:

The above amendment was recently reviewed by the Sub-Committee in correspondence .

Ethical opinion

The members of the Committee taking part in the review gave a **favourable ethical opinion** of the amendment on the basis described in the notice of amendment form and supporting documentation.

Please note the following minor points which do not affect the favourable opinion decision.

The amount of blood collected should also be amended to 35ml on the professional consultee info sheet (page 2)

Page 10 of the protocol, the amendment just before s.3.1 indicates that "Urine samples (10ml) either provided directly by the patient or drained from the urinary catheter will be obtained, processed and analysed to determine the presence of any metabolic signatures." Information sheets says they will only use tubes already in place.

A spell/grammar check of the amendment to the protocol at page 7-8 is recommended.

Approved documents

The documents reviewed and approved at the meeting were:

Document	Version	Date
Participant Information Sheet: Professional Consultee	1.7	01 August 2011
Participant Information Sheet: Patient Regaining Capacity	1.7	01 August 2011
Participant Information Sheet: Personal Consultee	1.7	01 August 2011
Investigator CV	Dr. J. Handy	
Protocol	1.7, August 2011	
Notice of Substantial Amendment (non-CTIMPs)		

Membership of the Committee

The members of the Committee who took part in the review are listed on the attached sheet.

R&D approval

All investigators and research collaborators in the NHS should notify the R&D office for the relevant NHS care organisation of this amendment and check whether it affects R&D approval of the research.

Statement of compliance

The Committee is constituted in accordance with the Governance Arrangements for Research Ethics Committees (July 2001) and complies fully with the Standard Operating Procedures for Research Ethics Committees in the UK.

10/H0709/77:	Please quote this number on all correspondence
---------------------	---

Yours sincerely

Dr Jan Downer
Chair

E-mail: alison.okane@nwlh.nhs.uk

Enclosures: List of names and professions of members who took part in the review

*Copy to: Becky Ward, Joint Research Office, Imperial College London and Imperial College Healthcare NHS Trust
Miss Becky Ward, Imperial College London and Imperial College Healthcare NHS Trust*

NRES Committee London - Harrow

Sub-Committee of the REC in correspondence meeting on 23 September 2011.

Dr. J. Downer (Chair)
Ms. Shelly Glaister-Young

Consultant Anaesthetist
Lay Member

Joint Research Office
 Academic Health Science Centre
 Imperial College London and Imperial College Healthcare NHS Trust
 St Mary's Hospital
 Faculty of Medicine
 Room GM14,
 Ground Mezzanine Floor,
 Praed Street Wing
 (Ex Diagnostic Bacteriology Space)
 W2 1 PG

4 March 2011

Dr Anthony Gordon
 Department of Critical Care
 Charing Cross Hospital,
 Fulham Palace Road,
 London W6 8RF

Dear Dr Anthony Gordon

Project Title: Mechanisms of monocyte priming and tolerance in vitro and in vivo involving tumour necrosis factor alpha converting enzyme.

Short Title: Mechanisms of monocyte priming and tolerance

Joint Research Office Reference number: JROHH0192

Ethics reference number: 10/H0709/77

Principal Investigator: Dr Anthony Gordon

I confirm that this project has now been approved by the Joint Research Office. The project may now start at Imperial College Healthcare NHS Trust sites. Please note that the start date of the project is the date of this letter and the duration is the same as that provided in your application form.

The list of documents reviewed and approved by the Joint Research Office under requirements of the Research Governance Framework are as follows:

Document	Version	Date
Ethics favourable opinion letter		
R&D form	42882/161998/14/491	23/10/2010
SSI form	42882/171336/6/547/44286/199054	03/12/2010
Protocol	1.6	November 2010
Participant information sheet: for patient	1.5	
Participant consent form: for subjects unable to give consent	1.5	
Participant information sheet: healthy volunteers	1.6	November 2010
Participant information sheet: personal legal representative	1.5	
Participant information sheet: patient regaining capacity	1.6	November 2010
Participant information sheet: professional consultee	1.6	November 2010
Participant consent form: healthy volunteers	1.6	November 2010
Participant consent form: for patients able to give consent	1.6	November 2010

Participant consent form: Professional consultee assent form	1.6	November 2010
Participant consent form: Assent form for personal consultees	1.6	November 2010
Participant consent form: for patient regaining capacity	1.6	November 2010
Covering statement for personal consultee	1.6	November 2010
Investigator's CV		

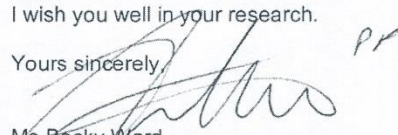
Before you commence your research, please note that you must be aware of your obligations to comply with the minimum requirements for compliance with the Research Governance indicators 17 (Data Protection); 25 (Health and Safety) and 22 (Financial Probity). Details of the requirements to be met can be found in the Research Governance Framework available on www.dh.gov.uk.

Under the Research Governance regulations, Serious Adverse Event Reports, Adverse Reactions and amendments to the protocol or other supporting documents must be forwarded to the Joint Research Office and Ethics Committee.

In accordance with the Research Governance Framework, research projects carried out in the Trust will be randomly chosen by the Joint Research Office for auditing. Please see the attached checklist for documentation that will be required during the audit.

I wish you well in your research.

Yours sincerely,

 *PP*
 Ms Becky Ward
 Research Governance Manager
 Academic Health Science Centre
 Joint Research Office
 Imperial College London and Imperial College Healthcare NHS Trust
 Hammersmith Hospital

Mechanisms of Monocyte Priming & Tolerance

Ethics committee: North London REC 3

REC reference: 10/H0709/77

Name of Principal Investigator: Dr Anthony Gordon

ASSENT FORM FOR PERSONAL CONSULTTEES

Please initial box

1. I confirm that I have read and understood the Personal Consultee Information Sheet dated August 2011 version 1.7 for the above study and have had the opportunity to ask questions which have been

answered fully.

2. I understand that I am giving this assent based on what I believe would be my

relative/friend/partner's wishes. In my opinion they would wish to participate.

3. I understand that my relative/friend/partner's participation is voluntary and I am free to change my advice about their wish to participate and to withdraw assent at any time, without giving any reason

and without their medical care or legal rights being affected.

4. I understand that sections of any of my relative/friend/partner's medical notes may be looked at by responsible individuals from Imperial College/Imperial College Healthcare NHS Trust or from regulatory authorities where it is relevant to my taking part in this research.

I assent to these individuals accessing my relative/friend/partner's records that are relevant to this research.

5. I assent to the use of my relative/friend/partner's samples for future ethically approved research projects and for their blood to be used for DNA testing in inflammation research. I understand that this

information will be kept confidential at all times.

6. The compensation arrangements have been discussed with me.

7. I assent to my relative/friend/partner taking part in the above study.

8. I realise that my relative/friend/partner's consent will override my assent when they are able to give informed consent.

9. I assent to data being stored in anonymous form for up to 10 years & used in future, ethically approved, projects

Name of patient

I am the patient's _____
(please write your relationship to the patient e.g. wife / brother etc.)

Name of personal consultee

Signature

Date

Name of researcher taking assent

Signature

Date

1 copy for subject; 1 copy for Principal Investigator; 1 copy to be kept with hospital notes

Mechanisms of Monocyte Priming & Tolerance

Name of Principal Investigator: Dr Anthony Gordon

Ethics committee: North London REC 3

REC reference: 10/H0709/77

PROFESSIONAL CONSULTEE ASSENT FORM

Regarding patient _____

This form should be completed by a doctor who is unconnected with the research study only in situations where the patient is temporarily unable to provide informed consent for themselves and if there is no relative / friend / partner willing and capable to act as the nominated personal consultee. The doctor primarily responsible for the medical treatment of the patient, or a person nominated by the relevant health care provider, can act as a professional consultee for the patient provided that they are not connected with the conduct of this study.

I, Dr / Mr / Ms / Prof _____ as the clinician treating this patient declare by signing this form that I have read the Professional Consultee Information Sheet version - ____ dated _____ and have no objection for this patient to be entered into this research study. I also understand that should the patient regain consciousness they will be fully informed of the decision to enter them into this research study and consent will be sought from them for their continued participation. I agree that the patient's consent will override my assent when the patient is able to give consent.

Name of Professional Consultee

Signature

Date

Name of researcher taking assent

Signature

Date

Mechanisms of Monocyte Priming & Tolerance

Name of Principal Investigator: Dr Anthony Gordon

Ethics committee: North London REC 3

REC reference: 10/H0709/77

PATIENT REGAINING CAPACITY CONSENT FORM**Please initial each box**

1. I confirm that I have read and understand the Patient Regaining Capacity Information Sheet dated August 2011 version 1.7 for the above study and have had the opportunity to ask questions

which have been answered fully.

2. I understand that my continued participation is voluntary and I am free to withdraw at any time,

without giving any reason, without my medical care or legal rights being affected.

3. I understand that sections of any of my medical notes may have been looked at by responsible individuals from Imperial College London/Imperial College Healthcare NHS Trust or from regulatory authorities where it is relevant to my taking part in this research.

I give permission for these individuals to access/continue to access records that are relevant to this research.

4. I agree to the use of my samples for future ethically approved research projects and for my blood to be used for DNA testing in inflammation research. I understand that this information will

be kept confidential at all times.

5. The compensation arrangements have been discussed with me.

6. I agree to my continued participation in the above study.

7. I agree that data can be stored in anonymous form for up to 10 years & used in future, ethically approved projects.

Name of Subject

Signature

Date

Name of Person
taking consent

Signature

Date

1 copy for subject; 1 copy for Principal Investigator; 1 copy to be kept with hospital note

Appendix III Bedside Clinical Data Collection Sheet

Date:

Sample Code:

Serum Taken	Time on Ice	Time off Ice	Time Centrifuge	Time Out	Time Cryotube	Time -80	RTube On	RTube Off	Time Cryotube	Time -80
Urine Taken	Time Centrifuge	Time Out	Time Cryotube	Time -80						

	Before Collection	During Collection	After Collection	Data for 24h prior to 8:00am	
				Min	Max
Ventilation Mode					
PEEP					
FiO2					
RR set					
RR measured					
Insp TV					
Exp TV					
PS/PC					
Exp MV					
PPeak					
PPlat					
Pmean					
I:E					
HR					
SBP					
MAP					
DBP					
Sats					
GCS	-	-	-		
Temp	-	-	-		
CVP	-	-	-		
U/O					
U/O Total					
Total IV Fluid input					
Total Oral Input					
PaO2					
FiO2					
PaCO2					
pH					
HCO3					
BE					
Lactate					
Glucose					

